Inverse Problems and Optimal Power Flow in Active Distribution Networks

Thèse N° 9456

Présentée le 27 septembre 2019

à la Faculté informatique et communications
Laboratoire pour les communications informatiques et leurs applications 2
Programme doctoral en informatique et communications

pour l'obtention du grade de Docteur ès Sciences

par

Cong WANG

Acceptée sur proposition du jury

Prof. O. N. A. Svensson, président du jury
Prof. J.-Y. Le Boudec, directeur de thèse
Dr A. Bernstein, rapporteur
Prof. Y. Chen, rapporteuse
Prof. M. Paolone, rapporteur

2019

ÉCOLE POLYTECHNIQUE
FÉDÉRALE DE LAUSANNE

If you want to find the secrets of the universe,
think in terms of energy, frequency and vibration.
- Nikola Tesla

Acknowledgements

First and foremost, I would like to express my deepest gratitude to my thesis director, Prof. Jean-Yves Le Boudec. Your inspiring ideas, scientific expertise, and warm encouragement make my PhD a wonderful and unique experience.

I would also like to express my sincere gratitude to Prof. Ola Svensson, Prof. Mario Paolone, Dr. Andrey Bernstein, and Prof. Yu Chen for both accepting to serve in my PhD thesis committee and providing valuable discussions.

During my PhD, I was very fortunate to do joint research with many brilliant people. Thank you, Mario, for sharing with me your expertise in power system. Then, I would like to thank Andrey for helping me solve the challenging problems during my PhD. Eleni, thank you for the nice idea of CoDistFlow and the collaboration in the last two years of my PhD. Thanks, Emiliano, for the support on multi-phase networks and OpenDSS.

Apart from the research, I felt very happy as a member of LCA2 and enjoyed every moment with my PhD colleagues Roman, Ehsan, Marguerite, Wajeb, and Maaz. They have been like a second family in the past few years.

Also, I would like to thank several alumni of LCA2. In particular, Nadia for guiding me to the area of power system; Sergio for offering me the experience of network engineering; Dan and Niek for the fun time in my first two years.

I also owe thanks to our secretaries Patricia, Angela, and our editor Holly. With their help, my PhD work became smooth and efficient.

Finally, my special thanks go to all my friends at EPFL for being around with me. Because of you, I never felt lonely during the course of the PhD.

Lausanne, 2019
Cong Wang

Abstract

During the last decade, distribution networks have experienced essential changes driven by the integration of renewable-energy sources, batteries, electric-vehicle charging stations, etc. This results in not only opportunities, but also operational problems. For example, the renewable power generation and the charging-station power consumption can be very large, leading to line congestion and over-/under-voltage issues. To solve the operational problems, we can develop methods that consist in directly manipulating the power; this is feasible by means of power-electronic devices and local controllers. For example, to address the line congestion and over-/under-voltage issues, we can either perform power curtailment at the energy sources and charging stations, or use batteries and demand response to avoid excessive power. So far, there is a growing number of works on managing distribution networks via direct power manipulation. These works include both the typical ones, such as regulating voltage/frequency by active/reactive power, and the pioneering ones, such as the Commelec that controls distribution networks by multi-agent systems and explicit power setpoints. With the integrated loads/sources and the direct power manipulation, the essence of distribution networks has changed. This gives us the concept of active distribution networks (ADNs). In this thesis, we focus on how to ensure network security and achieve optimality in ADNs.

First, we study the AC power-flow problem in generically modelled multi-phase ADNs, which is an inverse problem. It determines whether a target system power injection has a corresponding system electrical state that fulfills the security constraints and might need to be repeatedly solved in real time. For this problem, we apply the fixed-point theory and establish explicit conditions for the existence and uniqueness of the power-flow solution. When the conditions are satisfied, we guarantee the existence of a power-flow solution and analytically specify a domain in which this solution is unique. For this guaranteed solution, we further provide an efficient iterative method to numerically compute it.

Second, we take into account that the actual system power injection might be different from the target one, due to improperly modelled system dynamics, reaction delays, and renewable-energy disturbances. As a consequence, it is important to see whether we can ensure that the actual system electrical state always satisfies the security constraints, given that the actual system power injection resides in some known uncertainty set. We refer to this as the admissibility problem, which is another

inverse problem. For it, a major difficulty is that each system power injection might correspond to zero or multiple system electrical states. We layout the theoretical foundations for solving this problem. In addition, we develop two concrete solution methods that can be implemented in practical ADNs.

Third, to decide the optimal system power injection, we study an AC optimal power flow problem in generically modelled multi-phase ADNs. In this problem, we consider wye/delta load/source connections and incorporate the non-singularity constraint. We solve this problem by developing a successive local exploration method.

All proposed theories and methods have been numerically evaluated via IEEE/CIGRE test feeders.

Keywords: active distribution network, inverse problem, power-flow solvability, fixed-point theory ,non-singular Jacobian, security constraint, admissibility, multi-phase optimal power flow, uncertain power injection, wye/delta connection.

Résumé

Au cours de la dernière décennie, les réseaux de distribution ont évolué pour s'adapter à l'intégration de sources d'énergie renouvelable, de batteries, de stations de recharge de véhicules électriques, etc. Ces changements ouvrent non seulement sur de nouvelles opportunités, mais également sur certains problèmes opérationnels. Par exemple, la génération d'énergie renouvelable ou la consommation d'énergie par les stations de recharge peuvent être très grandes, ce qui peut entraîner la congestion de lignes et occasionner des problèmes de sur ou sous-tension. Afin de résoudre les problèmes opérationnels, nous pouvons développer des méthodes qui consistent à manipuler directement la puissance ; ceci peut se faire par le biais d'outils d'électronique de puissance ou de contrôleurs locaux. Par exemple, pour répondre aux problèmes de congestion de lignes causant une sur ou sous-tension, nous pouvons soit avoir recours à une réduction de production d'énergie au niveau des sources ainsi qu'au niveau des stations de recharge, soit avoir recours à des batteries avec des consommations flexibles afin d'éviter une consommation excessive d'énergie. Un nombre grandissant de travaux portent sur la gestion de réseaux de distribution par le biais d'une manipulation de la puissance. Ces travaux incluent des solutions classiques comme la régulation de la tension ou de la fréquence par la puissance active ou réactive. Ils incluent également des solutions plus novatrices comme Commelec qui contrôle les réseaux de distribution grâce à des systèmes multi-agents et à l'utilisation de consignes de puissance explicites. Avec l'intégration de nouvelles ressources et la manipulation directe des puissances, l'essence des réseaux de distribution a changé pour donner naissance aux réseaux dynamiques de distribution (RDDs). Dans cette thèse, nous nous intéressons aux méthodes permettant d'assurer la sécurité des réseaux et permettant une utilisation optimale des RDDs.

Dans un premier temps, nous étudions le problème de l'écoulement des charges dans les RDDs multi-phasés modélisés de façon générique, ce qui est un problème inverse. Ceci permet de déterminer si l'injection de puissance d'un système correspond à un état électrique qui satisfait les contraintes de sécurité. Cet état devra éventuellement être recalculé en temps réel. Pour ce problème, nous appliquons la théorie du point fixe et établissons des conditions explicites pour l'existence et l'unicité d'une solution aux équations du problème d'écoulement de charges. Lorsque les conditions sont satisfaites , nous garantissons l'existence d'une solution et précisons de manière analytique, le domaine dans lequel cette solution est unique. Nous fournissons également

une méthode efficace et itérative qui la calcule numériquement.

Dans un second temps, nous prenons en considération le fait que l'injection de puissance du système réel puisse être différente de celle du système modélisé. Ceci peut être dû à une mauvaise modélisation des dynamiques du système, à des réactions de délais ou à des perturbations des énergies renouvelables. Par conséquent, l'injection de puissance réelle du système réside dans un domaine d'incertitude connu. Celle-ci influe sur l'état électrique du système et il est important de savoir si celui-ci satisfait toujours les contraintes de sécurité ou non. Ce problème, également inverse, est appelé problème d'admissibilité. Une difficulté majeure dans la résolution de ce problème, est que chaque injection de puissance peut correspondre à zéro ou de multiples états électriques du système. Nous établissons les fondations théoriques pour résoudre ce problème. De plus, nous développons deux méthodes concrètes qui peuvent être implémentées en pratique dans les RDDs.

Dans un troisième temps, afin de décider l'injection optimale de puissance dans le système, nous étudions un problème d'écoulement de charges optimal (OPF) dans les RDDs multi-phasés génériquement modelés. Dans ce problème, nous considérons des connections de ressources wye/delta, et nous incorporons la contrainte de non-singularité. Nous résolvons ce problème en développant une méthode d'exploration locale successive.

Toutes les théories et méthodes proposées ont été évaluée numériquement sur les réseaux standardisés de IEEE et de CIGRE.

Mots clés : réseau dynamique de distribution, problem inverse, solvabilité de l'écoulement des charges, théorie des points fixes, Jacobienne non-singulière, contrainte de sécurité, admissibilité, écoulement des charges optimal multi-phasé, injection de puissance incertaine, connection wye/delta.

Contents

List of Figures

List of Tables

List of Notations

Latin Letters

$\mathbf{A}_{j,k}$	Matrix characterized by the transmission device of physical branch jk
$\mathcal{B}^{\text{aux}}$	Auxiliary set of $\mathbf{s}^{Y,\Delta}$, used in the solution method to the multi-phase optimal power flow problem
$\mathbf{C}_{j,k}$	Matrix characterized by the transmission device of physical branch jk
$\mathcal{D}_{\rho}$	Set of $\mathbf{v}$, for the existence and uniqueness of the power-flow solution
$\mathcal{E}$	Set of all physical branches
f	Arbitrary function
$\mathbf{F}$	Function of $\mathbf{v}$ that maps $\mathbf{v}$ to the corresponding $\mathbf{s}$
$\mathbf{F}^{Y,\Delta}$	Function of $\mathbf{v},\ \mathbf{i}^{\Delta}$ that maps $(\mathbf{v},\mathbf{i}^{\Delta})$ to the corresponding $\mathbf{s}^{Y,\Delta}$
$\mathbf{G}_{\mathbf{s}}$	Function of $\mathbf{v}$, used to express the fixed-point form of the multi-dimensional power-flow equation
$\mathbf{G}_{\mathbf{s}^{Y,\Delta}}$	Function of $\mathbf{v}$, used to express the fixed-point form of the augmented multi-dimensional power-flow equation
$\mathbf{H}$	Constant matrix that transforms the phase-to-ground quantities into the phase-to-phase quantities
$\mathbf{i}_j$	Complex nodal current at bus j
$\mathbf{i}$	Vector that collects $\mathbf{i}_j$ for $j \neq 0$
$\mathbf{i}_j^{\Delta}$	Complex phase-to-phase current of the delta connection at bus j
$\mathbf{i}^{\Delta}$	Vector that collects $\mathbf{i}_j^{\Delta}$ for $j \neq 0$
$\mathbf{i}_{jk}$	Complex branch current from bus j to k
$\mathbf{i}_{jk}^{\max}$	Upper security bound on the magnitude of $\mathbf{i}_{jk}$
$\mathbf{J}_{\mathbf{F}}$	Jacobian of $\mathbf{F}$, i.e., the power-flow Jacobian
$\mathbf{J}_{\mathbf{F}^{Y,\Delta}}$	Jacobian of $\mathbf{F}^{Y,\Delta}$, i.e., the augmented power-flow Jacobian
N	Number of PQ buses
N^{phase}	Number of phases
$\mathcal{N}$	Set of all buses (0 for the slack bus, $1,...,N$ for the PQ buses)
$\mathbf{s}_j$	Complex nodal power injection at bus j
$\mathbf{s}$	Vector that collects $\mathbf{s}_j$ for $j \neq 0$
$\mathbf{s}^{\text{initial}}$	Initial value of $\mathbf{s}$

$\mathbf{s}_j^Y$	Complex power injection of the wye connection at bus j
$\mathbf{s}^Y$	Vector that collects $\mathbf{s}_j^Y$ for $j \neq 0$
$\mathbf{s}_j^\Delta$	Complex power injection of the delta connection at bus j
$\mathbf{s}^\Delta$	Vector that collects $\mathbf{s}_j^\Delta$ for $j \neq 0$
$\mathbf{s}^{Y,\Delta}$	Vector that collects $\mathbf{s}^Y$ and $\mathbf{s}^\Delta$
$\mathcal{S}$	Arbitrary set of $\mathbf{s}$
$\mathcal{S}^{\text{uncertain}}$	Uncertainty set of $\mathbf{s}$
$\mathcal{S}^{Y,\Delta}$	Convex and compact set of $\mathbf{s}^{Y,\Delta}$
$\mathbf{v}_j$	Complex nodal voltage at bus j
$\mathbf{v}_j^{\max}$	Upper security bound on the magnitude of $\mathbf{v}_j$
$\mathbf{v}_j^{\min}$	Lower security bound on the magnitude of $\mathbf{v}_j$
$\mathbf{v}$	Vector that collects $\mathbf{v}_j$ for $j \neq 0$
$\mathbf{v}^{\text{initial}}$	Initial value of $\mathbf{v}$
$\mathcal{V}$	Arbitrary set of $\mathbf{v}$
$\mathcal{V}^\star$	Set of $\mathbf{v}$ that satisfies the security constraints and the non-singularity of the power-flow Jacobian
$\mathbf{w}$	Zero-injection value of $\mathbf{v}$
$\mathbf{W}$	Diagonal matrix with $\mathbf{w}$ on the main diagonal
$\mathbf{Y}$	Compound nodal admittance matrix
$\mathbf{Y}_{00}$, $\mathbf{Y}_{0L}$, $\mathbf{Y}_{L0}$	Sub-matrices of $\mathbf{Y}$
$\mathbf{Y}_{LL}$	Sub-matrix of $\mathbf{Y}$ that is invertible in practice

Greek Letters

α, β, γ	Functions of $\mathbf{v}$, used to guarantee the existence and uniqueness of the power-flow solution
$\mathbf{\Gamma}_{j,\ell}$	Matrix constructed using $\mathbf{A}_{j,k}$, $\mathbf{C}_{j,k}$, $\mathbf{Y}_{LL}$
$\boldsymbol{\delta}_j$	Vector related to the security of the guaranteed power-flow solution
ϵ	A bound that is used in the successive local exploration method
$\boldsymbol{\eta}_j$	Auxiliary vector, used by $\boldsymbol{\delta}_j$, $\boldsymbol{\tau}_{jk}$
ξ	Norm of $\mathbf{s}$, used to guarantee the existence and uniqueness of the power-flow solution
$\xi^{Y,\Delta}$	Norm of $\mathbf{s}^{Y,\Delta}$, used similarly to ξ
$\rho^\dagger$	A small radius of $\mathcal{D}_\rho$ for localizing the guaranteed power-flow solution
$\rho_{Y,\Delta}^\dagger$	A small radius of $\mathcal{D}_\rho$, used similarly to $\rho^\dagger$
$\rho^\ddagger$	A large radius of $\mathcal{D}_\rho$ for quantifying the domain of uniqueness
$\rho_{Y,\Delta}^\ddagger$	A large radius of $\mathcal{D}_\rho$, used similarly to $\rho^\ddagger$
$\boldsymbol{\tau}_{jk}$	Vector related to the security of the guaranteed power-flow solution
$\mathbf{\Upsilon}_{jk,\ell}$	Matrix constructed using $\mathbf{A}_{j,k}$, $\mathbf{C}_{j,k}$, $\mathbf{Y}_{LL}$

Other Math Notations

$(\cdot)_m$	m-th entry of a vector
$(\cdot)_{m,n}$	Entry on the m-th row and n-th column of a matrix
$\mathrm{Row}_m(\cdot)$	m-th row of a matrix
$\mathrm{diag}(\cdot)$	Diagonal matrix with a vector on the main diagonal
$\Re(\cdot)$	Real part
$\Im(\cdot)$	Imaginary part
$\bar{\cdot}$	Complex conjugation
$\hat{\cdot}$	Reference value
$.^T$	Transposition
$\lvert\cdot\rvert$	Component-wise absolute value
$\lVert\cdot\rVert_p$	ℓ_p norm of a vector or the induced ℓ_p norm of a matrix
$\bigcup, \bigcap$	Union and intersection of sets
$\mathrm{card}(\cdot)$	Cardinality of a set
$\partial\cdot$	Boundary of a set
$\mathrm{cl}(\cdot)$	Closure of a set
$>, \geq, <, \leq$	Component-wise inequalities

1 Introduction

Harmony and order emerge as from innate nature.

Chuang Tzu
ZHUANG ZHOU

1.1 Background and Motivation

For more than a century, electric-power delivery systems have been indispensable to our daily life. In general, they consist of two types of components: transmission networks and distribution networks. As described in, for example, [1, 2],

- Transmission networks are designed to deliver electric power, at high voltages, over long distances, from large centralized generating stations to distribution substations.
- Distribution networks deliver electric power to end users, such as town houses and relatively small commercial premises, at voltage levels lower than those of transmission networks.

Traditionally, distribution networks are passive in the sense that they receive one-way electric power from transmission networks at their substations and deliver it to end users. Indeed, distribution networks are traditionally viewed as synthesized loads of transmission networks. Guided by this point of view, the "connect and forget" principle is typically applied and the planning/operation are based mainly on worst-case or average loading conditions.

This situation has been going through radical changes for a decade, due to the integration of renewable-energy sources (such as photovoltaic panels and wind turbines), batteries, electric-vehicle charging stations, super capacitors. Consequently,

the electric power can flow bi-directionally between the transmission networks and end users. This is illustrated in Figure 1.1, where green and yellow arrows are used, respectively, to indicate the generation and consumption of electric power.

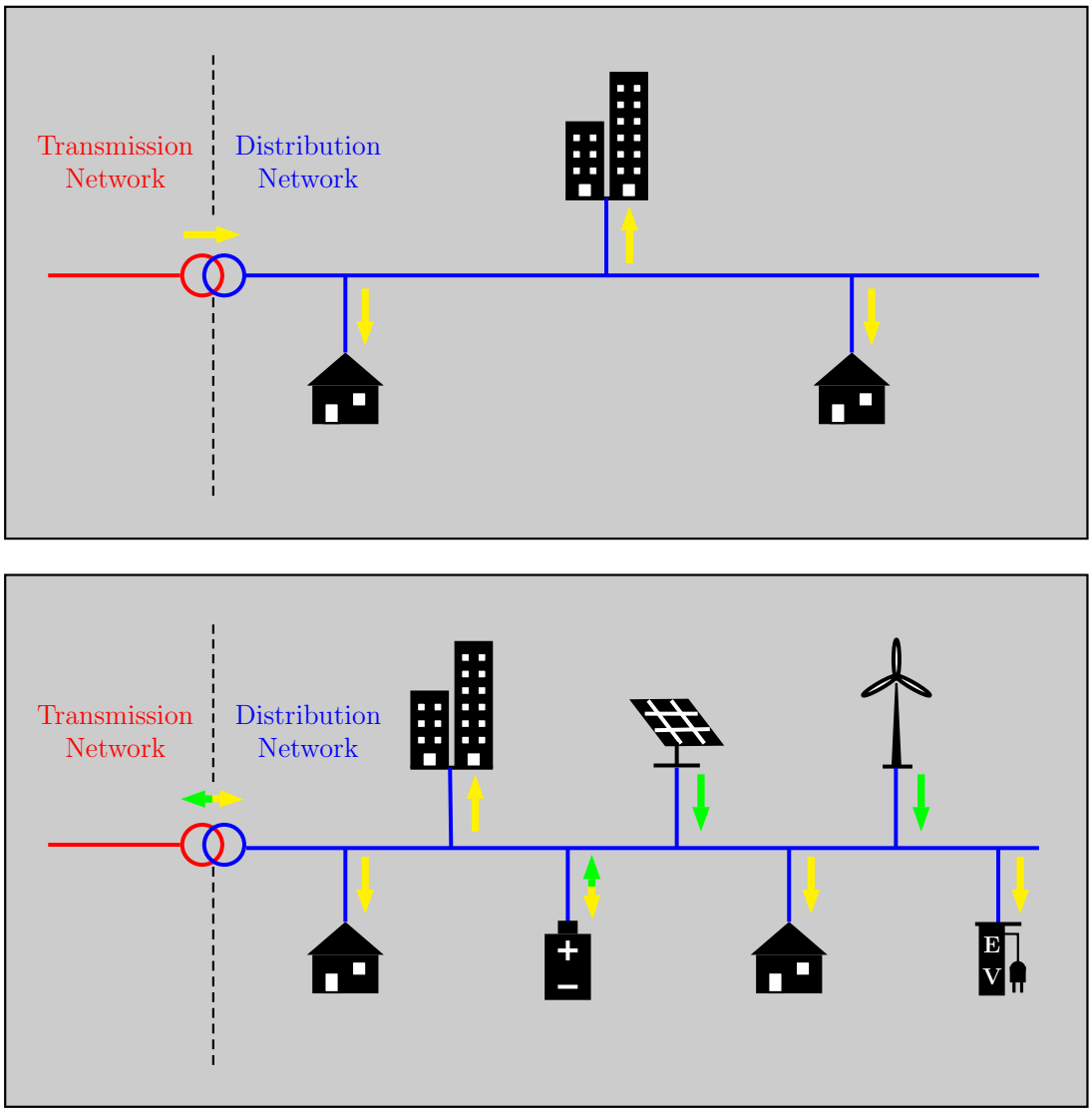

Figure 1.1 – (Top) Traditional distribution network. (Bottom) Distribution network with renewable-energy sources, batteries, and electrical-vehicle charging stations.

It is worth noticing that the integrated local power generation (e.g., from renewable-energy sources) and the integrated local power consumption (e.g., by electric-vehicle charging stations) should be viewed as a double-edged sword. On the one hand, the local power generation, together with the local power consumption, pose a threat to the network security, because the electric power flowing in both directions can be large enough to cause line congestion and over-/under-voltage issues [3, 4, 5]. On the other hand, the local power generation offers not only the chance to reduce the distribution networks' dependency on external networks, but also the possibility to achieve certain network optimality, such as minimizing the monetary cost of energy trade or the network power loss.

To address the threat to network security, one crude method would be to curtail the power generation and to reduce the power consumption. But, this is energy inefficient, and sometimes might not be feasible due to practical constraints (e.g., a charging station cannot arbitrarily reduce its power). A better method could be to properly deploy energy-storage devices and to control their power to avoid, as much as possible, the excessive power generation/consumption. In addition to the appropriate deployment and control of energy-storage devices, we can also develop an effective demand-response mechanism to shave the peak power generation/consumption.

As can be observed, when we want to preserve network security, the methods consist in properly manipulating the power in distribution networks. In fact, the same observation holds when we want to achieve certain network optimality. For example, to minimize the monetary cost of externally buying energy, the local power generation should be optimally determined for self-consumption.

Physically, it is feasible to directly manipulate the integrated local power generation and consumption, by virtue of the technological advances in power electronics and local control systems [6, 7, 8, 9, 10, 11, 12]. This facilitates a variety of works that aim to solve the operational problems in distribution networks via direct power manipulation. These works include not only the typical ones, such as regulating voltage/frequency via active/reactive power [13, 14, 15], but also the pioneering ones, such as the Commelec [16, 17] that uses multi-agent systems to manage distribution networks by explicit power setpoints.

So far, it is clear that the essence of distribution networks has been changed, due to the integration of local power generation and consumption, as well as the feasibility of direct power manipulation. Compared to the traditional counterparts, distribution networks now have both an enriched functionality resembling that in transmission networks, and an inherent peculiarity including the non-negligible resistance over reactance (R/X) ratios, phase imbalance, etc. All these factors, together, give rise to the notion of active distribution networks (ADNs).

1.2 Thesis Outline and Main Contributions

In this thesis, we study how to ensure network security and to achieve optimality in ADNs, by manipulating the power. Specifically, we consider three problems, one after another, in Chapters 2–4.

In Chapter 2: We focus on the AC power-flow problem in multi-phase ADNs, where we have the complex nodal power injections at all buses and would like to obtain the corresponding complex nodal voltages at all buses, by solving the non-linear multi-dimensional power-flow equation. This problem helps determine whether a target system power injection[1] has a corresponding system electrical state[2] that fulfills the security constraints. Due to non-linearity of the power-flow equation, the existence and uniqueness of the power-flow solution are not guaranteed globally. In fact, as reported in, e.g. [18, 19, 20, 21], the number of power-flow solutions can be zero or greater than one. With respect to this problem, our contributions are summarized as follows.

Summary of Contributions in Chapter 2

We take account of multi-phase networks, and we impose no restriction on the network topologies (i.e., they can be either radial or meshed). Both π-modelled transmission lines and complex-ratio transformers are included in our modelling.

- We show that, in practical ADNs, the power-flow problem can be expressed in a fixed-point form, called the implicit Z-bus formulation [22].
- Next, by applying the Banach fixed-point theorem [23] to the implicit Z-bus formulation of the power-flow problem, we establish explicit conditions for the existence and uniqueness of the power-flow solution. Whenever the conditions are satisfied, we guarantee the existence of a power-flow solution and analytically specify a domain in which this solution is unique. Moreover,
  - We provide an efficient iterative method for numerically computing this solution.
  - We show the non-singularity of the power-flow Jacobian at this solution.
- Last, we extend the above results to handle the various load and source connections. These connections include grounded wye, ungrounded delta, and a combination thereof.

[1] I.e., the collection of the complex nodal power injections at all buses.
[2] Represented by, e.g. the collection of the complex nodal voltages at all buses.

In Chapter 3: We take into account that the actual system power injection might be different from the target one, due to, for example, improperly modelled system dynamics, reaction delays, and renewable-energy disturbances. This motivates the "admissibility problem" that is formulated in the context of quasi-stationary analysis. Specifically, let $\mathcal{V}^\star$ collect all system electrical states that satisfy the security constraints and the non-singularity of the power-flow Jacobian, and let $\mathcal{S}^{\text{uncertain}}$ collect all possible actual system power injections. Since the system electrical state typically evolves as a continuous function of time due to the physical nature, our goal is to see whether we can ensure that the continuous path of the system electrical state remains in $\mathcal{V}^\star$, given that (i) it starts at some $\mathbf{v}^{\text{initial}} \in \mathcal{V}^\star$, and that (ii) the corresponding path of the actual system power injection belongs to $\mathcal{S}^{\text{uncertain}}$. If we can, then we say that $\mathcal{S}^{\text{uncertain}}$ is admissible for $\mathbf{v}^{\text{initial}}$. To make the description of this problem more clear, an illustration of the problem is shown in Figure 1.2. Indeed, the admissibility problem is of practical interest, as it reflects not only the common practice to indirectly control the electrical states via power injections, but also the fact that the local power generation/consumption can be volatile and inaccurately modelled by controllers.

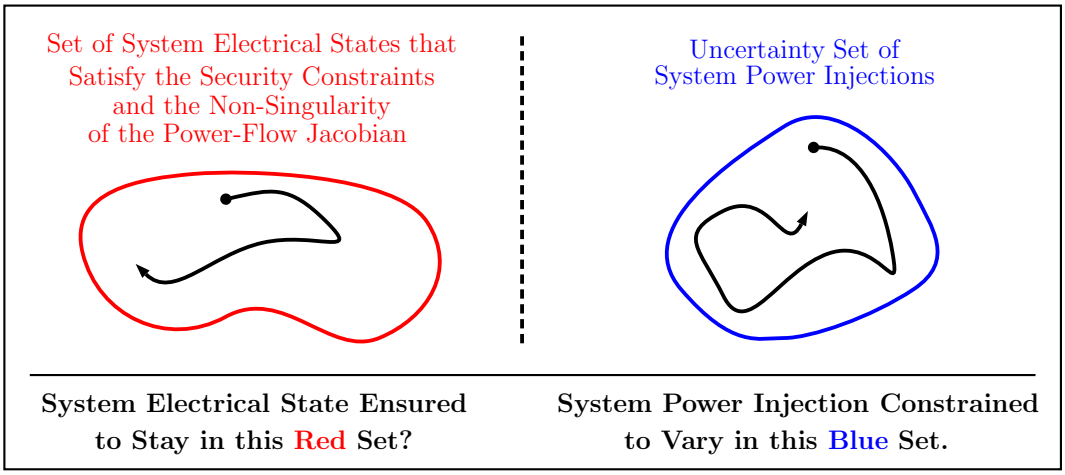

Figure 1.2 – Illustration of the admissibility problem.

To solve this problem, we contribute as follows.

Summary of Contributions in Chapter 3

- Let $\mathcal{V}$ be a set of system electrical states and $\mathcal{S}$ a set of system power injections. We introduce the auxiliary concept of "$\mathcal{V}$-control". More precisely, we say that $\mathcal{S}$ is a "domain of $\mathcal{V}$-control" if: any continuous path of the system electrical state that starts in $\mathcal{V}$ must stay in $\mathcal{V}$, as long as the corresponding path of the system power injection is constrained in $\mathcal{S}$. With the concept of $\mathcal{V}$-control, the

admissibility problem consists in whether there exists a set $\mathcal{V} \subseteq \mathcal{V}^\star$ such that (i) $\mathbf{v}^{\text{initial}} \in \mathcal{V}$, and (ii) $\mathcal{S}^{\text{uncertain}}$ is a domain of $\mathcal{V}$-control.

- We show that the "existence of a unique power-flow solution $\mathbf{v} \in \mathcal{V}$ for every $\mathbf{s} \in \mathcal{S}$" alone is neither sufficient nor necessary to ensure that $\mathcal{S}$ is a domain of $\mathcal{V}$-control.
- For $\mathcal{S}$ to be a domain of $\mathcal{V}$-control, we give additional conditions that complement the existence and uniqueness of the power-flow solution. Moreover, we propose theorems to ensure that there exists a unique power-flow solution $\mathbf{v} \in \mathcal{V}$ for every $\mathbf{s} \in \mathcal{S}$.
- Due to the real-quadratic nature of the multi-dimensional power-flow equation, we incidentally discover that local uniqueness implies non-singularity, which is the converse of the inverse function theorem.
- Using a subset of the theoretical results in this chapter, we develop a first solution method for the admissibility problem. Through numerical examples, we see that this method is tight in the sense that it almost finds the largest $\mathcal{S}^{\text{uncertain}}$ that is admissible for some given $\mathbf{v}^{\text{initial}} \in \mathcal{V}^\star$. However, we also see that the method has a relatively high computational complexity and requires large memory for data storage and manipulation. Thus, this method is not suitable for real-time applications in large networks.
- Using another subset of the theoretical results in this chapter and the results in Chapter 2, we develop a second solution method to the admissibility problem. Compared to the first solution method, this second solution method is less tight. But, it is suitable for real-time applications in large networks.

In Chapter 4: We consider an AC optimal power flow problem in multi-phase ADNs. In this problem,

- We take account of wye/delta load/source connections and incorporate the non-singularity of the power-flow Jacobian as a constraint.
- We would like to minimize an objective function that is convex in both the complex nodal voltages and the system power injection.

This problem is non-convex and NP-hard. Moreover, the existent linearization and convex-relaxation methods do not apply. With respect to the problem, our contributions are summarized below.

Summary of Contributions in Chapter 4

- We show that
  - This multi-phase optimal power flow problem might not be feasible, due to the non-singularity constraint.
  - Even if it is feasible, it might not have an optimal solution.
- We recall the results in Chapter 2 and show that, by properly restricting the system power injection to some local domains, we can obtain an explicit convex proxy for the feasible set of this problem.
- To solve this problem, we exploit the explicit convex proxy and develop a successive local exploration method. In each iteration of the method, we obtain a feasible point of this problem, by exploring around the feasible point obtained in the previous iteration. We ensure that the objective-function values at the obtained feasible points are monotonically non-increasing. For two consecutive iterations, if the difference between the objective-function values is less than some pre-specified error bound, then we terminate the method.
- We give theoretical results for the successive local exploration method. In detail,
  - We guarantee that the objective-function values at the obtained feasible points converge to a finite limit.
  - If the objective function does not explicitly contain the complex nodal voltages, then we give a-posteriori conditions to determine the local optimality for both the obtained feasible points and their limit points.

In the fifth chapter, we provide concluding remarks for the thesis.

2 Existence and Uniqueness of Power-Flow Solutions in Multi-Phase Networks

The very highest of heaven is hardly known.
Then comes what's recognized and praised.
Then comes what's feared.
Then comes what's defied.

Tao Te Ching
LAOCIUS

2.1 Introduction

Motivation

In this chapter, we study the AC power-flow problem in multi-phase distribution networks, which is an inverse problem. Specifically, given the system power injection, our goal is to obtain the corresponding system electrical state by solving the non-linear multi-dimensional power-flow equation.

Due to non-linearity, the existence and uniqueness of the power-flow solution are not guaranteed in general [18, 19, 20, 21]. Indeed, there can be zero or many power-flow solutions. Some upper bounds on the number of power-flow solutions are presented in [24, 25].

The lack of guaranteed existence and uniqueness of the power-flow solution creates an issue for network security. More precisely, when we have a target system power injection to implement, it is unknown whether this system power injection has a power-flow solution. Even if there is a power-flow solution, it might not satisfy the security constraints.

To address this issue, it is crucial to develop conditions that determine whether a

target system power injection has a guaranteed unique power-flow solution in some given domain. Moreover, as the power-flow problem might need to be repeatedly solved in real time for ADNs, we expect that

- These conditions can be verified at a low computational complexity.
- The guaranteed unique power-flow solution can be computed efficiently.

Contributions and Chapter Outline

In Sections 2.3–2.4, we consider the generic network model (i.e., with an arbitrary number of phases and an arbitrary network topology) and give the implicit Z-bus formulation of the power-flow problem.

By applying the Banach fixed-point theorem to the implicit Z-bus formulation, we establish Theorem 2.1 in Section 2.5.1, which contains explicit sufficient conditions on the existence and uniqueness of the power-flow solution. Whenever the conditions are satisfied, we guarantee the existence of a power-flow solution and analytically specify a domain in which this solution is unique.

In Theorem 2.1, we also provide an iterative method to numerically compute this solution; it converges in typically several iterations. If the iterative method is implemented by following the procedures in Remark 2.1, then each iteration has a computational complexity approximately linear in the number of buses and physical branches. Note that this per-iteration complexity is much lower than that of the widely deployed Newton-Raphson method.

We prove in Section 2.5.2 that the proposed conditions in Theorem 2.1 are better than the state of the art.

In Section 2.5.3, we give an explicit condition on the non-singularity of the power-flow Jacobian in Proposition 2.1. Using this condition, we show that the solution guaranteed by Theorem 2.1 has a non-singular power-flow Jacobian hence fulfills static voltage stability.

In Section 2.6, the above results are extended to networks with various load/source connections, including wye, delta, and a combination thereof. Specifically, we first extend the load/source model and the implicit Z-bus formulation in Sections 2.6.1–2.6.2. Then, in Section 2.6.3, we give

- Lemma 2.3 and Theorem 2.2 on the existence and uniqueness of the power-flow solution; they extend Theorem 2.1.
- Proposition 2.2 on the non-singularity of the power-flow Jacobian; it extends

Proposition 2.1.

All the proposed results are numerically validated in Section 2.7.

2.2 State of the Art

In [26], conditions for the existence and uniqueness of the solution to the "reactive power – voltage magnitude" problem are given and analyzed. Specifically, the authors decouple the power-flow equation, and consider only the non-linear relation between reactive power injections and nodal voltage magnitudes. This work is complemented by [27] that contains conditions for the existence and uniqueness of the solution to the "active power – voltage angle" problem. In both works, the authors assume that the power-flow equation can be decoupled into two separate ones, and establish all conditions on this assumption. Although the assumption is true in transmission networks, it does not hold in distribution networks. This is because the R/X ratios in distribution networks are much higher than those in transmission networks, which renders the decoupling of the power-flow equation invalid.

For balanced radial distribution networks, some asymptotic results on the existence and uniqueness of the feasible power-flow solution are given in [28], by exploiting the radial topology. There, "feasible" means that the solution belongs to some neighborhood of the zero-injection voltage profile. This result is extended to the unbalanced radial three-phase distribution networks in [29], using a similar method. In both works, the results are obtained by simply applying the limit theories. As a consequence, we do not know how to concretely determine whether a target system power injection has a unique solution. Moreover, the proofs are valid for only passive distribution networks, which do not have power sources. Therefore, the results in [28, 29] have very limited values in practical ADN applications.

Recently, the focus has been moved to fixed-point power-flow analysis, as the fixed-point theorems can be applied to guarantee the existence and uniqueness of the power-flow solution. In [30], the authors formulate the power-flow problem in balanced distribution networks as a fixed-point problem. Based on this formulation, the authors apply the Banach fixed-point theorem and obtain sufficient conditions to guarantee the existence and uniqueness of the power-flow solution. These sufficient conditions are further improved in [31]. However, as we show in Section 2.5.2 and Section 2.7, the conditions in our proposed Theorem 2.1 are better than the conditions in [30, 31]. More precisely, whenever the conditions in [30, 31] are satisfied, we have that the conditions in Theorem 2.1 are also satisfied; but the converse is not true.

In [32, 33, 34], other results on the existence and uniqueness of the power-flow solution are proposed. But these results are not of much interest in practical ADN

applications. In detail:

- The results in [32] are established for lossless networks. But, due to the relatively lower voltage level, it is inappropriate and impractical to neglect the power loss in distribution networks.
- The results in [33] do not contain sufficient information about the uniqueness of the power-flow solution. Similar to [28, 29], no method is provided to compute the guaranteed unique solution, and no domain is specified for the guaranteed uniqueness.
- The results in [34] are derived for only balanced networks that have radial topologies and equal R/X ratios in all transmission lines. Clearly, these results can hardly be applied to real-world networks.

To handle different load/source connections, the conditions in our proposed Theorem 2.1 are extended in [35]. However, compared to our extension of these conditions in Lemma 2.3 and Theorem 2.2, the conditions in [35] are weaker and apply only to networks with disjoint sets of wye and delta load/source connections.

2.3 Network Model and AC Power-Flow Equation

In this section, we describe the network model and the multi-dimensional AC power-flow equation. Specifically, we consider a distribution network that has one slack bus (indexed by 0), N PQ buses (indexed by 1,...,N), and a generic topology (i.e., either radial or meshed). The buses are physically connected through passive transmission devices, including π-modelled transmission lines and complex-ratio transformers.

First, we define the following sets to collectively express the physical buses and branches.

- $\mathcal{N} = \{0, 1, ..., N\}$,
- $\mathcal{E} = \{jk$: a transmission device exists between buses $j, k \in \mathcal{N}\}$.

Then, we denote the number of phases by N^{phase}, and let:

- $\mathbf{v}_j,\ \mathbf{i}_j,\ \mathbf{s}_j \in \mathbb{C}^{N^{\text{phase}}}$ be, respectively, the complex nodal voltage, current, and power injection at bus $j \in \mathcal{N}$, [1]

[1] For example, in three-phase networks, $N^{\text{phase}} = 3$, $\mathbf{v}_j = (v_j^a, v_j^b, v_j^c)^T$, $\mathbf{i}_j = (i_j^a, i_j^b, i_j^c)^T$, $\mathbf{s}_j = (s_j^a, s_j^b, s_j^c)^T$.

- $\mathbf{i}_{jk} \in \mathbb{C}^{N^{\text{phase}}}$ be the complex branch current entering branch $jk \in \mathcal{E}$ (i.e., from bus j to k).

According to [1, 36], passive transmission devices are typically modelled by means of longitudinal and transversal linear elements. As a consequence, for any $jk \in \mathcal{E}$, the branch current $\mathbf{i}_{jk}$ and the nodal voltages $\mathbf{v}_j$, $\mathbf{v}_k$ are linked through the following equation,

$$\mathbf{i}_{jk} = \mathbf{A}_{j,k}\mathbf{v}_j - \mathbf{C}_{j,k}\mathbf{v}_k \,, \tag{2.1}$$

where $\mathbf{A}_{j,k}$, $\mathbf{C}_{j,k} \in \mathbb{C}^{N^{\text{phase}} \times N^{\text{phase}}}$ are constant and specified by the corresponding transmission device.[2]

Next, take into account that

$$\mathbf{i}_j = \sum_{k:\ jk \in \mathcal{E}} \mathbf{i}_{jk} \,, \qquad \forall j \in \mathcal{N}. \tag{2.2}$$

By plugging (2.1) into (2.2), we obtain the linear relation between nodal currents and nodal voltages:

$$\mathbf{i}_j = \Bigg(\sum_{k:\ jk \in \mathcal{E}} \mathbf{A}_{j,k} \Bigg) \mathbf{v}_j - \sum_{k:\ jk \in \mathcal{E}} \mathbf{C}_{j,k}\mathbf{v}_k \,, \qquad \forall j \in \mathcal{N}. \tag{2.3}$$

In a more compact form, the linear relation (2.3) can be written as

$$\begin{bmatrix} \mathbf{i}_0 \\ \vdots \\ \mathbf{i}_N \end{bmatrix} = \mathbf{Y} \begin{bmatrix} \mathbf{v}_0 \\ \vdots \\ \mathbf{v}_N \end{bmatrix} \,, \tag{2.4}$$

where $\mathbf{Y}$ is the $N^{\text{phase}}(N+1)$-by-$N^{\text{phase}}(N+1)$ compound nodal admittance matrix of the network [1, 37].

Then, consider that

$$\begin{bmatrix} \mathbf{s}_0 \\ \vdots \\ \mathbf{s}_N \end{bmatrix} = \text{diag}\Bigg(\begin{bmatrix} \mathbf{v}_0 \\ \vdots \\ \mathbf{v}_N \end{bmatrix} \Bigg) \begin{bmatrix} \overline{\mathbf{i}_0} \\ \vdots \\ \overline{\mathbf{i}_N} \end{bmatrix} \,, \tag{2.5}$$

where $\text{diag}(\cdot)$ is a diagonal matrix with the entries of a vector on the main diagonal, and $\bar{\cdot}$ means the complex conjugation.

[2] To give an instance, we consider a π-modelled transmission line that connects buses j and k. Let $\mathbf{Y}^{\text{series}}$ be the series admittance between the two buses, and $\mathbf{Y}^{\text{shunt}}/2$ be the shunt admittance attached to each of the two buses. Then, we have $\mathbf{i}_{jk} = \mathbf{Y}^{\text{series}}(\mathbf{v}_j - \mathbf{v}_k) + (\mathbf{Y}^{\text{shunt}}/2)\mathbf{v}_j$. As it can be seen in this example, $\mathbf{A}_{j,k} = \mathbf{Y}^{\text{series}} + \mathbf{Y}^{\text{shunt}}/2$, and $\mathbf{C}_{j,k} = \mathbf{Y}^{\text{series}}$.

By combining (2.4) and (2.5), we obtain the following AC power-flow equation that links the nodal power injections with the nodal voltages:

$$\begin{bmatrix} \mathbf{s}_0 \\ \vdots \\ \mathbf{s}_N \end{bmatrix} = \mathrm{diag}\left(\begin{bmatrix} \mathbf{v}_0 \\ \vdots \\ \mathbf{v}_N \end{bmatrix} \right) \overline{\mathbf{Y}} \begin{bmatrix} \overline{\mathbf{v}_0} \\ \vdots \\ \overline{\mathbf{v}_N} \end{bmatrix} . \tag{2.6}$$

Note that the slack-bus voltage $\mathbf{v}_0$ and the nodal admittance matrix $\mathbf{Y}$ are both known in Equation (2.6).

2.4 Implicit Z-Bus Formulation of the Power-Flow Problem

In the conventional formulation of the AC power-flow problem, we have some given nodal power injections $\mathbf{s}_1$,...,$\mathbf{s}_N$, and we need to find the corresponding nodal voltages $\mathbf{v}_1$,...,$\mathbf{v}_N$, by solving the power-flow equation (2.6). In what follows, we give an equivalent formulation of the power-flow problem, which is called the implicit Z-bus formulation [22]. First, let us partition the nodal admittance matrix into four sub-matrices as follows. The sizes of these sub-matrices are listed in Table 2.1.

$$\mathbf{Y} = \begin{bmatrix} \mathbf{Y}_{00} & \mathbf{Y}_{0L} \\ \mathbf{Y}_{L0} & \mathbf{Y}_{LL} \end{bmatrix} . \tag{2.7}$$

$\mathbf{Y}_{00}$	$\mathbf{Y}_{0L}$	$\mathbf{Y}_{L0}$	$\mathbf{Y}_{LL}$
N^{phase}-by-N^{phase}	N^{phase}-by-$N^{\mathrm{phase}}N$	$N^{\mathrm{phase}}N$-by-N^{phase}	$N^{\mathrm{phase}}N$-by-$N^{\mathrm{phase}}N$

Table 2.1 – Sizes of sub-matrices in $\mathbf{Y}$.

Then, in accordance with the sizes of the sub-matrices, we define the following collective notations. As it can be seen, $\mathbf{v}$ fully represents the system electrical state, and $\mathbf{s}$ is the system power injection.

$$\mathbf{v} = \begin{bmatrix} \mathbf{v}_1 \\ \vdots \\ \mathbf{v}_N \end{bmatrix} \in \mathbb{C}^{N^{\mathrm{phase}}N}, \qquad \mathbf{i} = \begin{bmatrix} \mathbf{i}_1 \\ \vdots \\ \mathbf{i}_N \end{bmatrix} \in \mathbb{C}^{N^{\mathrm{phase}}N}, \qquad \mathbf{s} = \begin{bmatrix} \mathbf{s}_1 \\ \vdots \\ \mathbf{s}_N \end{bmatrix} \in \mathbb{C}^{N^{\mathrm{phase}}N} . \tag{2.8}$$

With the above partition and notations, the linear relation (2.4) and the AC power-flow

equation (2.6) can be written in the following forms.

$$\mathbf{i}_0 = \mathbf{Y}_{00}\mathbf{v}_0 + \mathbf{Y}_{0L}\mathbf{v}\,, \tag{2.9a}$$
$$\mathbf{i} = \mathbf{Y}_{L0}\mathbf{v}_0 + \mathbf{Y}_{LL}\mathbf{v}\,. \tag{2.9b}$$

$$\mathbf{s}_0 = \mathrm{diag}(\mathbf{v}_0)\left(\overline{\mathbf{Y}_{00}}\,\overline{\mathbf{v}_0} + \overline{\mathbf{Y}_{0L}}\,\overline{\mathbf{v}}\right)\,, \tag{2.10a}$$
$$\mathbf{s} = \mathrm{diag}(\mathbf{v})\left(\overline{\mathbf{Y}_{L0}}\,\overline{\mathbf{v}_0} + \overline{\mathbf{Y}_{LL}}\,\overline{\mathbf{v}}\right)\,. \tag{2.10b}$$

Here, observe that if all the nodal voltages are non-zero, then (2.10b) is equivalent to

$$\mathbf{Y}_{LL}\mathbf{v} = -\mathbf{Y}_{L0}\mathbf{v}_0 + \mathrm{diag}(\overline{\mathbf{v}})^{-1}\overline{\mathbf{s}}\,. \tag{2.11}$$

Moreover, as shown in [38, 39, 40, 41], $\mathbf{Y}_{LL}$ is invertible in practical distribution networks.[3] Therefore, we have

$$\mathbf{v} = \mathbf{w} + \mathbf{Y}_{LL}^{-1}\mathrm{diag}(\overline{\mathbf{v}})^{-1}\overline{\mathbf{s}}\,, \tag{2.12}$$

with

$$\mathbf{w} = -\mathbf{Y}_{LL}^{-1}\mathbf{Y}_{L0}\mathbf{v}_0\,. \tag{2.13}$$

Here, it is worth noticing that

- $\mathbf{w}$ is the zero-injection voltage profile of the network.
- (2.10b) can be expressed as

  $$\mathbf{s} = \mathbf{F}(\mathbf{v})\,, \tag{2.14}$$

  where

  $$\mathbf{F}(\mathbf{v}) = \mathrm{diag}(\mathbf{v})\overline{\mathbf{Y}_{LL}}(\overline{\mathbf{v}} - \overline{\mathbf{w}}) \tag{2.15}$$

  is the continuously differentiable function that maps a system electrical state, $\mathbf{v}$, to its corresponding system power injection.
- (2.12) is a direct result of the superposition theorem and can be written as

  $$\mathbf{v} = \mathbf{G}_{\mathbf{s}}(\mathbf{v})\,, \tag{2.16}$$

[3] For completeness, a proof is provided in Appendix 2.A.

with

$$\mathbf{G}_{\mathbf{s}}(\mathbf{v}) = \mathbf{w} + \mathbf{Y}_{LL}^{-1}\mathrm{diag}(\overline{\mathbf{v}})^{-1}\overline{\mathbf{s}}\,. \tag{2.17}$$

Using (2.16), we give the implicit Z-bus formulation of the power-flow problem as follows.

Problem 2.1 (*Implicit Z-Bus Formulation*)

Given the target system power injection $\mathbf{s}$*, solve equation* (2.16) *to find the corresponding system electrical state* $\mathbf{v}$*.*

2.5 Application of the Banach Fixed-Point Theorem to Power-Flow Solvability

2.5.1 Explicit Conditions to Guarantee the Existence and Uniqueness of the Power-Flow Solution

Observe that Equation (2.16) has a fixed-point form. According to the Banach fixed-point theorem [23], if $\mathbf{G}_{\mathbf{s}}$ is a contraction mapping (i.e., a self-mapping with contraction property) in some domain $\mathcal{D}$, then we have: in this domain $\mathcal{D}$, there exists a unique $\mathbf{v}$ that satisfies $\mathbf{v} = \mathbf{G}_{\mathbf{s}}(\mathbf{v})$. Moreover, this $\mathbf{v}$ can be computed through the iterative method

$$\mathbf{v}^{(k+1)} = \mathbf{G}_{\mathbf{s}}(\mathbf{v}^{(k)})\,, \tag{2.18}$$

with arbitrary $\mathbf{v}^{(0)} \in \mathcal{D}$. Therefore, in order to solve Problem 2.1, we need to find a proper domain, in which $\mathbf{G}_{\mathbf{s}}$ is a contraction mapping.

For this purpose, we assume the knowledge of a reference system electrical state $\hat{\mathbf{v}}$ and its corresponding system power injection $\hat{\mathbf{s}} = \mathbf{F}(\hat{\mathbf{v}})$. This reference system electrical state $\hat{\mathbf{v}}$ can be interpreted as the present one that is typically obtained through measurement units and state estimation processes [42,43,44,45,46]. In the cases where there is no knowledge of the present system electrical state, a trivial choice for $\hat{\mathbf{v}},\ \hat{\mathbf{s}}$ is $\mathbf{w},\ \mathbf{0}$.

With the knowledge of $\hat{\mathbf{v}}$ and $\hat{\mathbf{s}}$, we want to find a domain that contains $\hat{\mathbf{v}}$, in which $\mathbf{G}_{\mathbf{s}}$ is a contraction mapping for $\mathbf{s}$ around $\hat{\mathbf{s}}$. In other words, we want to explore the power-flow solvability in some neighbourhoods of $\hat{\mathbf{v}},\ \hat{\mathbf{s}}$. To do so, we first propose a lemma for the self-mapping property of $\mathbf{G}_{\mathbf{s}}$, which uses the notations in Table 2.2.[4]

[4]For any M-by-K matrix $\mathbf{A}$, $\|\mathbf{A}\|_\infty$ means the induced ℓ_∞ norm, which is defined as $\|\mathbf{A}\|_\infty = \max_{1\le m\le M}\sum_{k=1}^{K}|(\mathbf{A})_{m,k}|$.

The corresponding proof can be found in Appendix 2.B.

Notation	Definition
$\mathbf{W}$	$\mathrm{diag}(\mathbf{w})$
$\xi(\mathbf{s})$	$\left\|\mathbf{W}^{-1}\mathbf{Y}_{LL}^{-1}\overline{\mathbf{W}}^{-1}\mathrm{diag}(\bar{\mathbf{s}})\right\|_\infty$
$\alpha(\mathbf{v})$	$\min_j \dfrac{\lvert(\mathbf{v})_j\rvert}{\lvert(\mathbf{w})_j\rvert}$
$\rho^\ddagger(\mathbf{v})$	$\dfrac{1}{2}\left(\alpha(\mathbf{v}) - \dfrac{\xi(\mathbf{F}(\mathbf{v}))}{\alpha(\mathbf{v})}\right)$
$\rho^\dagger(\mathbf{v},\tilde{\mathbf{s}})$	$\rho^\ddagger(\mathbf{v}) - \sqrt{\left(\rho^\ddagger(\mathbf{v})\right)^2 - \xi\left(\tilde{\mathbf{s}} - \mathbf{F}(\mathbf{v})\right)}$

Table 2.2 – Notations for the proof of contraction mapping.

Lemma 2.1

Let $\mathbf{s}$ *be the target system power injection,* $\hat{\mathbf{v}}$ *represent the reference system electrical state, and* $\hat{\mathbf{s}} = \mathbf{F}(\hat{\mathbf{v}})$ *be the reference system power injection.*

Suppose that $\hat{\mathbf{v}}$ *and* $\mathbf{s} - \hat{\mathbf{s}}$ *satisfy*

$$\rho^\ddagger(\hat{\mathbf{v}}) > 0\,, \tag{2.19}$$

$$\xi(\mathbf{s} - \hat{\mathbf{s}}) < \left(\rho^\ddagger(\hat{\mathbf{v}})\right)^2. \tag{2.20}$$

Then, $\mathbf{G}_\mathbf{s}$ *is a self-mapping in*

$$\mathcal{D}_\rho(\hat{\mathbf{v}}) = \left\{\mathbf{v} : \lvert(\mathbf{v})_j - (\hat{\mathbf{v}})_j\rvert \le \rho\lvert(\mathbf{w})_j\rvert,\ j = 1, ..., N^{\mathrm{phase}}N\right\}, \tag{2.21}$$

for $\rho \in \left[\rho^\dagger(\hat{\mathbf{v}},\mathbf{s}), \rho^\ddagger(\hat{\mathbf{v}})\right]$.

Note that, in Lemma 2.1, we specify a lower bound $\rho^\dagger(\hat{\mathbf{v}},\mathbf{s})$ for ρ that depends on the target system power injection $\mathbf{s}$. This lower bound will be used later to provide a better localization for the power-flow solution. Also, notice that ξ is a norm and $\xi(\mathbf{s} - \hat{\mathbf{s}})$ is a distance between the system power injections $\mathbf{s}$, $\hat{\mathbf{s}}$. This is because

- $\xi(\kappa\mathbf{s}) = \lvert\kappa\rvert\xi(\mathbf{s})$ for any $\kappa \in \mathbb{C}$,

- $\xi(\mathbf{s}+\mathbf{s}') \leq \xi(\mathbf{s}) + \xi(\mathbf{s}')$ due to the triangle inequality of the induced matrix norm,
- $\xi(\mathbf{s}) = 0 \;\Rightarrow\; \mathbf{W}^{-1}\mathbf{Y}_{LL}^{-1}\overline{\mathbf{W}}^{-1}\mathrm{diag}(\overline{\mathbf{s}}) = \mathbf{0} \;\Rightarrow\; \mathbf{s} = \mathbf{0}$.

Next, we proceed and propose a lemma for the contraction property of $\mathbf{G}_{\mathbf{s}}$. The proof of this lemma is given in Appendix 2.C.

Lemma 2.2

Let $\mathbf{s}$ *be the target system power injection,* $\hat{\mathbf{v}}$ *represent the reference system electrical state, and* $\hat{\mathbf{s}} = \mathbf{F}(\hat{\mathbf{v}})$ *be the reference system power injection.*

Suppose that $\hat{\mathbf{v}}$ *and* $\mathbf{s} - \hat{\mathbf{s}}$ *satisfy conditions* (2.19)–(2.20)*. Then,* $\mathbf{G}_{\mathbf{s}}$ *is a contraction mapping in* $\mathcal{D}_\rho(\hat{\mathbf{v}})$*, for* $\rho \in \left[\rho^\dagger(\hat{\mathbf{v}}, \mathbf{s}), \rho^\ddagger(\hat{\mathbf{v}})\right)$.

Using Lemma 2.2, we have the following theorem that comes naturally from the Banach fixed-point theorem. To facilitate the comprehension of this theorem, we provide a graphical illustration in Figure 2.1.

Theorem 2.1

Let $\mathbf{s}$ *be the target system power injection,* $\hat{\mathbf{v}}$ *represent the reference system electrical state, and* $\hat{\mathbf{s}} = \mathbf{F}(\hat{\mathbf{v}})$ *be the reference system power injection.*

Suppose that $\hat{\mathbf{v}}$ *and* $\mathbf{s} - \hat{\mathbf{s}}$ *satisfy conditions* (2.19)–(2.20)*. Then, in domain* $\mathcal{D}_\rho(\hat{\mathbf{v}})$ *with* $\rho = \rho^\ddagger(\hat{\mathbf{v}})$*, there exists a unique solution* $\mathbf{v}$ *to* (2.16)*. Moreover, this solution is located in the smaller domain* $\mathcal{D}_\rho(\hat{\mathbf{v}})$ *with* $\rho = \rho^\dagger(\hat{\mathbf{v}}, \mathbf{s})$*, and can be computed through the iterative method* (2.18) *with arbitrary* $\mathbf{v}^{(0)} \in \mathcal{D}_\rho(\hat{\mathbf{v}})$*,* $\rho = \rho^\ddagger(\hat{\mathbf{v}})$.

As can be seen in Theorem 2.1, $\mathcal{D}_\rho(\hat{\mathbf{v}})$ with $\rho = \rho^\ddagger(\hat{\mathbf{v}})$ depends only on the choice of the reference system electrical state $\hat{\mathbf{v}}$, whereas $\mathcal{D}_\rho(\hat{\mathbf{v}})$ with $\rho = \rho^\dagger(\hat{\mathbf{v}}, \mathbf{s})$ depends on both $\hat{\mathbf{v}}$ and the target system power injection $\mathbf{s}$. If the distance $\xi(\mathbf{s} - \hat{\mathbf{s}})$ decreases, then the value of $\rho^\dagger(\hat{\mathbf{v}}, \mathbf{s})$ also decreases. When the distance $\xi(\mathbf{s} - \hat{\mathbf{s}})$ becomes 0 (i.e., $\mathbf{s} = \hat{\mathbf{s}}$), we have that $\rho^\dagger(\hat{\mathbf{v}}, \mathbf{s})$ becomes 0 hence the guaranteed solution $\mathbf{v}$ becomes $\hat{\mathbf{v}}$.

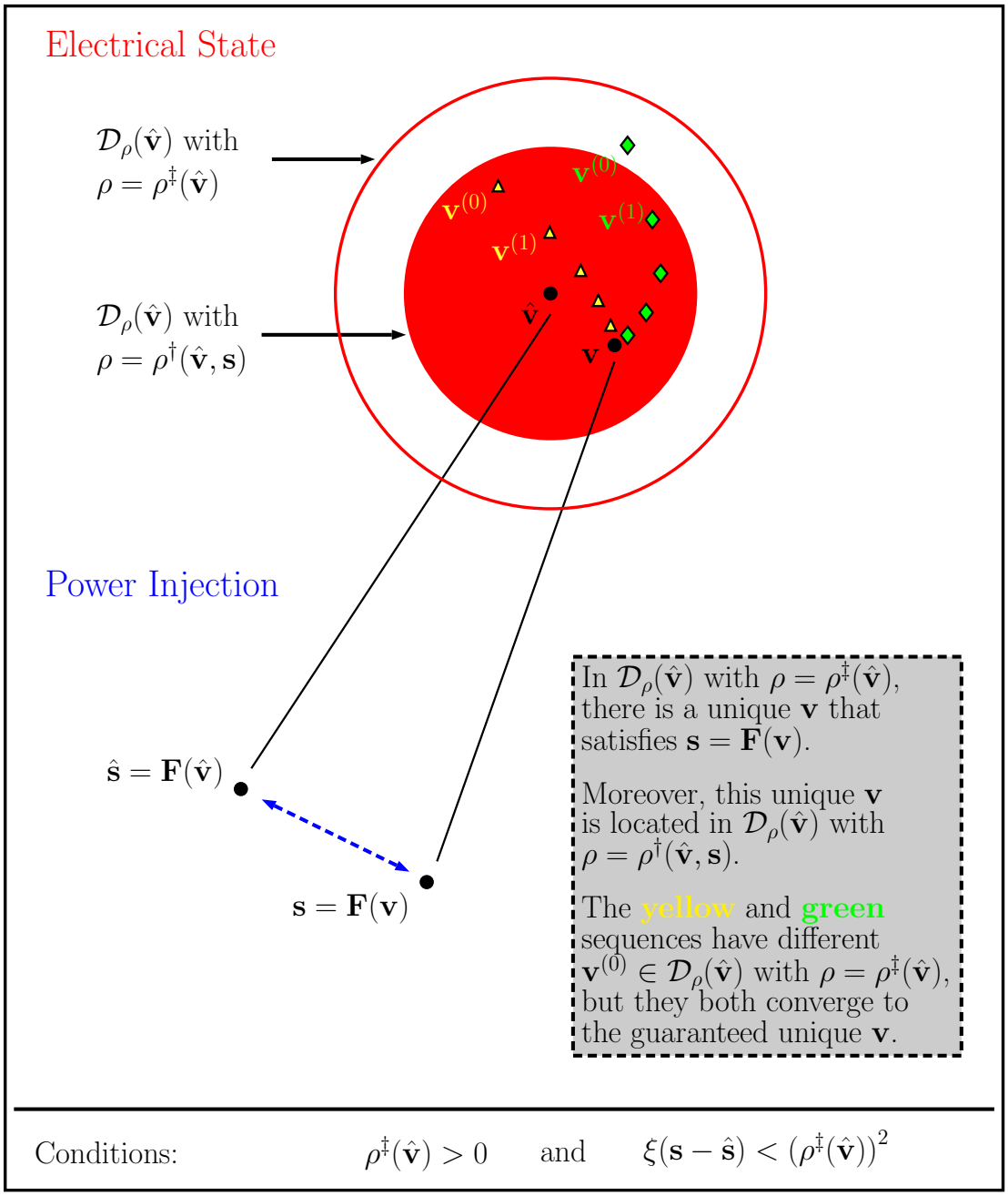

Figure 2.1 – Illustration of Theorem 2.1.

Remark 2.1 (*Computational Complexity Related to Theorem 2.1*)

1. *The complexity of verifying the conditions* (2.19)–(2.20) *is quadratic in* $N^{\text{phase}}N$. *Indeed, when computing the values of* $\xi(\hat{\mathbf{s}})$ *and* $\xi(\mathbf{s}-\hat{\mathbf{s}})$, *we need to perform* $(N^{\text{phase}}N)^2$ *multiplications and additions due to the fact that the constant matrix* $\mathbf{W}^{-1}\mathbf{Y}_{LL}^{-1}\overline{\mathbf{W}}^{-1}$ *is a full matrix.*

2. *The complexity of obtaining* $\mathbf{v}^{(k+1)}$ *in* (2.18) *is quadratic in* $N^{\text{phase}}N$ *if we directly compute* $\mathbf{w}+\mathbf{Y}_{LL}^{-1}\text{diag}(\overline{\mathbf{v}^{(k)}})^{-1}\overline{\mathbf{s}}$. *This is because* $\mathbf{Y}_{LL}^{-1}$ *is a full matrix. However, we observe that the matrix* $\mathbf{Y}_{LL}$ *is sparse in practice, since the real-world distribution networks are typically radial or weakly meshed. By virtue of this observation, the complexity of obtaining* $\mathbf{v}^{(k+1)}$ *can be considerably reduced by means of LU decomposition with complete Markowitz pivoting [47, 48, 49]. In detail, we first apply Gaussian elimination with Markowitz pivoting to* $\mathbf{Y}_{LL}$, *which identifies permutation matrices* $\mathbf{P}$, $\mathbf{Q}$, *lower-triangular matrix* $\mathbf{L}$, *and upper-triangular matrix* $\mathbf{U}$ *such that*

$$\mathbf{P}\mathbf{Y}_{LL}\mathbf{Q}=\mathbf{L}\mathbf{U}\,. \tag{2.22}$$

Due to the merit of Markowitz pivoting, the number of non-zero entries in $\mathbf{L}$ *and* $\mathbf{U}$ *is usually only a few more than that in* $\mathbf{Y}_{LL}$. *With the matrices* $\mathbf{P}$, $\mathbf{Q}$, $\mathbf{L}$, *and* $\mathbf{U}$, *we can obtain* $\mathbf{v}^{(k+1)}$ *by sequentially solving the following equations, which involves mainly permutations and forward/backward substitutions.*

$$\begin{aligned}\mathbf{L}\mathbf{d}=&\mathbf{P}\text{diag}(\overline{\mathbf{v}^{(k)}})^{-1}\overline{\mathbf{s}} &\text{(2.23a)}\\ \mathbf{U}\mathbf{g}=&\mathbf{d} &\text{(2.23b)}\\ \mathbf{h}=&\mathbf{Q}\mathbf{g} &\text{(2.23c)}\\ \mathbf{v}^{(k+1)}=&\mathbf{h}+\mathbf{w} &\text{(2.23d)}\end{aligned}$$

In this way, if we pre-store the matrices $\mathbf{P}$, $\mathbf{Q}$, $\mathbf{L}$, $\mathbf{U}$, *then the complexity of obtaining* $\mathbf{v}^{(k+1)}$ *is usually linear in* $N^{\text{phase}}N$ *and* $N^{\text{phase}}\text{card}(\mathcal{E})$, *where* $\text{card}(\cdot)$ *means the cardinality of a set.*

2.5.2 Comparison with State of the Art

In this section, we compare Theorem 2.1 with the results in [30, 31]. To the best of our knowledge, these results are the state of the art on the existence and uniqueness of AC power-flow solutions. Specifically,

- In [30], the authors propose the following sufficient condition on the existence

of a unique AC power-flow solution in distribution networks[5]: $\exists p \in [1,\infty],\ q = p/(p-1)$ such that

$$\left\| \mathbf{W}^{-1}\mathbf{Y}_{LL}^{-1}\overline{\mathbf{W}}^{-1} \right\|_p^* \|\mathbf{s}\|_q < 0.25\,, \tag{2.24}$$

where, for any matrix $\mathbf{A}$, $\|\mathbf{A}\|_p^* = \max_m \|\mathrm{Row}_m(\mathbf{A})\|_p$. However, they do not analytically specify the domain in which the guaranteed solution is unique.

- In [31], the sufficient condition of [30] is improved as follows: $\exists p \in [1,\infty],\ q = p/(p-1)$ and real invertible diagonal matrix $\mathbf{\Lambda}$ such that

$$\left\| \mathbf{W}^{-1}\mathbf{Y}_{LL}^{-1}\overline{\mathbf{W}}^{-1}\mathbf{\Lambda} \right\|_p^* \|\mathbf{\Lambda}^{-1}\mathbf{s}\|_q < 0.25\,. \tag{2.25}$$

  Same as in [30], the authors do not analytically specify the domain in which the guaranteed solution is unique.

As there is no assumption of non-trivial $\hat{\mathbf{v}}$ and $\hat{\mathbf{s}}$ in [30,31], we present below a corollary in order to make a fair comparison. This corollary is straightforwardly obtained by choosing $\hat{\mathbf{v}} = \mathbf{w}$ and $\hat{\mathbf{s}} = \mathbf{0}$ in our Theorem 2.1. Later, in Section 2.7, we give numerical examples where Theorem 2.1 can be applied to guarantee the existence and uniqueness of the power-flow solution, but this corollary cannot. In other words, Theorem 2.1 is strictly stronger than the corollary.

Corollary 2.1

Suppose that the target system power injection $\mathbf{s}$ *satisfies*

$$\xi(\mathbf{s}) < 0.25\,. \tag{2.26}$$

Then, in domain $\mathcal{D}_\rho(\mathbf{w})$ *with* $\rho = 0.5$*, there exists a unique solution* $\mathbf{v}$ *to* (2.16)*. Moreover, this solution is located in the smaller domain* $\mathcal{D}_\rho(\mathbf{w})$ *with* $\rho = \rho^\dagger(\mathbf{w},\mathbf{s})$*, and can be computed through the iterative method* (2.18) *with arbitrary* $\mathbf{v}^{(0)} \in \mathcal{D}_\rho(\mathbf{w})$*,* $\rho = 0.5$ *.*

[5] Although the original derivation in [30] is based on balanced networks, the obtained result has the same mathematical form for more general unbalanced networks.

Now, we compare Corollary 2.1 with the results in [30, 31]. Specifically, we show that $\xi(\mathbf{s}) < 0.25$ whenever (2.25) is true. First, observe that

$$\begin{aligned}\xi(\mathbf{s}) &= \left\|\mathbf{W}^{-1}\mathbf{Y}_{LL}^{-1}\overline{\mathbf{W}}^{-1}\mathrm{diag}(\overline{\mathbf{s}})\right\|_\infty \\ &= \left\|\left(\mathbf{W}^{-1}\mathbf{Y}_{LL}^{-1}\overline{\mathbf{W}}^{-1}\mathbf{\Lambda}\right)\left(\mathbf{\Lambda}^{-1}\mathrm{diag}(\overline{\mathbf{s}})\right)\right\|_\infty \\ &= \max_m \sum_n \left|\left(\mathbf{W}^{-1}\mathbf{Y}_{LL}^{-1}\overline{\mathbf{W}}^{-1}\mathbf{\Lambda}\right)_{m,n}\right|\left|\left(\mathbf{\Lambda}^{-1}\mathbf{s}\right)_n\right|. \end{aligned} \tag{2.27}$$

Then, for any m, we apply the Holder's inequality and obtain

$$\begin{aligned}&\sum_n \left|\left(\mathbf{W}^{-1}\mathbf{Y}_{LL}^{-1}\overline{\mathbf{W}}^{-1}\mathbf{\Lambda}\right)_{m,n}\right|\left|\left(\mathbf{\Lambda}^{-1}\mathbf{s}\right)_n\right| \\ \leq &\left\|\mathrm{Row}_m\left(\mathbf{W}^{-1}\mathbf{Y}_{LL}^{-1}\overline{\mathbf{W}}^{-1}\mathbf{\Lambda}\right)\right\|_p\left\|\mathbf{\Lambda}^{-1}\mathbf{s}\right\|_q \\ \leq &\left\|\mathbf{W}^{-1}\mathbf{Y}_{LL}^{-1}\overline{\mathbf{W}}^{-1}\mathbf{\Lambda}\right\|_p^*\left\|\mathbf{\Lambda}^{-1}\mathbf{s}\right\|_q. \end{aligned} \tag{2.28}$$

By combination of (2.27) and (2.28), we have

$$\xi(\mathbf{s}) \leq \left\|\mathbf{W}^{-1}\mathbf{Y}_{LL}^{-1}\overline{\mathbf{W}}^{-1}\mathbf{\Lambda}\right\|_p^*\left\|\mathbf{\Lambda}^{-1}\mathbf{s}\right\|_q, \tag{2.29}$$

which completes our proof.

Later, in Section 2.7, we give numerical examples where Corollary 2.1 can be applied to guarantee the existence and uniqueness of the power-flow solution, but the results in [30, 31] cannot. In other words, Corollary 2.1 is, in fact, strictly stronger than the results in [30, 31] (i.e., the condition in Corollary 2.1 is strictly weaker than the counterparts in [30, 31]).

2.5.3 Non-Singularity of the Power-Flow Jacobian at the Guaranteed Solutions

In what follows, we give results on the non-singularity of the power-flow Jacobian.

First, let $\mathbf{J}_\mathbf{F}(\mathbf{v})$ denote the Jacobian of $\mathbf{F}$ evaluated at $\mathbf{v}$. As $\mathbf{F}$ is the continuously differentiable function that maps a system electrical state into its corresponding system power injection, we have that $\mathbf{J}_\mathbf{F}$ is the power-flow Jacobian [1, 50]. According to the mathematical expression of $\mathbf{F}$ in equation (2.15), the action of $\mathbf{J}_\mathbf{F}(\mathbf{v})$ on arbitrary $\mathbf{d} \in \mathbb{C}^{N^{\mathrm{phase}}N}$ is as follows.

$$\mathbf{J}_\mathbf{F}(\mathbf{v})\cdot\mathbf{d} = \mathrm{diag}\left(\overline{\mathbf{Y}_{LL}}(\overline{\mathbf{v}} - \overline{\mathbf{w}})\right)\mathbf{d} + \mathrm{diag}(\mathbf{v})\overline{\mathbf{Y}_{LL}\mathbf{d}}\,. \tag{2.30}$$

Then, we give the following proposition on the non-singularity of $\mathbf{J_F}$. The corresponding proof can be found in Appendix 2.D. Note that

- This proposition contains an explicit condition $\rho^{\ddagger}(\mathbf{v}) > 0$ on the non-singularity of the power-flow Jacobian at $\mathbf{v}$.
- In general, the existence and uniqueness do not imply non-singularity. Here, we have this proposition because the power-flow problem has a real-quadratic nature in rectangular coordinates.

.

Proposition 2.1

In Theorem 2.1,

1. *The satisfaction of $\rho^{\ddagger}(\hat{\mathbf{v}}) > 0$ implies that $\mathbf{J_F}(\hat{\mathbf{v}})$ is non-singular.*
2. *Moreover, in domain $\mathcal{D}_{\rho}(\hat{\mathbf{v}})$ with $\rho = \rho^{\ddagger}(\hat{\mathbf{v}})$, the guaranteed unique solution $\mathbf{v}$ satisfies $\rho^{\ddagger}(\mathbf{v}) > 0$, which implies that $\mathbf{J_F}(\mathbf{v})$ is non-singular.*

According to [51,52,53], the non-singularity of the power-flow Jacobian represents a sufficient condition for the static voltage stability of the operating point. This means that the guaranteed unique solution $\mathbf{v}$ in Theorem 2.1 satisfies the static voltage stability.

Remark 2.2 (*Relation Between Theorem 2.1 and the Inverse Function Theorem [54]*)

On the one hand, the proposed Theorem 2.1 is consistent with the inverse function theorem, since the condition (2.19) *in Theorem 2.1 is essentially a requirement for $\hat{\mathbf{v}}$ to have a non-singular power-flow Jacobian.*

On the other hand, Theorem 2.1 and the inverse function theorem give different amounts of information. Specifically,

- *In the inverse function theorem, the non-singular Jacobian at $\hat{\mathbf{v}}$ implies that there exists a neighborhood $\mathcal{U}_v$ of $\hat{\mathbf{v}}$ and a neighborhood $\mathcal{U}_s$ of $\hat{\mathbf{s}} = \mathbf{F}(\hat{\mathbf{v}})$ such that $\mathbf{F}$ maps $\mathcal{U}_v$ bijectively to $\mathcal{U}_s$. But, the neighborhoods $\mathcal{U}_v, \mathcal{U}_s$ do not have explicit forms and might not have bounded radii.*
- *By contrast, in Theorem 2.1, we explicitly specify a set $\left\{\mathbf{s} : \xi(\mathbf{s} - \hat{\mathbf{s}}) < \left(\rho^{\ddagger}(\hat{\mathbf{v}})\right)^2\right\}$ such that, for every system power injection in this set, there exists a unique solution in $\mathcal{D}_{\rho}(\hat{\mathbf{v}}),\ \rho = \rho^{\ddagger}(\hat{\mathbf{v}})$.*

2.6 Extension of the Proposed Results to Networks with Various Load and Source Connections

2.6.1 Details of Connections and Augmentation of the Multi-Dimensional Power-Flow Equation

In this section, we make an extension of the modeling in Section 2.5, by considering different load/source connections. Specifically, these connections include wye, delta, and a combination thereof. To cover the most general cases, the extension is formulated in three-phase networks, i.e., $N^{\text{phase}} = 3$.

First, we show the wye and delta connections in Figure 2.2.

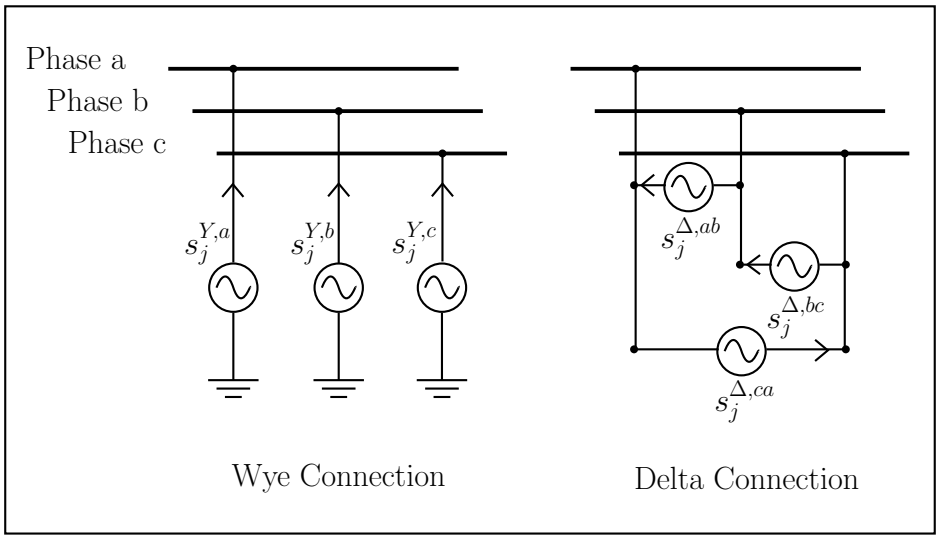

Figure 2.2 – Illustration of wye and delta connections.

Then, let us introduce some new notations:

- $\mathbf{s}_j^Y = \left(s_j^{Y,a}, s_j^{Y,b}, s_j^{Y,c}\right)^T \in \mathbb{C}^3$ is the power injection of the wye-connected load/-source at bus j,
- $\mathbf{s}_j^\Delta = \left(s_j^{\Delta,ab}, s_j^{\Delta,bc}, s_j^{\Delta,ca}\right)^T \in \mathbb{C}^3$ is the power injection of the delta-connected load/source at bus j,
- $\mathbf{i}_j^\Delta = \left(i_j^{\Delta,ab}, i_j^{\Delta,bc}, i_j^{\Delta,ca}\right)^T \in \mathbb{C}^3$ is the phase-to-phase current for the delta-connected load/source at bus j, [6]

[6] $i_j^{\Delta,ab}$ means the current from phase b to phase a.

- $\mathbf{s}^Y = \left(\left(\mathbf{s}_1^Y\right)^T, ..., \left(\mathbf{s}_N^Y\right)^T\right)^T \in \mathbb{C}^{3N}$, $\mathbf{s}^\Delta = \left(\left(\mathbf{s}_1^\Delta\right)^T, ..., \left(\mathbf{s}_N^\Delta\right)^T\right)^T \in \mathbb{C}^{3N}$, and $\mathbf{i}^\Delta = \left(\left(\mathbf{i}_1^\Delta\right)^T, ..., \left(\mathbf{i}_N^\Delta\right)^T\right)^T \in \mathbb{C}^{3N}$ are, respectively, the vectors that collect $\mathbf{s}_j^Y$, $\mathbf{s}_j^\Delta$, $\mathbf{i}_j^\Delta$ for all $j \in \mathcal{N} \setminus \{0\}$,

- $\mathbf{T} \in \mathbb{R}^{3\times 3}$ and $\mathbf{H} \in \mathbb{R}^{3N\times 3N}$ are auxiliary constant matrices, defined as follows.

$$\mathbf{T} = \begin{bmatrix} 1 & -1 & 0 \\ 0 & 1 & -1 \\ -1 & 0 & 1 \end{bmatrix}, \qquad \mathbf{H} = \begin{bmatrix} \mathbf{T} & & \\ & \ddots & \\ & & \mathbf{T} \end{bmatrix}. \tag{2.31}$$

With the above notations, we have the following equations for each bus $j \in \mathcal{N} \setminus \{0\}$.

$$\mathbf{s}_j = \mathbf{s}_j^Y + \mathrm{diag}(\mathbf{v}_j)\mathbf{T}^T\overline{\mathbf{i}_j^\Delta}\,, \tag{2.32}$$

$$\mathbf{s}_j^\Delta = \mathrm{diag}(\mathbf{T}\mathbf{v}_j)\overline{\mathbf{i}_j^\Delta}\,. \tag{2.33}$$

These equations can be collectively expressed as follows.

$$\mathbf{s} = \mathbf{s}^Y + \mathrm{diag}(\mathbf{v})\mathbf{H}^T\overline{\mathbf{i}^\Delta}\,, \tag{2.34}$$

$$\mathbf{s}^\Delta = \mathrm{diag}(\mathbf{H}\mathbf{v})\overline{\mathbf{i}^\Delta}\,. \tag{2.35}$$

Since $\mathbf{s} = \mathrm{diag}(\mathbf{v})\overline{\mathbf{Y}_{LL}}(\overline{\mathbf{v}} - \overline{\mathbf{w}})$, Equation (2.34) can be re-organized as

$$\mathbf{s}^Y = \mathrm{diag}(\mathbf{v})\overline{\mathbf{Y}_{LL}}(\overline{\mathbf{v}} - \overline{\mathbf{w}}) - \mathrm{diag}(\mathbf{v})\mathbf{H}^T\overline{\mathbf{i}^\Delta}\,. \tag{2.36}$$

Notice that (2.35)–(2.36) together define an augmentation of the multi-dimensional power-flow equation in this network. Moreover, $\begin{bmatrix}\mathbf{v}\\ \mathbf{i}^\Delta\end{bmatrix}$ represents the augmented system electrical state, and $\begin{bmatrix}\mathbf{s}^Y\\ \mathbf{s}^\Delta\end{bmatrix}$ is the augmented system power injection. To ease the exposition, we enclose (2.35)–(2.36) in the following form.

$$\mathbf{s}^{Y,\Delta} = \begin{bmatrix}\mathbf{s}^Y\\ \mathbf{s}^\Delta\end{bmatrix}, \qquad \mathbf{s}^{Y,\Delta} = \mathbf{F}^{Y,\Delta}\left(\mathbf{v}, \mathbf{i}^\Delta\right). \tag{2.37}$$

2.6.2 Extended Implicit Z-Bus Formulation of the Power-Flow Problem

Assume that all the nodal voltages are non-zero, then (2.36) can be equivalently written as

$$\mathbf{Y}_{LL}(\mathbf{v}-\mathbf{w}) = \mathrm{diag}(\overline{\mathbf{v}})^{-1}\overline{\mathbf{s}^{Y}} + \mathbf{H}^{T}\mathbf{i}^{\Delta}\,. \tag{2.38}$$

Furthermore, assume that all the entries in vector $\mathbf{Hv}$ are non-zero, which is true in practice. Then, (2.35) is equivalent to

$$\mathbf{i}^{\Delta} = \mathrm{diag}(\mathbf{H}\overline{\mathbf{v}})^{-1}\overline{\mathbf{s}^{\Delta}}\,. \tag{2.39}$$

By plugging (2.39) into (2.38), we obtain

$$\mathbf{Y}_{LL}(\mathbf{v}-\mathbf{w}) = \mathrm{diag}(\overline{\mathbf{v}})^{-1}\overline{\mathbf{s}^{Y}} + \mathbf{H}^{T}\mathrm{diag}(\mathbf{H}\overline{\mathbf{v}})^{-1}\overline{\mathbf{s}^{\Delta}}\,. \tag{2.40}$$

Since $\mathbf{Y}_{LL}$ is invertible, there is

$$\mathbf{v} = \mathbf{w} + \mathbf{Y}_{LL}^{-1}\left(\mathrm{diag}(\overline{\mathbf{v}})^{-1}\overline{\mathbf{s}^{Y}} + \mathbf{H}^{T}\mathrm{diag}(\mathbf{H}\overline{\mathbf{v}})^{-1}\overline{\mathbf{s}^{\Delta}}\right). \tag{2.41}$$

Observe that equation (2.41) is an extension of (2.12), and can be written as

$$\mathbf{v} = \mathbf{G}_{\mathbf{s}^{Y,\Delta}}(\mathbf{v})\,, \tag{2.42}$$

where

$$\mathbf{G}_{\mathbf{s}^{Y,\Delta}}(\mathbf{v}) = \mathbf{w} + \mathbf{Y}_{LL}^{-1}\left(\mathrm{diag}(\overline{\mathbf{v}})^{-1}\overline{\mathbf{s}^{Y}} + \mathbf{H}^{T}\mathrm{diag}(\mathbf{H}\overline{\mathbf{v}})^{-1}\overline{\mathbf{s}^{\Delta}}\right). \tag{2.43}$$

As $\mathbf{i}^{\Delta}$ can be straightforwardly recovered from $\mathbf{v}$ via (2.39), we only need to focus on finding the solution $\mathbf{v}$ to (2.42), which leads to the following extended implicit Z-bus formulation of the power-flow problem.

Problem 2.2 (*Extended Implicit Z-Bus Formulation*)

Given the target system power injection $\mathbf{s}^{Y,\Delta}$, find the solution $\mathbf{v}$ to equation (2.42).

2.6.3 Extended Results on Existence, Uniqueness, and Non-Singularity

In what follows, we extend the theoretical results in Theorem 2.1 and Proposition 2.1. To this end, we first give the notations in Table 2.3. As can be seen, the notations in Table 2.3 are extensions of their counterparts in Table 2.2. Then, we present the following lemma and prove it in Appendix 2.E.

Notation	Definition
$\beta(\mathbf{v})$	$\min_j \frac{\lvert(\mathbf{H}\mathbf{v})_j\rvert}{(\lvert\mathbf{H}\rvert\lvert\mathbf{w}\rvert)_j}$
$\gamma(\mathbf{v})$	$\min\{\alpha(\mathbf{v}),\, \beta(\mathbf{v})\}$
$\xi^Y(\mathbf{s}^{Y,\Delta})$	$\left\lVert \mathbf{W}^{-1}\mathbf{Y}_{LL}^{-1}\overline{\mathbf{W}}^{-1}\mathrm{diag}(\overline{\mathbf{s}^Y})\right\rVert_\infty$
$\xi^\Delta(\mathbf{s}^{Y,\Delta})$	$\left\lVert \mathbf{W}^{-1}\mathbf{Y}_{LL}^{-1}\mathbf{H}^T\mathrm{diag}(\lvert\mathbf{H}\rvert\lvert\mathbf{w}\rvert)^{-1}\mathrm{diag}(\overline{\mathbf{s}^\Delta})\right\rVert_\infty$
$\xi^{Y,\Delta}(\mathbf{s}^{Y,\Delta})$	$\xi^Y(\mathbf{s}^{Y,\Delta}) + \xi^\Delta(\mathbf{s}^{Y,\Delta})$
$\rho^\ddagger_{Y,\Delta}(\mathbf{v},\mathbf{s}^{Y,\Delta})$	$\frac{1}{2}\left(\gamma(\mathbf{v}) - \frac{\xi^{Y,\Delta}(\mathbf{s}^{Y,\Delta})}{\gamma(\mathbf{v})}\right)$
$\rho^\dagger_{Y,\Delta}(\mathbf{v},\mathbf{s}^{Y,\Delta},\tilde{\mathbf{s}}^{Y,\Delta})$	$\rho^\ddagger_{Y,\Delta}(\mathbf{v},\mathbf{s}^{Y,\Delta}) - \sqrt{\left(\rho^\ddagger_{Y,\Delta}(\mathbf{v},\mathbf{s}^{Y,\Delta})\right)^2 - \xi^{Y,\Delta}\left(\tilde{\mathbf{s}}^{Y,\Delta} - \mathbf{s}^{Y,\Delta}\right)}$

Table 2.3 – Notations for the extended results on solvability and non-singularity.

Lemma 2.3

Let $\mathbf{s}^{Y,\Delta}$ *be the target system power injection,* $\begin{bmatrix}\hat{\mathbf{v}}\\ \hat{\mathbf{i}}^\Delta\end{bmatrix}$ *represent the reference system electrical state, and* $\hat{\mathbf{s}}^{Y,\Delta} = \mathbf{F}^{Y,\Delta}\left(\hat{\mathbf{v}},\hat{\mathbf{i}}^\Delta\right)$ *be the reference system power injection.*

Suppose that there exists a $\rho \in (0,\gamma(\hat{\mathbf{v}}))$ *such that*

$$\frac{\xi^Y(\mathbf{s}^{Y,\Delta}-\hat{\mathbf{s}}^{Y,\Delta}) + \dfrac{\xi^Y(\hat{\mathbf{s}}^{Y,\Delta})}{\alpha(\hat{\mathbf{v}})}\rho}{\alpha(\hat{\mathbf{v}})-\rho} + \frac{\xi^\Delta(\mathbf{s}^{Y,\Delta}-\hat{\mathbf{s}}^{Y,\Delta}) + \dfrac{\xi^\Delta(\hat{\mathbf{s}}^{Y,\Delta})}{\beta(\hat{\mathbf{v}})}\rho}{\beta(\hat{\mathbf{v}})-\rho} \le \rho\,, \tag{2.44}$$

$$\frac{\xi^Y(\mathbf{s}^{Y,\Delta})}{\left(\alpha(\hat{\mathbf{v}})-\rho\right)^2} + \frac{\xi^\Delta(\mathbf{s}^{Y,\Delta})}{\left(\beta(\hat{\mathbf{v}})-\rho\right)^2} < 1\,. \tag{2.45}$$

Then, in domain $\mathcal{D}_\rho(\hat{\mathbf{v}})$*, there exists a unique solution* $\mathbf{v}$ *to* (2.42)*. Moreover, this solution can be computed via*

$$\mathbf{v}^{(k+1)} = \mathbf{G}_{\mathbf{s}^{Y,\Delta}}(\mathbf{v}^{(k)})\,, \tag{2.46}$$

with arbitrary $\mathbf{v}^{(0)} \in \mathcal{D}_\rho(\hat{\mathbf{v}})$*.*

Notice that the iterative method (2.46) can be efficiently implemented by following the procedures in Remark 2.1. The only difference is that the right-hand side of (2.23a) is replaced by $\mathbf{P}\left(\mathrm{diag}(\overline{\mathbf{v}^{(k)}})^{-1}\overline{\mathbf{s}^{Y}} + \mathbf{H}^{T}\mathrm{diag}(\mathbf{H}\overline{\mathbf{v}^{(k)}})^{-1}\overline{\mathbf{s}^{\Delta}}\right)$.

By comparing Lemma 2.3 with Theorem 2.1, it is clear that Lemma 2.3 does not provide an explicit condition for the existence and uniqueness of $\mathbf{v}$, hence it is hard to apply in practice. Indeed, to find an appropriate ρ, we have to scan all possible values, which is computationally intensive. To address this issue, we sacrifice the tightness of (2.44)–(2.45) and propose the following theorem. The corresponding proof is given in Appendix 2.F.

Theorem 2.2

Let $\mathbf{s}^{Y,\Delta}$ be the target system power injection, $\begin{bmatrix}\hat{\mathbf{v}}\\ \hat{\mathbf{i}}^{\Delta}\end{bmatrix}$ represent the reference system electrical state, and $\hat{\mathbf{s}}^{Y,\Delta} = \mathbf{F}^{Y,\Delta}\left(\hat{\mathbf{v}}, \hat{\mathbf{i}}^{\Delta}\right)$ be the reference system power injection.

Suppose that

$$\rho^{\ddagger}_{Y,\Delta}(\hat{\mathbf{v}}, \hat{\mathbf{s}}^{Y,\Delta}) > 0\,, \tag{2.47}$$

$$\xi^{Y,\Delta}\left(\mathbf{s}^{Y,\Delta} - \hat{\mathbf{s}}^{Y,\Delta}\right) < \left(\rho^{\ddagger}_{Y,\Delta}(\hat{\mathbf{v}}, \hat{\mathbf{s}}^{Y,\Delta})\right)^{2}. \tag{2.48}$$

Then, in domain $\mathcal{D}_{\rho}(\hat{\mathbf{v}})$ with $\rho = \rho^{\ddagger}_{Y,\Delta}(\hat{\mathbf{v}}, \hat{\mathbf{s}}^{Y,\Delta})$, there exists a unique solution $\mathbf{v}$ to (2.42). Moreover, this solution is located in the smaller domain $\mathcal{D}_{\rho}(\hat{\mathbf{v}})$ with $\rho = \rho^{\dagger}_{Y,\Delta}(\hat{\mathbf{v}}, \hat{\mathbf{s}}^{Y,\Delta}, \mathbf{s}^{Y,\Delta})$ and can be computed through the iterative method (2.46) with arbitrary $\mathbf{v}^{(0)} \in \mathcal{D}_{\rho}(\hat{\mathbf{v}})$, $\rho = \rho^{\ddagger}_{Y,\Delta}(\hat{\mathbf{v}}, \hat{\mathbf{s}}^{Y,\Delta})$.

We see that Theorem 2.2 gives explicit conditions for guaranteeing the existence and uniqueness of the power-flow solution; they extend the corresponding conditions in Theorem 2.1.

In the following text, we give results on the non-singularity of the augmented power-flow Jacobian. First, let us denote the augmented power-flow Jacobian by $\mathbf{J}_{\mathbf{F}^{Y,\Delta}}(\mathbf{v}, \mathbf{i}^{\Delta})$; it is the Jacobian of $\mathbf{F}^{Y,\Delta}$ evaluated at $(\mathbf{v}, \mathbf{i}^{\Delta})$. Specifically, for arbitrary $\mathbf{d} \in \mathbb{C}^{3N}$ and

$\mathbf{g} \in \mathbb{C}^{3N}$, the action of $\mathbf{J}_{\mathbf{F}^{Y,\Delta}}(\mathbf{v}, \mathbf{i}^{\Delta})$ on $\begin{bmatrix}\mathbf{d}\\ \mathbf{g}\end{bmatrix}$ is expressed as follows.

$$\begin{aligned}&\mathbf{J}_{\mathbf{F}^{Y,\Delta}}(\mathbf{v}, \mathbf{i}^{\Delta}) \cdot \begin{bmatrix}\mathbf{d}\\ \mathbf{g}\end{bmatrix}\\ &= \begin{bmatrix}\left(\operatorname{diag}\left(\overline{\mathbf{Y}_{LL}}(\overline{\mathbf{v}} - \overline{\mathbf{w}})\right) - \operatorname{diag}\left(\mathbf{H}^T\overline{\mathbf{i}^{\Delta}}\right)\right)\mathbf{d} + \operatorname{diag}(\mathbf{v})\overline{\mathbf{Y}_{LL}\mathbf{d}} - \operatorname{diag}(\mathbf{v})\mathbf{H}^T\overline{\mathbf{g}}\\ \operatorname{diag}\left(\overline{\mathbf{i}^{\Delta}}\right)\mathbf{H}\mathbf{d} + \operatorname{diag}(\mathbf{H}\mathbf{v})\overline{\mathbf{g}}\end{bmatrix}.\end{aligned} \tag{2.49}$$

Then, we give the following proposition on the non-singularity of $\mathbf{J}_{\mathbf{F}^{Y,\Delta}}(\mathbf{v}, \mathbf{i}^{\Delta})$. The corresponding proof can be found in Appendix 2.G. Here, recall that given $\mathbf{v}$ and $\mathbf{s}^{Y,\Delta}$, we can recover $\mathbf{i}^{\Delta}$ via (2.39).

Proposition 2.2

In Theorem 2.2,

1. *The satisfaction of $\rho^{\ddagger}_{Y,\Delta}(\hat{\mathbf{v}}, \hat{\mathbf{s}}^{Y,\Delta}) > 0$ implies that $\mathbf{J}_{\mathbf{F}^{Y,\Delta}}(\hat{\mathbf{v}}, \hat{\mathbf{i}}^{\Delta})$ is non-singular.*
2. *Moreover, in domain $\mathcal{D}_{\rho}(\hat{\mathbf{v}})$ with $\rho = \rho^{\ddagger}_{Y,\Delta}(\hat{\mathbf{v}}, \hat{\mathbf{s}}^{Y,\Delta})$, the guaranteed unique solution $\mathbf{v}$ satisfies $\rho^{\ddagger}_{Y,\Delta}(\mathbf{v}, \mathbf{s}^{Y,\Delta}) > 0$, which implies that $\mathbf{J}_{\mathbf{F}^{Y,\Delta}}(\mathbf{v}, \mathbf{i}^{\Delta})$ is non-singular.*

Remark 2.3 (*Comparison with the State of the Art*)

In [35], the authors extend the proposed Theorem 2.1 to address ZIP loads. Therein, they consider both wye and delta connections. However, compared to our results in this section, their results do not handle the combination of wye and delta connections at a bus. In other words, their results require only one type of connection per bus. Additionally, they do not assume the knowledge of a reference system electrical state and its corresponding system power injection. As a consequence, it is easy to find a situation where the results in this section are applicable, whereas the results in [35] are not. Last but not least, there is no result on the non-singularity of the power-flow Jacobian in [35].

2.6.4 Discussion on General Multi-Phase Networks

Observe that the developed results in Sections 2.6.1–2.6.3 can be easily adapted to handle the general multi-phase networks where one-, two-, three-phase buses coexist. Specifically, for such networks,

- $\mathbf{v}$, $\mathbf{w}$, and $\mathbf{s}^Y$ collect their corresponding electrical quantities for only the existent phases,
- $\mathbf{s}^\Delta$ collects the corresponding electrical quantities for only the existent phase-to-phase connections,
- $\mathbf{H}$ contains rows that correspond to only the existent phase-to-phase connections and columns that correspond to only the existent phases,
- $\mathbf{Y}_{LL}$ contains rows and columns in $\mathbf{Y}$ that correspond to the existent phases at PQ buses.

With these adaptations, we preserve the mathematical forms and correctness for all the proposed theories.

2.7 Numerical Evaluation

In this section, we present the numerical evaluation of the proposed theories, using a two-bus network and two IEEE networks [55, 56]. All the experiments are conducted on a Macbook Pro with 3 GHz Intel Core i7 and 16 GB 1600 MHz DDR3.

2.7.1 Numerical Experiments for Section 2.5

A Two-Bus Network

We consider a balanced network that has one three-phase PQ bus (namely, $N^{\text{phase}} = 3$ and $N = 1$). This PQ bus is directly connected to the slack bus via a transmission line. The per-unit line admittance matrix is given as follows,

$$\begin{bmatrix} 7-\jmath 12 & -1+\jmath 2 & -1+\jmath 2 \\ -1+\jmath 2 & 7-\jmath 12 & -1+\jmath 2 \\ -1+\jmath 2 & -1+\jmath 2 & 7-\jmath 12 \end{bmatrix}.$$

Moreover, we assume that the shunt elements are negligible and the slack-bus voltage is $\mathbf{v}_0 = (1, e^{-\jmath\frac{2\pi}{3}}, e^{\jmath\frac{2\pi}{3}})^T$ p.u. In this way,

$$\mathbf{w} = \mathbf{v}_0, \qquad \mathbf{Y}_{LL} = \begin{bmatrix} 7-\jmath 12 & -1+\jmath 2 & -1+\jmath 2 \\ -1+\jmath 2 & 7-\jmath 12 & -1+\jmath 2 \\ -1+\jmath 2 & -1+\jmath 2 & 7-\jmath 12 \end{bmatrix}. \tag{2.50}$$

Now, let the power injection $\mathbf{s} = \mathbf{s}_1$ be balanced in all phases. As a consequence, there is $\mathbf{v}_1 = (v_1^a)\mathbf{v}_0$, which means that $\mathbf{v} = \mathbf{v}_1$ is determined by $v_1^a \in \mathbb{C}$.

On the top of Figure 2.3, we plot the region (a filled circle) in which the condition

(2.19) holds. It can be seen that this region covers almost all the v_1^a with a secured magnitude and an angle between $\pm 35.78°$, which is of practical significance. Also, note that the region contains v_1^a with a magnitude much higher than 1 p.u., which corresponds to the case of strong reverse power flow.

On the bottom of Figure 2.3, we take $\hat{v}_1^a = 1$ p.u. (i.e., $\hat{\mathbf{v}} = \mathbf{w}$, $\hat{\mathbf{s}} = \mathbf{0}$), $\mathbf{s} = (1.5 + \jmath 0.9, 1.5 + \jmath 0.9, 1.5 + \jmath 0.9)^T$ p.u., and we plot the domain $\mathcal{D}_\rho(\hat{\mathbf{v}})$ for $\rho^\ddagger(\hat{\mathbf{v}})$, $\rho^\dagger(\hat{\mathbf{v}}, \mathbf{s})$. We see that when taking the target system power injection $\mathbf{s}$ into account, the guaranteed solution is localized more accurately using $\mathcal{D}_\rho(\hat{\mathbf{v}})$ with $\rho = \rho^\dagger(\hat{\mathbf{v}}, \mathbf{s})$.

In Table 2.4, we show the update of $(v_1^a)^{(k)}$ during the iterations. By observing the third column, it is clear that the iterative update gradually converges. In the fourth column, we give the convergence rate that is upper bounded by the contraction modulus $\dfrac{\xi(\mathbf{s})}{\Big(\alpha(\hat{\mathbf{v}}) - \rho^\dagger(\hat{\mathbf{v}}, \mathbf{s})\Big)^2} = 0.3264$.

We note that the true convergence rate is usually less than a third of the contraction modulus. As a consequence, when our conditions hold, the iterative method generally reaches a precision of 10^{-6} in several iterations.

k	$(v_1^a)^{(k)}$	$\left\lvert (v_1^a)^{(k)} - (v_1^a)^{(k-1)} \right\rvert$	$\dfrac{\lvert (v_1^a)^{(k+1)} - (v_1^a)^{(k)} \rvert}{\lvert (v_1^a)^{(k)} - (v_1^a)^{(k-1)} \rvert}$
0	$1.0000 + \jmath 0.0000$		
1	$1.0946 + \jmath 0.0531$	0.1085	0.0990
2	$1.0839 + \jmath 0.0526$	0.0107	0.0912
3	$1.0847 + \jmath 0.0531$	0.0010	0.0921
4	$1.0846 + \jmath 0.0531$	0.0001	

Table 2.4 – Update of v_1^a in the iterations.

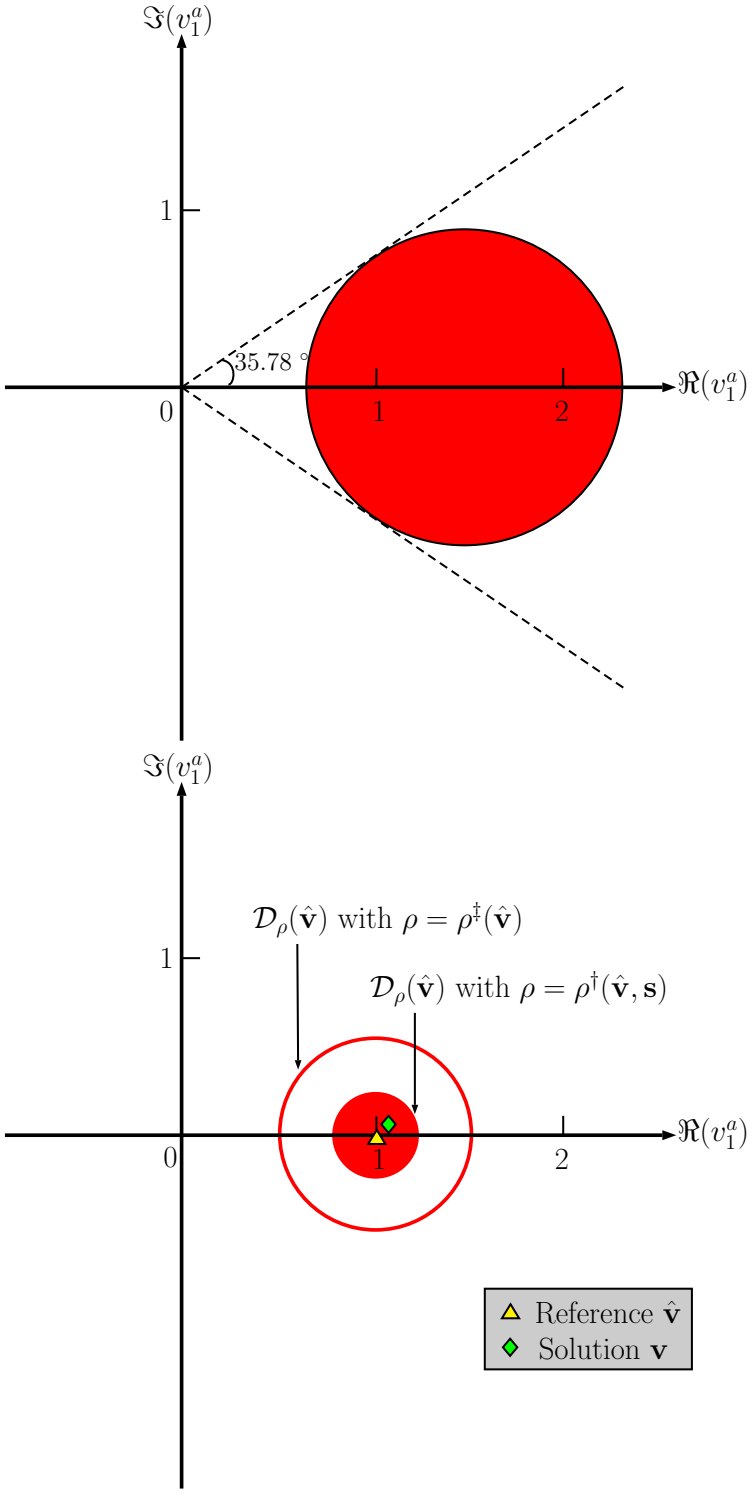

Figure 2.3 – (Top) The region where condition (2.19) holds. (Bottom) The domain $\mathcal{D}_\rho(\hat{\mathbf{v}})$ and the guaranteed solution $\mathbf{v}$ (projected on the space of v_1^a).

Modified IEEE 34-Bus Test Feeder

In this modified IEEE 34-Bus Test Feeder,

- The three-phase line configuration 300 is applied to all transmission lines,
- Both regulators are set to default values,
- All loads are considered to be wye-connected and constant-power.

Let the IEEE benchmark system power injection be $\mathbf{s}^{\text{bench}}$. In addition, let $\hat{\mathbf{v}} = \mathbf{w}$ and $\hat{\mathbf{s}} = \mathbf{0}$. Then, $\rho^{\ddagger}(\hat{\mathbf{v}}) = 0.5$ and $\xi(\mathbf{s}^{\text{bench}} - \hat{\mathbf{s}}) = \xi(\mathbf{s}^{\text{bench}}) = 0.1042 < 0.25$, which takes 0.5 ms to compute. Clearly, the conditions (2.19)–(2.20) in Theorem 2.1 are satisfied.[7] Therefore, there exists a unique solution $\mathbf{v}$ in $\mathcal{D}_{\rho}(\hat{\mathbf{v}})$ with $\rho = \rho^{\dagger}(\hat{\mathbf{v}}, \mathbf{s}^{\text{bench}}) = 0.1182$. We compute this guaranteed solution $\mathbf{v}$ via the iterative method (2.18). In this example, the iterative method converges in 6 iterations. On average, each iteration takes 0.08 ms if we follow the efficient computation procedures in Remark 2.1. We observe that this solution $\mathbf{v}$ is identical to the one obtained from the Newton-Raphson method (up to the machine precision). However, the total runtime of the Newton-Raphson method is approximately 80 times longer than that of our iterative method.

Next, we perform the continuation power-flow analysis [50, 57]. Specifically, we let the target system power injection be $\mathbf{s} = \kappa \mathbf{s}^{\text{bench}}$, where $\kappa \in [0, \infty)$. By varying κ, we find

- The conditions in [30] are satisfied for $\mathbf{s}$ belonging to Interval 1 in Figure 2.4,[8]
- The conditions in [31] are satisfied for $\mathbf{s}$ belonging to Interval 2 in Figure 2.4,[9]
- The conditions (2.19)–(2.20) in our Theorem 2.1 are satisfied for $\mathbf{s}$ belonging to Interval 3 in Figure 2.4.

Clearly, Interval 3 is much larger than Intervals 1 and 2. Furthermore, let $\mathbf{s}^{(1)}$ be the rightmost system power injection in Interval 3 and denote its guaranteed solution by $\mathbf{v}^{(1)}$. By taking $\hat{\mathbf{s}} = \mathbf{s}^{(1)}$ and $\hat{\mathbf{v}} = \mathbf{v}^{(1)}$, we obtain Interval 4 in Figure 2.4. For all $\mathbf{s}$ belonging to Interval 4, we guarantee the existence of a power-flow solution that is unique in a neighborhood of $\mathbf{v}^{(1)}$. Note that Interval 4 cannot be obtained using the proposed Corollary 2.1 and the results in [30, 31].

[7] Note that Corollary 2.1 also applies in this case.

[8] We choose the best values of p and q through parameter scanning.

[9] In addition to the best values of p and q, we take $(\mathbf{\Lambda})_{k,k} = 1/\max_h |(\mathbf{W}^{-1}\mathbf{Y}_{LL}^{-1}\overline{\mathbf{W}}^{-1})_{h,k}|$ as suggested in [31].

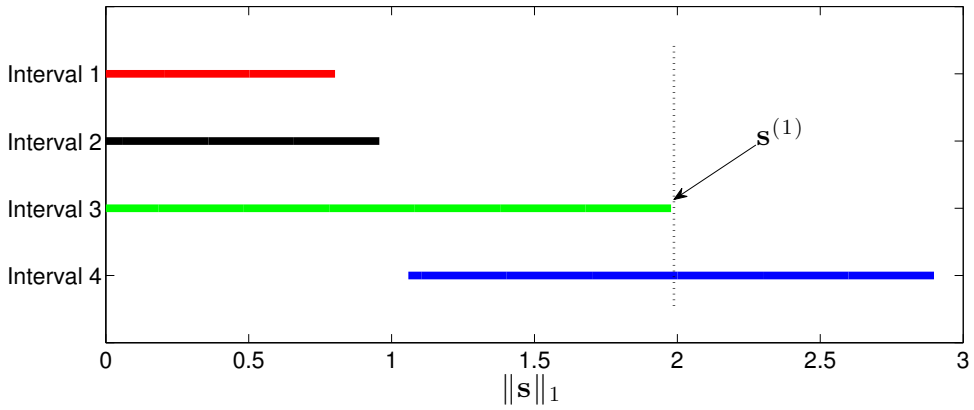

Figure 2.4 – The conditions in [30] are satisfied by system power injections in Interval 1. The conditions in [31] are satisfied by system power injections in Interval 2. The conditions in Theorem 2.1 are satisfied by system power injections in Intervals 3 and 4.

2.7.2 Numerical Experiments for Section 2.6.3

IEEE 123-Bus Test Feeder

The IEEE 123-Bus Test Feeder is a large multi-phase network with unbalanced one-, two-, and three-phase loads/sources. As mentioned in Section 2.6.4, let us first delete in $\mathbf{H}$ the rows that correspond to the lacking phase-to-phase connections and the columns that correspond to the lacking phases.

Similarly to part of the previous example on the modified IEEE 34-Bus Test Feeder, we set the regulators to their default values and perform the continuation power-flow analysis. Specifically, denote the IEEE benchmark system power injection by $\left(\mathbf{s}^{Y,\Delta}\right)^{\text{bench}}$, and the target system power injection by $\mathbf{s}^{Y,\Delta} = \kappa\left(\mathbf{s}^{Y,\Delta}\right)^{\text{bench}}$ with $\kappa \in [0,\infty)$. As there is no combined wye/delta connection, the conditions in [35] are applicable.

First, let $\hat{\mathbf{v}} = \mathbf{w}$ and $\hat{\mathbf{s}}^{Y,\Delta} = \mathbf{0}$. Through varying κ, we find

- The conditions in [35] are satisfied for $\mathbf{s}^{Y,\Delta}$ belonging to Interval 1 in Figure 2.5,[10]
- The conditions (2.44)–(2.45) in Lemma 2.3 are satisfied for $\mathbf{s}^{Y,\Delta}$ belonging to Interval 2 in Figure 2.5,
- The conditions (2.47)–(2.48) in Theorem 2.2 are satisfied for $\mathbf{s}^{Y,\Delta}$ belonging to Interval 3 in Figure 2.5.

Note that the verification of the explicit conditions (2.47)–(2.48) takes 12 ms on average,

[10] As suggested by the authors of [35], we let their diagonal matrix $\mathbf{\Lambda}$ be $\mathbf{W}$.

which is much faster than the other conditions.

Then, let $\left(\mathbf{s}^{Y,\Delta}\right)^{(1)}$ be the rightmost power injection in Interval 2, and its guaranteed solution be $\mathbf{v}^{(1)}$ (which is computed via the iterative method in (2.46)). By choosing $\hat{\mathbf{v}} = \mathbf{v}^{(1)}$ and $\hat{\mathbf{s}}^{Y,\Delta} = \left(\mathbf{s}^{Y,\Delta}\right)^{(1)}$, we obtain Interval 4 via Lemma 2.3 and Interval 5 via Theorem 2.2. These two intervals cannot be obtained from the results in [35].

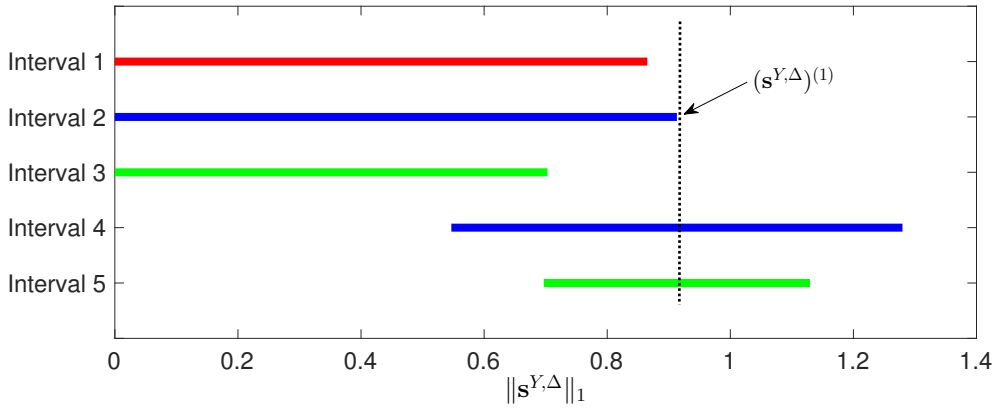

Figure 2.5 – The conditions in [35] are satisfied by system power injections in Interval 1. The conditions in Lemma 2.3 are satisfied by system power injections in Intervals 2 and 4. The conditions in Theorem 2.2 are satisfied by system power injections in Intervals 3 and 5.

IEEE 123-Bus Test Feeder (with Combined Wye/Delta Connections)

Here, we modify the IEEE 123-Bus Test Feeder by adding the loads and sources in Table 2.5 to the benchmark system power injection. In this way, we create combined wye/delta connections, which renders the results in [35] inapplicable. With the modified benchmark system power injection, we repeat the continuation power-flow analysis in the previous example and obtain 4 intervals in Figure 2.6. Specifically, Intervals 1 and 3 correspond to Lemma 2.3; Intervals 2 and 4 correspond to Theorem 2.2. Within each interval, we notice that

- For a target system power injection, the computation of the guaranteed solution converges in typically less than 10 iterations of (2.46). On average, each iteration takes 0.49 ms.
- The guaranteed unique solutions in Theorem 2.2 and Lemma 2.3 match with those obtained from OpenDSS [58]. OpenDSS is the only freely-available solver that works with combined wye/delta connections.

Bus	Type	Phase-Phase ab / Phase a (p.u.)	Phase-Phase bc / Phase b (p.u.)	Phase-Phase ca / Phase c (p.u.)
1	delta	$-0.03 - \jmath 0.01$	$-0.03 - \jmath 0.01$	$-0.03 - \jmath 0.01$
35	wye	-0.02	-0.02	-0.02
76	wye	$0.04 + \jmath 0.01$	$0.04 + \jmath 0.01$	$0.04 + \jmath 0.01$
99	delta	$-0.02 - \jmath 0.01$	$-0.02 - \jmath 0.01$	$-0.02 - \jmath 0.01$

Table 2.5 – Additional loads and sources in IEEE 123-Bus Test Feeder.

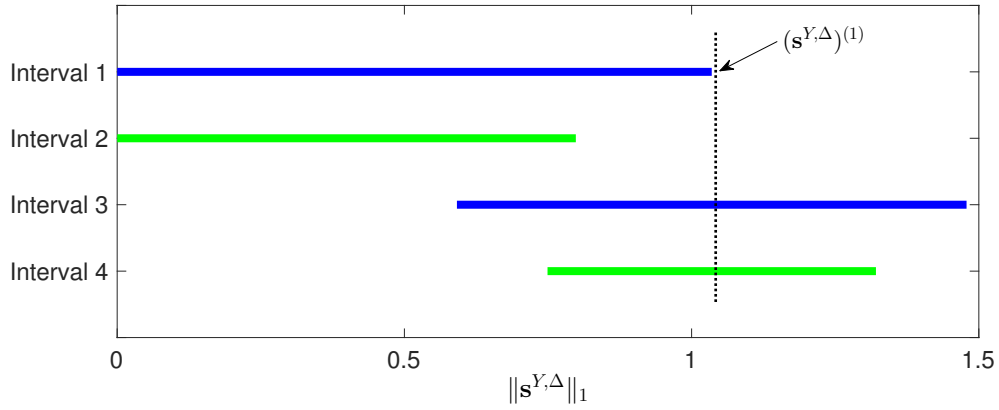

Figure 2.6 – The conditions in Lemma 2.3 are satisfied by system power injections in Intervals 1 and 3. The conditions in Theorem 2.2 are satisfied by system power injections in Intervals 2 and 4.

2.8 Conclusions

We have proposed explicit sufficient conditions on the existence and uniqueness of the power-flow solution. Once the conditions are satisfied, we guarantee the existence of a power-flow solution and provide an analytically specified domain in which this guaranteed solution is unique. In addition, we have also provided an iterative method to compute this solution; it can be efficiently implemented by means of LU decomposition with Markowitz pivoting. Moreover, we have provided an explicit condition on the non-singularity of power-flow Jacobian and have shown that the guaranteed solution has a non-singular power-flow Jacobian. All these results have been extended to account for various load/source connections, including wye, delta, and a combination thereof.

Appendix

2.A Proof of Invertibility of $\mathbf{Y}_{LL}$

The proof is based on the following assumptions, which hold in a large number of practical distribution networks.

- The connection from the slack bus to a PQ bus can be realized in three ways: (i) a transmission line, (ii) a $\mathrm{Delta}-\mathrm{Wye_G}$ transformer, or (iii) a $\mathrm{Wye_G}-\mathrm{Wye_G}$ transformer;
- The connection between two PQ buses can be realized through either a transmission line or a $\mathrm{Wye_G}-\mathrm{Wye_G}$ transformer;
- For all transmission lines, the series admittances and shunt admittances are described by circulant matrices.
- For all transformers, we employ the models in [36], which include both the longitudinal winding admittances and the transversal core-related admittances.
- Transmission lines and transformers do not generate active power, and their longitudinal elements have positive resistance in zero-, positive-, negative sequences.

With the above assumptions, we prove the invertibility of $\mathbf{Y}_{LL}$, by showing: if $\mathbf{Y}_{LL}\mathbf{v}=\mathbf{0}$, then we must have $\mathbf{v}=\mathbf{0}$. To this end, we view $\mathbf{Y}_{LL}$ as the nodal admittance matrix of a fictitious N-bus network (i.e., the original network with the slack bus grounded), and let $\mathcal{N}^{\mathrm{slack}}$ be the set of PQ buses that are directly connected to the slack bus in the original $(N+1)$-bus network. Then, the total power injection into this N-bus network is $s^{\mathrm{total}}=\mathbf{v}^T\overline{\mathbf{Y}_{LL}}\overline{\mathbf{v}}=0$. Notice that s^{total} equals the total power loss and can be further decomposed as

$$s^{\mathrm{total}}=s^{\mathrm{slack}}+s^{\mathrm{series}}+s^{\mathrm{shunt}}+s^{\mathrm{winding}}+s^{\mathrm{core}}\,, \tag{2.51}$$

where

- s^{slack} results from the transmission devices between the grounded slack bus and the PQ buses $j\in\mathcal{N}^{\mathrm{slack}}$,
- s^{series} and s^{shunt} result from the transmission lines between the PQ buses,
- s^{winding} and s^{core} result from the transformers between the PQ buses.

By our last assumption, $s^{\mathrm{total}}=0$ implies that all the five terms have zero real parts. Consequently, we have

1. $\mathbf{v}_j = \mathbf{0}, \forall j \in \mathcal{N}^{\text{slack}}$.
2. $\mathbf{v}_j = \mathbf{v}_k$, if buses $j,\ k \in \{1, ..., N\}$ are connected through a transmission line.
3. $\mathbf{v}_j = \mathrm{x}_{jk}\mathbf{v}_k$, if buses $j,\ k \in \{1, ..., N\}$ are connected through a transformer with ratio x_{jk}.

Since $\mathcal{N}^{\text{slack}}$ is non-empty, there is at least one $\mathbf{v}_j$ equal to zero. This zero voltage propagates throughout the N-bus network. Thus, we have $\mathbf{v} = \mathbf{0}$.

■

2.B Proof of Lemma 2.1

First, let us define $\mathbf{u} = \mathbf{W}^{-1}\mathbf{v}$, which can be viewed as the normalized system electrical state. Then, Equation (2.16) is equivalent to

$$\mathbf{u} = \tilde{\mathbf{G}}_{\mathbf{s}}(\mathbf{u}) \,, \tag{2.52}$$

where

$$\tilde{\mathbf{G}}_{\mathbf{s}}(\mathbf{u}) = \mathbf{1} + \mathbf{W}^{-1}\mathbf{Y}_{LL}^{-1}\overline{\mathbf{W}}^{-1}\mathrm{diag}(\overline{\mathbf{u}})^{-1}\overline{\mathbf{s}} \,. \tag{2.53}$$

Since $\mathbf{W}$ defines an invertible relation between $\mathbf{u}$ and $\mathbf{v}$, we can complete the proof by showing: given the satisfaction of conditions (2.19)–(2.20), $\tilde{\mathbf{G}}_{\mathbf{s}}(\mathbf{u})$ is a self-mapping in domain

$$\tilde{\mathcal{D}}_{\rho}(\hat{\mathbf{u}}) = \left\{ \mathbf{u} : |(\mathbf{u})_j - (\hat{\mathbf{u}})_j| \leq \rho,\ j = 1, ..., N^{\text{phase}}N \right\} , \tag{2.54}$$

for $\rho \in \left[\rho^{\dagger}(\hat{\mathbf{v}}, \mathbf{s}), \rho^{\ddagger}(\hat{\mathbf{v}}) \right]$ and $\hat{\mathbf{u}} = \mathbf{W}^{-1}\hat{\mathbf{v}}$.

In other words, we need to show: given the satisfaction of conditions (2.19)–(2.20),

$$\left\| \mathbf{u} - \hat{\mathbf{u}} \right\|_{\infty} \leq \rho \qquad \Rightarrow \qquad \left\| \tilde{\mathbf{G}}_{\mathbf{s}}(\mathbf{u}) - \hat{\mathbf{u}} \right\|_{\infty} \leq \rho \,, \tag{2.55}$$

for $\rho \in \left[\rho^{\dagger}(\hat{\mathbf{v}}, \mathbf{s}), \rho^{\ddagger}(\hat{\mathbf{v}}) \right]$.

To this end, consider that

$$\begin{aligned}\tilde{\mathbf{G}}_{\mathbf{s}}(\mathbf{u})-\hat{\mathbf{u}} =&\mathbf{W}^{-1}\mathbf{Y}_{LL}^{-1}\overline{\mathbf{W}}^{-1}\left(\operatorname{diag}(\overline{\mathbf{u}})^{-1}\overline{\mathbf{s}}-\operatorname{diag}(\overline{\hat{\mathbf{u}}})^{-1}\overline{\hat{\mathbf{s}}}\right)\\ =&\mathbf{W}^{-1}\mathbf{Y}_{LL}^{-1}\overline{\mathbf{W}}^{-1}\left(\operatorname{diag}(\overline{\mathbf{u}})^{-1}\overline{\mathbf{s}}-\operatorname{diag}(\overline{\mathbf{u}})^{-1}\overline{\hat{\mathbf{s}}}\right)\\ &+\mathbf{W}^{-1}\mathbf{Y}_{LL}^{-1}\overline{\mathbf{W}}^{-1}\left(\operatorname{diag}(\overline{\mathbf{u}})^{-1}\overline{\hat{\mathbf{s}}}-\operatorname{diag}(\overline{\hat{\mathbf{u}}})^{-1}\overline{\hat{\mathbf{s}}}\right). \end{aligned} \tag{2.56}$$

For the terms on the right-hand side of (2.56), we can re-arrange as follows:

$$\begin{aligned}&\mathbf{W}^{-1}\mathbf{Y}_{LL}^{-1}\overline{\mathbf{W}}^{-1}\left(\operatorname{diag}(\overline{\mathbf{u}})^{-1}\overline{\mathbf{s}}-\operatorname{diag}(\overline{\mathbf{u}})^{-1}\overline{\hat{\mathbf{s}}}\right)\\ =&\mathbf{W}^{-1}\mathbf{Y}_{LL}^{-1}\overline{\mathbf{W}}^{-1}\operatorname{diag}\left(\overline{\mathbf{s}}-\overline{\hat{\mathbf{s}}}\right)\begin{bmatrix}(\overline{\mathbf{u}})_1^{-1}\\ \vdots\\ (\overline{\mathbf{u}})_{N^{\text{phase}}N}^{-1}\end{bmatrix},\end{aligned} \tag{2.57}$$

$$\begin{aligned}&\mathbf{W}^{-1}\mathbf{Y}_{LL}^{-1}\overline{\mathbf{W}}^{-1}\left(\operatorname{diag}(\overline{\mathbf{u}})^{-1}\overline{\hat{\mathbf{s}}}-\operatorname{diag}(\overline{\hat{\mathbf{u}}})^{-1}\overline{\hat{\mathbf{s}}}\right)\\ =&\mathbf{W}^{-1}\mathbf{Y}_{LL}^{-1}\overline{\mathbf{W}}^{-1}\operatorname{diag}(\overline{\hat{\mathbf{s}}})\begin{bmatrix}\dfrac{(\overline{\hat{\mathbf{u}}})_1-(\overline{\mathbf{u}})_1}{(\overline{\hat{\mathbf{u}}})_1(\overline{\mathbf{u}})_1}\\ \vdots\\ \dfrac{(\overline{\hat{\mathbf{u}}})_{N^{\text{phase}}N}-(\overline{\mathbf{u}})_{N^{\text{phase}}N}}{(\overline{\hat{\mathbf{u}}})_{N^{\text{phase}}N}(\overline{\mathbf{u}})_{N^{\text{phase}}N}}\end{bmatrix}.\end{aligned} \tag{2.58}$$

In this way, for $\rho<\alpha(\hat{\mathbf{v}})$, $\|\mathbf{u}-\hat{\mathbf{u}}\|_\infty\leq\rho$ implies that

$$\begin{aligned}\left\|\tilde{\mathbf{G}}_{\mathbf{s}}(\mathbf{u})-\hat{\mathbf{u}}\right\|_\infty\leq&\left\|\mathbf{W}^{-1}\mathbf{Y}_{LL}^{-1}\overline{\mathbf{W}}^{-1}\left(\operatorname{diag}(\overline{\mathbf{u}})^{-1}\overline{\mathbf{s}}-\operatorname{diag}(\overline{\mathbf{u}})^{-1}\overline{\hat{\mathbf{s}}}\right)\right\|_\infty\\ &+\left\|\mathbf{W}^{-1}\mathbf{Y}_{LL}^{-1}\overline{\mathbf{W}}^{-1}\left(\operatorname{diag}(\overline{\mathbf{u}})^{-1}\overline{\hat{\mathbf{s}}}-\operatorname{diag}(\overline{\hat{\mathbf{u}}})^{-1}\overline{\hat{\mathbf{s}}}\right)\right\|_\infty\\ \leq&\frac{\xi(\mathbf{s}-\hat{\mathbf{s}})}{\alpha(\hat{\mathbf{v}})-\rho}+\frac{\xi(\hat{\mathbf{s}})\rho}{\Big(\alpha(\hat{\mathbf{v}})-\rho\Big)\alpha(\hat{\mathbf{v}})}.\end{aligned} \tag{2.59}$$

Furthermore, observe that

$$\begin{aligned}&\frac{\xi(\mathbf{s}-\hat{\mathbf{s}})}{\alpha(\hat{\mathbf{v}})-\rho}+\frac{\xi(\hat{\mathbf{s}})\rho}{\Big(\alpha(\hat{\mathbf{v}})-\rho\Big)\alpha(\hat{\mathbf{v}})}-\rho\\ =&\frac{\rho^2-\left(\alpha(\hat{\mathbf{v}})-\dfrac{\xi(\hat{\mathbf{s}})}{\alpha(\hat{\mathbf{v}})}\right)\rho+\xi(\mathbf{s}-\hat{\mathbf{s}})}{\alpha(\hat{\mathbf{v}})-\rho}\\ =&\frac{\rho^2-2\rho^{\ddagger}(\hat{\mathbf{v}})\rho+\xi(\mathbf{s}-\hat{\mathbf{s}})}{\alpha(\hat{\mathbf{v}})-\rho}\,.\end{aligned}\tag{2.60}$$

Given the satisfaction of conditions (2.19)–(2.20), we have

$$\rho^2-2\rho^{\ddagger}(\hat{\mathbf{v}})\rho+\xi(\mathbf{s}-\hat{\mathbf{s}})\leq 0\,,\tag{2.61}$$

$$\alpha(\hat{\mathbf{v}})-\rho>0\,,\tag{2.62}$$

for $\rho\in\Big[\rho^{\dagger}(\hat{\mathbf{v}},\mathbf{s}),\rho^{\ddagger}(\hat{\mathbf{v}})\Big]$. Specifically, (2.61) is true because: the satisfaction of (2.19)–(2.20) ensures that the convex polynomial $\rho^2-2\rho^{\ddagger}(\hat{\mathbf{v}})\rho+\xi(\mathbf{s}-\hat{\mathbf{s}})$ has two positive real roots $\rho^{\dagger}(\hat{\mathbf{v}},\mathbf{s}),\ 2\rho^{\ddagger}(\hat{\mathbf{v}})-\rho^{\dagger}(\hat{\mathbf{v}},\mathbf{s})$, hence $\rho^2-2\rho^{\ddagger}(\hat{\mathbf{v}})\rho+\xi(\mathbf{s}-\hat{\mathbf{s}})$ is non-positive between its small root $\rho^{\dagger}(\hat{\mathbf{v}},\mathbf{s})$ and its axis of symmetry $\rho^{\ddagger}(\hat{\mathbf{v}})$.

As a result of (2.61) and (2.62), we obtain

$$\frac{\xi(\mathbf{s}-\hat{\mathbf{s}})}{\alpha(\hat{\mathbf{v}})-\rho}+\frac{\xi(\hat{\mathbf{s}})\rho}{\Big(\alpha(\hat{\mathbf{v}})-\rho\Big)\alpha(\hat{\mathbf{v}})}\leq\rho\,,\tag{2.63}$$

for $\rho\in\Big[\rho^{\dagger}(\hat{\mathbf{v}},\mathbf{s}),\rho^{\ddagger}(\hat{\mathbf{v}})\Big]$.

By combination of (2.59) and (2.63), there is

$$\left\|\tilde{\mathbf{G}}_{\mathbf{s}}(\mathbf{u})-\hat{\mathbf{u}}\right\|_{\infty}\leq\rho\,,\tag{2.64}$$

for $\rho\in\Big[\rho^{\dagger}(\hat{\mathbf{v}},\mathbf{s}),\rho^{\ddagger}(\hat{\mathbf{v}})\Big]$, which completes the proof.

■

2.C Proof of Lemma 2.2

In this proof, we continue using the notations in Appendix 2.B. Here, our goal is to show: given the satisfaction of conditions (2.19)–(2.20), $\tilde{\mathbf{G}}_{\mathbf{s}}(\mathbf{u})$ is a contraction mapping in domain $\tilde{\mathcal{D}}_{\rho}(\hat{\mathbf{u}})$ for $\rho\in\Big[\rho^{\dagger}(\hat{\mathbf{v}},\mathbf{s}),\rho^{\ddagger}(\hat{\mathbf{v}})\Big]$.

In other words, we need to show: given the satisfaction of conditions (2.19)–(2.20),

$$\left\|\tilde{\mathbf{G}}_{\mathbf{s}}(\mathbf{u})-\tilde{\mathbf{G}}_{\mathbf{s}}(\mathbf{u}')\right\|_{\infty}<\left\|\mathbf{u}-\mathbf{u}'\right\|_{\infty},\quad \forall \mathbf{u},\ \mathbf{u}'\in\tilde{\mathcal{D}}_{\rho}(\hat{\mathbf{u}})\,, \tag{2.65}$$

holds for $\rho\in\left[\rho^{\dagger}(\hat{\mathbf{v}},\mathbf{s}),\rho^{\ddagger}(\hat{\mathbf{v}})\right)$.

To this end, consider that

$$\tilde{\mathbf{G}}_{\mathbf{s}}(\mathbf{u})-\tilde{\mathbf{G}}_{\mathbf{s}}(\mathbf{u}')=\mathbf{W}^{-1}\mathbf{Y}_{LL}^{-1}\overline{\mathbf{W}}^{-1}\left(\mathrm{diag}(\overline{\mathbf{u}})^{-1}\overline{\mathbf{s}}-\mathrm{diag}(\overline{\mathbf{u}'})^{-1}\overline{\mathbf{s}}\right). \tag{2.66}$$

Similar to (2.58), the right-hand side of (2.66) can be re-arranged as follows.

$$\begin{aligned}&\mathbf{W}^{-1}\mathbf{Y}_{LL}^{-1}\overline{\mathbf{W}}^{-1}\left(\mathrm{diag}(\overline{\mathbf{u}})^{-1}\overline{\mathbf{s}}-\mathrm{diag}(\overline{\mathbf{u}'})^{-1}\overline{\mathbf{s}}\right)\\ =&\mathbf{W}^{-1}\mathbf{Y}_{LL}^{-1}\overline{\mathbf{W}}^{-1}\mathrm{diag}(\overline{\mathbf{s}})\begin{bmatrix}\dfrac{(\overline{\mathbf{u}'})_1-(\overline{\mathbf{u}})_1}{(\overline{\mathbf{u}'})_1(\overline{\mathbf{u}})_1}\\ \vdots\\ \dfrac{(\overline{\mathbf{u}'})_{N^{\mathrm{phase}}N}-(\overline{\mathbf{u}})_{N^{\mathrm{phase}}N}}{(\overline{\mathbf{u}'})_{N^{\mathrm{phase}}N}(\overline{\mathbf{u}})_{N^{\mathrm{phase}}N}}\end{bmatrix}.\end{aligned} \tag{2.67}$$

In this way, for $\rho<\alpha(\hat{\mathbf{v}})$, $\mathbf{u},\ \mathbf{u}'\in\tilde{\mathcal{D}}_{\rho}(\hat{\mathbf{u}})$ implies that

$$\left\|\tilde{\mathbf{G}}_{\mathbf{s}}(\mathbf{u})-\tilde{\mathbf{G}}_{\mathbf{s}}(\mathbf{u}')\right\|_{\infty}\leq\frac{\xi(\mathbf{s})}{\left(\alpha(\hat{\mathbf{v}})-\rho\right)^2}\left\|\mathbf{u}-\mathbf{u}'\right\|_{\infty}. \tag{2.68}$$

Further, given the satisfaction of conditions (2.19)–(2.20), we have

$$\begin{aligned}\xi(\mathbf{s})\leq&\xi(\hat{\mathbf{s}})+\xi(\mathbf{s}-\hat{\mathbf{s}})\\ <&\xi(\hat{\mathbf{s}})+\frac{1}{4}\left(\alpha(\hat{\mathbf{v}})-\frac{\xi(\hat{\mathbf{s}})}{\alpha(\hat{\mathbf{v}})}\right)^2\\ =&\frac{1}{4}\left(\alpha(\hat{\mathbf{v}})+\frac{\xi(\hat{\mathbf{s}})}{\alpha(\hat{\mathbf{v}})}\right)^2\\ =&\left(\alpha(\hat{\mathbf{v}})-\rho^{\ddagger}(\hat{\mathbf{v}})\right)^2.\end{aligned} \tag{2.69}$$

Therefore, we obtain that

$$\xi(\mathbf{s})<\left(\alpha(\hat{\mathbf{v}})-\rho\right)^2, \tag{2.70}$$

for $\rho\in\left[\rho^{\dagger}(\hat{\mathbf{v}},\mathbf{s}),\rho^{\ddagger}(\hat{\mathbf{v}})\right)$.

By combination of (2.68) and (2.70), there is

$$\left\|\tilde{\mathbf{G}}_{\mathbf{s}}(\mathbf{u}) - \tilde{\mathbf{G}}_{\mathbf{s}}(\mathbf{u}')\right\|_{\infty} < \left\|\mathbf{u} - \mathbf{u}'\right\|_{\infty}, \tag{2.71}$$

for $\rho \in \left[\rho^{\dagger}(\hat{\mathbf{v}}, \mathbf{s}), \rho^{\ddagger}(\hat{\mathbf{v}})\right]$, which completes the proof.

■

2.D Proof of Proposition 2.1

For the First Item

In order to prove that $\mathbf{J}_{\mathbf{F}}(\hat{\mathbf{v}})$ is non-singular, we need to show

$$\mathbf{J}_{\mathbf{F}}(\mathbf{v}) \cdot \mathbf{d} = \mathbf{0} \qquad \Rightarrow \qquad \mathbf{d} = \mathbf{0}\,. \tag{2.72}$$

This can be done by the method of contradiction. First, let us assume that there exists a $\mathbf{d} \neq \mathbf{0}$ such that $\mathbf{J}_{\mathbf{F}}(\mathbf{v}) \cdot \mathbf{d} = \mathbf{0}$. Clearly, for any $\epsilon > 0$, $\epsilon\mathbf{d}$ satisfies

$$\mathbf{J}_{\mathbf{F}}(\mathbf{v}) \cdot (\epsilon\mathbf{d}) = \mathbf{0}\,. \tag{2.73}$$

Then, let $\mathbf{v}_{\epsilon}{}' = \hat{\mathbf{v}} + \epsilon\mathbf{d}$ and $\mathbf{v}_{\epsilon}{}'' = \hat{\mathbf{v}} - \epsilon\mathbf{d}$ be two different system electrical states. Note that $\mathbf{v}_{\epsilon}{}'$ and $\mathbf{v}_{\epsilon}{}''$ correspond to the same system power injection, since

$$\begin{aligned}
\mathbf{F}(\mathbf{v}_{\epsilon}{}') =& \operatorname{diag}(\hat{\mathbf{v}} + \epsilon\mathbf{d})\overline{\mathbf{Y}_{LL}}(\overline{\hat{\mathbf{v}}} + \epsilon\overline{\mathbf{d}} - \overline{\mathbf{w}}) \\
=& \hat{\mathbf{s}} + \mathbf{J}_{\mathbf{F}}(\mathbf{v}) \cdot (\epsilon\mathbf{d}) + \operatorname{diag}(\epsilon\mathbf{d})\overline{\mathbf{Y}_{LL}}(\epsilon\overline{\mathbf{d}}) \\
=& \hat{\mathbf{s}} - \mathbf{J}_{\mathbf{F}}(\mathbf{v}) \cdot (\epsilon\mathbf{d}) + \operatorname{diag}(\epsilon\mathbf{d})\overline{\mathbf{Y}_{LL}}(\epsilon\overline{\mathbf{d}}) \\
=& \operatorname{diag}(\hat{\mathbf{v}} - \epsilon\mathbf{d})\overline{\mathbf{Y}_{LL}}(\overline{\hat{\mathbf{v}}} - \epsilon\overline{\mathbf{d}} - \overline{\mathbf{w}}) \\
=& \mathbf{F}(\mathbf{v}_{\epsilon}{}'')\,.
\end{aligned} \tag{2.74}$$

Next, we find a small enough $\epsilon^* > 0$ such that

- The difference of power injections $\mathbf{F}(\mathbf{v}_{\epsilon}{}') - \hat{\mathbf{s}}$ satisfies condition (2.20),
- Both $\mathbf{v}_{\epsilon}{}'$ and $\mathbf{v}_{\epsilon}{}''$ are included in domain $\mathcal{D}_{\rho}(\hat{\mathbf{v}})$ with $\rho = \rho^{\ddagger}(\hat{\mathbf{v}})$.

This creates a contradiction, since Theorem 2.1 enforces that $\mathbf{v}_{\epsilon}{}' = \mathbf{v}_{\epsilon}{}''$. Therefore, $\mathbf{d}$ must be $\mathbf{0}$ and $\mathbf{J}_{\mathbf{F}}(\hat{\mathbf{v}})$ is non-singular.

For the Second Item

As the guaranteed solution $\mathbf{v}$ belongs to domain $\mathcal{D}_\rho(\hat{\mathbf{v}})$ with $\rho = \rho^\ddagger(\hat{\mathbf{v}})$, we have

$$\begin{aligned}\frac{|(\mathbf{v})_j|}{|(\mathbf{w})_j|} &\geq \frac{|(\hat{\mathbf{v}})_j|}{|(\mathbf{w})_j|} - \rho^\ddagger(\hat{\mathbf{v}}) \\ &\geq \alpha(\hat{\mathbf{v}}) - \rho^\ddagger(\hat{\mathbf{v}}) \,, \qquad \forall j \,. \end{aligned} \tag{2.75}$$

This implies that

$$\alpha(\mathbf{v}) \geq \alpha(\hat{\mathbf{v}}) - \rho^\ddagger(\hat{\mathbf{v}}) \,. \tag{2.76}$$

Then, we have

$$\begin{aligned}\rho^\ddagger(\mathbf{v}) &= \frac{1}{2}\left(\alpha(\mathbf{v}) - \frac{\xi\Big(\mathbf{F}(\mathbf{v})\Big)}{\alpha(\mathbf{v})}\right) \\ &\geq \frac{1}{2}\left(\Big(\alpha(\hat{\mathbf{v}}) - \rho^\ddagger(\hat{\mathbf{v}})\Big) - \frac{\xi\Big(\mathbf{F}(\mathbf{v})\Big)}{\Big(\alpha(\hat{\mathbf{v}}) - \rho^\ddagger(\hat{\mathbf{v}})\Big)}\right) \\ &= \frac{\Big(\alpha(\hat{\mathbf{v}}) - \rho^\ddagger(\hat{\mathbf{v}})\Big)^2 - \xi\Big(\mathbf{F}(\mathbf{v})\Big)}{2\Big(\alpha(\hat{\mathbf{v}}) - \rho^\ddagger(\hat{\mathbf{v}})\Big)} \,. \end{aligned} \tag{2.77}$$

Next, according to (2.69) in Appendix 2.C, there is

$$\xi\Big(\mathbf{F}(\mathbf{v})\Big) = \xi(\mathbf{s}) < \Big(\alpha(\hat{\mathbf{v}}) - \rho^\ddagger(\hat{\mathbf{v}})\Big)^2 \,. \tag{2.78}$$

By plugging (2.78) into (2.77), we obtain

$$\rho^\ddagger(\mathbf{v}) > 0 \,, \tag{2.79}$$

which completes the proof.

■

2.E Proof of Lemma 2.3

Let $\mathbf{u} = \mathbf{W}^{-1}\mathbf{v}$ and notice that (2.42) is equivalent to

$$\mathbf{u} = \tilde{\mathbf{G}}_{\mathbf{s}^{Y,\Delta}}(\mathbf{u}) \,, \tag{2.80}$$

where

$$\tilde{\mathbf{G}}_{\mathbf{s}^{Y,\Delta}}(\mathbf{u}) = \mathbf{1} + \mathbf{W}^{-1}\mathbf{Y}_{LL}^{-1}\overline{\mathbf{W}}^{-1}\mathrm{diag}(\overline{\mathbf{u}})^{-1}\overline{\mathbf{s}^{Y}} + \mathbf{W}^{-1}\mathbf{Y}_{LL}^{-1}\mathbf{H}^{T}\mathrm{diag}(\mathbf{H}\overline{\mathbf{W}}\overline{\mathbf{u}})^{-1}\overline{\mathbf{s}^{\Delta}}\,. \tag{2.81}$$

Then, by the Banach fixed-point theorem, we need to show that $\tilde{\mathbf{G}}_{\mathbf{s}^{Y,\Delta}}$ is a contraction mapping in

$$\tilde{\mathcal{D}}_{\rho}(\hat{\mathbf{u}}) = \left\{\mathbf{u} : |(\mathbf{u})_j - (\hat{\mathbf{u}})_j| \leq \rho,\ j = 1, ..., 3N\right\},$$

for $\hat{\mathbf{u}} = \mathbf{W}^{-1}\hat{\mathbf{v}}$ and some $\rho \in (0, \gamma(\hat{\mathbf{v}}))$ that satisfies (2.44)–(2.45).[11] To do so, we sequentially prove the self-mapping property and the contraction property of $\tilde{\mathbf{G}}_{\mathbf{s}^{Y,\Delta}}$.

Self-Mapping Property

Assuming that $\|\mathbf{u} - \hat{\mathbf{u}}\|_{\infty} \leq \rho$, our goal is to show $\|\tilde{\mathbf{G}}_{\mathbf{s}^{Y,\Delta}}(\mathbf{u}) - \hat{\mathbf{u}}\|_{\infty} \leq \rho$.

Since $\hat{\mathbf{u}} = \tilde{\mathbf{G}}_{\mathbf{s}^{Y,\Delta}}(\hat{\mathbf{u}})$, we have

$$\begin{aligned}
\tilde{\mathbf{G}}_{\mathbf{s}^{Y,\Delta}}(\mathbf{u}) - \hat{\mathbf{u}} =& \mathbf{W}^{-1}\mathbf{Y}_{LL}^{-1}\overline{\mathbf{W}}^{-1}\left(\mathrm{diag}(\overline{\mathbf{u}})^{-1}\overline{\mathbf{s}^{Y}} - \mathrm{diag}(\overline{\hat{\mathbf{u}}})^{-1}\overline{\hat{\mathbf{s}}^{Y}}\right) \\
&+ \mathbf{W}^{-1}\mathbf{Y}_{LL}^{-1}\mathbf{H}^{T}\left(\mathrm{diag}(\mathbf{H}\overline{\mathbf{W}}\overline{\mathbf{u}})^{-1}\overline{\mathbf{s}^{\Delta}} - \mathrm{diag}(\mathbf{H}\overline{\mathbf{W}}\hat{\mathbf{u}})^{-1}\overline{\hat{\mathbf{s}}^{\Delta}}\right), \\
=& \mathbf{W}^{-1}\mathbf{Y}_{LL}^{-1}\overline{\mathbf{W}}^{-1}\left(\mathrm{diag}(\overline{\mathbf{u}})^{-1}\overline{\mathbf{s}^{Y}} - \mathrm{diag}(\overline{\mathbf{u}})^{-1}\overline{\hat{\mathbf{s}}^{Y}}\right) \\
&+ \mathbf{W}^{-1}\mathbf{Y}_{LL}^{-1}\overline{\mathbf{W}}^{-1}\left(\mathrm{diag}(\overline{\mathbf{u}})^{-1}\overline{\hat{\mathbf{s}}^{Y}} - \mathrm{diag}(\overline{\hat{\mathbf{u}}})^{-1}\overline{\hat{\mathbf{s}}^{Y}}\right) \\
&+ \mathbf{W}^{-1}\mathbf{Y}_{LL}^{-1}\mathbf{H}^{T}\left(\mathrm{diag}(\mathbf{H}\overline{\mathbf{W}}\overline{\mathbf{u}})^{-1}\overline{\mathbf{s}^{\Delta}} - \mathrm{diag}(\mathbf{H}\overline{\mathbf{W}}\overline{\mathbf{u}})^{-1}\overline{\hat{\mathbf{s}}^{\Delta}}\right) \\
&+ \mathbf{W}^{-1}\mathbf{Y}_{LL}^{-1}\mathbf{H}^{T}\left(\mathrm{diag}(\mathbf{H}\overline{\mathbf{W}}\overline{\mathbf{u}})^{-1}\overline{\hat{\mathbf{s}}^{\Delta}} - \mathrm{diag}(\mathbf{H}\overline{\mathbf{W}}\hat{\mathbf{u}})^{-1}\overline{\hat{\mathbf{s}}^{\Delta}}\right).
\end{aligned} \tag{2.82}$$

Therefore,

$$\begin{aligned}
\left\|\tilde{\mathbf{G}}_{\mathbf{s}^{Y,\Delta}}(\mathbf{u}) - \hat{\mathbf{u}}\right\|_{\infty} \leq& \left\|\mathbf{W}^{-1}\mathbf{Y}_{LL}^{-1}\overline{\mathbf{W}}^{-1}\left(\mathrm{diag}(\overline{\mathbf{u}})^{-1}\overline{\mathbf{s}^{Y}} - \mathrm{diag}(\overline{\mathbf{u}})^{-1}\overline{\hat{\mathbf{s}}^{Y}}\right)\right\|_{\infty} \\
&+ \left\|\mathbf{W}^{-1}\mathbf{Y}_{LL}^{-1}\overline{\mathbf{W}}^{-1}\left(\mathrm{diag}(\overline{\mathbf{u}})^{-1}\overline{\hat{\mathbf{s}}^{Y}} - \mathrm{diag}(\overline{\hat{\mathbf{u}}})^{-1}\overline{\hat{\mathbf{s}}^{Y}}\right)\right\|_{\infty} \\
&+ \left\|\mathbf{W}^{-1}\mathbf{Y}_{LL}^{-1}\mathbf{H}^{T}\left(\mathrm{diag}(\mathbf{H}\overline{\mathbf{W}}\overline{\mathbf{u}})^{-1}\overline{\mathbf{s}^{\Delta}} - \mathrm{diag}(\mathbf{H}\overline{\mathbf{W}}\overline{\mathbf{u}})^{-1}\overline{\hat{\mathbf{s}}^{\Delta}}\right)\right\|_{\infty} \\
&+ \left\|\mathbf{W}^{-1}\mathbf{Y}_{LL}^{-1}\mathbf{H}^{T}\left(\mathrm{diag}(\mathbf{H}\overline{\mathbf{W}}\overline{\mathbf{u}})^{-1}\overline{\hat{\mathbf{s}}^{\Delta}} - \mathrm{diag}(\mathbf{H}\overline{\mathbf{W}}\hat{\mathbf{u}})^{-1}\overline{\hat{\mathbf{s}}^{\Delta}}\right)\right\|_{\infty}.
\end{aligned} \tag{2.83}$$

[11] Recall that $\tilde{\mathcal{D}}_{\rho}(\hat{\mathbf{u}})$ is defined in (2.54).

According to the proof of Lemma 2.1, we have

$$\left\|\mathbf{W}^{-1}\mathbf{Y}_{LL}^{-1}\overline{\mathbf{W}}^{-1}\left(\mathrm{diag}(\overline{\mathbf{u}})^{-1}\overline{\mathbf{s}^{Y}}-\mathrm{diag}(\overline{\mathbf{u}})^{-1}\overline{\hat{\mathbf{s}}^{Y}}\right)\right\|_{\infty}\leq\frac{\xi^{Y}(\mathbf{s}^{Y,\Delta}-\hat{\mathbf{s}}^{Y,\Delta})}{\alpha(\hat{\mathbf{v}})-\rho}\,, \tag{2.84}$$

$$\left\|\mathbf{W}^{-1}\mathbf{Y}_{LL}^{-1}\overline{\mathbf{W}}^{-1}\left(\mathrm{diag}(\overline{\mathbf{u}})^{-1}\overline{\hat{\mathbf{s}}^{Y}}-\mathrm{diag}(\overline{\hat{\mathbf{u}}})^{-1}\overline{\hat{\mathbf{s}}^{Y}}\right)\right\|_{\infty}\leq\frac{\xi^{Y}(\hat{\mathbf{s}}^{Y,\Delta})\rho}{\Big(\alpha(\hat{\mathbf{v}})-\rho\Big)\alpha(\hat{\mathbf{v}})}\,. \tag{2.85}$$

Furthermore, consider that

$$\begin{aligned}&\mathbf{W}^{-1}\mathbf{Y}_{LL}^{-1}\mathbf{H}^{T}\left(\mathrm{diag}(\mathbf{H}\overline{\mathbf{W}}\overline{\mathbf{u}})^{-1}\overline{\mathbf{s}^{\Delta}}-\mathrm{diag}(\mathbf{H}\overline{\mathbf{W}}\overline{\mathbf{u}})^{-1}\overline{\hat{\mathbf{s}}^{\Delta}}\right)\\ =&\mathbf{W}^{-1}\mathbf{Y}_{LL}^{-1}\mathbf{H}^{T}\mathrm{diag}(|\mathbf{H}||\mathbf{w}|)^{-1}\mathrm{diag}\left(\overline{\mathbf{s}^{\Delta}}-\overline{\hat{\mathbf{s}}^{\Delta}}\right)\begin{bmatrix}\dfrac{1}{\left(\dfrac{(\mathbf{H}\overline{\mathbf{W}}\overline{\mathbf{u}})_1}{(|\mathbf{H}||\mathbf{w}|)_1}\right)}\\ \vdots\\ \dfrac{1}{\left(\dfrac{(\mathbf{H}\overline{\mathbf{W}}\overline{\mathbf{u}})_{3N}}{(|\mathbf{H}||\mathbf{w}|)_{3N}}\right)}\end{bmatrix},\end{aligned} \tag{2.86}$$

$$\begin{aligned}&\mathbf{W}^{-1}\mathbf{Y}_{LL}^{-1}\mathbf{H}^{T}\left(\mathrm{diag}(\mathbf{H}\overline{\mathbf{W}}\overline{\mathbf{u}})^{-1}\overline{\hat{\mathbf{s}}^{\Delta}}-\mathrm{diag}(\mathbf{H}\overline{\mathbf{W}}\hat{\mathbf{u}})^{-1}\overline{\hat{\mathbf{s}}^{\Delta}}\right)\\ =&\mathbf{W}^{-1}\mathbf{Y}_{LL}^{-1}\mathbf{H}^{T}\mathrm{diag}(|\mathbf{H}||\mathbf{w}|)^{-1}\mathrm{diag}\left(\overline{\hat{\mathbf{s}}^{\Delta}}\right)\begin{bmatrix}\dfrac{\left(\dfrac{(\mathbf{H}\overline{\mathbf{W}}\hat{\mathbf{u}})_1}{(|\mathbf{H}||\mathbf{w}|)_1}\right)-\left(\dfrac{(\mathbf{H}\overline{\mathbf{W}}\overline{\mathbf{u}})_1}{(|\mathbf{H}||\mathbf{w}|)_1}\right)}{\left(\dfrac{(\mathbf{H}\overline{\mathbf{W}}\hat{\mathbf{u}})_1}{(|\mathbf{H}||\mathbf{w}|)_1}\right)\left(\dfrac{(\mathbf{H}\overline{\mathbf{W}}\overline{\mathbf{u}})_1}{(|\mathbf{H}||\mathbf{w}|)_1}\right)}\\ \vdots\\ \dfrac{\left(\dfrac{(\mathbf{H}\overline{\mathbf{W}}\hat{\mathbf{u}})_{3N}}{(|\mathbf{H}||\mathbf{w}|)_{3N}}\right)-\left(\dfrac{(\mathbf{H}\overline{\mathbf{W}}\overline{\mathbf{u}})_{3N}}{(|\mathbf{H}||\mathbf{w}|)_{3N}}\right)}{\left(\dfrac{(\mathbf{H}\overline{\mathbf{W}}\hat{\mathbf{u}})_{3N}}{(|\mathbf{H}||\mathbf{w}|)_{3N}}\right)\left(\dfrac{(\mathbf{H}\overline{\mathbf{W}}\overline{\mathbf{u}})_{3N}}{(|\mathbf{H}||\mathbf{w}|)_{3N}}\right)}\end{bmatrix},\end{aligned} \tag{2.87}$$

$$|(\mathbf{HWu})_j-(\mathbf{HW}\hat{\mathbf{u}})_j|\leq\rho(|\mathbf{H}||\mathbf{w}|)_j\,,\qquad\forall j=1,...,3N\,, \tag{2.88}$$

$$|(\mathbf{HWu})_j|\geq(\beta(\hat{\mathbf{v}})-\rho)(|\mathbf{H}||\mathbf{w}|)_j\,,\qquad\forall j=1,...,3N\,. \tag{2.89}$$

We obtain

$$\left\|\mathbf{W}^{-1}\mathbf{Y}_{LL}^{-1}\mathbf{H}^T\left(\mathrm{diag}(\mathbf{H}\overline{\mathbf{W}}\overline{\mathbf{u}})^{-1}\overline{\mathbf{s}^{\Delta}}-\mathrm{diag}(\mathbf{H}\overline{\mathbf{W}}\overline{\mathbf{u}})^{-1}\overline{\hat{\mathbf{s}}^{\Delta}}\right)\right\|_{\infty}\leq\frac{\xi^{\Delta}(\mathbf{s}^{Y,\Delta}-\hat{\mathbf{s}}^{Y,\Delta})}{\beta(\hat{\mathbf{v}})-\rho}\,, \tag{2.90}$$

$$\left\|\mathbf{W}^{-1}\mathbf{Y}_{LL}^{-1}\mathbf{H}^T\left(\mathrm{diag}(\mathbf{H}\overline{\mathbf{W}}\overline{\mathbf{u}})^{-1}\overline{\hat{\mathbf{s}}^{\Delta}}-\mathrm{diag}(\mathbf{H}\overline{\mathbf{W}}\overline{\hat{\mathbf{u}}})^{-1}\overline{\hat{\mathbf{s}}^{\Delta}}\right)\right\|_{\infty}\leq\frac{\xi^{\Delta}(\hat{\mathbf{s}}^{Y,\Delta})\rho}{\Big(\beta(\hat{\mathbf{v}})-\rho\Big)\beta(\hat{\mathbf{v}})}\,. \tag{2.91}$$

By combination of equations (2.83)–(2.85) and (2.90)–(2.91), we get

$$\left\|\tilde{\mathbf{G}}_{\mathbf{s}^{Y,\Delta}}(\mathbf{u})-\hat{\mathbf{u}}\right\|_{\infty}\leq\frac{\xi^{Y}(\mathbf{s}^{Y,\Delta}-\hat{\mathbf{s}}^{Y,\Delta})+\dfrac{\xi^{Y}(\hat{\mathbf{s}}^{Y,\Delta})}{\alpha(\hat{\mathbf{v}})}\rho}{\alpha(\hat{\mathbf{v}})-\rho}+\frac{\xi^{\Delta}(\mathbf{s}^{Y,\Delta}-\hat{\mathbf{s}}^{Y,\Delta})+\dfrac{\xi^{\Delta}(\hat{\mathbf{s}}^{Y,\Delta})}{\beta(\hat{\mathbf{v}})}\rho}{\beta(\hat{\mathbf{v}})-\rho}\,. \tag{2.92}$$

This implies that $\left\|\tilde{\mathbf{G}}_{\mathbf{s}^{Y,\Delta}}(\mathbf{u})-\hat{\mathbf{u}}\right\|_{\infty}\leq\rho$, since ρ satisfies condition (2.44).

Contraction Property

In this part, we assume that $\mathbf{u}$ and $\mathbf{u}'$ are arbitrary elements in $\tilde{\mathcal{D}}_{\rho}(\hat{\mathbf{v}})$. Our goal is to show $\left\|\tilde{\mathbf{G}}_{\mathbf{s}^{Y,\Delta}}(\mathbf{u})-\tilde{\mathbf{G}}_{\mathbf{s}^{Y,\Delta}}(\mathbf{u}')\right\|_{\infty}<\|\mathbf{u}-\mathbf{u}'\|_{\infty}$. Similar to the proof of self-mapping property, we first take the subtraction

$$\begin{aligned}\tilde{\mathbf{G}}_{\mathbf{s}^{Y,\Delta}}(\mathbf{u})-\tilde{\mathbf{G}}_{\mathbf{s}^{Y,\Delta}}(\mathbf{u}')=&\mathbf{W}^{-1}\mathbf{Y}_{LL}^{-1}\overline{\mathbf{W}}^{-1}\left(\mathrm{diag}(\overline{\mathbf{u}})^{-1}\overline{\mathbf{s}^{Y}}-\mathrm{diag}(\overline{\mathbf{u}'})^{-1}\overline{\mathbf{s}^{Y}}\right)\\&+\mathbf{W}^{-1}\mathbf{Y}_{LL}^{-1}\mathbf{H}^T\left(\mathrm{diag}(\mathbf{H}\overline{\mathbf{W}}\overline{\mathbf{u}})^{-1}\overline{\mathbf{s}^{\Delta}}-\mathrm{diag}(\mathbf{H}\overline{\mathbf{W}}\overline{\mathbf{u}'})^{-1}\overline{\mathbf{s}^{\Delta}}\right).\end{aligned} \tag{2.93}$$

Then, there is

$$\begin{aligned}\left\|\tilde{\mathbf{G}}_{\mathbf{s}^{Y,\Delta}}(\mathbf{u})-\tilde{\mathbf{G}}_{\mathbf{s}^{Y,\Delta}}(\mathbf{u}')\right\|_{\infty}\leq&\left\|\mathbf{W}^{-1}\mathbf{Y}_{LL}^{-1}\overline{\mathbf{W}}^{-1}\left(\mathrm{diag}(\overline{\mathbf{u}})^{-1}\overline{\mathbf{s}^{Y}}-\mathrm{diag}(\overline{\mathbf{u}'})^{-1}\overline{\mathbf{s}^{Y}}\right)\right\|_{\infty}\\&+\left\|\mathbf{W}^{-1}\mathbf{Y}_{LL}^{-1}\mathbf{H}^T\left(\mathrm{diag}(\mathbf{H}\overline{\mathbf{W}}\overline{\mathbf{u}})^{-1}\overline{\mathbf{s}^{\Delta}}-\mathrm{diag}(\mathbf{H}\overline{\mathbf{W}}\overline{\mathbf{u}'})^{-1}\overline{\mathbf{s}^{\Delta}}\right)\right\|_{\infty}\\\leq&\left(\frac{\xi^{Y}(\mathbf{s}^{Y,\Delta})}{\Big(\alpha(\hat{\mathbf{v}})-\rho\Big)^2}+\frac{\xi^{\Delta}(\mathbf{s}^{Y,\Delta})}{\Big(\beta(\hat{\mathbf{v}})-\rho\Big)^2}\right)\|\mathbf{u}-\mathbf{u}'\|_{\infty}\end{aligned} \tag{2.94}$$

Since ρ satisfies condition (2.45), we have $\left\|\tilde{\mathbf{G}}_{\mathbf{s}^{Y,\Delta}}(\mathbf{u})-\tilde{\mathbf{G}}_{\mathbf{s}^{Y,\Delta}}(\mathbf{u}')\right\|_{\infty}<\|\mathbf{u}-\mathbf{u}'\|_{\infty}$, which completes the proof.

■

2.F Proof of Theorem 2.2

Given conditions (2.47)–(2.48) are satisfied, we need to show that conditions (2.44)–(2.45) are true for $\rho \in \left[\rho^{\dagger}_{Y,\Delta}(\hat{\mathbf{v}}, \hat{\mathbf{s}}^{Y,\Delta}, \mathbf{s}^{Y,\Delta}), \rho^{\ddagger}_{Y,\Delta}(\hat{\mathbf{v}}, \hat{\mathbf{s}}^{Y,\Delta})\right]$.

First, notice that

$$\begin{aligned}
&\frac{\xi^{Y}(\mathbf{s}^{Y,\Delta} - \hat{\mathbf{s}}^{Y,\Delta}) + \dfrac{\xi^{Y}(\hat{\mathbf{s}}^{Y,\Delta})}{\alpha(\hat{\mathbf{v}})}\rho}{\alpha(\hat{\mathbf{v}}) - \rho} + \frac{\xi^{\Delta}(\mathbf{s}^{Y,\Delta} - \hat{\mathbf{s}}^{Y,\Delta}) + \dfrac{\xi^{\Delta}(\hat{\mathbf{s}}^{Y,\Delta})}{\beta(\hat{\mathbf{v}})}\rho}{\beta(\hat{\mathbf{v}}) - \rho} \\
\leq &\frac{\xi^{Y}(\mathbf{s}^{Y,\Delta} - \hat{\mathbf{s}}^{Y,\Delta}) + \dfrac{\xi^{Y}(\hat{\mathbf{s}}^{Y,\Delta})}{\gamma(\hat{\mathbf{v}})}\rho}{\gamma(\hat{\mathbf{v}}) - \rho} + \frac{\xi^{\Delta}(\mathbf{s}^{Y,\Delta} - \hat{\mathbf{s}}^{Y,\Delta}) + \dfrac{\xi^{\Delta}(\hat{\mathbf{s}}^{Y,\Delta})}{\gamma(\hat{\mathbf{v}})}\rho}{\gamma(\hat{\mathbf{v}}) - \rho} \\
= &\frac{\xi^{Y,\Delta}(\mathbf{s}^{Y,\Delta} - \hat{\mathbf{s}}^{Y,\Delta}) + \dfrac{\xi^{Y,\Delta}(\hat{\mathbf{s}}^{Y,\Delta})}{\gamma(\hat{\mathbf{v}})}\rho}{\gamma(\hat{\mathbf{v}}) - \rho} .
\end{aligned} \tag{2.95}$$

Analogous to the derivation of (2.63), we have

$$\frac{\xi^{Y,\Delta}(\mathbf{s}^{Y,\Delta} - \hat{\mathbf{s}}^{Y,\Delta}) + \dfrac{\xi^{Y,\Delta}(\hat{\mathbf{s}}^{Y,\Delta})}{\gamma(\hat{\mathbf{v}})}\rho}{\gamma(\hat{\mathbf{v}}) - \rho} \leq \rho \,, \tag{2.96}$$

for $\rho \in \left[\rho^{\dagger}_{Y,\Delta}(\hat{\mathbf{v}}, \hat{\mathbf{s}}^{Y,\Delta}, \mathbf{s}^{Y,\Delta}), \rho^{\ddagger}_{Y,\Delta}(\hat{\mathbf{v}}, \hat{\mathbf{s}}^{Y,\Delta})\right]$. In this way, we obtain that condition (2.44) is true for $\rho \in \left[\rho^{\dagger}_{Y,\Delta}(\hat{\mathbf{v}}, \hat{\mathbf{s}}^{Y,\Delta}, \mathbf{s}^{Y,\Delta}), \rho^{\ddagger}_{Y,\Delta}(\hat{\mathbf{v}}, \hat{\mathbf{s}}^{Y,\Delta})\right]$.

Next, we consider that

$$\begin{aligned}
&\frac{\xi^{Y}(\mathbf{s}^{Y,\Delta})}{\Big(\alpha(\hat{\mathbf{v}}) - \rho\Big)^2} + \frac{\xi^{\Delta}(\mathbf{s}^{Y,\Delta})}{\Big(\beta(\hat{\mathbf{v}}) - \rho\Big)^2} \\
\leq &\frac{\xi^{Y}(\mathbf{s}^{Y,\Delta})}{\Big(\gamma(\hat{\mathbf{v}}) - \rho\Big)^2} + \frac{\xi^{\Delta}(\mathbf{s}^{Y,\Delta})}{\Big(\gamma(\hat{\mathbf{v}}) - \rho\Big)^2} \\
= &\frac{\xi^{Y,\Delta}(\mathbf{s}^{Y,\Delta})}{\Big(\gamma(\hat{\mathbf{v}}) - \rho\Big)^2} .
\end{aligned} \tag{2.97}$$

By analogy to the derivation of (2.70), we have

$$\frac{\xi^{Y,\Delta}(\mathbf{s}^{Y,\Delta})}{\Big(\gamma(\hat{\mathbf{v}})-\rho\Big)^2}<1\,, \tag{2.98}$$

for $\rho\in\Big[\rho^{\dagger}_{Y,\Delta}(\hat{\mathbf{v}},\hat{\mathbf{s}}^{Y,\Delta},\mathbf{s}^{Y,\Delta}),\rho^{\ddagger}_{Y,\Delta}(\hat{\mathbf{v}},\hat{\mathbf{s}}^{Y,\Delta})\Big]$. In this way, we obtain that condition (2.45) is true for $\rho\in\Big[\rho^{\dagger}_{Y,\Delta}(\hat{\mathbf{v}},\hat{\mathbf{s}}^{Y,\Delta},\mathbf{s}^{Y,\Delta}),\rho^{\ddagger}_{Y,\Delta}(\hat{\mathbf{v}},\hat{\mathbf{s}}^{Y,\Delta})\Big]$, which completes the proof.

■

2.G Proof of Proposition 2.2

For the First Item

In order to prove that $\mathbf{J}_{\mathbf{F}^{Y,\Delta}}(\hat{\mathbf{v}},\hat{\mathbf{i}}^{\Delta})$ is non-singular, we need to show

$$\mathbf{J}_{\mathbf{F}^{Y,\Delta}}(\hat{\mathbf{v}},\hat{\mathbf{i}}^{\Delta})\cdot\begin{bmatrix}\mathbf{d}\\ \mathbf{g}\end{bmatrix}=\mathbf{0}\qquad\Rightarrow\qquad\begin{bmatrix}\mathbf{d}\\ \mathbf{g}\end{bmatrix}=\mathbf{0}\,. \tag{2.99}$$

Similar to the proof of Proposition 2.1, we show by contradiction. First, we assume that there exists a $\begin{bmatrix}\mathbf{d}\\ \mathbf{g}\end{bmatrix}\neq\mathbf{0}$ such that $\mathbf{J}_{\mathbf{F}^{Y,\Delta}}(\hat{\mathbf{v}},\hat{\mathbf{i}}^{\Delta})\cdot\begin{bmatrix}\mathbf{d}\\ \mathbf{g}\end{bmatrix}=\mathbf{0}$. Clearly, for any $\epsilon>0$, $\epsilon\begin{bmatrix}\mathbf{d}\\ \mathbf{g}\end{bmatrix}$ satisfies

$$\mathbf{J}_{\mathbf{F}^{Y,\Delta}}(\hat{\mathbf{v}},\hat{\mathbf{i}}^{\Delta})\cdot\left(\epsilon\begin{bmatrix}\mathbf{d}\\ \mathbf{g}\end{bmatrix}\right)=\mathbf{0}\,. \tag{2.100}$$

Then, let $\begin{bmatrix}\mathbf{v}_\epsilon{}'\\ (\mathbf{i}^{\Delta}_\epsilon)'\end{bmatrix}=\begin{bmatrix}\hat{\mathbf{v}}+\epsilon\mathbf{d}\\ \hat{\mathbf{i}}^{\Delta}+\epsilon\mathbf{g}\end{bmatrix}$ and $\begin{bmatrix}\mathbf{v}_\epsilon{}''\\ (\mathbf{i}^{\Delta}_\epsilon)''\end{bmatrix}=\begin{bmatrix}\hat{\mathbf{v}}-\epsilon\mathbf{d}\\ \hat{\mathbf{i}}^{\Delta}-\epsilon\mathbf{g}\end{bmatrix}$. Notice that, these two system electrical states correspond to the same system power injection, i.e., $\mathbf{F}^{Y,\Delta}(\mathbf{v}_\epsilon{}',(\mathbf{i}^{\Delta}_\epsilon)')=\mathbf{F}^{Y,\Delta}(\mathbf{v}_\epsilon{}'',(\mathbf{i}^{\Delta}_\epsilon)'')$.

Next, we find a small enough $\epsilon^*>0$ such that

- The system power injection $\mathbf{F}^{Y,\Delta}(\mathbf{v}_\epsilon{}',(\mathbf{i}^{\Delta}_\epsilon)')$ satisfies condition (2.48),
- Both $\mathbf{v}_\epsilon{}'$ and $\mathbf{v}_\epsilon{}''$ are included in domain $\mathcal{D}_\rho(\hat{\mathbf{v}})$ with $\rho=\rho^{\ddagger}_{Y,\Delta}(\hat{\mathbf{v}},\hat{\mathbf{s}}^{Y,\Delta})$.

This creates a contradiction, since Theorem 2.2 and equation (2.39) enforce that $\begin{bmatrix}\mathbf{v}_\epsilon{}'\\ (\mathbf{i}^{\Delta}_\epsilon)'\end{bmatrix}=\begin{bmatrix}\mathbf{v}_\epsilon{}''\\ (\mathbf{i}^{\Delta}_\epsilon)''\end{bmatrix}$. Therefore, both $\mathbf{d}$ and $\mathbf{g}$ must be $\mathbf{0}$, and $\mathbf{J}_{\mathbf{F}^{Y,\Delta}}(\hat{\mathbf{v}},\hat{\mathbf{i}}^{\Delta})$ is non-singular.

For the Second Item

As the guaranteed solution $\mathbf{v}$ belongs to domain $\mathcal{D}_\rho(\hat{\mathbf{v}})$ with $\rho = \rho^{\ddagger}_{Y,\Delta}(\hat{\mathbf{v}}, \hat{\mathbf{s}}^{Y,\Delta})$, we have

$$\begin{aligned}\gamma(\hat{\mathbf{v}}) - \rho^{\ddagger}_{Y,\Delta}(\hat{\mathbf{v}}, \hat{\mathbf{s}}^{Y,\Delta}) \leq & \alpha(\hat{\mathbf{v}}) - \rho^{\ddagger}_{Y,\Delta}(\hat{\mathbf{v}}, \hat{\mathbf{s}}^{Y,\Delta}) \\ \leq & \alpha(\mathbf{v}) \,, \end{aligned} \tag{2.101}$$

$$\begin{aligned}\gamma(\hat{\mathbf{v}}) - \rho^{\ddagger}_{Y,\Delta}(\hat{\mathbf{v}}, \hat{\mathbf{s}}^{Y,\Delta}) \leq & \beta(\hat{\mathbf{v}}) - \rho^{\ddagger}_{Y,\Delta}(\hat{\mathbf{v}}, \hat{\mathbf{s}}^{Y,\Delta}) \\ \leq & \beta(\mathbf{v}) \,. \end{aligned} \tag{2.102}$$

Combining the two inequalities, we get

$$\gamma(\hat{\mathbf{v}}) - \rho^{\ddagger}_{Y,\Delta}(\hat{\mathbf{v}}, \hat{\mathbf{s}}^{Y,\Delta}) \leq \gamma(\mathbf{v}) \,. \tag{2.103}$$

Furthermore, by (2.98), there is

$$\xi^{Y,\Delta}(\mathbf{s}^{Y,\Delta}) < \Big(\gamma(\mathbf{v})\Big)^2 \,, \tag{2.104}$$

which is equivalent to $\rho^{\ddagger}_{Y,\Delta}(\mathbf{v}, \mathbf{s}^{Y,\Delta}) > 0$ and completes the proof.

■

3 Admissibility of Uncertain Power Injections

She melts into the throng with trails of scents.
In the crowd once and again,
I look for her in vain.
When all at once I turn my head,
I find her there where lantern light is dimly shed.

The Lantern Festival Night
XIN QIJI

3.1 Introduction

Motivation

In the last chapter, we have studied the existence and uniqueness of the power-flow solution that is used to determine whether, for a target system power injection, there exists a system electrical state that satisfies the security constraints. In this chapter, we continue focusing on the network security and take into account that the actual system power injection might be uncertain and different from the target one in practical ADNs due to, for example, uncaptured system dynamics, reaction delays, and disturbances from the nature of renewable energy.

Formally, let us assume that the distribution network is steered by a network control system (e.g., the Commelec [16, 17]). At some time t_0, the network control system obtains the initial system electrical state $\mathbf{v}^{\text{initial}}$ via state estimation processes and decides the target system power injection for some future time instant t_1. During the time interval $[t_0, t_1]$, the actual system power injection is uncertain and is supposed to reside in some set $\mathcal{S}^{\text{uncertain}}$ that includes both the initial and the target system power injections. As a result of the uncertainty in the system power injection, the actual system electrical state cannot be predicted precisely during $[t_0, t_1]$, which makes it

difficult to ensure the satisfaction of the security constraints.

The above issue motivates another inverse problem that is referred to as the "admissibility problem". More precisely, let set $\mathcal{V}^\star$ collect all system electrical states that satisfy the security constraints and the non-singularity of the power-flow Jacobian. Consider that the system electrical state typically evolves as a continuous function of time due to the physical nature, our goal is to see whether we can ensure that the continuous path of the actual system electrical state remains in $\mathcal{V}^\star$, given that (i) it starts at $\mathbf{v}^{\text{initial}} \in \mathcal{V}^\star$, and that (ii) the corresponding path of the actual system power injection belongs to $\mathcal{S}^{\text{uncertain}}$. If we can, then we say that $\mathcal{S}^{\text{uncertain}}$ is admissible for $\mathbf{v}^{\text{initial}}$. To solve the admissibility problem, a major difficulty is that each system power injection might correspond to zero or multiple system electrical states. Specifically,

1. Some of the system power injections in $\mathcal{S}^{\text{uncertain}}$ might not have corresponding system electrical states in $\mathcal{V}^\star$. As a result, it is impossible for the system electrical state to stay in $\mathcal{V}^\star$ when any of these system power injections is implemented.

2. Even if every system power injection in $\mathcal{S}^{\text{uncertain}}$ has at least one corresponding system electrical state in $\mathcal{V}^\star$, we still might not be able to ensure that the system electrical state remains in $\mathcal{V}^\star$. For example, let us consider the single-phase radial network given in [18], which is shown in Figure 3.1.

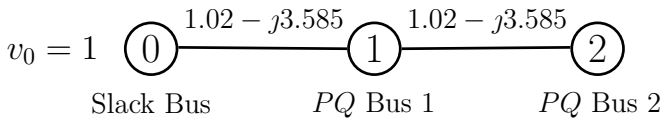

Figure 3.1 – The radial network in [18]. The slack-bus voltage and line parameters are given in p.u.

   In this network, a system electrical state satisfies the security constraints if the nodal voltage magnitudes at both PQ buses are between 0.9 and 1.1 p.u. With per-unit initial system power injection $\mathbf{s}^{\text{initial}}$=$(-1.105 + \jmath 1, -1 + \jmath 1.105)^T$, there are two system electrical states in $\mathcal{V}^\star$. They are marked by "diamond" and "square" in Figure 3.2. Now, let $\mathcal{S}^{\text{uncertain}}$ collect all system power injections that are obtained by linearly scaling the initial system power injection with a real factor in $[0.992, 1]$. Suppose that the system electrical state is initialized at the diamond in $\mathcal{V}^\star$ and continuously moves along the "Voltage Branch A" in Figure 3.2. In the meantime, the system power injection continuously decreases in $\mathcal{S}^{\text{uncertain}}$. As can be seen, the system electrical state immediately exits $\mathcal{V}^\star$. But, there is a corresponding system electrical state in $\mathcal{V}^\star$ on "Voltage Branch B" for every system power injection in $\mathcal{S}^{\text{uncertain}}$.

Evidently, the admissibility problem is harder than the AC power-flow problem.

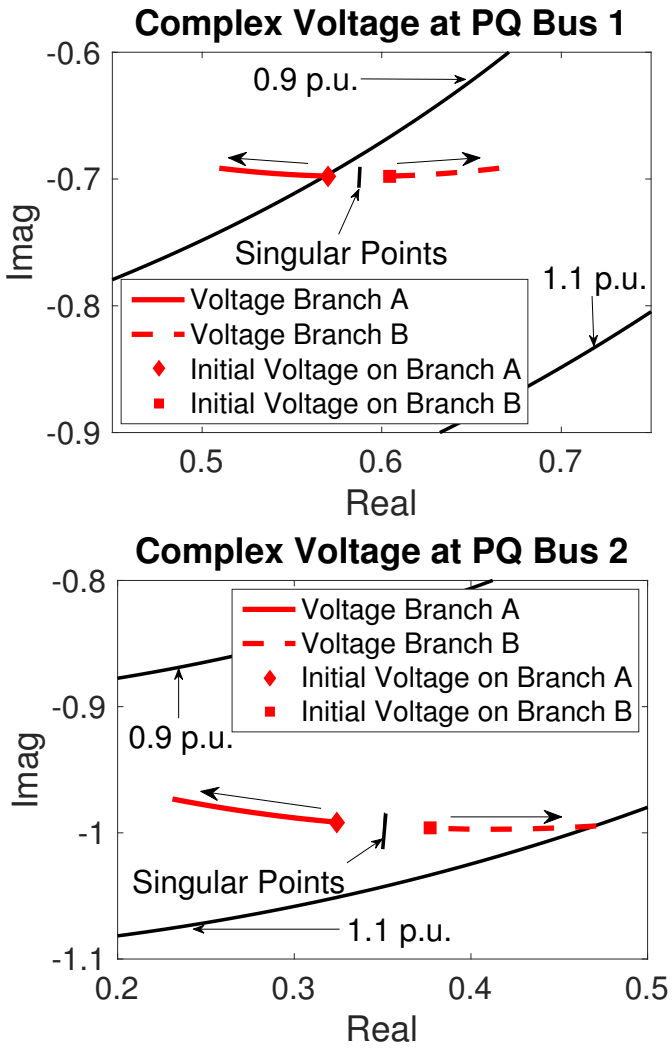

Figure 3.2 – For initial system power injection $\mathbf{s}^{\text{initial}}=(-1.105+\jmath 1, -1+\jmath 1.105)^T$, there are two system electrical states in $\mathcal{V}^\star$. They are marked by "diamond" $(0.901\angle -0.886, 1.043\angle -0.857)^T$ and "square" $(0.923\angle -1.255, 1.065\angle -1.209)^T$. If we continuously scale down the system power injection by a real factor from 1 to 0.992, then the system electrical state moves along either "Voltage Branch A" or "Voltage Branch B", depending on its own initialization.

Contributions and Chapter Outline

In Section 3.3.1, we mathematically formulate the admissibility problem.

In Section 3.3.2, we layout the theoretical foundations for solving the admissibility problem:

1. We introduce the auxiliary concept of $\mathcal{V}$-control. More precisely, we say that $\mathcal{S}$ is a "domain of $\mathcal{V}$-control" if: any continuous path of the system electrical state that starts in $\mathcal{V}$ must stay in $\mathcal{V}$, as long as the corresponding path of the system power injection is constrained in $\mathcal{S}$. With the concept of $\mathcal{V}$-control, the admissibility problem consists in whether there exists a set $\mathcal{V} \subseteq \mathcal{V}^\star$ such that (i) $\mathbf{v}^{\text{initial}} \in \mathcal{V}$, and (ii) $\mathcal{S}^{\text{uncertain}}$ is a domain of $\mathcal{V}$-control.

2. According to our discussions at the beginning of this chapter, we see that $\mathcal{V}$-control might not hold due to zero or multiple power-flow solutions. This could lead to a conjecture that $\mathcal{V}$-control holds if and only if there exists a unique power-flow solution $\mathbf{v} \in \mathcal{V}$ for every $\mathbf{s} \in \mathcal{S}$. We disprove this conjecture by examples. Specifically,

   - We give an example where there exists a unique power-flow solution $\mathbf{v} \in \mathcal{V}$ for every $\mathbf{s} \in \mathcal{S}$, but $\mathcal{S}$ is not a domain of $\mathcal{V}$-control.
   - We give another example where $\mathcal{S}$ is a domain of $\mathcal{V}$-control, but there exists more than one power-flow solution in $\mathcal{V}$ for almost every $\mathbf{s} \in \mathcal{S}$.

3. For $\mathcal{S}$ to be a domain of $\mathcal{V}$-control, we give sufficient conditions in Lemma 3.1, including

   - the openness of $\mathcal{V}$,
   - the existence of a unique power-flow solution $\mathbf{v} \in \mathcal{V}$ for every $\mathbf{s} \in \mathcal{S}$,
   - the continuity of the inverse power-flow mapping from $\mathcal{S}$ to $\mathcal{V}$.

   By using the inverse function theorem, we replace the continuity condition in Lemma 3.1 with the non-singularity of the power-flow Jacobian in $\mathcal{V}$, which gives us Theorem 3.1. Compared to Lemma 3.1, Theorem 3.1 has better practical applicability.

   Further, by the real-quadratic nature of $\mathbf{F}$ in rectangular coordinates, we obtain Theorem 3.2 as an alternative to Theorem 3.1. The difference between the two theorems is that the non-singularity condition in Theorem 3.1 is replaced by the openness of $\mathcal{S}$ in Theorem 3.2.

4. We give Theorems 3.3 and 3.4 that can be used to ensure the existence of a unique power-flow solution $\mathbf{v} \in \mathcal{V}$ for every $\mathbf{s} \in \mathcal{S}$. Specifically,

   - In Theorem 3.3, we show that if $\mathcal{V}$ is convex and the power-flow Jacobian $\mathbf{J_F}$ is non-singular everywhere in $\mathcal{V}$, then $\mathcal{V}$ is a domain of uniqueness (i.e., $\mathbf{F}(\mathbf{v}) = \mathbf{F}(\mathbf{v}') \Rightarrow \mathbf{v} = \mathbf{v}',\ \forall \mathbf{v}, \mathbf{v}' \in \mathcal{V}$).
   - In Theorem 3.4, we provide sufficient conditions to ensure that there exists a power-flow solution $\mathbf{v} \in \mathcal{V}$ for every $\mathbf{s} \in \mathcal{S}$, by exploiting the topological properties of $\mathcal{V}$ and $\mathcal{S}$.

5. We incidentally obtain in Theorem 3.5 that $\mathbf{J_F}$ is non-singular throughout $\mathcal{V}$ if $\mathcal{V}$ is open and a domain of uniqueness. Note that
   - this is the converse of the inverse function theorem,
   - this is true due to the real-quadratic nature of $\mathbf{F}$ in rectangular coordinates.

In Section 3.4, we develop a first solution method for the admissibility problem, using Theorems 3.1, 3.3, and 3.4. Specifically,

- In Section 3.4.1, we establish a high-level framework that contains the general ideas and the key steps of our first solution method. The framework requires an explicit condition on the non-singularity of $\mathbf{J_F}$ and needs to perform infeasibility check for a group of optimization problems.
- In Section 3.4.2, we concretize the high-level framework and obtain our first solution method. During the infeasibility check, this method employs the semi-definite programming relaxation of polynomial optimizations [59, 60, 61].

Through numerical examples, we see that this method is tight in the sense that it almost finds the largest $\mathcal{S}^{\text{uncertain}}$ that is admissible for some given $\mathbf{v}^{\text{initial}} \in \mathcal{V}^{\star}$. However, we also see that the method has a relatively high computational complexity and requires large memory for data storage and manipulation. Thus, this method is not suitable for real-time applications in large networks.

In Section 3.5, we develop a second solution method for the admissibility problem, using Theorem 3.2 and the results in Chapter 2. Compared to the first solution method, this second solution method is less tight. But, it is suitable for real-time applications in large networks.

3.2 State of the Art

In the pioneering work of Commelec [16, 17], the authors investigate how to ensure that the actual system electrical state satisfies the security constraints, given that the actual system power injection is constrained in the uncertainty set. There, the main idea is to check whether the extreme values of the nodal-voltage and branch-current magnitudes violate the security constraints. To this end, the authors assume:

(A1) For any system power injection in the uncertainty set, if there exists a power-flow solution that satisfies the security constraints, then this solution is unique.

(A2) The nodal-voltage magnitudes and the branch-current magnitudes are monotonic functions of the nodal power injections; the extreme values of the nodal-

voltage and branch-current magnitudes are obtained at the extreme values of the nodal power injections.

However, these two assumptions might not hold in practice:

- As shown in Figure 3.2, there can be more than one power-flow solution satisfying the security constraints.
- In Section 3.5.3, we give an example where the extreme values of the nodal-voltage magnitudes are not obtained at the extreme values of the nodal power injections.

In [62], another method is developed to ensure that the security constraints are always satisfied, given that the system power injection is constrained in the uncertainty set. The development of this method is based on the results in [63, 64] that are originally established for robust optimal power flow. In order to apply this method, the following assumptions are made:

(A1') There exists a high-voltage power-flow solution for every system power injection in the uncertainty set.

(A2') All possible low-voltage power-flow solutions can be precluded by some lower bounds on the nodal-voltage magnitudes.

If both (A1') and (A2') are true, then the method is able to determine whether the security constraints are always ensured, by relaxing the multi-dimensional power-flow equation and iteratively solving a collection of optimization problems. Note that this method is problematic, because

- There is no means to guarantee that (A1') and (A2') are true.
- There is no theoretical guarantee on the performance and convergence.
- There is no proof for the ensured satisfaction of the security constraints.

In [65], rigorous sufficient conditions are proposed to ensure that, for every system power injection in the uncertainty set, there exists a system electrical state that satisfies the security constraints. These conditions exploit the non-singularity of the power-flow Jacobian as well as the topological properties in both the space of system electrical states and the space of system power injections, which essentially share the same spirit with the conditions in our Theorem 3.4. In addition to the proposed sufficient conditions, a practical method is developed for testing whether the sufficient conditions

are satisfied by the uncertainty set. This method uses the semi-definite programming relaxation of polynomial optimizations, which is inspired by the works [66, 67, 68].

Note that the results in [65] do not solve the admissibility problem, as the existence of a power-flow solution $\mathbf{v} \in \mathcal{V}^\star$ for every $\mathbf{s} \in \mathcal{S}^{\text{uncertain}}$ is only a necessary condition for the admissibility.

3.3 Admissibility Problem and Theoretical Foundations of Solution Methods

3.3.1 Definition of Admissibility and Problem Formulation

Let $\mathcal{S}^{\text{uncertain}}$ be the uncertainty set that constrains the actual system power injection. Additionally, let

$$\mathcal{V}^\star = \left\{ \mathbf{v} : \ f_\ell(\mathbf{v}) > 0, \ \ell \in \{1, ..., L^{\text{secure}}\}, \text{ and } \mathbf{J}_{\mathbf{F}}(\mathbf{v}) \text{ is non-singular} \right\}, \tag{3.1}$$

where

- $f_\ell, \ \ell \in \{1, ..., L^{\text{secure}}\}$ are continuous functions,
- $f_\ell(\mathbf{v}) > 0, \ \ell \in \{1, ..., L^{\text{secure}}\}$ are security constraints on the system electrical state.

In this chapter, we consider the linear relation (2.1) between the branch currents $\mathbf{i}_{jk}$ and the complex nodal voltages $\mathbf{v}_j$, $\mathbf{v}_k$, and we take the following concrete forms of $f_\ell(\mathbf{v}) > 0, \ \ell \in \{1, ..., L^{\text{secure}}\}$:

$$\mathbf{v}_j^{\min} < |\mathbf{v}_j| < \mathbf{v}_j^{\max}, \qquad j \in \mathcal{N} \setminus \{0\}, \tag{3.2a}$$

$$|\mathbf{A}_{j,k}\mathbf{v}_j - \mathbf{C}_{j,k}\mathbf{v}_k| < \mathbf{i}_{jk}^{\max}, \qquad jk \in \mathcal{E}, \tag{3.2b}$$

where

- $\mathbf{v}_j^{\min} \in \mathbb{R}^{N^{\text{phase}}}$, $\mathbf{v}_j^{\max} \in \mathbb{R}^{N^{\text{phase}}}$, $\mathbf{i}_{jk}^{\max} \in \mathbb{R}^{N^{\text{phase}}}$ are some pre-determined positive real security bounds,
- $<$ means the component-wise less-than inequality,[1]
- $|\cdot|$ means the component-wise absolute value.

[1] Similar definitions hold for $>$, $\leq$, and $\geq$.

The security constraints (3.2a)–(3.2b) can also be written as the following 2-degree polynomial inequalities in $\Re(\mathbf{v})$ and $\Im(\mathbf{v})$,

$$\operatorname{diag}\Big(|\mathbf{v}_j|\Big)|\mathbf{v}_j| - \operatorname{diag}\Big(\mathbf{v}_j^{\min}\Big)\mathbf{v}_j^{\min} > \mathbf{0}\,, \qquad j \in \mathcal{N} \setminus \{0\}\,, \tag{3.3a}$$

$$-\operatorname{diag}\Big(|\mathbf{v}_j|\Big)|\mathbf{v}_j| + \operatorname{diag}\Big(\mathbf{v}_j^{\max}\Big)\mathbf{v}_j^{\max} > \mathbf{0}\,, \qquad j \in \mathcal{N} \setminus \{0\}\,, \tag{3.3b}$$

$$-\operatorname{diag}\Big(|\mathbf{A}_{j,k}\mathbf{v}_j - \mathbf{C}_{j,k}\mathbf{v}_k|\Big)|\mathbf{A}_{j,k}\mathbf{v}_j - \mathbf{C}_{j,k}\mathbf{v}_k| + \operatorname{diag}\Big(\mathbf{i}_{jk}^{\max}\Big)\mathbf{i}_{jk}^{\max} > \mathbf{0}\,, \qquad jk \in \mathcal{E}\,, \tag{3.3c}$$

which are useful in Section 3.4.2.

As discussed at the beginning of this chapter, we are interested in ensuring $\mathbf{v} \in \mathcal{V}^\star$ by maintaining $\mathbf{s} \in \mathcal{S}^{\text{uncertain}}$, for which we introduce the following definition of "admissibility".

Definition 3.1

Given any initial system electrical state $\mathbf{v}^{\text{initial}}$ and uncertainty set $\mathcal{S}^{\text{uncertain}}$ of system power injections such that

(I1) $\mathbf{v}^{\text{initial}} \in \mathcal{V}^\star$,

(I2) $\mathbf{F}(\mathbf{v}^{\text{initial}}) \in \mathcal{S}^{\text{uncertain}}$.

We say $\mathcal{S}^{\text{uncertain}}$ is admissible *for $\mathbf{v}^{\text{initial}}$ if, for any continuous function $\mathbf{v}(t), t \in [0,1]$ such that $\mathbf{v}(0) = \mathbf{v}^{\text{initial}}$ and $\mathbf{F}(\mathbf{v}(t)) \in \mathcal{S}^{\text{uncertain}}, \forall t \in [0,1]$, we have that $\mathbf{v}(t) \in \mathcal{V}^\star, \forall t \in [0,1]$.*

Clearly, given any $\mathbf{v}^{\text{initial}}$ and $\mathcal{S}^{\text{uncertain}}$ that satisfy (I1)–(I2) in Definition 3.1, if $\mathcal{S}^{\text{uncertain}}$ is admissible for $\mathbf{v}^{\text{initial}}$ and the system electrical state moves as a continuous function of time, then the system electrical state must stay in $\mathcal{V}^\star$.

Using the above formal definition of admissibility, we formulate the problem of interest as follows.

Problem 3.1 (*Admissibility Problem*)

Given an initial system electrical state $\mathbf{v}^{\text{initial}}$ and an uncertainty set $\mathcal{S}^{\text{uncertain}}$ of system power injections that satisfy the conditions (I1)–(I2) in Definition 3.1, is $\mathcal{S}^{\text{uncertain}}$ admissible for $\mathbf{v}^{\text{initial}}$?

3.3.2 Theoretical Foundations of Solution Methods

In this section, we progressively layout the theoretical foundations for solving the admissibility problem.

Auxiliary Concept of $\mathcal{V}$-Control and Its Relation with Admissibility

First, we introduce the following auxiliary concept of $\mathcal{V}$-control.

Definition 3.2

For a set $\mathcal{V}$ of system electrical states and a set $\mathcal{S}$ of system power injections: $\mathcal{S}$ is a domain of $\mathcal{V}$-control *if, for any continuous path $\mathbf{v}(t), t \in [0,1]$ such that $\mathbf{v}(0) \in \mathcal{V}$ and $\mathbf{F}(\mathbf{v}(t)) \in \mathcal{S}, \forall t \in [0,1]$, we have $\mathbf{v}(t) \in \mathcal{V}, \forall t \in [0,1]$.*

In Definition 3.2, the concept of $\mathcal{V}$-control can be interpreted as: keeping the continuous path $\mathbf{v}(t)$ in $\mathcal{V}$ by maintaining the continuous path $\mathbf{s}(t)$ in $\mathcal{S}$. For $\mathcal{S}$ to be a domain of $\mathcal{V}$-control, a necessary condition is the existence of a power-flow solution in $\mathcal{V}$ for every $\mathbf{s} \in \mathcal{S}$.

Through comparison between Definitions 3.1 and 3.2, we have:

$\mathcal{S}^{\text{uncertain}}$ is admissible for $\mathbf{v}^{\text{initial}}$ if there exists a set $\mathcal{V}$ such that

(O1) $\mathcal{V} \subseteq \mathcal{V}^{\star}$,

(O2) $\mathbf{v}^{\text{initial}} \in \mathcal{V}$,

(O3) $\mathcal{S}^{\text{uncertain}}$ is a domain of $\mathcal{V}$-control.

As can be seen, in order to solve the admissibility problem, we need to find sufficient conditions for $\mathcal{V}$-control.

Existence and Uniqueness of the Power-Flow Solution $\nLeftrightarrow$ $\mathcal{V}$-Control

According to our discussions at the beginning of this chapter, we see that $\mathcal{V}$-control might not hold due to zero or multiple power-flow solutions. This could give us a wrong impression that $\mathcal{V}$-control holds if and only if there exists a unique power-flow solution $\mathbf{v} \in \mathcal{V}$ for every $\mathbf{s} \in \mathcal{S}$. We clarify this by the following two examples.

(**E1**) First, we give an example where there exists a unique power-flow solution $\mathbf{v} \in \mathcal{V}$ for every $\mathbf{s} \in \mathcal{S}$, but $\mathcal{S}$ is not a domain of $\mathcal{V}$-control.

Consider again the single-phase network in Figure 3.1. In this network, when $\mathbf{s} = 0.999915\mathbf{s}^{\text{initial}}$, the corresponding system electrical state on "Voltage Branch A" of Figure 3.2 touches the lower voltage-security bound. In view of this, let us assume that

- $\mathcal{S} = \mathcal{S}^{\text{A}} \bigcup \mathcal{S}^{\text{B}}$ where
  - $\mathcal{S}^{\text{A}} = \{\mathbf{s} : \mathbf{s} = \kappa \mathbf{s}^{\text{initial}}, \kappa \in (0.999915, 1]\}$,
  - $\mathcal{S}^{\text{B}} = \{\mathbf{s} : \mathbf{s} = \kappa \mathbf{s}^{\text{initial}}, \kappa \in [0.999, 0.999915]\}$.
- $\mathcal{V} = \mathcal{V}^{\text{A}} \bigcup \mathcal{V}^{\text{B}}$ where
  - $\mathcal{V}^{\text{A}} = \{\mathbf{v} \in \text{Voltage Branch A} : \mathbf{F}(\mathbf{v}) \in \mathcal{S}^{\text{A}}\}$,
  - $\mathcal{V}^{\text{B}} = \{\mathbf{v} \in \text{Voltage Branch B} : \mathbf{F}(\mathbf{v}) \in \mathcal{S}^{\text{B}}\}$.

Clearly, for any $\mathbf{s} \in \mathcal{S}$, there exists a unique $\mathbf{v} \in \mathcal{V}$ such that $\mathbf{F}(\mathbf{v}) = \mathbf{s}$. But $\mathcal{S}$ is not a domain of $\mathcal{V}$-control. To prove this, we show $\mathcal{V}^{\text{A}}$ and $\mathcal{V}^{\text{B}}$ in Figure 3.3, by magnifying the regions near the "diamond" and "square" in Figure 3.2. Suppose that the system electrical state is initialized at the "diamond" in Figure 3.3(a) and moves along "Voltage Branch A" from the "diamond" to the "ring". Once the system electrical state reaches the "ring", it exits $\mathcal{V}$. Nonetheless, the system power injection $\mathbf{s}$ still belongs to $\mathcal{S}$, which completes the proof.

(**E2**) Second, we give an example where $\mathcal{S}$ is a domain of $\mathcal{V}$-control, but there exists more than one power-flow solution in $\mathcal{V}$ for almost every $\mathbf{s} \in \mathcal{S}$.

Consider a single-phase two-bus network where the only PQ bus is connected to the slack bus via a purely resistive transmission line. Assume that

- the slack-bus voltage is 1 p.u.,
- the resistance of the transmission line is 1 p.u.,
- $\mathcal{S} = \{\mathbf{s} : \Re(\mathbf{s}) \in [-0.25, 0] \, , \, \Im(\mathbf{s}) = 0\}$.

Then, it can be derived that for any $\mathbf{s} \in \mathcal{S}$, the power-flow solution $\mathbf{v}$ must satisfy:

- $\Re(\mathbf{v})\Big(\Re(\mathbf{v}) - 1\Big) = \Re(\mathbf{s})$,
- $\Im(\mathbf{v}) = 0$.

As a consequence,

- there exists a unique power-flow solution $\mathbf{v} = 0.5$ p.u. for $\mathbf{s} = -0.25$ p.u.,
- there exist two power-flow solutions, $0.5 \pm \sqrt{0.25 + \Re(\mathbf{s})}$, for every $\mathbf{s} \in \mathcal{S} \setminus \{-0.25\}$.

It can be easily verified that $\mathcal{S}$ is a domain of $\mathcal{V}$-control for $\mathcal{V} = \{\mathbf{v} : \Re(\mathbf{v}) \in [0, 1] \, , \, \Im(\mathbf{v}) = 0\}$. However, there exists more than one power-flow solution in $\mathcal{V}$ for all but one $\mathbf{s} \in \mathcal{S}$.

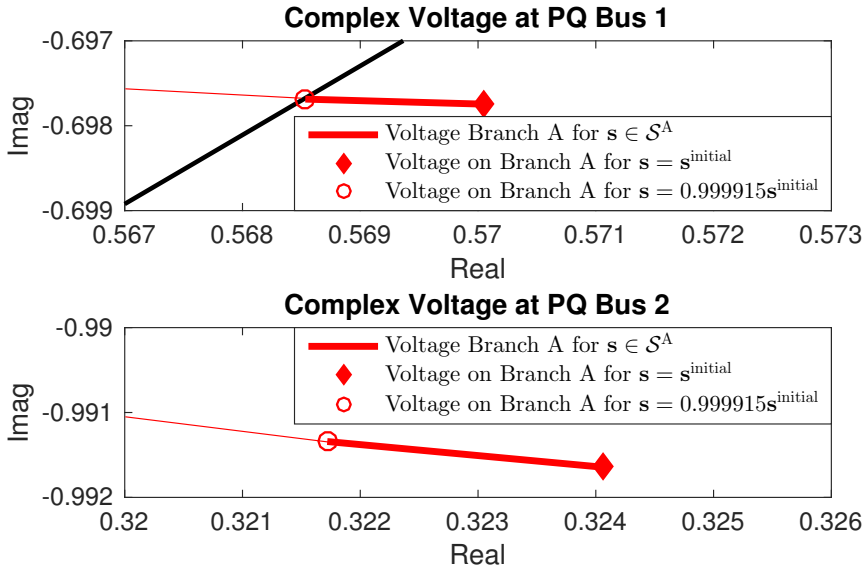

(a)

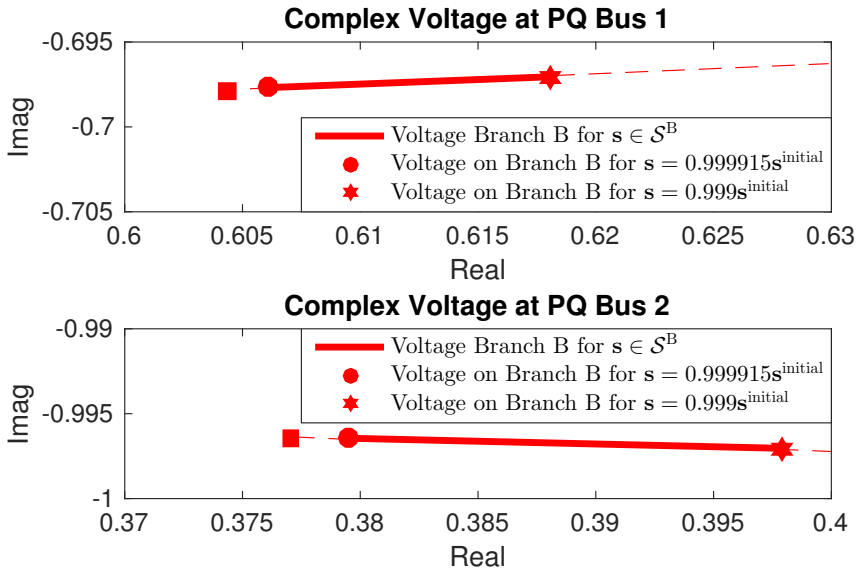

(b)

Figure 3.3 – In (a), "diamond" and "ring", respectively, represent the system electrical states on the "Voltage Branch A" in Figure 3.2 for $\mathbf{s} = \mathbf{s}^{\mathrm{initial}}$ and $\mathbf{s} = 0.999915\mathbf{s}^{\mathrm{initial}}$. In (b), "circle" and "hexagram", respectively, represent the system electrical states on the "Voltage Branch B" in Figure 3.2 for $\mathbf{s} = 0.999915\mathbf{s}^{\mathrm{initial}}$ and $\mathbf{s} = 0.999\mathbf{s}^{\mathrm{initial}}$.

Sufficient Conditions for $\mathcal{V}$-Control

We start with the following lemma that mainly relies on the openness of $\mathcal{V}$ and the continuous inverse of $\mathbf{F}$ from $\mathcal{S}$ to $\mathcal{V}$. The proof is included in Appendix 3.A. It is easy to see that the important hypotheses of the openness and the continuity in this lemma are violated in the previous example E1.

Lemma 3.1

Assume that

1. *$\mathcal{V}$ is open,*
2. *For any $\mathbf{s} \in \mathcal{S}$, there exists a unique $\mathbf{v} \in \mathcal{V}$ such that $\mathbf{F}(\mathbf{v}) = \mathbf{s}$,*
3. *The unique $\mathbf{v} \in \mathcal{V}$ depends continuously on $\mathbf{s} \in \mathcal{S}$.*

Then $\mathcal{S}$ is a domain of $\mathcal{V}$-control.

As the continuity of the inverse is hard to ensure in practice, we give below a theorem that contains sufficient conditions for the continuity. These sufficient conditions are obtained using the inverse function theorem. Detailed proof is included in Appendix 3.B.

Definition 3.3

A set $\mathcal{V}$ of system electrical states is non-singular *if the Jacobian $\mathbf{J}_{\mathbf{F}}(\mathbf{v})$ is non-singular $\forall \mathbf{v} \in \mathcal{V}$.*

Theorem 3.1

Assume that

1. *$\mathcal{V}$ is open and non-singular,*
2. *For any $\mathbf{s} \in \mathcal{S}$, there exists a unique $\mathbf{v} \in \mathcal{V}$ such that $\mathbf{F}(\mathbf{v}) = \mathbf{s}$.*

Then there is a continuous mapping $\mathbf{\Phi} : \mathcal{S} \to \mathcal{V}$ such that $\mathbf{F}(\mathbf{\Phi}(\mathbf{s})) = \mathbf{s}, \forall \mathbf{s} \in \mathcal{S}$, and $\mathcal{S}$ is a domain of $\mathcal{V}$-control.

By virtue of the real-quadratic nature of $\mathbf{F}$ in rectangular coordinates, we can replace the condition of the non-singularity in Theorem 3.1 and obtain the following alternative theorem for $\mathcal{V}$-control. Its proof is given in Appendix 3.F.

Theorem 3.2

Assume that

1. *$\mathcal{V}$ is open,*
2. *$\mathcal{S}$ is open,*
3. *For any $\mathbf{s} \in \mathcal{S}$, there exists a unique $\mathbf{v} \in \mathcal{V}$ such that $\mathbf{F}(\mathbf{v}) = \mathbf{s}$.*

Then, $\mathbf{J}_{\mathbf{F}}(\mathbf{v})$ is non-singular at any $\mathbf{v} \in \mathcal{V}$ such that $\mathbf{F}(\mathbf{v}) \in \mathcal{S}$. Moreover, there exists a continuous mapping $\mathbf{\Phi} : \mathcal{S} \to \mathcal{V}$ such that $\mathbf{F}(\mathbf{\Phi}(\mathbf{s})) = \mathbf{s}, \forall \mathbf{s} \in \mathcal{S}$, and $\mathcal{S}$ is a domain of $\mathcal{V}$-control.

In the forthcoming Section 3.4 and Section 3.5, we will use Theorem 3.1 and Theorem 3.2, respectively, to develop practical solution methods for the admissibility problem.

Beyond $\mathcal{V}$-Control

A key component of the obtained sufficient conditions for $\mathcal{V}$-control is the existence of a unique power-flow solution $\mathbf{v} \in \mathcal{V}$ for every $\mathbf{s} \in \mathcal{S}$. In the following, we give Theorem 3.3 and Theorem 3.4 that can be used to satisfy this key component. Their proofs are included in Appendices 3.C and 3.D. Note that

- the proof of Theorem 3.3 uses only the real-quadratic nature of $\mathbf{F}$ in rectangular coordinates,
- the proof of Theorem 3.4 essentially depends on the differentiability of $\mathbf{F}$.

Definition 3.4

A set $\mathcal{V}$ of system electrical states is a domain of uniqueness *if* $\mathbf{F}(\mathbf{v}) = \mathbf{F}(\mathbf{v}') \Rightarrow \mathbf{v} = \mathbf{v}'$, $\forall \mathbf{v}, \mathbf{v}' \in \mathcal{V}$.

Theorem 3.3

If a set $\mathcal{V}$ of system electrical states is non-singular and convex, then it is a domain of uniqueness.

Theorem 3.4

Let $\mathcal{V}$ be a set of system electrical states, $\mathcal{S}$ be a set of system power injections, and $\partial\mathcal{V}$ denote the topological boundary of $\mathcal{V}$. Assume that

1. *$\mathcal{V}$ is bounded, open and non-singular,*
2. *$\mathcal{S}$ is connected,*
3. *$\mathbf{F}(\mathcal{V}) \bigcap \mathcal{S}$ is non-empty,*
4. *$\mathbf{F}(\partial\mathcal{V}) \bigcap \mathcal{S}$ is empty.*

Then, for any $\mathbf{s} \in \mathcal{S}$, there exists a $\mathbf{v} \in \mathcal{V}$ such that $\mathbf{F}(\mathbf{v}) = \mathbf{s}$.

Besides Theorems 3.3 and 3.4, we incidentally find that the local uniqueness in a neighborhood of a system electrical state $\mathbf{v}$ implies the non-singularity of $\mathbf{J}_{\mathbf{F}}(\mathbf{v})$. This is true due to the real-quadratic nature of $\mathbf{F}$ in rectangular coordinates. Moreover, this is the converse of the inverse function theorem. To formalize, we give the following theorem and prove it in Appendix 3.E.

Theorem 3.5

If $\mathcal{V}$ is open and a domain of uniqueness, then $\mathcal{V}$ is non-singular.

Remark 3.1 (*Interpretation of Theorem 3.4*)

In essence, Theorem 3.4 asserts that every $\mathbf{s} \in \mathcal{S}$ has a corresponding system electrical state in $\mathcal{V}$, provided that

- *$\mathcal{V}$ is bounded, open and non-singular,*
- *$\mathcal{S}$ is connected,*
- *At least one $\mathbf{s}^* \in \mathcal{S}$ has a corresponding system electrical state in $\mathcal{V}$,*
- *It is impossible for any $\mathbf{s} \in \mathcal{S}$ to have a corresponding system electrical state on the boundary of $\mathcal{V}$.*

Intuitively, this is because: if there would be an $\mathbf{s}^{**} \in \mathcal{S}$ that has no corresponding system electrical state in $\mathcal{V}$, then in order to continuously move from $\mathbf{s}^*$ to $\mathbf{s}^{**}$, the corresponding path in the system electrical state space must either hit a singular point in $\mathcal{V}$ or exit $\mathcal{V}$ by crossing the boundary $\partial\mathcal{V}$; but this is made impossible by conditions 1 and 4 in Theorem 3.4.

3.4 A First Solution Method for the Admissibility Problem

In this section, we develop a first solution method for the admissibility problem. Specifically,

- In Section 3.4.1, we establish a high-level framework that contains the general ideas and the key steps of our first solution method. In the framework, we need to find a $\mathcal{V} \subseteq \mathcal{V}^\star$ such that $\mathcal{S}^{\text{uncertain}}$ is a domain of $\mathcal{V}$-control. To this purpose, we apply Theorem 3.1 for $\mathcal{V}$-control. Additionally, to satisfy condition 2 in Theorem 3.1 (i.e., the existence and uniqueness of the power-flow solution), we employ Theorems 3.3 and 3.4.
- In Section 3.4.2, we concretize the framework and obtain our first solution method. Here, we would like to emphasize that the concretization of the framework is not unique, and we just explore one possibility.

Through numerical examples in Section 3.4.4, we demonstrate that

- The obtained solution method is tight in the sense that it almost finds the largest $\mathcal{S}^{\text{uncertain}}$ that is admissible for some given $\mathbf{v}^{\text{initial}} \in \mathcal{V}^\star$.
- However, the obtained solution method has a relatively high computational complexity and requires large memory for data storage and manipulation, which makes it unsuitable for real-time applications in large networks.

3.4.1 Framework for Development of the First Solution Method

As we have observed in Section 3.3.2, $\mathcal{S}^{\text{uncertain}}$ is admissible for $\mathbf{v}^{\text{initial}}$ if there exists a set $\mathcal{V}$ such that

(O1) $\mathcal{V} \subseteq \mathcal{V}^\star$,

(O2) $\mathbf{v}^{\text{initial}} \in \mathcal{V}$,

(O3) $\mathcal{S}^{\text{uncertain}}$ is a domain of $\mathcal{V}$-control.

By this observation, our framework consists in constructing a large set $\mathcal{V}$ such that the hypotheses (O1)–(O3) are satisfied:

- In step 1, we find a large open set $\tilde{\mathcal{V}}$ such that its closure $\text{cl}(\tilde{\mathcal{V}})$ is non-singular and convex, using some sufficient conditions on non-singularity. Then, let $\mathcal{V}$ be the intersection of $\tilde{\mathcal{V}}$ and $\mathcal{V}^\star$, which fulfills (O1). Note that the obtained set $\mathcal{V}$ is open and non-singular. Moreover, by Theorem 3.3, it is also a domain of uniqueness.

- In step 2, we first verify (O2) by inspection. Then, we test whether $\forall \mathbf{s} \in \mathcal{S}^{\text{uncertain}}$, there is no corresponding system electrical state on the boundary $\partial\mathcal{V}$. This is done by checking the infeasibility of a number of optimization problems (see detailed descriptions below). By Theorem 3.4, this will guarantee that there exists a corresponding system electrical state $\mathbf{v} \in \mathcal{V}$ for every $\mathbf{s} \in \mathcal{S}^{\text{uncertain}}$. Further, by Theorem 3.1, this will guarantee that (O3) is satisfied.

According to the above reasoning, the framework is as follows.

Framework

Input: An initial system electrical state $\mathbf{v}^{\text{initial}}$ and a connected uncertainty set $\mathcal{S}^{\text{uncertain}}$ such that (I1)–(I2) in Definition 3.1 are satisfied.

Output: $\mathcal{S}^{\text{uncertain}}$ is admissible for $\mathbf{v}^{\text{initial}}$, or we are unsure of the admissibility.

(Step 1) Construct $\mathcal{V}$ as follows:

- Find some appropriate continuous functions f_ℓ, $\ell \in \{L^{\text{secure}}+1, ..., L\}$ such that $\tilde{\mathcal{V}} = \{\mathbf{v} : f_\ell(\mathbf{v}) > 0,\ \ell = L^{\text{secure}}+1, ..., L\}$ is large and its closure is non-singular and convex, [2]
- Then, let $\mathcal{V} = \{\mathbf{v} : f_\ell(\mathbf{v}) > 0,\ \ell = 1, ..., L\}$ (i.e., let $\mathcal{V} = \tilde{\mathcal{V}} \bigcap \mathcal{V}^\star$).

(Step 2) Test whether

- $\mathbf{v}^{\text{initial}} \in \mathcal{V}$,
- The following optimization problems are infeasible for all ℓ.

$$
\begin{aligned}
[\mathbf{P0}(\ell)] \qquad \min \ & \sum_{j=1}^{N^{\text{phase}}N} \Big(\Re\Big((\mathbf{v})_j\Big) + \Im\Big((\mathbf{v})_j\Big) \Big) \\
\text{s.t.} : \ & f_{\ell'}(\mathbf{v}) \geq 0\,, \qquad \forall \ell' \in \{1, ..., L\} \setminus \{\ell\}\,, \\
& f_\ell(\mathbf{v}) = 0\,, \\
& \mathbf{F}(\mathbf{v}) \in \mathcal{S}^{\text{uncertain}}\,.
\end{aligned}
$$

If both tests succeed, then declare that $\mathcal{S}^{\text{uncertain}}$ is admissible for $\mathbf{v}^{\text{initial}}$. Otherwise, we are unsure of the admissibility.

---

[2] The closure of $\tilde{\mathcal{V}}$ is $\text{cl}(\tilde{\mathcal{V}}) = \{\mathbf{v} : f_\ell(\mathbf{v}) \geq 0,\ \ell = L^{\text{secure}}+1, ..., L\}$.

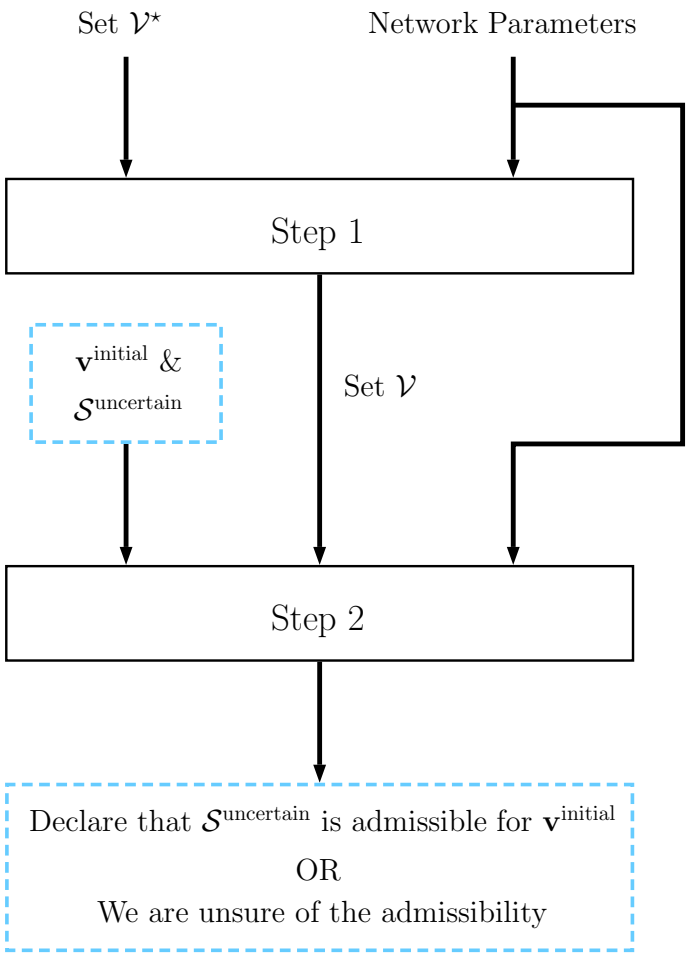

Figure 3.4 – Flow chart of the framework.

For this framework, we highlight its structure in Figure 3.4 and propose the following theorem on its validity (proof can be found in Appendix 3.G).

Theorem 3.6

The proposed framework is correct in the sense that, whenever it declares $\mathcal{S}^{\text{uncertain}}$ *admissible for* $\mathbf{v}^{\text{initial}}$*, it* is *so.*

Before proceeding to the next section, we would like to emphasize that it is always beneficial to have $\mathcal{V}$ as large as possible in step 1 of the framework. This might not be obvious at the first glimpse, since the fact that $\mathcal{S}^{\text{uncertain}}$ is a domain of $\mathcal{V}$-control might not automatically extend to a superset of $\mathcal{V}$. However, this extension of $\mathcal{V}$-control is not an issue in our framework, as we use Theorems 3.3 and 3.4. To formalize this point, we give below a theorem and prove it in Appendix 3.H.

Theorem 3.7

Assume that we are given two implementations, $\mathbf{A}$ and $\mathbf{A}'$, of the framework, where, in step 1, $\mathbf{A}$ constructs $\mathcal{V}$ and $\mathbf{A}'$ constructs $\mathcal{V}' \supseteq \mathcal{V}$. Also assume that the ground truth is that $\mathcal{S}^{\text{uncertain}}$ is admissible for $\mathbf{v}^{\text{initial}}$. If $\mathbf{A}$ declares $\mathcal{S}^{\text{uncertain}}$ admissible for $\mathbf{v}^{\text{initial}}$, then so does $\mathbf{A}'$.

3.4.2 Concretization of the Framework and the First Solution Method

Now we show one concretization of the framework, which gives us the first solution method. Corresponding to the framework, this first solution method has two steps.

Step 1 of the First Solution Method

As in step 1 of the framework, we need to find an open set $\tilde{\mathcal{V}}$ such that its closure $\text{cl}(\tilde{\mathcal{V}})$ is non-singular and convex. For this purpose, take into account that

- The singularity of the power-flow Jacobian $\mathbf{J_F}$ usually occurs due to high power generation and high power consumption,
- High power generation and high power consumption are both linked to large magnitudes of the branch and nodal currents.

Therefore, for $\text{cl}(\tilde{\mathcal{V}})$ to be non-singular, we need to ensure that no system electrical state in $\text{cl}(\tilde{\mathcal{V}})$ has very large branch and nodal currents. Based on this consideration, we let $\tilde{\mathcal{V}}$ be

$$\tilde{\mathcal{V}} = \Bigg\{ \mathbf{v} : \text{Inequalities in (3.3c) are satisfied, and} \\ - \left| \text{Row}_j(\mathbf{Y}_{LL})(\mathbf{v}-\mathbf{w}) \right|^2 + \left(I_j^{\text{node}} \right)^2 > 0,\ \forall j \in \{1,...,N^{\text{phase}}N\} \Bigg\}, \tag{3.4}$$

where I_j^{node} are some auxiliary constants.

Obviously, the set $\tilde{\mathcal{V}}$ defined in (3.4) is open and has a convex closure. Thus, we only need to find appropriate values for constants $I_j^{\text{node}},\ j \in \{1,...,N^{\text{phase}}N\}$ such that the set $\text{cl}(\tilde{\mathcal{V}})$ is non-singular. To this end, we recall that a necessary condition for $\mathbf{J_F}(\mathbf{v})$ to be singular is given by (8) in [69] as follows:

$$\exists m \in \{1,...,N^{\text{phase}}N\} \text{ such that } \sum_{n=1}^{N^{\text{phase}}N} \left| (\mathbf{Y}_{LL}^{-1})_{m,n} (\mathbf{i})_n \right| \geq |(\mathbf{v})_m|. \tag{3.5}$$

Clearly, if none of the elements in $\mathrm{cl}(\tilde{\mathcal{V}})$ satisfies this necessary condition for singularity, then $\mathrm{cl}(\tilde{\mathcal{V}})$ is non-singular. This leads to the following proposition. The corresponding proof can be found in Appendix 3.I.

Proposition 3.1

For the set $\tilde{\mathcal{V}}$ in (3.4)*, its closure $\mathrm{cl}(\tilde{\mathcal{V}})$ is non-singular if the following second-order cone programming problems are infeasible for all $m, n \in \{1, ..., N^{\mathrm{phase}}N\}$ and $\psi, \phi \in \{1, -1\}$.*

$$
\begin{aligned}
[\mathbf{P1}(m,n,\psi,\phi)] \qquad \min \; & \sum_{j=1}^{N^{\mathrm{phase}}N} \Big(\Re\Big((\mathbf{v})_j\Big) + \Im\Big((\mathbf{v})_j\Big) \Big) \\
\text{s.t.} : \; & \mathbf{v} \in \mathrm{cl}(\tilde{\mathcal{V}}) \,, \\
& \|\mathrm{Row}_m(\mathbf{Y}_{LL}^{-1})\|_1 \Big(\psi \Re\Big(\mathrm{Row}_n(\mathbf{Y}_{LL})(\mathbf{v}-\mathbf{w}) \Big) \\
& \qquad + \phi \Im\Big(\mathrm{Row}_n(\mathbf{Y}_{LL})(\mathbf{v}-\mathbf{w}) \Big) \Big) \geq |(\mathbf{v})_m| \,, \\
& \psi \Re\Big(\mathrm{Row}_n(\mathbf{Y}_{LL})(\mathbf{v}-\mathbf{w}) \Big) \geq 0 \,, \\
& \phi \Im\Big(\mathrm{Row}_n(\mathbf{Y}_{LL})(\mathbf{v}-\mathbf{w}) \Big) \geq 0 \,.
\end{aligned}
$$

By synthesizing the above discussions, we develop step 1 of the first solution method as follows.

First Solution Method (Step 1)

(1-a) Choose some positive reference values for I_j^{node} and denote them by $\hat{I}_j^{\mathrm{node}}$, $j \in \{1, ..., N^{\mathrm{phase}}N\}$. Here, we could let $\hat{I}_j^{\mathrm{node}}$ be the peak value of the nodal-current magnitude $|(\mathbf{i})_j|$ in real-world operation, or simply let all $\hat{I}_j^{\mathrm{node}}$ be the same.

(1-b) Next, let $I_j^{\mathrm{node}} = \lambda \hat{I}_j^{\mathrm{node}}$, $\forall j \in \{1, ..., N^{\mathrm{phase}}N\}$, where λ is a positive scaling factor that will vary in the subsequent (1-c). In addition, for every j, specify some positive threshold $I_j^{\mathrm{threshold}}$ that should be an upper bound on the largest possible value of the nodal-current magnitude $|(\mathbf{i})_j|$. These thresholds are used as stopping criteria of the subsequent (1-c).

(1-c) We start with a sufficiently small $\lambda \in \left(0, \min_j \dfrac{I_j^{\mathrm{threshold}}}{\hat{I}_j^{\mathrm{node}}}\right)$ such that the problems P1(m, n, ψ, ϕ) are all infeasible, and we gradually increase it by a fixed

step size $\Delta\lambda$ until either (i) P1(m,n,ψ,ϕ) are no longer simultaneously infeasible for all $m,n \in \{1,...,N^{\text{phase}}N\}$, $\psi,\phi \in \{1,-1\}$, or (ii) $\lambda \geq \min_j \frac{I_j^{\text{threshold}}}{\hat{I}_j^{\text{node}}}$.

(1-d) With the penultimate value of λ, we obtain I_j^{node}, $\forall j \in \{1,...,N^{\text{phase}}N\}$ and the set $\tilde{\mathcal{V}}$ that is defined in (3.4).

(1-e) Last, we let $\mathcal{V} = \tilde{\mathcal{V}} \bigcap \mathcal{V}^{\star}$.

Step 2 of the First Solution Method

According to step 2 of the proposed framework, our main task amounts to checking the infeasibility of P0(ℓ) for every $\ell \in \{1,...,L\}$. Observe that for each optimization problem P0(ℓ), we have that

- The objective function is polynomial in $\Re(\mathbf{v})$, $\Im(\mathbf{v})$,
- By (3.3)–(3.4), $f_\ell(\mathbf{v}),\ \ell \in \{1,...,L\}$ are all polynomial in $\Re(\mathbf{v})$, $\Im(\mathbf{v})$,
- $\mathbf{F}(\mathbf{v})$ is a collection of polynomials in $\Re(\mathbf{v})$ and $\Im(\mathbf{v})$.

Therefore, P0(ℓ), $\forall \ell$ become standard polynomial optimization problems if we add the following assumption.

Assumption 3.1

$\mathcal{S}^{\text{uncertain}}$ is the Cartesian product of $\mathcal{S}_j^{\text{uncertain}}$, $\forall j \in \{1,...,N^{\text{phase}}N\}$, and each $\mathcal{S}_j^{\text{uncertain}}$ is either a convex polygon or a singleton.

Note that $\mathcal{S}^{\text{uncertain}}$ is a connected set under Assumption 3.1, as it is path-connected. Furthermore, note that these polynomial optimization problems are not convex. To address this issue, we could apply convex relaxation to them and check whether the relaxed problems are infeasible. Indeed, the infeasibility of the relaxed problem implies the infeasibility of the original problem. As proposed in [59], these non-convex polynomial optimization problems can be effectively approximated by a hierarchy of semi-definite programming relaxations. This hierarchy is arranged by a positive integer called relaxation order. As the relaxation order increases, the relaxed problem becomes closer to the original problem, in terms of the optimal value and feasibility. Despite the theoretical beauty of this hierarchy of relaxations, it gradually becomes computationally intractable as the number of variables and the relaxation order increase. To cope with this, a sparsity-exploiting counterpart of this hierarchy is developed later

in [60, 61], where the level of sparsity depends mainly on the cross terms in the polynomial constraints. For completeness, a brief description for the sparsity-exploiting hierarchy of semi-definite programming relaxations is included in Appendix 3.K.

Taking the above into consideration, we develop step 2 of the first solution method below.

First Solution Method (Step 2)

(2-a) Given the set $\mathcal{V}$ obtained in First Solution Method (Step 1), check whether $\mathbf{v}^{\text{initial}} \in \mathcal{V}$.

(2-b) With this $\mathcal{V}$ and the sparsity-exploiting hierarchy of semi-definite programming relaxations in [60, 61], check whether the relaxed P0(ℓ) are all infeasible for some relaxation order.[3]

(2-c) If both (2-a) and (2-b) are true, then we declare that $\mathcal{S}^{\text{uncertain}}$ is admissible for $\mathbf{v}^{\text{initial}}$. Otherwise, we are unsure of the admissibility.

3.4.3 Computational Complexity and Implementation Issues of the First Solution Method

Computational Complexity

We give below a proposition on the computational complexity of the first solution method. Its proof is straightforward and can be found in Appendix 3.J.

[3] Under Assumption 3.1, an empirically good choice of the relaxation order is 2.

Proposition 3.2

For the proposed first solution method, we have:

- *The complexity of step 1 is equal to that of at most*

$$4\Big(N^{\text{phase}}N\Big)^2\left\lceil \min_j \frac{I_j^{\text{threshold}}}{\hat{I}_j^{\text{node}}\Delta\lambda}\right\rceil$$

  second-order cone programming feasibility problems, where $\lceil\cdot\rceil$ *means ceiling.*

- *Under Assumption 3.1, the complexity of step 2 is equal to that of* $N^{\text{phase}}\Big(3N+\text{card}(\mathcal{E})\Big)$ *semi-definite programming feasibility problems, where* $\text{card}(\cdot)$ *means cardinality.*

From the theoretical perspective, the complexity of a second-order cone programming feasibility problem and the complexity of a semi-definite programming feasibility problem remain as open research topics [70, 71, 72]. Despite this fact, in practice, these feasibility problems can be solved efficiently. This can be seen in Table 3.1 of the next section.

Implementation Issues

We present some implementation issues as follows:

- Given the network configuration (i.e., topology and line parameters), step 1 of the method needs to be implemented only once.
- In step 1 of the method, the infeasibility of each P1(m,n,ψ,ϕ) can be checked independently. Thus, step 1 of the method can be implemented in parallel through a multi-core CPU/GPU or a networked computing infrastructure. Similarly, in step 2 of the method, the infeasibility of each relaxed P0(ℓ) can also be checked independently. Therefore, step 2 of the method can be implemented in parallel as well.

3.4.4 Numerical Evaluation of the First Solution Method

In this section, we evaluate the performance of the first solution method, using one meshed grid and two benchmark radial grids in [55, 56, 73]. Topologies of these grids are shown in Figures 3.5, 3.6 and 3.7, respectively.[4] In all evaluations, we assume

[4] For the convenience of branch references, we adjust the bus indexes in the benchmark networks.

that (i) the slack-bus voltage is nominal, and that (ii) the semi-definite programming relaxation order is 2.

Note that the results in this chapter are generated on a Macbook Pro that is equipped with a 3.0 GHz Intel Core i7 CPU and 16 GB 1600 MHz DDR3 memory. In particular, we implement the method using MATLAB tools YALMIP, Mosek and SparsePOP [74, 75, 76].

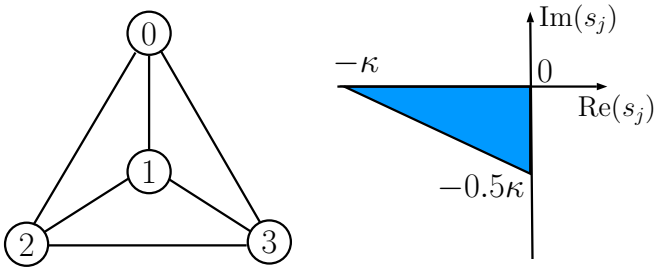

Figure 3.5 – Topology and uncertainty set (in p.u.) for the meshed network, where κ is a positive real parameter.

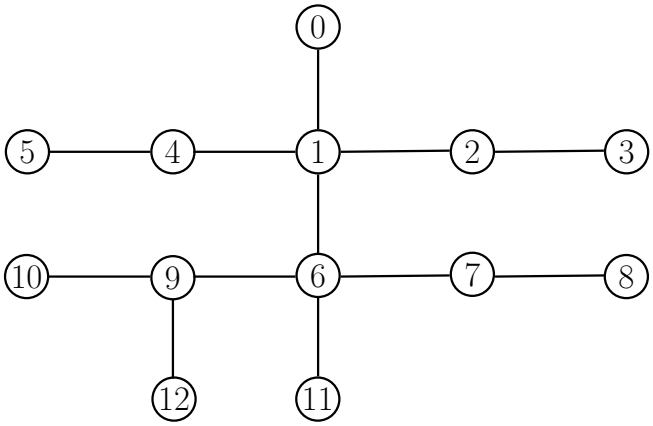

Figure 3.6 – Topology of the IEEE 13-Bus Test Feeder.

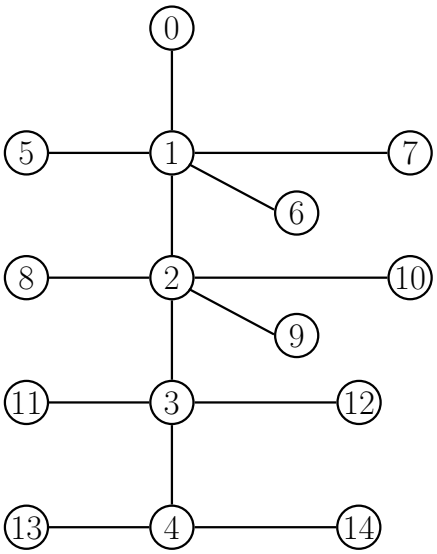

Figure 3.7 – Topology of the CIGRE North American LV Distribution Network (residential part).

Evaluation 1

We consider the single-phase meshed network shown on the left-hand side of Figure 3.5. Assume that (i) each transmission line has a series admittance $5 - \jmath 3.6$ p.u., (ii) the security bounds on the nodal-voltage magnitudes are 0.95 and 1.05 p.u., (iii) the security bounds on the branch-current magnitudes are 0.6 p.u., and (iv) $\forall j$, $(\mathbf{s})_j$ belongs to the triangular region on the right-hand side of Figure 3.5 that specifies $\mathcal{S}^{\text{uncertain}}$. [5] Clearly, this grid is stressed when parameter $\kappa \in (0, \infty)$ increases.

Now, let $\mathbf{v}^{\text{initial}} = \mathbf{w}$. We would like to find the maximum value for κ such that $\mathcal{S}^{\text{uncertain}}$ is admissible for $\mathbf{v}^{\text{initial}}$. In step 1 of the method, we choose $I_j^{\text{node}} = 0.8$ p.u. for all j, and obtain a valid $\mathcal{V}$. Then, in step 2 of the method, we verify that $\mathbf{v}^{\text{initial}} \in \mathcal{V}$ and find that the maximum value for κ to preserve admissibility is 0.35. With $\kappa = 0.35$ and $(\mathbf{s})_j = -\kappa$ p.u. for all j, we find that there is a corresponding system electrical state that has the following features:

- All nodal-voltage magnitudes are 0.9506 p.u., which indicates that the method is tight in terms of the obtained maximum value of κ,
- All branch-current magnitudes are much lower than the security bounds,
- For all j, $|(\mathbf{i})_j|$ is far below I_j^{node}, which means that the introduction of I_j^{node} does not limit the performance.

[5] We intentionally choose the triangular shape to demonstrate that our method works for polygonal uncertainty sets.

Evaluation 2

The IEEE 13-Bus Test Feeder shown in Figure 3.6 is a medium-voltage network that has shunt elements and a MV/LV transformer.[6] In this network, we (i) take IEEE benchmark configuration 602 for all transmission lines, (ii) remove the regulator between buses 0 and 1, and (iii) do positive-sequence analysis for the network.

Let $\mathbf{s}^{\text{initial}}$ be the initial system power injection, for which $(\mathbf{s}^{\text{initial}})_j$ is the phase-average of the IEEE benchmark power injections at bus j. In addition, let $\mathbf{v}^{\text{initial}}$ be its corresponding state that is guaranteed to be unique around $\mathbf{w}$ by Theorem 2.1. To ensure that $\mathbf{v}^{\text{initial}}$ satisfies the security constraints, we let

- the security bounds on the nodal-voltage magnitudes be 0.9 and 1.1 p.u.,
- the security bounds on the branch-current magnitudes be:
  - 1 p.u. for branches 01 and 10,
  - 0.45 p.u. for branches 16 and 61,
  - 0.3 p.u. for the remaining branches.

Assume that the system power injection fluctuates significantly in this network. More precisely, $\mathcal{S}^{\text{uncertain}}$ is a set such that $\forall j,\ \mathcal{S}_j^{\text{uncertain}} = [\kappa\Re((\mathbf{s}^{\text{initial}})_j), 0] \times [\kappa\Im((\mathbf{s}^{\text{initial}})_j), 0]$, where $\kappa \in [1, \infty)$ is a scalar. As κ increases, $\mathcal{S}^{\text{uncertain}}$ will eventually violate the admissibility for the given $\mathbf{v}^{\text{initial}}$. Hence, in the following, we look for the maximum value of κ such that $\mathcal{S}^{\text{uncertain}}$ is admissible for $\mathbf{v}^{\text{initial}}$.

According to the method, we first obtain a set $\mathcal{V}$, by choosing $I_j^{\text{node}},\ \forall j$ as: $I_1^{\text{node}} = I_6^{\text{node}} = 0.2$ p.u., $I_2^{\text{node}} = I_3^{\text{node}} = I_4^{\text{node}} = I_5^{\text{node}} = I_8^{\text{node}} = 0.15$ p.u., and $I_7^{\text{node}} = I_9^{\text{node}} = I_{10}^{\text{node}} = I_{11}^{\text{node}} = I_{12}^{\text{node}} = 0.1$ p.u. Next, in step 2 of our method, we have that $\mathbf{v}^{\text{initial}} \in \mathcal{V}$ and the maximum value for κ to preserve admissibility is 1.96. When $\kappa = 1.96$, we find that $\kappa\mathbf{s}^{\text{initial}}$ has a corresponding system electrical state that possesses the following features:

- The lowest nodal-voltage magnitude is $|(\mathbf{v})_8| = 0.9016$ p.u.,
- The branch-current magnitudes between buses 1 and 6 are 0.4128 p.u., and all the other branch-current magnitudes are far below the security bounds,
- $|(\mathbf{i})_j| < I_j^{\text{node}},\ \forall j$.

[6] The transformer lies between buses 2 and 3. By [36] and [37], it is modeled as the serial combination of a winding admittance and an ideal MV/LV transformer. We describe the voltage and current at bus 3 by their equivalents at the MV side of the ideal transformer. Moreover, we do not consider any power limit of this transformer.

Thus, the method almost finds the largest possible value for κ.

In addition to the tightness, we show the measured time in Table 3.1. Here, note that the time of step 1 is reported per choice of λ. Clearly, for the IEEE 13-Bus Test Feeder, the method does not have a real-time performance. As the computational complexity increases along with the size of the network, we know that the method is not suitable for real-time applications in large networks.

Table 3.1 – The measured time for Evaluations 2 and 3.

	Execution Time of Parallel Implementation (in seconds)		Accumulated Time of Sequential Implementation (in minutes)	
	Step 1	Step 2	Step 1	Step 2
Evaluation 2	less than 1	4–9	9	6
Evaluation 3	roughly 1	7–15	12–13	10

Evaluation 3

The residential part of the CIGRE North American LV Distribution Network in Figure 3.7 is a low-voltage network, where every bus is either on the main lateral or directly linked to the main lateral. In this network, $|\mathbf{i}_{jk}| = |\mathbf{i}_{kj}|$ holds everywhere, since shunt elements are completely ignored due to short transmission lines. Additionally, the R/X ratios are much larger than 1, which is different from the previous network.

We assume that each of the buses 1–4 has an extra energy source. Moreover,

- Each of these sources is balanced across the neutral line,
- Each of these sources has a real-valued power in $[(1-\kappa)\times 20, (1+\kappa)\times 20]$ kW, where scalar $\kappa \in [0,1)$,
- These sources are independent of each other.

By fixing the benchmark peak power injections for the other buses, we construct a set $\mathcal{S}^{\text{uncertain}}$. Now, let (i) $\mathbf{s}^{\text{initial}}$ be the central point in $\mathcal{S}^{\text{uncertain}}$, and (ii) $\mathbf{v}^{\text{initial}}$ be the corresponding system electrical state that is guaranteed to be unique around $\mathbf{w}$ by Theorem 2.1. To ensure that $\mathbf{v}^{\text{initial}}$ satisfies the security constraints, let

- the security bounds on the nodal-voltage magnitudes be 0.95 and 1.05 p.u.,
- the security bounds on the branch-current magnitudes be:

- 1 p.u. for branches 01 and 10,
- 0.8 p.u. for branches 12 and 21,
- 0.6 p.u. for branches 23 and 32,
- 0.5 p.u. for branches 34 and 43,
- 0.4 p.u. for the remaining branches.

Similarly to the last evaluation, we look for the maximum value of κ such that $\mathcal{S}^{\text{uncertain}}$ is admissible for $\mathbf{v}^{\text{initial}}$. In step 1 of the method, we choose $I_j^{\text{node}} = 0.6$ p.u. for all j. In this way, we obtain a set $\mathcal{V}$. Next, in step 2 of the method, we find that $\mathbf{v}^{\text{initial}} \in \mathcal{V}$ and the maximum value for κ to preserve admissibility is 0.11. When $\kappa = 0.11$, if each of the four extra sources at buses 1–4 has a power injection equal to $(1+\kappa) \times 20$ kW, then there is a resultant system electrical state that has the following features:

- All nodal-voltage magnitudes are close to 1 p.u.,
- The branch-current magnitudes between buses 0 and 1 are 0.9498 p.u.,
- The branch-current magnitudes between buses 1 and 2 are 0.7813 p.u.,
- The branch-current magnitudes between buses 2 and 3 are 0.5428 p.u.,
- The other branch-current magnitudes are far below their security bounds,
- $|(\mathbf{i})_j| < I_j^{\text{node}}$, $\forall j$.

The method is tight in the sense that it almost finds the largest possible value for κ.

In terms of the measured time, we give the details in Table 3.1. Same as before, the time of step 1 is reported per choice of λ. Again, we observe that the method is not suitable for real-time applications in large networks.

3.5 A Second Solution Method for the Admissibility Problem

In this section, we continue making Assumption 3.1 and develop a second solution method for the admissibility problem. In this method, we apply Theorem 3.2 for $\mathcal{V}$-control and the results in Chapter 2 for the power-flow solvability.

Through numerical examples, we demonstrate that this method is less tight than the first solution method, but it can solve the admissibility problem in real time for large networks.

3.5.1 Development of the Method

According to our observation in Section 3.3.2, $\mathcal{S}^{\text{uncertain}}$ is admissible for $\mathbf{v}^{\text{initial}}$ if there exists a set $\mathcal{V}$ such that

(O1) $\mathcal{V} \subseteq \mathcal{V}^{\star}$,

(O2) $\mathbf{v}^{\text{initial}} \in \mathcal{V}$,

(O3) $\mathcal{S}^{\text{uncertain}}$ is a domain of $\mathcal{V}$-control.

By Theorem 3.2, we could instead see whether there exists a set $\mathcal{V}$ such that

(O1) $\mathcal{V} \subseteq \mathcal{V}^{\star}$,

(O2) $\mathbf{v}^{\text{initial}} \in \mathcal{V}$,

(O3a) $\mathcal{V}$ is open and a domain of uniqueness,

(O3b) $\mathbf{F}(\mathcal{V})$ is open and includes $\mathcal{S}^{\text{uncertain}}$.

Indeed, if $\mathcal{V}$ satisfies (O3a) and $\mathbf{F}(\mathcal{V})$ is open, then $\mathbf{F}(\mathcal{V})$ is a domain of $\mathcal{V}$-control by Theorem 3.2. Furthermore, if $\mathcal{S}^{\text{uncertain}}$ is a subset of $\mathbf{F}(\mathcal{V})$, then we have that $\mathcal{S}^{\text{uncertain}}$ is also a domain of $\mathcal{V}$-control.

In the following, we gradually develop a method that determines whether there exists a set $\mathcal{V}$ such that (O1)–(O3b) are satisfied.

Candidate Pair and Its Solution Set

First, we show how to construct a set of system electrical states that is non-singular and a domain of uniqueness. This is useful for the satisfaction of hypotheses (O1) and (O3a). To make the construction computationally efficient under Assumption 3.1, we exploit the results in Chapter 2 rather than Theorems 3.3 and 3.4. The thorough complexity analysis as well as the detailed implementation issues will be given later in Section 3.5.2.

As the results in Chapter 2 rely on a reference system electrical state $\hat{\mathbf{v}}$, we assume the knowledge of such $\hat{\mathbf{v}}$ in the subsequent development. With $\hat{\mathbf{v}}$, we introduce the following definitions of the candidate pair and its solution set.

Definition 3.5

For a reference system electrical state $\hat{\mathbf{v}}$ and a set $\mathcal{S}$ of system power injections: We say that $(\hat{\mathbf{v}}, \mathcal{S})$ is a candidate pair *if*

1. $\rho^{\ddagger}(\hat{\mathbf{v}}) > 0$,
2. $\xi(\mathbf{s} - \mathbf{F}(\hat{\mathbf{v}})) < \left(\rho^{\ddagger}(\hat{\mathbf{v}})\right)^2$, $\forall \mathbf{s} \in \mathcal{S}$.

In addition, whenever $(\hat{\mathbf{v}}, \mathcal{S})$ is a candidate pair, we define its solution set *as*

$$\mathcal{V}(\hat{\mathbf{v}}, \mathcal{S}) = \left\{ \mathbf{v} : \mathbf{F}(\mathbf{v}) \in \mathcal{S},\ \mathbf{v} \in \mathcal{D}_{\rho}(\hat{\mathbf{v}}), \rho = \rho^{\ddagger}(\hat{\mathbf{v}}) \right\}. \tag{3.6}$$

By Theorem 2.1, if $(\hat{\mathbf{v}}, \mathcal{S})$ is a candidate pair, then its solution set $\mathcal{V}(\hat{\mathbf{v}}, \mathcal{S})$ is a domain of uniqueness. Furthermore, by Proposition 2.1, we have that the solution set $\mathcal{V}(\hat{\mathbf{v}}, \mathcal{S})$ is also non-singular. These findings are summarized in the following proposition.

Proposition 3.3

For any candidate pair $(\hat{\mathbf{v}}, \mathcal{S})$, the solution set $\mathcal{V}(\hat{\mathbf{v}}, \mathcal{S})$ is non-singular and a domain of uniqueness.

Satisfaction of the Security Constraints by Elements in a Solution Set

Now, we derive conditions to ensure that all system electrical states in $\mathcal{V}(\hat{\mathbf{v}}, \mathcal{S})$ satisfy the security constraints. This is useful for the satisfaction of hypothesis (O1). To this end, we give several auxiliary notations to ease the exposition of the conditions.

- $\boldsymbol{\eta}_{\ell}(\hat{\mathbf{v}}, \mathbf{s}) = \alpha(\hat{\mathbf{v}})|\mathbf{s}_{\ell} - \mathbf{F}_{\ell}(\hat{\mathbf{v}})| + \rho^{\dagger}(\hat{\mathbf{v}}, \mathbf{s})|\mathbf{F}_{\ell}(\hat{\mathbf{v}})|$, where $\mathbf{w}_{\ell} \in \mathbb{C}^{N^{\text{phase}}}$ is the zero-injection nodal voltage at bus ℓ and $\mathbf{F}_{\ell}$ is the function that maps $\mathbf{v}$ to $\mathbf{s}_{\ell}$.
- $\boldsymbol{\Gamma}_{j,\ell}$ is the N^{phase}-by-N^{phase} sub-matrix formed by rows from $\left(N^{\text{phase}}(j-1)+1\right)$ to $(N^{\text{phase}}j)$ and columns from $\left(N^{\text{phase}}(\ell-1)+1\right)$ to $(N^{\text{phase}}\ell)$ of $\mathbf{Y}_{LL}^{-1}$.
- $\boldsymbol{\Upsilon}_{jk,\ell}$ is an N^{phase}-by-N^{phase} matrix defined by

$$\boldsymbol{\Upsilon}_{jk,\ell} = \begin{cases} -\mathbf{C}_{j,k}\boldsymbol{\Gamma}_{k,\ell}\,, & j = 0, k \neq 0\,, \\ \mathbf{A}_{j,k}\boldsymbol{\Gamma}_{j,\ell}\,, & j \neq 0, k = 0\,, \\ \mathbf{A}_{j,k}\boldsymbol{\Gamma}_{j,\ell} - \mathbf{C}_{j,k}\boldsymbol{\Gamma}_{k,\ell}\,, & j \neq 0, k \neq 0\,. \end{cases} \tag{3.7}$$

With the above auxiliary notations, we give the following proposition that contains bounds on $\mathbf{v}_j$ and $\mathbf{i}_{jk}$ for each system electrical state in $\mathcal{V}(\hat{\mathbf{v}}, \mathcal{S})$. The corresponding proof is in Appendix 3.L.

Proposition 3.4

Let $(\hat{\mathbf{v}}, \mathcal{S})$ be a candidate pair, $\mathcal{V}(\hat{\mathbf{v}}, \mathcal{S})$ be its solution set, and $\hat{\mathbf{i}}_{jk} = \mathbf{A}_{j,k}\hat{\mathbf{v}}_j - \mathbf{C}_{j,k}\hat{\mathbf{v}}_k$, $\forall jk \in \mathcal{E}$.

Then, for any system electrical state $\mathbf{v} \in \mathcal{V}(\hat{\mathbf{v}}, \mathcal{S})$, we have that the complex nodal voltages $\mathbf{v}_j$, $j \in \mathcal{N} \setminus \{0\}$ satisfy

$$|\mathbf{v}_j - \hat{\mathbf{v}}_j| \leq \boldsymbol{\delta}_j(\hat{\mathbf{v}}, \mathbf{s}) \,, \tag{3.8}$$

$$\boldsymbol{\delta}_j(\hat{\mathbf{v}}, \mathbf{s}) = \frac{\sum_{\ell=1}^{N} |\boldsymbol{\Gamma}_{j,\ell}||\mathrm{diag}(\mathbf{w}_\ell)^{-1}|\boldsymbol{\eta}_\ell(\hat{\mathbf{v}}, \mathbf{s})}{\alpha(\hat{\mathbf{v}})\Big(\alpha(\hat{\mathbf{v}}) - \rho^{\dagger}(\hat{\mathbf{v}}, \mathbf{s})\Big)} \,. \tag{3.9}$$

In addition, the branch currents $\mathbf{i}_{jk} = \mathbf{A}_{j,k}\mathbf{v}_j - \mathbf{C}_{j,k}\mathbf{v}_k$, $jk \in \mathcal{E}$ satisfy

$$|\mathbf{i}_{jk} - \hat{\mathbf{i}}_{jk}| \leq \boldsymbol{\tau}_{jk}(\hat{\mathbf{v}}, \mathbf{s}) \,, \tag{3.10}$$

$$\boldsymbol{\tau}_{jk}(\hat{\mathbf{v}}, \mathbf{s}) = \frac{\sum_{\ell=1}^{N} |\boldsymbol{\Upsilon}_{jk,\ell}||\mathrm{diag}(\mathbf{w}_\ell)^{-1}|\boldsymbol{\eta}_\ell(\hat{\mathbf{v}}, \mathbf{s})}{\alpha(\hat{\mathbf{v}})\Big(\alpha(\hat{\mathbf{v}}) - \rho^{\dagger}(\hat{\mathbf{v}}, \mathbf{s})\Big)} \,. \tag{3.11}$$

Using Proposition 3.4 and the triangle inequality, we obtain the following proposition in which we give conditions to ensure that all system electrical states in $\mathcal{V}(\hat{\mathbf{v}}, \mathcal{S})$ satisfy the security constraints. The proof is included in Appendix 3.M.

Definition 3.6

A candidate pair $(\hat{\mathbf{v}}, \mathcal{S})$ is strongly secured *if*

$$\mathbf{v}_j^{\min} + \boldsymbol{\delta}_j(\hat{\mathbf{v}}, \mathbf{s}) < |\hat{\mathbf{v}}_j| < \mathbf{v}_j^{\max} - \boldsymbol{\delta}_j(\hat{\mathbf{v}}, \mathbf{s}) \,, \qquad \forall j \in \mathcal{N} \setminus \{0\} \,, \tag{3.12}$$

$$|\hat{\mathbf{i}}_{jk}| < \mathbf{i}_{jk}^{\max} - \boldsymbol{\tau}_{jk}(\hat{\mathbf{v}}, \mathbf{s}) \,, \qquad \forall jk \in \mathcal{E} \,, \tag{3.13}$$

are satisfied $\forall \mathbf{s} \in \mathcal{S}$.

Proposition 3.5

If $(\hat{\mathbf{v}}, \mathcal{S})$ is a strongly secured candidate pair, then the security constraints (3.2a)–(3.2b) *are satisfied for all system electrical states in $\mathcal{V}(\hat{\mathbf{v}}, \mathcal{S})$.*

Consistency Between Candidate Pairs and Patching of Their Solution Sets

So far, if the uncertainty set $\mathcal{S}^{\text{uncertain}}$ is not very large, then the admissibility problem could be solved by the already obtained results. Specifically, let $\tilde{\mathcal{S}}$ be an open superset of $\mathcal{S}^{\text{uncertain}}$. If $(\mathbf{v}^{\text{initial}}, \tilde{\mathcal{S}})$ is a strongly secured candidate pair, then we have that $\mathcal{V}(\mathbf{v}^{\text{initial}}, \tilde{\mathcal{S}})$ satisfies the hypotheses (O1), (O2), (O3a), (O3b):

- $\mathcal{V}(\mathbf{v}^{\text{initial}}, \tilde{\mathcal{S}}) \subseteq \mathcal{V}^{\star}$, according to our previous discussion.
- $\mathbf{v}^{\text{initial}} \in \mathcal{V}(\mathbf{v}^{\text{initial}}, \tilde{\mathcal{S}})$, as $\mathbf{F}(\mathbf{v}^{\text{initial}}) \in \mathcal{S}^{\text{uncertain}}$ and $\mathcal{S}^{\text{uncertain}} \subseteq \tilde{\mathcal{S}}$.
- $\mathcal{V}(\mathbf{v}^{\text{initial}}, \tilde{\mathcal{S}})$ is open, since (i) $\mathcal{V}(\mathbf{v}^{\text{initial}}, \tilde{\mathcal{S}})$ is included in the interior of $\mathcal{D}_{\rho}(\mathbf{v}^{\text{initial}})$, $\rho = \rho^{\ddagger}(\mathbf{v}^{\text{initial}})$, and (ii) $\mathcal{V}(\mathbf{v}^{\text{initial}}, \tilde{\mathcal{S}})$ is included in the pre-image of the open set $\tilde{\mathcal{S}}$ under continuous function $\mathbf{F}$.
- $\mathcal{V}(\mathbf{v}^{\text{initial}}, \tilde{\mathcal{S}})$ is a domain of uniqueness, by our previous discussion.
- $\mathbf{F}\Big(\mathcal{V}(\mathbf{v}^{\text{initial}}, \tilde{\mathcal{S}})\Big) = \tilde{\mathcal{S}}$ is open and includes $\mathcal{S}^{\text{uncertain}}$.

However, in the case where $\mathcal{S}^{\text{uncertain}}$ is very large, there might not be an open set $\tilde{\mathcal{S}}$ such that $(\mathbf{v}^{\text{initial}}, \tilde{\mathcal{S}})$ is a strongly secured candidate pair. To address this issue, our idea is to first cover $\mathcal{S}^{\text{uncertain}}$ by overlapped smaller pieces such that we can construct a strongly secured candidate pair for every piece, and then patch the solution sets together. This gives rise to a question whether multiple solution sets can be compatibly patched (in the sense that the union of these solution sets is a domain of uniqueness). In what follows, we give a proposition that answers this question. The proof is in Appendix 3.N.

Definition 3.7

Candidate pairs $(\hat{\mathbf{v}}, \mathcal{S})$, $(\hat{\mathbf{v}}', \mathcal{S}')$ *are* consistent *if*

$$\|\mathbf{W}^{-1}(\hat{\mathbf{v}} - \hat{\mathbf{v}}')\|_{\infty} < \max\left\{\rho^{\ddagger}(\hat{\mathbf{v}}) - \sup_{\mathbf{s}' \in \mathcal{S}'} \rho^{\dagger}(\hat{\mathbf{v}}', \mathbf{s}'),\ \rho^{\ddagger}(\hat{\mathbf{v}}') - \sup_{\mathbf{s} \in \mathcal{S}} \rho^{\dagger}(\hat{\mathbf{v}}, \mathbf{s})\right\}. \tag{3.14}$$

Proposition 3.6

Let $\mathcal{L}$ *be a finite collection of candidate pairs. If* $(\hat{\mathbf{v}}, \mathcal{S})$ *and* $(\hat{\mathbf{v}}', \mathcal{S}')$ *are consistent* $\forall (\hat{\mathbf{v}}, \mathcal{S}), (\hat{\mathbf{v}}', \mathcal{S}') \in \mathcal{L}$*, then* $\bigcup_{(\hat{\mathbf{v}}, \mathcal{S}) \in \mathcal{L}} \mathcal{V}(\hat{\mathbf{v}}, \mathcal{S})$ *is a domain of uniqueness.*

Based on Proposition 3.6, we arrive at the following theorem. This theorem lays out the theoretical foundation for our second solution method. The corresponding proof can be found in Appendix 3.O.

Theorem 3.8

Suppose that the uncertainty set $\mathcal{S}^{\text{uncertain}}$ is compact.

If we have a finite collection $\mathcal{L}$ of candidate pairs such that

1. $\bigcup_{(\hat{\mathbf{v}},\mathcal{S})\in\mathcal{L}} \mathcal{S} = \mathcal{S}^{\text{uncertain}}$,
2. $\hat{\mathbf{v}} = \mathbf{v}^{\text{initial}}$ *for at least one* $(\hat{\mathbf{v}},\mathcal{S}) \in \mathcal{L}$,
3. $\forall(\hat{\mathbf{v}},\mathcal{S}) \in \mathcal{L}$, $\mathcal{S}$ *is closed and includes* $\mathbf{F}(\hat{\mathbf{v}})$,
4. $\forall(\hat{\mathbf{v}},\mathcal{S}) \in \mathcal{L}$, $(\hat{\mathbf{v}},\mathcal{S})$ *is strongly secured,*
5. $\forall(\hat{\mathbf{v}},\mathcal{S}),(\hat{\mathbf{v}}',\mathcal{S}') \in \mathcal{L}$, $(\hat{\mathbf{v}},\mathcal{S})$ *and* $(\hat{\mathbf{v}}',\mathcal{S}')$ *are consistent.*

Then there exists a set $\mathcal{V}$ that satisfies requirements (O1), (O2), (O3a), (O3b), hence $\mathcal{S}^{\text{uncertain}}$ is admissible for $\mathbf{v}^{\text{initial}}$.

From Theorem 3.8 to the Second Solution Method

The second solution method is developed on the basis of Theorem 3.8. In the method, we assume that $\mathbf{v}^{\text{initial}}$ satisfies $\rho^{\ddagger}(\mathbf{v}^{\text{initial}}) > 0$, which is usually the case during real-world operation. The purpose of this method is to incrementally construct a collection $\mathcal{L}$ of candidate pairs that satisfy the five items in Theorem 3.8. To do so, we dynamically maintain an auxiliary collection $\mathcal{L}^{\text{aux}}$ that represents the "unsolved" fraction of the admissibility problem. Each element in $\mathcal{L}^{\text{aux}}$ is a pair $(\check{\mathbf{v}},\mathcal{S})$ such that

- $\mathcal{S}$ is closed and includes $\mathbf{F}(\check{\mathbf{v}})$,
- $\mathcal{S}$ is contained in the closure of $\mathcal{S}^{\text{uncertain}} \setminus \bigcup_{(\hat{\mathbf{v}}',\mathcal{S}')\in\mathcal{L}} \mathcal{S}'$.

In the initial stage of the method, we let $\mathcal{L} = \{(\mathbf{v}^{\text{initial}}, \{\mathbf{F}(\mathbf{v}^{\text{initial}})\})\}$ and $\mathcal{L}^{\text{aux}} = \{(\mathbf{v}^{\text{initial}}, \mathcal{S}^{\text{uncertain}})\}$. Then, in the intermediate stage of the method, we take out the elements from $\mathcal{L}^{\text{aux}}$ one at a time and heuristically transform each of them into either a new element of $\mathcal{L}$, or multiple new elements of $\mathcal{L}^{\text{aux}}$. In both cases, we ensure that

- $\mathcal{L}$ fulfills items 3–5 in Theorem 3.8,
- $\left(\bigcup_{(\check{\mathbf{v}},\mathcal{S})\in\mathcal{L}^{\text{aux}}} \mathcal{S}\right) \cup \left(\bigcup_{(\hat{\mathbf{v}}',\mathcal{S}')\in\mathcal{L}} \mathcal{S}'\right) = \mathcal{S}^{\text{uncertain}}$.

In the final stage of the method, we declare that $\mathcal{S}^{\text{uncertain}}$ is admissible for $\mathbf{v}^{\text{initial}}$ if $\mathcal{L}^{\text{aux}}$ becomes empty (otherwise, we are unsure of the admissibility).

The full description of our second solution method is given below. Note that Assumption 3.1 is made, as we mentioned at the beginning of this section. Moreover, for all elements in $\mathcal{L}$ and $\mathcal{L}^{\text{aux}}$, we always ensure that $\mathcal{S}$ is the Cartesian product of $\mathcal{S}_j$, $j = 1, ..., N^{\text{phase}}N$, where each $\mathcal{S}_j$ is either a convex polygon or a singleton.

Second Solution Method

Input: An initial system electrical state $\mathbf{v}^{\text{initial}}$ and a compact uncertainty set $\mathcal{S}^{\text{uncertain}}$ such that (I1)–(I2) in Definition 3.1 are satisfied.

Output: $\mathcal{S}^{\text{uncertain}}$ is admissible for $\mathbf{v}^{\text{initial}}$, or we are unsure of the admissibility.

Initial Stage: Let $\mathcal{L} = \{(\mathbf{v}^{\text{initial}}, \{\mathbf{F}(\mathbf{v}^{\text{initial}})\})\}$ and $\mathcal{L}^{\text{aux}} = \{(\mathbf{v}^{\text{initial}}, \mathcal{S}^{\text{uncertain}})\}$.

Intermediate Stage: Repeat the following steps until $\mathcal{L}^{\text{aux}}$ is empty or some predefined maximum round of repetition is exceeded.

(Step 1) Take an element $(\check{\mathbf{v}}, \mathcal{S})$ out of $\mathcal{L}^{\text{aux}}$.

(Step 2) Let vector $\mathbf{s}^{\text{c}} \in \mathbb{C}^{N^{\text{phase}}N}$ be such that $(\mathbf{s}^{\text{c}})_j$, $\forall j$ is the arithmetic mean of all vertices in $\mathcal{S}_j$, which can be viewed as the center of $\mathcal{S}$. In addition, let

$$\hat{\mathbf{s}} = \left(1 - \min\left\{\frac{\left(\rho^{\ddagger}(\check{\mathbf{v}})\right)^2}{2\xi(\mathbf{s}^{\text{c}} - \mathbf{F}(\check{\mathbf{v}}))}, 1\right\}\right)\mathbf{F}(\check{\mathbf{v}}) + \left(\min\left\{\frac{\left(\rho^{\ddagger}(\check{\mathbf{v}})\right)^2}{2\xi(\mathbf{s}^{\text{c}} - \mathbf{F}(\check{\mathbf{v}}))}, 1\right\}\right)\mathbf{s}^{\text{c}}\,, \tag{3.15}$$

which is close to $\mathbf{s}^{\text{c}}$ and satisfies $\xi(\hat{\mathbf{s}} - \mathbf{F}(\check{\mathbf{v}})) \leq \frac{1}{2}\left(\rho^{\ddagger}(\check{\mathbf{v}})\right)^2$.

(Step 3) Compute the power-flow solution $\hat{\mathbf{v}}$ for the system power injection $\hat{\mathbf{s}}$, via (2.18) with $\mathbf{v}^{(0)} = \check{\mathbf{v}}$.

(Step 4) Check whether $(\hat{\mathbf{v}}, \mathcal{S})$ is a strongly secured candidate pair that is consistent with all elements in $\mathcal{L}$. [7]

(Step 5) If it does, then add it to $\mathcal{L}$; otherwise, partition $\mathcal{S}$ and update $\mathcal{L}^{\text{aux}}$ in the following way (see Figure 3.8):

- Find index j^* such that the convex polygon $\mathcal{S}_{j^*}$ has the largest area,

[7] $\rho^{\ddagger}(\hat{\mathbf{v}}) > 0$ is guaranteed by Proposition 2.1 .

- Partition $\mathcal{S}_{j^*}$ into smaller pieces by connecting $(\hat{\mathbf{s}})_{j^*}$ to the middle points of all edges in $\mathcal{S}_{j^*}$,
- Cut every non-convex piece into two smaller triangular pieces along the diagonal stemming at $(\hat{\mathbf{s}})_{j^*}$,
- For each piece, first obtain a new system power injection set by replacing $\mathcal{S}_{j^*}$ of $\mathcal{S}$ with the closure of this piece, then add to $\mathcal{L}^{\text{aux}}$ an element formed by $\hat{\mathbf{v}}$ and the resultant new system power injection set.

Final Stage: Check whether $\mathcal{L}^{\text{aux}}$ is empty. If yes, then declare that $\mathcal{S}^{\text{uncertain}}$ is admissible for $\mathbf{v}^{\text{initial}}$. Otherwise, we are unsure of the admissibility.

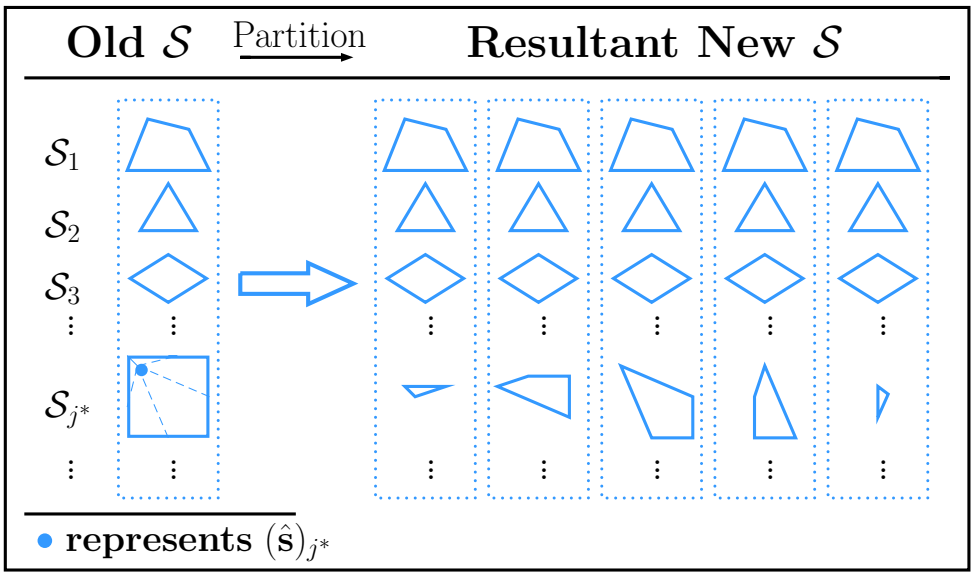

Figure 3.8 – Illustration of step 5 in the intermediate stage of the second solution method. The leftmost column represents the original system power injection set $\mathcal{S}$. First, we find the $\mathcal{S}_{j^*}$ that has the largest area, which is a rectangle in the example. Then, we connect $(\hat{\mathbf{s}})_{j^*}$ (shown with a $\circ$) to the middle points of all edges in $\mathcal{S}_{j^*}$, hence break $\mathcal{S}_{j^*}$ into four pieces. Next, taking into account that the Boomerang-like piece on the top-left corner of $\mathcal{S}_{j^*}$ is non-convex, we therefore cut it into two triangular pieces. All of these procedures can be efficiently realized in computer programming. After partition, the original $\mathcal{S}$ is broken into five new system power injection sets, every of which contains $\hat{\mathbf{s}}$. As a result, we need to add five elements to $\mathcal{L}^{\text{aux}}$ in this illustration. Each of the five elements is a pair formed by $\hat{\mathbf{v}}$ and one of the five new system power injection sets.

For the second solution method, we give the following theorem on its validity. The corresponding proof is included in Appendix 3.P.

Theorem 3.9

The proposed second solution method is correct in the sense that, whenever it declares $\mathcal{S}^{\text{uncertain}}$ *admissible for* $\mathbf{v}^{\text{initial}}$*, it* is *so.*

3.5.2 Computational Complexity and Implementation Issues

In what follows, we analyze the computational complexity of our second solution method. Meanwhile, we show that some steps can be implemented in parallel.

- **For Step 2 in the Intermediate Stage:** The computational complexity of $\mathbf{s}^{\text{c}}$ depends linearly on the number of vertices in $\mathcal{S}_j$, $j = 1, ..., N^{\text{phase}}N$. In addition, the computational complexity of $\hat{\mathbf{s}}$ is quadratic in $N^{\text{phase}}N$, according to our analysis in Remark 2.1.
- **For Step 3 in the Intermediate Stage:** If the iterative method (2.18) is implemented by following the procedures in Remark 2.1, then each iteration has a computational complexity approximately linear in the number of buses and physical branches.
- **For Step 4 in the Intermediate Stage:**

  (i) In order to check whether $(\hat{\mathbf{v}}, \mathcal{S})$ is a strongly secured candidate pair, we need to find the following values.

  - $\max_{\mathbf{s}\in\mathcal{S}} \xi(\mathbf{s} - \mathbf{F}(\hat{\mathbf{v}}))$,
  - $\max_{\mathbf{s}\in\mathcal{S}} \rho^{\dagger}(\hat{\mathbf{v}}, \mathbf{s})$,
  - $\max_{\mathbf{s}\in\mathcal{S}} \left(\boldsymbol{\delta}_j(\hat{\mathbf{v}}, \mathbf{s})\right)_{\ell}$, $j = 1, ..., N$, $\ell = 1, ..., N^{\text{phase}}$,
  - $\max_{\mathbf{s}\in\mathcal{S}} \left(\boldsymbol{\tau}_{jk}(\hat{\mathbf{v}}, \mathbf{s})\right)_{\ell}$, $j = 1, ..., N$, $\ell = 1, ..., N^{\text{phase}}$.

  Taking into consideration that

  - The $N^{\text{phase}}N$ entries in $|\mathbf{s} - \mathbf{F}(\hat{\mathbf{v}})|$ are independent of each other,
  - $\xi(\mathbf{s} - \mathbf{F}(\hat{\mathbf{v}})) = \max\limits_{m=1,...,N^{\text{phase}}N} \sum\limits_{n=1}^{N^{\text{phase}}N} \left|\left(\mathbf{W}^{-1}\mathbf{Y}_{LL}^{-1}\overline{\mathbf{W}}^{-1}\right)_{m,n}\right| |(\mathbf{s} - \mathbf{F}(\hat{\mathbf{v}}))_n|$,
  - $\rho^{\dagger}(\hat{\mathbf{v}}, \mathbf{s})$ is a monotonically increasing function of $\xi(\mathbf{s} - \mathbf{F}(\hat{\mathbf{v}}))$,
  - All entries in $\boldsymbol{\delta}_j(\hat{\mathbf{v}}, \mathbf{s})$, $\boldsymbol{\tau}_{jk}(\hat{\mathbf{v}}, \mathbf{s})$ are monotonically increasing with respect to both $\rho^{\dagger}(\hat{\mathbf{v}}, \mathbf{s})$ and the entries in $|\mathbf{s} - \mathbf{F}(\hat{\mathbf{v}})|$,

we obtain

- $\max_{\mathbf{s}\in\mathcal{S}} \xi(\mathbf{s}-\mathbf{F}(\hat{\mathbf{v}})) = \xi(\mathbf{s}^*-\mathbf{F}(\hat{\mathbf{v}}))$,
- $\max_{\mathbf{s}\in\mathcal{S}} \rho^\dagger(\hat{\mathbf{v}},\mathbf{s}) = \rho^\dagger(\hat{\mathbf{v}},\mathbf{s}^*)$,
- $\max_{\mathbf{s}\in\mathcal{S}} \Big(\boldsymbol{\delta}_j(\hat{\mathbf{v}},\mathbf{s})\Big)_\ell = \Big(\boldsymbol{\delta}_j(\hat{\mathbf{v}},\mathbf{s}^*)\Big)_\ell$, $j=1,...,N$, $\ell=1,...,N^{\text{phase}}$,
- $\max_{\mathbf{s}\in\mathcal{S}} \Big(\boldsymbol{\tau}_{jk}(\hat{\mathbf{v}},\mathbf{s})\Big)_\ell = \Big(\boldsymbol{\tau}_{jk}(\hat{\mathbf{v}},\mathbf{s}^*)\Big)_\ell$, $j=1,...,N$, $\ell=1,...,N^{\text{phase}}$,

with $\mathbf{s}^*\in\mathcal{S}$ being a vector such that $(\mathbf{s}^*)_j$ maximizes $|(\mathbf{s}^*)_j-(\hat{\mathbf{s}})_j|$, $j=1,...,N^{\text{phase}}N$. As each $\mathcal{S}_j$ is either a polygon or a singleton, the computational complexity of $\mathbf{s}^*$ depends linearly on the number of vertices in $\mathcal{S}_j$, $j=1,...,N^{\text{phase}}N$. Further, as the entries in $\mathbf{s}^*$ are independent, we can assign the computation of each entry in $\mathbf{s}^*$ to a thread of multi-core CPU and GPU. In this way, the computation can be executed in parallel for acceleration. With the obtained value of $\mathbf{s}^*$, we can compute $\boldsymbol{\delta}_j(\hat{\mathbf{v}},\mathbf{s}^*)$, $\boldsymbol{\tau}_{jk}(\hat{\mathbf{v}},\mathbf{s}^*)$ in parallel via a group of threads, since these variables are also independent of each other.

(ii) In order to determine whether $(\hat{\mathbf{v}},\mathcal{S})$ is consistent with an element in $\mathcal{L}$, we need to verify the condition (3.14). The computational complexity of this verification is linear in $N^{\text{phase}}N$, due to the left-hand side of (3.14). Note that the verification for different elements in $\mathcal{L}$ can be executed in parallel, since they do not rely on each other.

- **For Step 5 in the Intermediate Stage:** The major computational complexity comes from the identification of the index j^*. To find j^*, we first need to compute the area for every S_j. This process can be executed in parallel, and the corresponding computational complexity for each S_j depends linearly on the number of vertices in S_j [77]. Then, we compare the computed areas and obtain the value of j^*, for which the computational complexity is linear in $N^{\text{phase}}N$.

3.5.3 Numerical Evaluation

In this section, we give numerical examples on modified IEEE Test Feeders [55], [56]. Specifically, we first illustrate the second solution method in Section 3.5.1 on a modified IEEE 13-Bus Test Feeder. Then, we evaluate the performance and scalability of the method on modified IEEE 37-Bus and 123-Bus Test Feeders.

Illustration of the Method

We modify the IEEE 13-Bus Test Feeder by (i) taking the three-phase configuration 602 for all transmission lines, and (ii) removing the regulator. Denote the benchmark system power injection of this network by $\mathbf{s}^{\text{initial}}$, and let $\mathbf{v}^{\text{initial}}$ be the corresponding system electrical state around $\mathbf{w}$ that is guaranteed by Theorem 2.1. Let us assume:

- For phase b at bus 634, phase c at bus 671, and phase a at bus 652, the power injections are uncertain and belong to the domains in Figure 3.9.
- For the other phases and buses, the power injections are fixed to the benchmark values.

This specifies the uncertainty set $\mathcal{S}^{\text{uncertain}}$. Clearly, $\mathcal{S}^{\text{uncertain}}$ includes $\mathbf{s}^{\text{initial}}$. As some of the nodal-voltage magnitudes are below 0.95 p.u. and some of the branch-current magnitudes are over 0.3 p.u. for $\mathbf{v}^{\text{initial}}$, we let

- the security bounds on the nodal-voltage magnitudes be 0.9 and 1.1 p.u.,
- the security bounds on the branch-current magnitudes be 0.4 p.u.

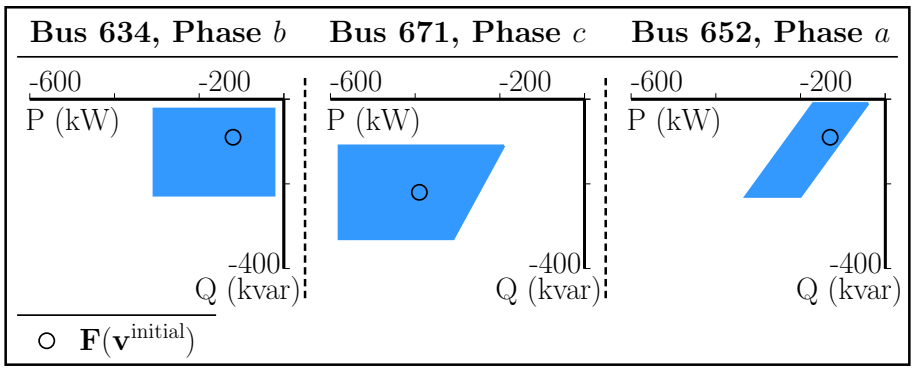

Figure 3.9 – The uncertainty set of system power injections.

In Figure 3.10, we show a step-by-step illustration of the second solution method. After the initial stage of the method, we enter the 1-st round of the intermediate stage. In this round, $(\hat{\mathbf{v}}, \mathcal{S})$ is not a strongly secured candidate pair. Therefore, we partition the system power injection set and add four elements to $\mathcal{L}^{\text{aux}}$. Next, in the 2-nd to 4-th rounds, we sequentially add three elements into $\mathcal{L}$. However, in the 5-th round, $(\hat{\mathbf{v}}, \mathcal{S})$ is not a strongly secured candidate pair again. Hence, we partition the system power injection set and add four elements to $\mathcal{L}^{\text{aux}}$. Then, in the 6-th to 9-th rounds, we sequentially add four elements to $\mathcal{L}$ and stop the intermediate stage. In the final stage, we declare that $\mathcal{S}^{\text{uncertain}}$ is admissible for $\mathbf{v}^{\text{initial}}$, since $\mathcal{L}^{\text{aux}}$ is empty.

The example is completed in 0.07 seconds, using non-parallel MATLAB implementation.

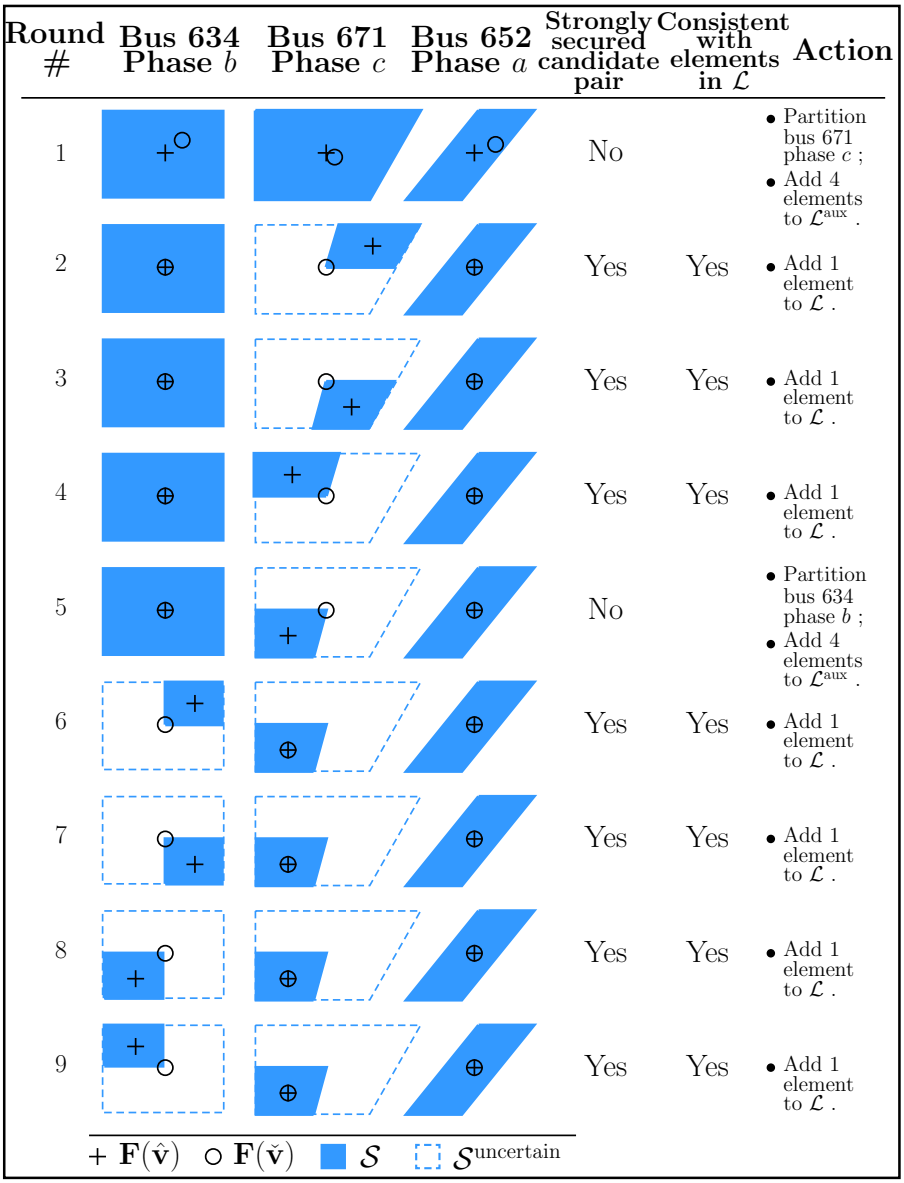

Figure 3.10 – Illustration of the second solution method.

Performance Evaluation

Consider that the number of partitions is a major factor that affects the computational complexity of the method, we keep the security bounds in the previous example and analyze this factor via two new examples on a modified IEEE 37-Bus Test Feeder.

1. In the first example, we denote the benchmark system power injection by $\mathbf{s}^{\text{initial}}$, and let $\mathbf{v}^{\text{initial}}$ be its solution around $\mathbf{w}$ that is guaranteed by Theorem 2.1. In addition, we assume that there is a single-phase power source, for which the power injection is uncertain and belongs to the domain in Figure 3.11. We attach

this power source to the phase c of a previously unloaded bus, and fix the power injections of the other phases and buses. In this way, we specify the set $\mathcal{S}^{\text{uncertain}}$.

- Case 1: If the power source is attached to bus 702 that is close to the slack bus, we have that the needed number of partitions increases faster as κ gets closer to 1. When $\kappa = 1$, one of the branch-current magnitudes reaches its security bound.
- Case 2: If the power source is attached to bus 709 that is in the middle of this network, we again have that the needed number of partitions increases faster as κ gets closer to 1. When $\kappa = 1$, one of the nodal-voltage magnitudes reaches its upper security bound.
- Case 3: If the power source is attached to bus 711 that is almost the farthest from the slack bus, we obtain a result that is similar to the one in Case 2.

Clearly, in all three cases, we need no partition for $\kappa \leq 0.75$ and at most 2–3 partitions for $\kappa \leq 0.938$. For $\kappa = 0.992$, the method terminates in approximately 0.2 seconds.

As a by-product, in Cases 2 and 3, we notice that the monotonicity assumption in [16] does not hold, since the lowest value of the nodal-voltage magnitudes is achieved at ($\kappa P^{\max}$,0).

2. In the second example, we let $\mathbf{v}^{\text{initial}} = \mathbf{w}$ and assume that the real and imaginary parts of all power injections can vary independently between 0 and κ times of their benchmark values (i.e., $\kappa = 1$ corresponds to the benchmark values). In this way, we specify the set $\mathcal{S}^{\text{uncertain}}$ such that each of the 32 loaded phases has a rectangular domain of uncertain power injections. Obviously, as κ increases, (i) the size of $\mathcal{S}^{\text{uncertain}}$ grows, and (ii) the worst-case voltage/current magnitudes move toward the security bounds. Taking these into account, we increase the value of κ from 0 and observe the number of partitions. Through numerical experiments, we find that the method terminates in around 0.01 to 0.02 seconds without performing any set partition for $\kappa \in [0, 1.15]$. After $\kappa = 1.15$, the number of partitions starts to increase exponentially with respect to κ, which follows the heuristic nature of the method. This example demonstrates the applicability of the method to real-world problems, because (i) $\mathcal{S}^{\text{uncertain}}$ represents the uncertainty of 32 phases, (ii) the size of $\mathcal{S}^{\text{uncertain}}$ is large for $\kappa = 1.15$. Apart from this, we have that the method is not conservative in terms of tightness, as the lowest nodal-voltage magnitude for $\kappa = 1.15$ is only 0.017 p.u. away from the corresponding security bound.

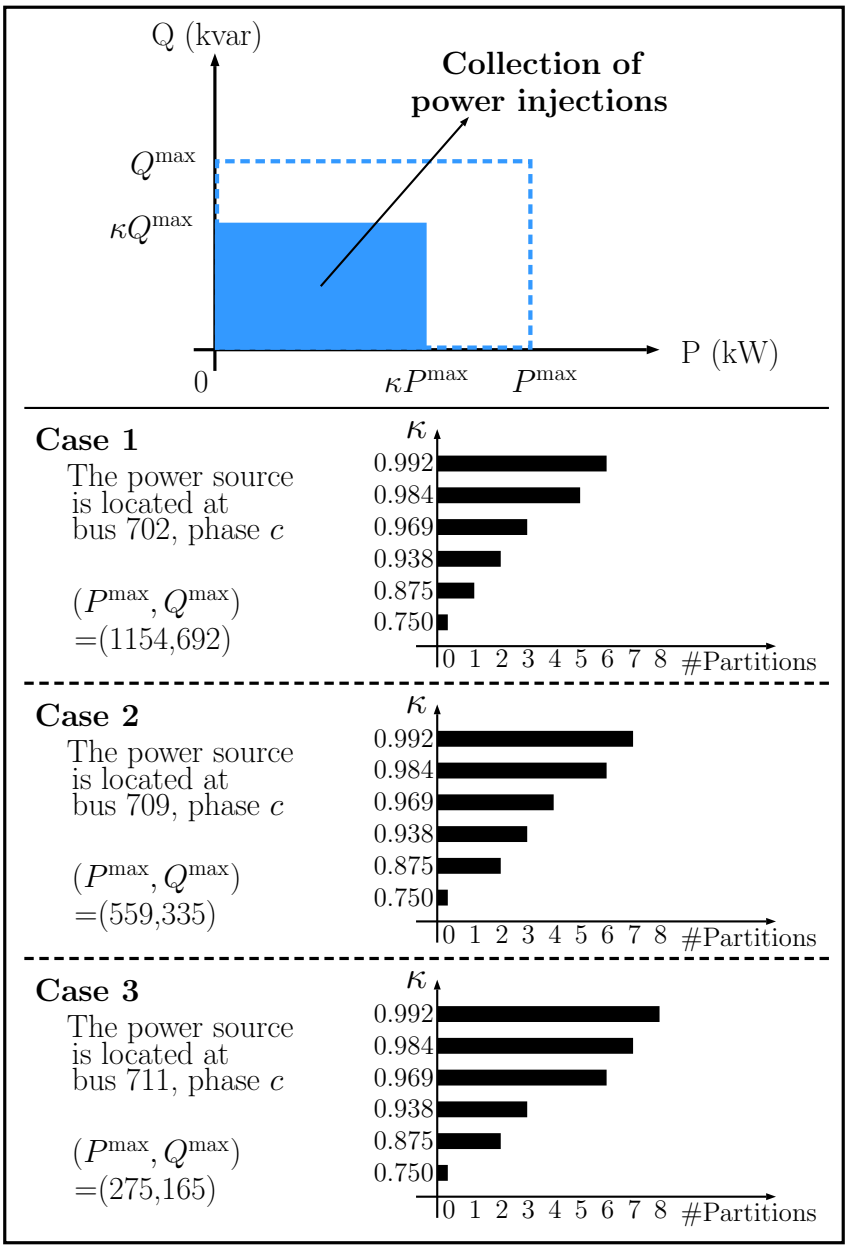

Figure 3.11 – Performance evaluation. $\kappa \in [0, 1]$ is a real scaling factor.

Scalability Test

Now, we take a modified IEEE 123-Bus Test Feeder for scalability test. Specifically, we (i) take the three-phase configuration 1 for all transmission lines, (ii) model the switches by 10-feet lines, (iii) remove the regulators, and (iv) keep the security bounds the same as before. Similarly to the previous evaluation on IEEE 37-Bus Test Feeder, we are interested in the needed number of partitions.

Denote the benchmark system power injection by $\mathbf{s}^{\text{initial}}$, and let $\mathbf{v}^{\text{initial}}$ be its solution around $\mathbf{w}$ that is guaranteed by Theorem 2.1. Consider that if $\mathbf{v}_0 = (1, e^{\frac{-\jmath 2\pi}{3}}, e^{\frac{\jmath 2\pi}{3}})^T$, then the lowest nodal-voltage magnitude in $\mathbf{v}^{\text{initial}}$ is already below the corresponding security bound. Therefore, we take $\mathbf{v}_0 = (1.05, 1.05e^{\frac{-\jmath 2\pi}{3}}, 1.05e^{\frac{\jmath 2\pi}{3}})^T$.

In this example, we assume that the real and imaginary parts of all power injections can vary independently between $1 - \frac{\kappa}{2}$ and $1 + \frac{\kappa}{2}$ times of their benchmark values (i.e., $\kappa = 0$ corresponds to the benchmark values). In this way, we specify the set $\mathcal{S}^{\text{uncertain}}$ such that each of the 95 loaded phases has a rectangular domain of uncertain power injections.

Same as in the previous example, as κ increases, (i) the size of $\mathcal{S}^{\text{uncertain}}$ grows, and (ii) the worst-case voltage/current magnitudes move toward the security bounds. Let us increase the value of κ from 0 and observe the number of partitions. Through numerical experiments, it is found that the method terminates in around 0.03 seconds without performing any set partition for $\kappa \in [0, 0.31]$. After $\kappa = 0.31$, the number of partitions starts to increase exponentially with respect to κ. For $\kappa = 0.31$, we find that the highest branch-current magnitude is only 0.032 p.u. below the corresponding security bound. This example demonstrates that the method is efficient for large networks and is not conservative in terms of tightness.

3.6 Conclusions

We have studied the admissibility problem in ADNs. In order to solve this problem, we have introduced the auxiliary concept of $\mathcal{V}$-control. Specifically, given a set $\mathcal{S}$ of system power injections and a set $\mathcal{V}$ of system electrical states, we say that $\mathcal{S}$ is a domain of $\mathcal{V}$-control if: any continuous path of the system electrical state that starts in $\mathcal{V}$ must stay in $\mathcal{V}$, as long as the corresponding path of the system power injection is constrained in $\mathcal{S}$. With the concept of $\mathcal{V}$-control, the admissibility problem consists in whether there exists a set $\mathcal{V} \subseteq \mathcal{V}^\star$ such that (i) $\mathbf{v}^{\text{initial}} \in \mathcal{V}$, and (ii) $\mathcal{S}^{\text{uncertain}}$ is a domain of $\mathcal{V}$-control. We have shown that the "existence of a unique power-flow solution $\mathbf{v} \in \mathcal{V}$ for every $\mathbf{s} \in \mathcal{S}$" alone is neither sufficient nor necessary to ensure that $\mathcal{S}$ is a domain of $\mathcal{V}$-control. For $\mathcal{S}$ to be a domain of $\mathcal{V}$-control, we have given additional conditions that complement the existence and uniqueness of the power-flow solution. Moreover, we have proposed theorems to ensure that there exists a unique power-flow solution $\mathbf{v} \in \mathcal{V}$ for every $\mathbf{s} \in \mathcal{S}$. Due to the real-quadratic nature of the multi-dimensional power-flow equation, we have incidentally discovered that local uniqueness implies non-singularity. This is the converse of the inverse function theorem. Using a subset of the theoretical results in this chapter, we have developed a first solution method for the admissibility problem. This method is tight, but not suitable for real-time applications in large networks. With another subset of the theoretical results in this chapter and the results in Chapter 2, we have developed a second solution method for the admissibility

problem. This method is less tight than the first solution method, but it is suitable for real-time applications in large networks.

Appendix

3.A Proof of Lemma 3.1

Let $\mathbf{v} : [0,1] \to \mathbb{C}^{N^{\text{phase}}N}$ be a continuous path such that $\mathbf{v}(0) \in \mathcal{V}$ and $\mathbf{F}(\mathbf{v}(t)) \in \mathcal{S}, \forall t \in [0,1]$. We want to show that $\mathbf{v}(t) \in \mathcal{V}, \forall t \in [0,1]$.

First, denote the continuous inverse of $\mathbf{F}$ from $\mathcal{S}$ to $\mathcal{V}$ by $\mathbf{\Phi}$. As $\mathbf{F}(\mathbf{v}(t)) \in \mathcal{S}, \forall t \in [0,1]$, we have that $\mathbf{\Phi}(\mathbf{F}(\mathbf{v}(t))) \in \mathcal{V}$ is well-defined. Next, let $\mathcal{T} = \{t \in [0,1] : \mathbf{v}(t) \in \mathcal{V}\}$. Note that $\mathcal{T}$ can also be represented by $\{t \in [0,1] : \mathbf{v}(t) = \mathbf{\Phi}(\mathbf{F}(\mathbf{v}(t)))\}$ due to the following reasons:

- $\mathbf{v}(t) \in \mathcal{V} \Rightarrow \mathbf{v}(t) = \mathbf{\Phi}(\mathbf{F}(\mathbf{v}(t)))$, since $\mathbf{v}(t), \mathbf{\Phi}(\mathbf{F}(\mathbf{v}(t))) \in \mathcal{V}$ have the same image by $\mathbf{F}$.
- $\mathbf{v}(t) \in \mathcal{V} \Leftarrow \mathbf{v}(t) = \mathbf{\Phi}(\mathbf{F}(\mathbf{v}(t)))$, since $\mathbf{\Phi}(\mathbf{F}(\mathbf{v}(t))) \in \mathcal{V}$.

Now, let us prove $\mathbf{v}(t) \in \mathcal{V}, \forall t \in [0,1]$ by showing that $\mathcal{T} = [0,1]$. Consider:

- $\mathcal{T}$ is non-empty because $0 \in \mathcal{T}$.
- $\mathcal{T}$ is open in $[0,1]$ because $\mathcal{T} = \{t \in [0,1] : \mathbf{v}(t) \in \mathcal{V}\}$, $\mathcal{V}$ is an open set, and $\mathbf{v}$ is continuous.
- $\mathcal{T}$ is closed in $[0,1]$ because $\mathcal{T} = \{t \in [0,1] : \mathbf{v}(t) = \mathbf{\Phi}(\mathbf{F}(\mathbf{v}(t)))\}$, and $\mathbf{v}$, $\mathbf{F}$, $\mathbf{\Phi}$ are continuous.

It follows that $\mathcal{T}$ is a non-empty, closed and open subset of $[0,1]$. Since $[0,1]$ is connected, its only closed and open subsets are the empty set and itself. Thus, $\mathcal{T} = [0,1]$, which means that $\mathcal{S}$ is a domain of $\mathcal{V}$-control.

■

3.B Proof of Theorem 3.1

For $\mathbf{s} \in \mathcal{S}$, let $\mathbf{\Phi}(\mathbf{s})$ be the unique $\mathbf{v} \in \mathcal{V}$ such that $\mathbf{F}(\mathbf{v}) = \mathbf{s}$. This defines the mapping $\mathbf{\Phi}$. Consider that set $\mathcal{V}$ is open and non-singular. By the inverse function theorem, for any $\mathbf{s} \in \mathcal{S}$, there exist neighbourhoods $\mathcal{U}_v \subseteq \mathcal{V}$ of $\mathbf{\Phi}(\mathbf{s})$ and $\mathcal{U}_s$ of $\mathbf{s}$ such that $\mathbf{F}$

maps $\mathcal{U}_v$ bijectively to $\mathcal{U}_s$, and its inverse (say $\mathbf{\Phi_s}$) is differentiable hence continuous. Clearly, for any $\mathbf{s}' \in \mathcal{U}_s \bigcap \mathcal{S}$, we have $\mathbf{\Phi_s}(\mathbf{s}') \in \mathcal{U}_v \subseteq \mathcal{V}$. Since uniqueness is assume in the second item of this theorem, there is $\mathbf{\Phi}(\mathbf{s}') = \mathbf{\Phi_s}(\mathbf{s}'), \forall \mathbf{s}' \in \mathcal{U}_s \bigcap \mathcal{S}$. This proves that $\mathbf{\Phi}$ is continuous at $\mathbf{s}$. Moreover, as this is true for every $\mathbf{s} \in \mathcal{S}$, we conclude that $\mathbf{\Phi}$ is continuous in $\mathcal{S}$. Finally, by Lemma 3.1, it follows that $\mathcal{S}$ is a domain of $\mathcal{V}$-control.

■

3.C Proof of Theorem 3.3

We prove by contradiction. Let set $\mathcal{V}$ be non-singular and convex. In addition, suppose that there exist $\mathbf{v},\ \mathbf{v}' \in \mathcal{V}$ such that (i) $\mathbf{F}(\mathbf{v}) = \mathbf{F}(\mathbf{v}')$, and (ii) $\mathbf{v} \neq \mathbf{v}'$. Owing to convexity, there is $\dfrac{\mathbf{v}+\mathbf{v}'}{2} \in \mathcal{V}$. Furthermore, according to the non-singularity of $\mathcal{V}$, $\mathbf{J_F}\left(\dfrac{\mathbf{v}+\mathbf{v}'}{2}\right)$ is non-singular. However, by the Property 1 in [78], $\mathbf{J_F}\left(\dfrac{\mathbf{v}+\mathbf{v}'}{2}\right)$ should be singular, since $\mathbf{F}$ is real-quadratic in rectangular coordinates. This creates a contradiction.

■

3.D Proof of Theorem 3.4

We need to show that $\mathcal{S} \subseteq \mathbf{F}(\mathcal{V})$, i.e., $\mathbf{F}(\mathcal{V}) \bigcap \mathcal{S} = \mathcal{S}$. Since $\mathcal{S}$ is connected by condition 2, its closed and open subsets are $\mathcal{S}$ and the empty set. Based on this, consider that (i) $\mathbf{F}(\mathcal{V}) \bigcap \mathcal{S} \subseteq \mathcal{S}$, and (ii) $\mathbf{F}(\mathcal{V}) \bigcap \mathcal{S}$ is not empty by condition 3, we can prove $\mathbf{F}(\mathcal{V}) \bigcap \mathcal{S} = \mathcal{S}$ by showing that $\mathbf{F}(\mathcal{V}) \bigcap \mathcal{S}$ is both closed and open in $\mathcal{S}$, which we do next.

First, the openness of $\mathcal{V}$ implies $\partial\mathcal{V} = \mathrm{cl}(\mathcal{V}) \setminus \mathcal{V}$, where $\mathrm{cl}(\mathcal{V})$ is the closure of $\mathcal{V}$ (i.e., the set of limit points that can be approached from $\mathcal{V}$). As $\mathcal{V}$ is bounded, we have that the closure $\mathrm{cl}(\mathcal{V})$ is compact. Therefore, by continuity of $\mathbf{F}$, $\mathbf{F}(\mathrm{cl}(\mathcal{V}))$ is compact and $\mathbf{F}(\mathrm{cl}(\mathcal{V})) \bigcap \mathcal{S}$ is closed in $\mathcal{S}$. By condition 4, $\mathbf{F}(\mathrm{cl}(\mathcal{V}) \setminus \mathcal{V}) \bigcap \mathcal{S}$ is empty. Thus, we have $\mathbf{F}(\mathrm{cl}(\mathcal{V})) \bigcap \mathcal{S} = \mathbf{F}(\mathcal{V}) \bigcap \mathcal{S}$. So, $\mathbf{F}(\mathcal{V}) \bigcap \mathcal{S}$ is closed in $\mathcal{S}$.

Second, $\mathcal{V}$ is open and non-singular by condition 1. By the inverse function theorem, $\mathbf{F}(\mathcal{V})$ is open and therefore $\mathbf{F}(\mathcal{V}) \bigcap \mathcal{S}$ is open in $\mathcal{S}$. Thus, $\mathbf{F}(\mathcal{V}) \bigcap \mathcal{S}$ is a non-empty, closed and open subset in $\mathcal{S}$, which means that $\mathbf{F}(\mathcal{V}) \bigcap \mathcal{S} = \mathcal{S}$ and completes the proof.

■

3.E Proof of Theorem 3.5

First, we show that if $\mathbf{J_F}(\mathbf{v})$ is singular, then there is a non-zero vector $\boldsymbol{\mu} \in \mathbb{C}^{N^{\text{phase}}N}$ such that $\mathbf{F}(\mathbf{v}+\theta\boldsymbol{\mu}) = \mathbf{F}(\mathbf{v}-\theta\boldsymbol{\mu}), \forall\theta \in \mathbb{R}$. To this end, let $\boldsymbol{\mu}$ be an eigenvector with eigenvalue 0 of the Jacobian $\mathbf{J_F}(\mathbf{v})$, i.e., $\mathbf{J_F}(\mathbf{v}) \cdot \boldsymbol{\mu} = \mathbf{0}$. For $\theta \in \mathbb{R}$, define $\boldsymbol{\Psi}(\theta) = \mathbf{F}(\mathbf{v}+\theta\boldsymbol{\mu})$. Since $\mathbf{F}$ is real-quadratic in rectangular coordinates, there exist some vectors $\mathbf{a},\ \mathbf{b},\ \mathbf{c} \in \mathbb{C}^{N^{\text{phase}}N}$ such that $\boldsymbol{\Psi}(\theta) = \theta^2\mathbf{a} + \theta\mathbf{b} + \mathbf{c}$. Consider that $\dfrac{\mathrm{d}\boldsymbol{\Psi}(\theta)}{\mathrm{d}\theta} = 2\theta\mathbf{a} + \mathbf{b}$ and by chain rule $\left.\dfrac{\mathrm{d}\boldsymbol{\Psi}(\theta)}{\mathrm{d}\theta}\right|_{\theta=0} = \mathbf{J_F}(\mathbf{v}) \cdot \boldsymbol{\mu}$. We obtain $\mathbf{b} = \mathbf{0}$. Thus, $\boldsymbol{\Psi}(\theta) = \theta^2\mathbf{a} + \mathbf{c} = \boldsymbol{\Psi}(-\theta)$.

Next, we prove the theorem by contradiction. Assume that there exists $\mathbf{v} \in \mathcal{V}$ such that $\mathbf{J_F}(\mathbf{v})$ is singular. Then, there is a non-zero vector $\boldsymbol{\mu}$ such that $\mathbf{F}(\mathbf{v}+\theta\boldsymbol{\mu}) = \mathbf{F}(\mathbf{v}-\theta\boldsymbol{\mu}), \forall\theta \in \mathbb{R}$. As $\mathcal{V}$ is open, there is some $\epsilon > 0$ such that $\mathbf{v}+\theta\boldsymbol{\mu} \in \mathcal{V}$ whenever $|\theta| < \epsilon$. This contradicts that $\mathcal{V}$ is a domain of uniqueness, and completes the proof.

■

3.F Proof of Theorem 3.2

Let $\mathbf{F}^{-1}(\mathcal{S}) = \{\mathbf{v} \in \mathbb{C}^{N^{\text{phase}}N} : \mathbf{F}(\mathbf{v}) \in \mathcal{S}\}$. Because $\mathbf{F}$ is continuous and $\mathcal{S}$ is open, we have that $\mathbf{F}^{-1}(\mathcal{S})$ is open. Therefore, $\mathcal{V}' = \mathbf{F}^{-1}(\mathcal{S}) \bigcap \mathcal{V}$ is open and a domain of uniqueness. Further, by Theorem 3.5, $\mathcal{V}'$ is non-singular.

According to Theorem 3.1, $\mathcal{S}$ is a domain of $\mathcal{V}'$-control. As the unique solution in $\mathcal{V}$ is in $\mathcal{V}'$, we have that $\mathcal{S}$ is also a domain of $\mathcal{V}$-control.

■

3.G Proof of Theorem 3.6

We need to show that $\mathcal{S}^{\text{uncertain}}$ is a domain of $\mathcal{V}$-control. By Theorem 3.1, as $\mathcal{V}$ is already open and non-singular, we only need to prove that $\forall\mathbf{s} \in \mathcal{S}^{\text{uncertain}}$, there exists a unique $\mathbf{v} \in \mathcal{V}$ such that $\mathbf{F}(\mathbf{v}) = \mathbf{s}$.

According to Theorem 3.3, $\mathcal{V}$ is a domain of uniqueness because it is included in a non-singular and convex set. In this way, it suffices to show that there exists a $\mathbf{v} \in \mathcal{V}$ such that $\mathbf{F}(\mathbf{v}) = \mathbf{s}$, for every $\mathbf{s} \in \mathcal{S}^{\text{uncertain}}$. To this end, we check the four conditions in Theorem 3.4.

In Theorem 3.4, conditions 1 and 2 are automatically satisfied by construction. Condition 3 follows from $\mathbf{F}(\mathbf{v}^{\text{initial}}) \in \mathcal{S}^{\text{uncertain}}$.

Now, let us focus on condition 4. Since P0(ℓ) are infeasible for all ℓ, we have that set

$$\mathbf{F}\left(\bigcup_{\ell=1}^{L}\left\{\mathbf{v}: f_\ell(\mathbf{v})=0 \text{ and } f_{\ell'}(\mathbf{v})\geq 0,\ \ell'\in\{1,...,L\}\setminus\{\ell\}\right\}\right)$$

has an empty intersection with $\mathcal{S}^{\text{uncertain}}$. Therefore, we can complete the proof by showing that the boundary $\partial\mathcal{V}$ is contained in the set

$$\bigcup_{\ell=1}^{L}\left\{\mathbf{v}: f_\ell(\mathbf{v})=0 \text{ and } f_{\ell'}(\mathbf{v})\geq 0,\ \ell'\in\{1,...,L\}\setminus\{\ell\}\right\}.$$

Consider that all f_ℓ are continuous and the topological boundary of $\mathcal{V}$ is the set of points that are both limit points of $\mathcal{V}$ and limit points of the complement of $\mathcal{V}$. If $\mathbf{v}\in\partial\mathcal{V}$, then $\mathbf{v}$ is the limit of some infinite sequence $\mathbf{v}^{(n)}\in\mathcal{V}$, thus $f_\ell(\mathbf{v}^{(n)})>0$ and $f_\ell(\mathbf{v})\geq 0$ for all $\ell\in\{1,...,L\}$. Also, $\mathbf{v}$ is the limit of some infinite sequence $\mathbf{v}'^{(n)}$ outside $\mathcal{V}$. Since there are only finitely many inequalities, there must be at least one inequality, say with index ℓ^*, such that $f_{\ell^*}(\mathbf{v}'^{(n)})\leq 0$ for an infinite number of superscripts n. It follows that $f_{\ell^*}(\mathbf{v})\leq 0$ and thus $f_{\ell^*}(\mathbf{v})=0$.

■

3.H Proof of Theorem 3.7

By hypothesis, we have that $\mathcal{S}^{\text{uncertain}}$ and $\mathcal{V}$ satisfy the four conditions in Theorem 3.4. In addition, in step 1 of $\mathbf{A}'$, we have an open set $\tilde{\mathcal{V}}'$ such that (i) its closure $\text{cl}(\tilde{\mathcal{V}}')$ is non-singular and convex, and (ii) $\mathcal{V}'=\tilde{\mathcal{V}}'\bigcap\mathcal{V}^\star$. All we need to show is that $\mathcal{S}^{\text{uncertain}}$ and $\mathcal{V}'$ satisfy the four conditions in Theorem 3.4, which we do next.

First, the open set $\tilde{\mathcal{V}}'$ is non-singular, since its closure $\text{cl}(\tilde{\mathcal{V}}')$ is non-singular. Therefore, $\mathcal{V}'=\tilde{\mathcal{V}}'\bigcap\mathcal{V}^\star$ is bounded, open and non-singular, which means that condition 1 in Theorem 3.4 holds.

Next, condition 2 in Theorem 3.4 holds by hypothesis, and condition 3 in Theorem 3.4 holds because

- $\mathbf{F}(\mathcal{V})\bigcap\mathcal{S}$ is non-empty,
- $\Big(\mathbf{F}(\mathcal{V})\bigcap\mathcal{S}\Big)\subseteq\Big(\mathbf{F}(\mathcal{V}')\bigcap\mathcal{S}\Big)$.

Then, we show condition 4 in Theorem 3.4 by contradiction. Suppose that there exists $\mathbf{v}\in\partial\mathcal{V}'$ such that $\mathbf{F}(\mathbf{v})\in\mathcal{S}^{\text{uncertain}}$. Let $\mathbf{s}=\mathbf{F}(\mathbf{v})$ and consider:

- $\mathcal{S}^{\text{uncertain}}$ and $\mathcal{V}$ satisfy all the conditions in Theorem 3.4,
- $\mathcal{V} \subseteq \mathcal{V}'$, both of which are open and have empty intersection with $\partial\mathcal{V}'$.

We have that there exists $\mathbf{v}^* \in \mathcal{V}$ such that $\mathbf{F}(\mathbf{v}^*) = \mathbf{s}$ and $\mathbf{v}^* \neq \mathbf{v}$. In this way, we obtain two distinct elements in $\text{cl}(\tilde{\mathcal{V}}')$ that both correspond to $\mathbf{s} \in \mathcal{S}^{\text{uncertain}}$. However, this cannot be the case, since $\text{cl}(\tilde{\mathcal{V}}')$ is a domain of uniqueness according to Theorem 3.3. As a result, we have that condition 4 in Theorem 3.4 holds, which completes the proof.

■

3.I Proof of Proposition 3.1

First, let us construct in (3.16) a collection of sets:

$$\mathcal{V}_{m,n} = \Bigg\{ \mathbf{v} \in \text{cl}(\tilde{\mathcal{V}}) : \left\| \text{Row}_m(\mathbf{Y}_{LL}^{-1}) \right\|_1 \Bigg(\left| \Re\Big(\text{Row}_n(\mathbf{Y}_{LL})(\mathbf{v} - \mathbf{w}) \Big) \right| + \left| \Im\Big(\text{Row}_n(\mathbf{Y}_{LL})(\mathbf{v} - \mathbf{w}) \Big) \right| \Bigg) \geq |(\mathbf{v})_m| \Bigg\}, \tag{3.16}$$

where $m, n \in \{1, ..., N^{\text{phase}}N\}$. By inspection, we have that $\mathcal{V}_{m,n}$ is empty when P1(m, n, ψ, ϕ) is infeasible $\forall \psi, \phi \in \{1, -1\}$.

Next, we show that when $\mathcal{V}_{m,n}$ is empty for all $m, n \in \{1, ..., N^{\text{phase}}N\}$, the condition in (3.5) holds nowhere in $\text{cl}(\tilde{\mathcal{V}})$. Specifically,

- By the triangle inequality, the emptiness of $\mathcal{V}_{m,n}$ implies that the following inequality holds $\forall \mathbf{v} \in \text{cl}(\tilde{\mathcal{V}})$.

$$\left\| \text{Row}_m(\mathbf{Y}_{LL}^{-1}) \right\|_1 \left| \text{Row}_n(\mathbf{Y}_{LL})(\mathbf{v} - \mathbf{w}) \right| < |(\mathbf{v})_m| \,. \tag{3.17}$$

- Consequently, for each $m \in \{1, ..., N^{\text{phase}}N\}$, the following inequality holds $\forall \mathbf{v} \in \text{cl}(\tilde{\mathcal{V}})$.

$$\left\| \text{Row}_m(\mathbf{Y}_{LL}^{-1}) \right\|_1 \left\| \mathbf{Y}_{LL}(\mathbf{v} - \mathbf{w}) \right\|_\infty = \left\| \text{Row}_m(\mathbf{Y}_{LL}^{-1}) \right\|_1 \|\mathbf{i}\|_\infty < |(\mathbf{v})_m| \,. \tag{3.18}$$

- Furthermore, for each $m \in \{1, ..., N^{\text{phase}}N\}$, the following inequality holds $\forall \mathbf{v} \in \text{cl}(\tilde{\mathcal{V}})$.

$$\sum_{n=1}^{N^{\text{phase}}N} \left| (\mathbf{Y}_{LL}^{-1})_{m,n}(\mathbf{i})_n \right| \leq \left\| \text{Row}_m(\mathbf{Y}_{LL}^{-1}) \right\|_1 \|\mathbf{i}\|_\infty < |(\mathbf{v})_m| \,. \tag{3.19}$$

Thus, the closure of the set $\tilde{\mathcal{V}}$ in (3.4) is non-singular if the problems P1(m, n, ψ, ϕ) are all infeasible.

■

3.J Proof of Proposition 3.2

In step 1 of the method, we have at most $\left\lceil \min_j \frac{I_j^{\text{threshold}}}{\hat{I}_j^{\text{node}} \Delta\lambda} \right\rceil$ choices of λ, which correspond to at most $\left\lceil \min_j \frac{I_j^{\text{threshold}}}{\hat{I}_j^{\text{node}} \Delta\lambda} \right\rceil$ choices of I_j^{node}, $\forall j \in \{1, ..., N^{\text{phase}} N\}$. For each λ, we need to solve $4\Big(N^{\text{phase}} N\Big)^2$ second-order cone programming feasibility problems. Therefore, we solve at most $4\Big(N^{\text{phase}} N\Big)^2 \left\lceil \min_j \frac{I_j^{\text{threshold}}}{\hat{I}_j^{\text{node}} \Delta\lambda} \right\rceil$ second-order cone programming feasibility problems in total.

In step 2 of the method, we have that the total number of continuous functions is $L = N^{\text{phase}}\Big(3N + \text{card}(\mathcal{E})\Big)$. As a result, we have $N^{\text{phase}}\Big(3N + \text{card}(\mathcal{E})\Big)$ semi-definite programming feasibility problems to solve (namely, one feasibility problem per $\ell \in \{1, ..., L\}$).

■

3.K Basics for the Sparsity-Exploiting Hierarchy of Semi-Definite Programming Relaxations

In the following text, we give a brief description of the sparsity-exploiting hierarchy of semi-definite programming relaxations. Our description is based on the tutorial in [79].

Consider following polynomial optimization problem:

$$\begin{aligned} &\min\ f_0(\mathbf{x}) \\ &\text{s.t.}: f_k(\mathbf{x}) \geq 0\,, \qquad \forall k \in \mathcal{K}\,, \end{aligned}$$

where (i) $\mathcal{K} = \{1, ..., K\}$ is an index set, and (ii) f_0 and $f_k,\ k \in \mathcal{K}$ are all polynomials in $\mathbf{x} \in \mathbb{R}^M$.

For each polynomial f of $\mathbf{x}$, we can express it generically as $f(\mathbf{x}) = \sum_{\boldsymbol{\alpha} \in \mathbb{N}^M} c_f(\boldsymbol{\alpha}) \mathbf{x}^{\boldsymbol{\alpha}}$ with some $c_f : \mathbb{N}^M \to \mathbb{R}$, where $\mathbf{x}^{\boldsymbol{\alpha}} = x_1^{\alpha_1} \cdots x_M^{\alpha_M}$. Then, let us define

- $\mathcal{M} = \{1, ..., M\}$,
- $\omega_f = \lceil \deg(f)/2 \rceil$, where $\deg(f)$ is the degree of f,
- $\mathcal{I}_{f_k} = \{j \in \mathcal{M} : \exists \boldsymbol{\alpha} \in \mathbb{N}^M$ such that $\alpha_j > 0$ and $c_{f_k}(\boldsymbol{\alpha}) \neq 0\}, \forall k \in \mathcal{K}$, [8]
- $\mathcal{E}_{f_0} = \{\{j, \ell\} \subseteq \mathcal{M} : \exists \boldsymbol{\alpha} \in \mathbb{N}^M$ such that $\alpha_j > 0,\ \alpha_\ell > 0$ and $c_{f_0}(\boldsymbol{\alpha}) \neq 0\}$, [9]
- $\mathcal{E}_{f_k} = \{\{j, \ell\} \subseteq \mathcal{M} : j, \ell \in \mathcal{I}_{f_k}\}, \forall k \in \mathcal{K}$,
- $\mathcal{A}_\omega^{\mathcal{C}} = \{\boldsymbol{\alpha} \in \mathbb{N}^M : \alpha_j = 0, \forall j \notin \mathcal{C}$ and $\sum_{j=1}^M \alpha_j \leq \omega\}$, where $\mathcal{C} \subseteq \mathcal{M}$,
- $\boldsymbol{\varphi}(\mathbf{x}, \mathcal{A}_\omega^{\mathcal{C}})$ is a column vector formed by all monomials $\mathbf{x}^{\boldsymbol{\alpha}}$, $\boldsymbol{\alpha} \in \mathcal{A}_\omega^{\mathcal{C}}$.

To exploit sparsity, we need to first construct a graph with node set $\mathcal{M}$ and edge set $\mathcal{E}_{f_0} \bigcup \cdots \bigcup \mathcal{E}_{f_K}$. Next, we find a chordal extension of this graph [80], and denote the maximal cliques of this chordal extension by $\mathcal{C}_r,\ r \in \mathcal{R} = \{1, ..., R\}$ with R being the total number of maximal cliques. Clearly, there exists an index mapping $\theta : \mathcal{K} \to \mathcal{R}$ such that $\mathcal{I}_{f_k} \subseteq \mathcal{C}_{\theta(k)}, \forall k \in \mathcal{K}$.

Now, the original polynomial optimization problem can be equivalently transformed as follows:

$$\begin{aligned} &\min\ f_0(\mathbf{x}) \\ &\text{s.t.} : \boldsymbol{\varphi}(\mathbf{x}, \mathcal{A}_{\omega-\omega_{f_k}}^{\mathcal{C}_{\theta(k)}}) \boldsymbol{\varphi}(\mathbf{x}, \mathcal{A}_{\omega-\omega_{f_k}}^{\mathcal{C}_{\theta(k)}})^T f_k(\mathbf{x}) \succeq 0\,, \qquad \forall k \in \mathcal{K}\,, \\ &\qquad \boldsymbol{\varphi}(\mathbf{x}, \mathcal{A}_\omega^{\mathcal{C}_r}) \boldsymbol{\varphi}(\mathbf{x}, \mathcal{A}_\omega^{\mathcal{C}_r})^T \succeq 0\,, \qquad \forall r \in \mathcal{R}\,, \end{aligned}$$

where $\omega \geq \max\{\omega_{f_0}, ..., \omega_{f_K}\}$ and "$\succeq 0$" means positive semi-definite.

Observe that the above formulation can be re-written as

$$\begin{aligned} \min \quad & \sum_{\boldsymbol{\alpha} \in \bigcup_{\ell=1}^R \mathcal{A}_{2\omega}^{\mathcal{C}_\ell}} c_{f_0}(\boldsymbol{\alpha}) \mathbf{x}^{\boldsymbol{\alpha}} \\ \text{s.t.} : \quad & \sum_{\boldsymbol{\alpha} \in \bigcup_{\ell=1}^R \mathcal{A}_{2\omega}^{\mathcal{C}_\ell}} \mathbf{L}_k(\boldsymbol{\alpha}, \omega) \mathbf{x}^{\boldsymbol{\alpha}} \succeq 0\,, \qquad \forall k \in \mathcal{K}\,, \\ & \sum_{\boldsymbol{\alpha} \in \bigcup_{\ell=1}^R \mathcal{A}_{2\omega}^{\mathcal{C}_\ell}} \mathbf{M}_r(\boldsymbol{\alpha}, \omega) \mathbf{x}^{\boldsymbol{\alpha}} \succeq 0\,, \qquad \forall r \in \mathcal{R}\,, \end{aligned}$$

for some real symmetric matrices $\mathbf{L}_k(\boldsymbol{\alpha}, \omega)$ and $\mathbf{M}_r(\boldsymbol{\alpha}, \omega)$.

In this way, a semi-definite programming relaxation of the original problem is

[8] I.e., j is in $\mathcal{I}_{f_k}$ if x_j explicitly shows up in the polynomial f_k.
[9] I.e., $\{j, \ell\}$ belongs to $\mathcal{E}_{f_0}$ if x_j, x_ℓ explicitly appear together in a monomial of f_0.

obtained by replacing each monomial $\mathbf{x}^{\boldsymbol{\alpha}}$ with a single real variable $y_{\boldsymbol{\alpha}}$:

$$\begin{aligned}
\min \quad & \sum_{\boldsymbol{\alpha}\in\bigcup_{\ell=1}^{R}\mathcal{A}_{2\omega}^{\mathcal{C}_\ell}} c_{f_0}(\boldsymbol{\alpha}) y_{\boldsymbol{\alpha}} \\
\text{s.t.}: \quad & \sum_{\boldsymbol{\alpha}\in\bigcup_{\ell=1}^{R}\mathcal{A}_{2\omega}^{\mathcal{C}_\ell}} \mathbf{L}_k(\boldsymbol{\alpha},\omega) y_{\boldsymbol{\alpha}} \succeq 0\,, \qquad \forall k \in \mathcal{K}\,, \\
& \sum_{\boldsymbol{\alpha}\in\bigcup_{\ell=1}^{R}\mathcal{A}_{2\omega}^{\mathcal{C}_\ell}} \mathbf{M}_r(\boldsymbol{\alpha},\omega) y_{\boldsymbol{\alpha}} \succeq 0\,, \qquad \forall r \in \mathcal{R}\,, \\
& y_{\mathbf{0}} = 1\,.
\end{aligned}$$

Obviously, by varying ω, the size of the above semi-definite programming relaxation changes. In the literature, this parameter ω is referred to as the relaxation order. With ω being positive integers, we have a hierarchy of semi-definite programming relaxations.

3.L Proof of Proposition 3.4

(Since $\hat{\mathbf{s}}_\ell = \mathbf{F}_\ell(\hat{\mathbf{v}})$, we use the notation $\hat{\mathbf{s}}_\ell$ in this proof for ease of exposition.)

First, let us derive (3.8)–(3.9). Consider that, $\forall j \in \mathcal{N} \setminus \{0\}$, we have

$$\mathbf{v}_j = \mathbf{w}_j + \sum_{\ell=1}^{N} \boldsymbol{\Gamma}_{j,\ell} \mathrm{diag}(\overline{\mathbf{v}_\ell})^{-1} \overline{\mathbf{s}_\ell}\,, \tag{3.20}$$

$$\hat{\mathbf{v}}_j = \mathbf{w}_j + \sum_{\ell=1}^{N} \boldsymbol{\Gamma}_{j,\ell} \mathrm{diag}(\overline{\hat{\mathbf{v}}_\ell})^{-1} \overline{\hat{\mathbf{s}}_\ell}\,. \tag{3.21}$$

Taking the subtraction of these equations, we get

$$\mathbf{v}_j - \hat{\mathbf{v}}_j = \sum_{\ell=1}^{N} \boldsymbol{\Gamma}_{j,\ell} \Big(\mathrm{diag}(\overline{\mathbf{v}_\ell})^{-1} \overline{\mathbf{s}_\ell} - \mathrm{diag}(\overline{\hat{\mathbf{v}}_\ell})^{-1} \overline{\hat{\mathbf{s}}_\ell} \Big)\,. \tag{3.22}$$

Further, by taking the component-wise absolute value of (3.22), there is

$$\begin{aligned}
&|\mathbf{v}_j - \hat{\mathbf{v}}_j| \\
\leq &\sum_{\ell=1}^{N} |\mathbf{\Gamma}_{j,\ell}| \Big| \mathrm{diag}(\overline{\mathbf{v}_\ell})^{-1} \overline{\mathbf{s}_\ell} - \mathrm{diag}(\overline{\hat{\mathbf{v}}_\ell})^{-1} \overline{\hat{\mathbf{s}}_\ell} \Big| \\
\leq &\sum_{\ell=1}^{N} |\mathbf{\Gamma}_{j,\ell}| \Big| \mathrm{diag}(\overline{\mathbf{v}_\ell})^{-1} \overline{\mathbf{s}_\ell} - \mathrm{diag}(\overline{\mathbf{v}_\ell})^{-1} \overline{\hat{\mathbf{s}}_\ell} \Big| \\
&+ \sum_{\ell=1}^{N} |\mathbf{\Gamma}_{j,\ell}| \Big| \mathrm{diag}(\overline{\mathbf{v}_\ell})^{-1} \overline{\hat{\mathbf{s}}_\ell} - \mathrm{diag}(\overline{\hat{\mathbf{v}}_\ell})^{-1} \overline{\hat{\mathbf{s}}_\ell} \Big| .
\end{aligned} \tag{3.23}$$

For the first term on the right-hand side of (3.23), we have

$$\begin{aligned}
&\sum_{\ell=1}^{N} |\mathbf{\Gamma}_{j,\ell}| \Big| \mathrm{diag}(\overline{\mathbf{v}_\ell})^{-1} \overline{\mathbf{s}_\ell} - \mathrm{diag}(\overline{\mathbf{v}_\ell})^{-1} \overline{\hat{\mathbf{s}}_\ell} \Big| \\
= &\sum_{\ell=1}^{N} |\mathbf{\Gamma}_{j,\ell}| \Big| \mathrm{diag}(\mathbf{v}_\ell)^{-1} \Big| |\mathbf{s}_\ell - \hat{\mathbf{s}}_\ell| \\
\leq &\frac{\sum_{\ell=1}^{N} |\mathbf{\Gamma}_{j,\ell}| \Big| \mathrm{diag}(\mathbf{w}_\ell)^{-1} \Big| |\mathbf{s}_\ell - \hat{\mathbf{s}}_\ell|}{\alpha(\hat{\mathbf{v}}) - \rho^{\dagger}(\hat{\mathbf{v}}, \mathbf{s})} .
\end{aligned} \tag{3.24}$$

For the second term on the right-hand side of (3.23), we have

$$\begin{aligned}
&\sum_{\ell=1}^{N} |\mathbf{\Gamma}_{j,\ell}| \Big| \mathrm{diag}(\overline{\mathbf{v}_\ell})^{-1} \overline{\hat{\mathbf{s}}_\ell} - \mathrm{diag}(\overline{\hat{\mathbf{v}}_\ell})^{-1} \overline{\hat{\mathbf{s}}_\ell} \Big| \\
= &\sum_{\ell=1}^{N} |\mathbf{\Gamma}_{j,\ell}| \Big| \mathrm{diag}(\mathbf{v}_\ell)^{-1} - \mathrm{diag}(\hat{\mathbf{v}}_\ell)^{-1} \Big| |\hat{\mathbf{s}}_\ell| \\
\leq &\frac{\rho^{\dagger}(\hat{\mathbf{v}}, \mathbf{s}) \sum_{\ell=1}^{N} |\mathbf{\Gamma}_{j,\ell}| \Big| \mathrm{diag}(\mathbf{w}_\ell)^{-1} \Big| |\hat{\mathbf{s}}_\ell|}{\alpha(\hat{\mathbf{v}}) \Big(\alpha(\hat{\mathbf{v}}) - \rho^{\dagger}(\hat{\mathbf{v}}, \mathbf{s}) \Big)} .
\end{aligned} \tag{3.25}$$

Note that, in the last step of (3.25), we take account of

$$\begin{aligned}
&\left|\frac{1}{(\mathbf{v})_m}-\frac{1}{(\hat{\mathbf{v}})_m}\right| \\
=&\frac{|(\mathbf{v})_m-(\hat{\mathbf{v}})_m|}{|(\mathbf{v})_m||(\hat{\mathbf{v}})_m|} \\
\leq&\frac{\rho^{\dagger}(\hat{\mathbf{v}},\mathbf{s})|(\mathbf{w})_m|}{\Big(\alpha(\hat{\mathbf{v}})-\rho^{\dagger}(\hat{\mathbf{v}},\mathbf{s})\Big)|(\mathbf{w})_m||(\hat{\mathbf{v}})_m|} \\
\leq&\frac{\rho^{\dagger}(\hat{\mathbf{v}},\mathbf{s})}{\alpha(\hat{\mathbf{v}})\Big(\alpha(\hat{\mathbf{v}})-\rho^{\dagger}(\hat{\mathbf{v}},\mathbf{s})\Big)|(\mathbf{w})_m|}\,.
\end{aligned} \tag{3.26}$$

Therefore, by definition of $\boldsymbol{\eta}_\ell$ and inequalities (3.23)–(3.25), we have

$$|\mathbf{v}_j-\hat{\mathbf{v}}_j|\leq\frac{\displaystyle\sum_{\ell=1}^{N}|\boldsymbol{\Gamma}_{j,\ell}|\Big|\mathrm{diag}(\mathbf{w}_\ell)^{-1}\Big|\boldsymbol{\eta}_\ell(\hat{\mathbf{v}},\mathbf{s})}{\alpha(\hat{\mathbf{v}})\Big(\alpha(\hat{\mathbf{v}})-\rho^{\dagger}(\hat{\mathbf{v}},\mathbf{s})\Big)}\,, \tag{3.27}$$

which completes the proof of (3.8)–(3.9).

Next, let us cope with (3.10)–(3.11). Consider that, $\forall jk\in\mathcal{E}$, we have

$$\begin{aligned}
\mathbf{i}_{jk}-\hat{\mathbf{i}}_{jk}&=\Big(\mathbf{A}_{j,k}\mathbf{v}_j-\mathbf{C}_{j,k}\mathbf{v}_k\Big)-\Big(\mathbf{A}_{j,k}\hat{\mathbf{v}}_j-\mathbf{C}_{j,k}\hat{\mathbf{v}}_k\Big) \\
&=\mathbf{A}_{j,k}(\mathbf{v}_j-\hat{\mathbf{v}}_j)-\mathbf{C}_{j,k}(\mathbf{v}_k-\hat{\mathbf{v}}_k)\,.
\end{aligned} \tag{3.28}$$

Further, plug (3.22) into (3.28) and consider the definition in (3.7), there is

$$\mathbf{i}_{jk}-\hat{\mathbf{i}}_{jk}=\sum_{\ell=1}^{N}\boldsymbol{\Upsilon}_{jk,\ell}\Big(\mathrm{diag}(\overline{\mathbf{v}_\ell})^{-1}\overline{\mathbf{s}_\ell}-\mathrm{diag}(\overline{\hat{\mathbf{v}}_\ell})^{-1}\overline{\hat{\mathbf{s}}_\ell}\Big)\,. \tag{3.29}$$

Observe that (3.29) shares exactly the same structure with (3.22). Thus, similar to the derivations for (3.8)–(3.9), we obtain

$$|\mathbf{i}_{jk}-\hat{\mathbf{i}}_{jk}|\leq\frac{\displaystyle\sum_{\ell=1}^{N}|\boldsymbol{\Upsilon}_{jk,\ell}|\Big|\mathrm{diag}(\mathbf{w}_\ell)^{-1}\Big|\boldsymbol{\eta}_\ell(\hat{\mathbf{v}},\mathbf{s})}{\alpha(\hat{\mathbf{v}})\Big(\alpha(\hat{\mathbf{v}})-\rho^{\dagger}(\hat{\mathbf{v}},\mathbf{s})\Big)}\,, \tag{3.30}$$

which completes the proof of (3.10)–(3.11).

■

3.M Proof of Proposition 3.5

For any $\mathbf{v} \in \mathcal{V}(\hat{\mathbf{v}}, \mathcal{S})$, let $\mathbf{s} = \mathbf{F}(\mathbf{v})$ be its corresponding system power injection in $\mathcal{S}$. By Proposition 3.4 and the triangle inequality, we have

$$|\mathbf{v}_j| \leq |\hat{\mathbf{v}}_j| + \boldsymbol{\delta}_j(\hat{\mathbf{v}}, \mathbf{s}) \,, \qquad \forall j \in \mathcal{N} \setminus \{0\} \,, \tag{3.31a}$$

$$|\hat{\mathbf{v}}_j| - \boldsymbol{\delta}_j(\hat{\mathbf{v}}, \mathbf{s}) \leq |\mathbf{v}_j| \,, \qquad \forall j \in \mathcal{N} \setminus \{0\} \,, \tag{3.31b}$$

$$|\mathbf{i}_{jk}| \leq |\hat{\mathbf{i}}_{jk}| + \boldsymbol{\tau}_{jk}(\hat{\mathbf{v}}, \mathbf{s}) \,, \qquad \forall jk \in \mathcal{E} \,. \tag{3.31c}$$

Further by Definition 3.6, we have

$$|\hat{\mathbf{v}}_j| + \boldsymbol{\delta}_j(\hat{\mathbf{v}}, \mathbf{s}) < \mathbf{v}_j^{\max} \,, \qquad \forall j \in \mathcal{N} \setminus \{0\} \,, \tag{3.32a}$$

$$\mathbf{v}_j^{\min} < |\hat{\mathbf{v}}_j| - \boldsymbol{\delta}_j(\hat{\mathbf{v}}, \mathbf{s}) \,, \qquad \forall j \in \mathcal{N} \setminus \{0\} \,, \tag{3.32b}$$

$$|\hat{\mathbf{i}}_{jk}| + \boldsymbol{\tau}_{jk}(\hat{\mathbf{v}}, \mathbf{s}) < \mathbf{i}_{jk}^{\max} \,, \qquad \forall jk \in \mathcal{E} \,. \tag{3.32c}$$

Combining them together gives

$$\mathbf{v}_j^{\min} < |\mathbf{v}_j| < \mathbf{v}_j^{\max} \,, \qquad \forall j \in \mathcal{N} \setminus \{0\} \,, \tag{3.33a}$$

$$|\mathbf{i}_{jk}| < \mathbf{i}_{jk}^{\max} \,, \qquad \forall jk \in \mathcal{E} \,, \tag{3.33b}$$

which completes the proof.

■

3.N Proof of Proposition 3.6

To prove that $\bigcup_{(\hat{\mathbf{v}},\mathcal{S})\in\mathcal{L}} \mathcal{V}(\hat{\mathbf{v}}, \mathcal{S})$ is a domain of uniqueness, we have to show that $\forall \mathbf{v}, \mathbf{v}' \in \bigcup_{(\hat{\mathbf{v}},\mathcal{S})\in\mathcal{L}} \mathcal{V}(\hat{\mathbf{v}}, \mathcal{S})$, $\mathbf{F}(\mathbf{v}) = \mathbf{F}(\mathbf{v}') \Rightarrow \mathbf{v} = \mathbf{v}'$. To do so, we let $(\hat{\mathbf{v}}, \mathcal{S}) \in \mathcal{L}$ be any candidate pair such that $\mathbf{v} \in \mathcal{V}(\hat{\mathbf{v}}, \mathcal{S})$, and discuss as follows:

1. If $\mathbf{v}' \in \mathcal{V}(\hat{\mathbf{v}}, \mathcal{S})$, then $\mathbf{F}(\mathbf{v}) = \mathbf{F}(\mathbf{v}') \Rightarrow \mathbf{v} = \mathbf{v}'$ because $\mathcal{V}(\hat{\mathbf{v}}, \mathcal{S})$ is a domain of uniqueness.
2. Otherwise, let $(\hat{\mathbf{v}}', \mathcal{S}') \in \mathcal{L}$ be any candidate pair such that $\mathbf{v}' \in \mathcal{V}(\hat{\mathbf{v}}', \mathcal{S}')$, and take into account that
   - $\mathcal{V}(\hat{\mathbf{v}}, \mathcal{S}) \subseteq \mathcal{D}_\rho(\hat{\mathbf{v}})$ with $\rho = \sup_{\mathbf{s}\in\mathcal{S}} \rho^\dagger(\hat{\mathbf{v}}, \mathbf{s})$,
   - $\mathcal{D}_\rho(\hat{\mathbf{v}})$, $\rho = \sup_{\mathbf{s}\in\mathcal{S}} \rho^\dagger(\hat{\mathbf{v}}, \mathbf{s})$ is contained in $\mathcal{D}_\rho(\hat{\mathbf{v}}')$, $\rho = \rho^\ddagger(\hat{\mathbf{v}}')$ whenever $\|\mathbf{W}^{-1}(\hat{\mathbf{v}} - \hat{\mathbf{v}}')\|_\infty + \sup_{\mathbf{s}\in\mathcal{S}} \rho^\dagger(\hat{\mathbf{v}}, \mathbf{s}) < \rho^\ddagger(\hat{\mathbf{v}}')$.

   In this way, $\mathbf{v} \in \mathcal{D}_\rho(\hat{\mathbf{v}}'), \rho = \rho^\ddagger(\hat{\mathbf{v}}')$ when $\|\mathbf{W}^{-1}(\hat{\mathbf{v}} - \hat{\mathbf{v}}')\|_\infty + \sup_{\mathbf{s}\in\mathcal{S}} \rho^\dagger(\hat{\mathbf{v}}, \mathbf{s}) < \rho^\ddagger(\hat{\mathbf{v}}')$.

Since $\mathbf{v}'$ is the unique power-flow solution in $\mathcal{D}_\rho(\hat{\mathbf{v}}')$, $\rho = \rho^\ddagger(\hat{\mathbf{v}}')$ for system power injection $\mathbf{F}(\mathbf{v}')$, there is $\mathbf{F}(\mathbf{v}) = \mathbf{F}(\mathbf{v}') \Rightarrow \mathbf{v} = \mathbf{v}'$. In a similar way, we have $\mathbf{F}(\mathbf{v}) = \mathbf{F}(\mathbf{v}') \Rightarrow \mathbf{v} = \mathbf{v}'$ when $\|\mathbf{W}^{-1}(\hat{\mathbf{v}}' - \hat{\mathbf{v}})\|_\infty + \sup_{\mathbf{s}' \in \mathcal{S}'} \rho^\dagger(\hat{\mathbf{v}}', \mathbf{s}') < \rho^\ddagger(\hat{\mathbf{v}})$. As we have (3.14) according to Definition 3.7, it is ensured that $\mathbf{F}(\mathbf{v}) = \mathbf{F}(\mathbf{v}') \Rightarrow \mathbf{v} = \mathbf{v}'$.

Therefore, $\bigcup_{(\hat{\mathbf{v}}, \mathcal{S}) \in \mathcal{L}} \mathcal{V}(\hat{\mathbf{v}}, \mathcal{S})$ is a domain of uniqueness.

■

3.O Proof of Theorem 3.8

First, for every $(\hat{\mathbf{v}}, \mathcal{S}) \in \mathcal{L}$, let set $\tilde{\mathcal{S}}$ collect all $\tilde{\mathbf{s}}$ that satisfy the following items:[10]

1. $\xi(\tilde{\mathbf{s}} - \mathbf{F}(\hat{\mathbf{v}})) < \frac{1}{2}\left(\left(\rho^\ddagger(\hat{\mathbf{v}})\right)^2 + \max_{\mathbf{s} \in \mathcal{S}} \xi(\mathbf{s} - \mathbf{F}(\hat{\mathbf{v}}))\right)$,
2. (3.12)–(3.13),
3. $\rho^\dagger(\hat{\mathbf{v}}, \tilde{\mathbf{s}}) < \frac{1}{2}\left(\rho^\ddagger(\hat{\mathbf{v}}') + \max_{\mathbf{s} \in \mathcal{S}} \rho^\dagger(\hat{\mathbf{v}}, \mathbf{s}) - \|\mathbf{W}^{-1}(\hat{\mathbf{v}} - \hat{\mathbf{v}}')\|_\infty\right)$, $\forall (\hat{\mathbf{v}}', \mathcal{S}') \in \mathcal{L}$ such that $\rho^\ddagger(\hat{\mathbf{v}}') - \max_{\mathbf{s} \in \mathcal{S}} \rho^\dagger(\hat{\mathbf{v}}, \mathbf{s}) \geq \rho^\ddagger(\hat{\mathbf{v}}) - \max_{\mathbf{s}' \in \mathcal{S}'} \rho^\dagger(\hat{\mathbf{v}}', \mathbf{s}')$.

As can be seen, (i) $\tilde{\mathcal{S}}$ is open and contains $\mathcal{S}$, (ii) $(\hat{\mathbf{v}}, \tilde{\mathcal{S}})$ is a candidate pair.

Then, let $\tilde{\mathcal{L}}$ be the collection of all candidate pairs $(\hat{\mathbf{v}}, \tilde{\mathcal{S}})$. We have:

1. $\bigcup_{(\hat{\mathbf{v}}, \tilde{\mathcal{S}}) \in \tilde{\mathcal{L}}} \mathcal{V}(\hat{\mathbf{v}}, \tilde{\mathcal{S}})$ satisfies (O1), as every $(\hat{\mathbf{v}}, \tilde{\mathcal{S}})$ is strongly secured by construction.
2. $\bigcup_{(\hat{\mathbf{v}}, \tilde{\mathcal{S}}) \in \tilde{\mathcal{L}}} \mathcal{V}(\hat{\mathbf{v}}, \tilde{\mathcal{S}})$ satisfies (O2), since we assume in the theorem that at least one $\hat{\mathbf{v}}$ equals $\mathbf{v}^{\text{initial}}$.
3. $\bigcup_{(\hat{\mathbf{v}}, \tilde{\mathcal{S}}) \in \tilde{\mathcal{L}}} \mathcal{V}(\hat{\mathbf{v}}, \tilde{\mathcal{S}})$ is open, due to the openness of every $\mathcal{V}(\hat{\mathbf{v}}, \tilde{\mathcal{S}})$.
4. $\bigcup_{(\hat{\mathbf{v}}, \tilde{\mathcal{S}}) \in \tilde{\mathcal{L}}} \mathcal{V}(\hat{\mathbf{v}}, \tilde{\mathcal{S}})$ satisfies (O3b) because $\mathbf{F}\Big(\bigcup_{(\hat{\mathbf{v}}, \tilde{\mathcal{S}}) \in \tilde{\mathcal{L}}} \mathcal{V}(\hat{\mathbf{v}}, \tilde{\mathcal{S}})\Big)$ is open and includes $\mathcal{S}^{\text{uncertain}}$.

Clearly, the proof can be completed by showing that $\bigcup_{(\hat{\mathbf{v}}, \tilde{\mathcal{S}}) \in \tilde{\mathcal{L}}} \mathcal{V}(\hat{\mathbf{v}}, \tilde{\mathcal{S}})$ is a domain of uniqueness, which we do next. Since $\forall (\hat{\mathbf{v}}, \mathcal{S}), (\hat{\mathbf{v}}', \mathcal{S}') \in \mathcal{L}$, we have

$$\|\mathbf{W}^{-1}(\hat{\mathbf{v}} - \hat{\mathbf{v}}')\|_\infty < \max\left\{\rho^\ddagger(\hat{\mathbf{v}}) - \max_{\mathbf{s}' \in \mathcal{S}'} \rho^\dagger(\hat{\mathbf{v}}', \mathbf{s}'), \rho^\ddagger(\hat{\mathbf{v}}') - \max_{\mathbf{s} \in \mathcal{S}} \rho^\dagger(\hat{\mathbf{v}}, \mathbf{s})\right\}.$$

It follows that

[10] Here, the maximum exists in the definition of $\tilde{\mathcal{S}}$, since $\mathcal{S}$ is closed.

1. If $\rho^{\ddagger}(\hat{\mathbf{v}}') - \max\limits_{\mathbf{s}\in\mathcal{S}} \rho^{\dagger}(\hat{\mathbf{v}},\mathbf{s}) \geq \rho^{\ddagger}(\hat{\mathbf{v}}) - \max\limits_{\mathbf{s}'\in\mathcal{S}'} \rho^{\dagger}(\hat{\mathbf{v}}',\mathbf{s}')$, then

$$\begin{aligned}\|\mathbf{W}^{-1}(\hat{\mathbf{v}}-\hat{\mathbf{v}}')\|_{\infty} <& \frac{1}{2}\left(\rho^{\ddagger}(\hat{\mathbf{v}}') - \max_{\mathbf{s}\in\mathcal{S}} \rho^{\dagger}(\hat{\mathbf{v}},\mathbf{s}) + \|\mathbf{W}^{-1}(\hat{\mathbf{v}}-\hat{\mathbf{v}}')\|_{\infty}\right)\\ \leq& \rho^{\ddagger}(\hat{\mathbf{v}}') - \sup_{\tilde{\mathbf{s}}\in\tilde{\mathcal{S}}} \rho^{\dagger}(\hat{\mathbf{v}},\tilde{\mathbf{s}})\\ \leq& \max\left\{\rho^{\ddagger}(\hat{\mathbf{v}}) - \sup_{\tilde{\mathbf{s}}'\in\tilde{\mathcal{S}}'} \rho^{\dagger}(\hat{\mathbf{v}}',\tilde{\mathbf{s}}'),\ \rho^{\ddagger}(\hat{\mathbf{v}}') - \sup_{\tilde{\mathbf{s}}\in\tilde{\mathcal{S}}} \rho^{\dagger}(\hat{\mathbf{v}},\tilde{\mathbf{s}})\right\}.\end{aligned} \tag{3.34}$$

2. Similarly, if $\rho^{\ddagger}(\hat{\mathbf{v}}) - \max\limits_{\mathbf{s}'\in\mathcal{S}'} \rho^{\dagger}(\hat{\mathbf{v}}',\mathbf{s}') \geq \rho^{\ddagger}(\hat{\mathbf{v}}') - \max\limits_{\mathbf{s}\in\mathcal{S}} \rho^{\dagger}(\hat{\mathbf{v}},\mathbf{s})$, then

$$\begin{aligned}\|\mathbf{W}^{-1}(\hat{\mathbf{v}}-\hat{\mathbf{v}}')\|_{\infty} <& \rho^{\ddagger}(\hat{\mathbf{v}}) - \sup_{\tilde{\mathbf{s}}'\in\tilde{\mathcal{S}}'} \rho^{\dagger}(\hat{\mathbf{v}}',\tilde{\mathbf{s}}')\\ \leq& \max\left\{\rho^{\ddagger}(\hat{\mathbf{v}}) - \sup_{\tilde{\mathbf{s}}'\in\tilde{\mathcal{S}}'} \rho^{\dagger}(\hat{\mathbf{v}}',\tilde{\mathbf{s}}'),\ \rho^{\ddagger}(\hat{\mathbf{v}}') - \sup_{\tilde{\mathbf{s}}\in\tilde{\mathcal{S}}} \rho^{\dagger}(\hat{\mathbf{v}},\tilde{\mathbf{s}})\right\}.\end{aligned} \tag{3.35}$$

By combining the above two cases, we obtain that $(\hat{\mathbf{v}},\tilde{\mathcal{S}})$ and $(\hat{\mathbf{v}}',\tilde{\mathcal{S}}')$ are consistent. According to Proposition 3.6, $\bigcup_{(\hat{\mathbf{v}},\tilde{\mathcal{S}})\in\tilde{\mathcal{L}}} \mathcal{V}(\hat{\mathbf{v}},\tilde{\mathcal{S}})$ is a domain of uniqueness, which completes the proof.

■

3.P Proof of Theorem 3.9

We show that $\mathcal{L}$ satisfies the five items in Theorem 3.8 when $\mathcal{L}^{\text{aux}}$ becomes empty. Specifically,

- The method always ensures that $\left(\bigcup_{(\check{\mathbf{v}},\mathcal{S})\in\mathcal{L}^{\text{aux}}} \mathcal{S}\right) \bigcup \left(\bigcup_{(\hat{\mathbf{v}}',\mathcal{S}')\in\mathcal{L}} \mathcal{S}'\right) = \mathcal{S}^{\text{uncertain}}$. Therefore, the first item $\bigcup_{(\hat{\mathbf{v}},\mathcal{S})\in\mathcal{L}} \mathcal{S} = \mathcal{S}^{\text{uncertain}}$ holds when $\mathcal{L}^{\text{aux}}$ becomes empty.
- The second item is satisfied in the initial stage.
- For every element in $\mathcal{L}$ and $\mathcal{L}^{\text{aux}}$, $\mathcal{S}$ is closed. Moreover, $\mathcal{S}$ is convex and contains the $\hat{\mathbf{s}}$ obtained in (3.15). Therefore, all elements in $\mathcal{L}$ satisfy the third item.
- An element is added to $\mathcal{L}$ only if it is a strongly secured candidate pair and consistent with all the existent elements in $\mathcal{L}$. In this way, the fourth and fifth items are also fulfilled.

■

4 Multi-Phase Optimal Power Flow with Wye/Delta Load/Source Connections and Non-Singularity Constraint

All appearances are illusory.

The Diamond Sutra
BUDDHA

4.1 Introduction

Motivation

In this chapter, we shift our focus to network optimality and consider an AC optimal power flow problem in multi-phase ADNs. Specifically,

- We assume that
  - The network topology is generic,
  - The buses are linked via either π-modelled transmission lines or complex-ratio transformers,
  - The system power injection is unbalanced,
  - The loads and sources have various connections, including wye, delta, and a combination thereof.

- Our goal is to find a system power injection $\mathbf{s}^{Y,\Delta} = \begin{bmatrix} \mathbf{s}^{Y} \\ \mathbf{s}^{\Delta} \end{bmatrix}$ and a corresponding power-flow solution $\mathbf{v}$ such that
  - $(\mathbf{v}, \mathbf{s}^{Y,\Delta})$ minimizes an objective function that is convex in both $\mathbf{v}$ and $\mathbf{s}^{Y,\Delta}$.[1]
  - $\mathbf{s}^{Y,\Delta}$ belongs to a given convex and compact set.
  - $\mathbf{v}$ satisfies the nodal-voltage and branch-current security constraints (3.2a)–(3.2b).
  - The power-flow Jacobian $\mathbf{J}_{\mathbf{F}^{Y,\Delta}}\left(\mathbf{v}, \operatorname{diag}\left(\mathbf{H}\overline{\mathbf{v}}\right)^{-1}\overline{\mathbf{s}^{\Delta}}\right)$ (defined in (2.49)) is non-singular.[2]

This problem is meaningful for the operation of real-world ADNs. However, it is technically challenging. In detail,

- It is non-convex and NP-hard [82].
- It cannot be addressed by existent linearization and convex-relaxation methods (see Section 4.2).

Contributions and Chapter Outline

In Section 4.3, we give the mathematical formulation of the multi-phase optimal power flow problem and show that

- This problem might not be feasible, due to the non-singularity constraint.
- Even if it is feasible, it might not have an optimal solution.

[1] For example, assume that we would like to minimize the total monetary cost $f^{\text{external}}(\mathbf{s}_0)+f^{\text{local}}(\mathbf{s}^{Y,\Delta})$, where

* f^{external} is a convex function of the slack-bus power $\mathbf{s}_0$ and represents the monetary cost of importing power from the external networks.
* f^{local} is a convex function of $\mathbf{s}^{Y,\Delta}$ and represents the monetary cost of the local power generation.

By (2.10a) in Chapter 2, the slack-bus power $\mathbf{s}_0$ equals $\operatorname{diag}(\mathbf{v}_0)\left(\overline{\mathbf{Y}_{00}}\overline{\mathbf{v}_0} + \overline{\mathbf{Y}_{0L}}\overline{\mathbf{v}}\right)$. As $\mathbf{v}_0$, $\mathbf{Y}_{00}$, $\mathbf{Y}_{0L}$ are known and fixed, we have that the slack-bus power $\mathbf{s}_0$ is an affine function of $\overline{\mathbf{v}}$. Therefore, the objective function can be written as $\tilde{f}^{\text{external}}(\mathbf{v}) + f^{\text{local}}(\mathbf{s}^{Y,\Delta})$, which is convex in both $\mathbf{v}$ and $\mathbf{s}^{Y,\Delta}$.

[2] This is of practical interests, as non-singular power-flow Jacobian indicates the static voltage stability and cannot be implied by the satisfaction of the security constraints [81].

In Section 4.4, we present a successive local exploration method for solving the multi-phase optimal power flow problem. Specifically,

- In Section 4.4.1, we recall the results in Chapter 2 and show that, by properly restricting the system power injection to some local domains, we can obtain an explicit convex proxy for the feasible set of this problem.
- In Section 4.4.2, we exploit the finding in Section 4.4.1 and develop the successive local exploration method. In each iteration of the method, we obtain a feasible point of this problem, by exploring around the feasible point obtained in the previous iteration. We ensure that the objective-function values at the obtained feasible points are monotonically non-increasing. For two consecutive iterations, if the difference between the objective-function values is less than some pre-specified error bound, then we terminate the method.
- In Section 4.4.3, we give theoretical results for the successive local exploration method. Specifically,
  - We guarantee that the objective-function values at the obtained feasible points converge to a finite limit.
  - If the objective function does not explicitly contain $\mathbf{v}$, then we give a-posteriori conditions to determine the local optimality for both the obtained feasible points and their limit points.

In Section 4.5, we numerically evaluate the successive local exploration method.

In Section 4.6, we compare with our work [83].

4.2 State of the Art

To solve the considered problem, a fundamental method consists in replacing the non-singularity constraint by some indicator of non-singularity [84, 85] and applying the sequential linear programming technique [86]. However,

- The convergence of this method is not guaranteed. If it does not converge, then it might yield a solution that does not satisfy the security constraints.
- This method does not provide any information on the optimality of its solutions.

In [87], the authors attempt to address the unbalanced three-phase optimal power flow problem. Specifically, they replace the security constraints with a security-related penalty term in the objective function. As a result, the multi-dimensional power-flow equation is left as the only constraint. Then, they apply the well-known Newton iteration to solve this equality-constrained problem and obtain the optimal power flow solution. Their method has two major issues. First, it cannot ensure the satisfaction of the security constraints. Second, it has neither a guarantee on the convergence nor a result on the optimality.

The same problem is also studied in [88, 89]. Similarly to those of [87], the authors of [88, 89] handle the problem by well-known generic solvers and do not provide any results on the convergence and optimality.

In [90], the authors try to address the general multi-phase optimal power flow problem. To do so, they assume that all the constant-power loads/sources can be equivalently replaced by some constant-current loads/sources. In this way, the non-linear multi-dimensional power-flow equation is replaced by a linear relation between the nodal currents and the nodal voltages. Then, they solve the resultant problem by generic solvers, without giving any information of the convergence and optimality.

Different from the method in [90], a semi-definite programming relaxation method is proposed in [91] for solving the multi-phase optimal power flow problem. Specifically, the authors of [91] relax the original non-convex problem into a semi-definite programming problem. Then, they give a-posteriori rank conditions to guarantee that the optimal solution of the semi-definite programming problem is globally optimal for the original non-convex problem. This method has the following shortcomings:

- The computational complexity for solving a semi-definite programming problem does not scale well with respect to the size of the network. To cope with this issue, the authors develop a distributed semi-definite programming solver based on the ADMM technique [92]. Although this solver reduces the runtime for acquiring the solution, it is still inefficient for relatively large networks, due to the inevitable communication costs and the long-tail convergence property.
- The method does not consider delta and combined wye/delta connections, and it cannot be straightforwardly adapted for these connections.
- The method does not ensure that the obtained solution satisfies the non-singularity of the power-flow Jacobian.

The computational efficiency of the semi-definite programming relaxation method is improved in [93]. But the improvement is achieved for only radial networks that do not have any shunt element and any transformer. Furthermore, this improvement cannot be straightforwardly extended for delta and combined wye/delta connections.

In a recent work [94], the authors assume quadratic objective functions and formulate the multi-phase optimal power flow problem as a non-convex quadratically-constrained quadratic programming problem. Then, they solve this problem by applying the iterative convex approximation method in [95]. It is shown that this iterative method converges and returns a KKT point of the multi-phase optimal power flow problem. Moreover, if the method starts with a point that satisfies the security constraints, then the obtained KKT point also satisfies the security constraints. Despite the theoretical merits, this work handles only wye connections and cannot be easily adapted for the other connections.

4.3 The Multi-Phase Optimal Power Flow Problem

In the chapter, we make the following assumption on the network model.

Assumption 4.1

- *The network topology is generic (i.e., radial or meshed),*
- *The buses are linked via either π-modelled transmission lines or complex-ratio transformers,*
- *The system power injection is unbalanced,*
- *The loads and sources have various connections, including wye, delta, and a combination thereof.*

Based on this assumption, we formulate the multi-phase optimal power flow problem as follows.

Problem 4.1 (*Multi-Phase Optimal Power Flow Problem*)

Given that the network model follows Assumption 4.1. Solve

$$
\begin{aligned}
[\mathbf{GOPF}] \qquad & \min f(\mathbf{v}, \mathbf{s}^{Y,\Delta}) \\
& \text{s.t. } : \mathbf{s}^{Y,\Delta} \in \mathcal{S}^{Y,\Delta} \,, \\
& \quad \mathbf{v} = \mathbf{G}_{\mathbf{s}^{Y,\Delta}}(\mathbf{v}) \,, \\
& \quad \mathbf{v}^{\min} \leq |\mathbf{v}| \leq \mathbf{v}^{\max} \,, \\
& \quad |\mathbf{i}_{\mathcal{E}}(\mathbf{v})| \leq \mathbf{i}^{\max} \,, \\
& \quad \mathbf{J}_{\mathbf{F}^{Y,\Delta}}\left(\mathbf{v}, \operatorname{diag}\left(\mathbf{H}\overline{\mathbf{v}}\right)^{-1}\overline{\mathbf{s}^{\Delta}}\right) \textit{ is non-singular} \,,
\end{aligned}
$$

where

- f *is a function that is convex in both* $\mathbf{v}$ *and* $\mathbf{s}^{Y,\Delta}$*,*
- $\mathcal{S}^{Y,\Delta}$ *is a convex and compact set of* $\mathbf{s}^{Y,\Delta}$*,*
- $\mathbf{v} = \mathbf{G}_{\mathbf{s}^{Y,\Delta}}(\mathbf{v})$ *is the fixed-point power-flow equation* (2.42)*,*
- $\mathbf{v}^{\min} \leq |\mathbf{v}| \leq \mathbf{v}^{\max}$ *collects the nodal-voltage security constraints in* (3.2a)*,*
- $|\mathbf{i}_{\mathcal{E}}(\mathbf{v})| \leq \mathbf{i}^{\max}$ *collects the branch-current security constraints in* (3.2b)*,*
- $\mathbf{J}_{\mathbf{F}^{Y,\Delta}}\left(\mathbf{v}, \operatorname{diag}\left(\mathbf{H}\overline{\mathbf{v}}\right)^{-1}\overline{\mathbf{s}^{\Delta}}\right)$ *is the power-flow Jacobian defined by* (2.39) *and* (2.49)*.*

In this problem, the first four constraints

$$
\begin{aligned}
& \mathbf{s}^{Y,\Delta} \in \mathcal{S}^{Y,\Delta} \,, \\
& \mathbf{v} = \mathbf{G}_{\mathbf{s}^{Y,\Delta}}(\mathbf{v}) \,, \\
& \mathbf{v}^{\min} \leq |\mathbf{v}| \leq \mathbf{v}^{\max} \,, \\
& |\mathbf{i}_{\mathcal{E}}(\mathbf{v})| \leq \mathbf{i}^{\max}
\end{aligned}
$$

specify a closed set of $(\mathbf{v}, \mathbf{s}^{Y,\Delta})$. However, the non-singularity of the power-flow Jacobian (i.e., the last constraint) specifies an open set of $(\mathbf{v}, \mathbf{s}^{Y,\Delta})$. As a result, this problem might not be feasible. Furthermore, even if it is feasible, it might not have an optimal solution (see Figure 4.1 for an illustration).

For such a problem, we develop a solution method in the next section. As long as the problem is feasible, our solution method at least finds sub-optimal solutions.

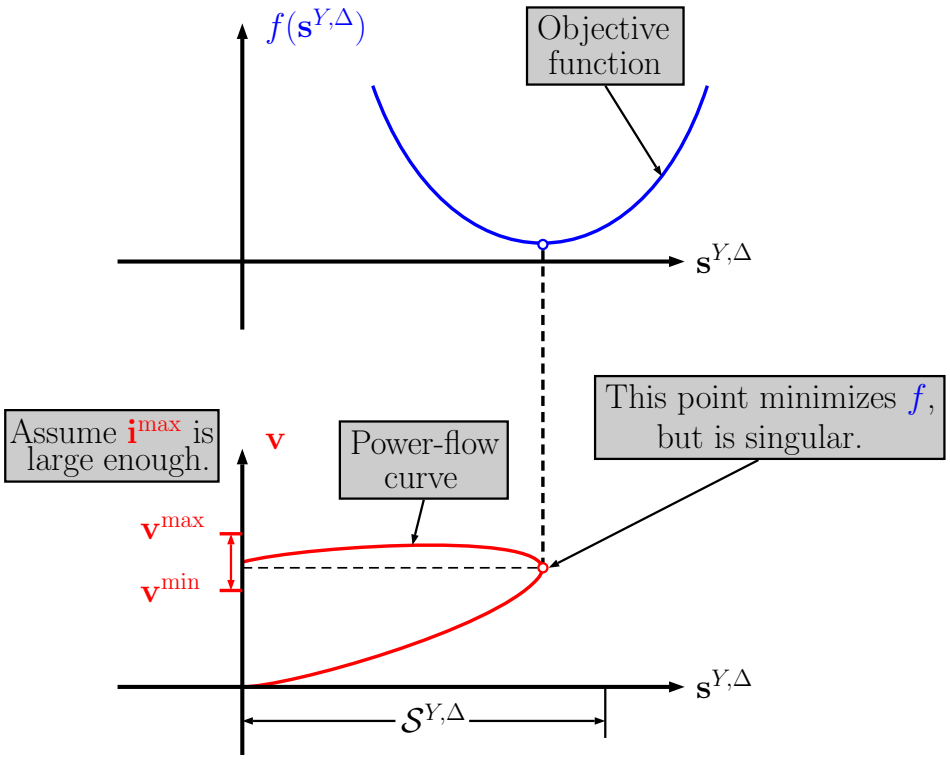

Figure 4.1 – Assume that the objective function does not explicitly contain $\mathbf{v}$ (i.e., it can be written as $f(\mathbf{s}^{Y,\Delta})$). Then, for the case shown in this figure, GOPF is feasible but does not have an optimal solution.

4.4 Solving the Multi-Phase Optimal Power Flow Problem by Successive Local Explorations

In this section, we present a successive local exploration method for solving the multi-phase optimal power flow problem, GOPF . Specifically,

- In Section 4.4.1, we recall the results in Chapter 2 and show that, by properly restricting the system power injection to some local domains, we can obtain an explicit convex proxy for the feasible set of GOPF .
- In Section 4.4.2, we exploit the finding in Section 4.4.1 and develop the successive local exploration method.
- In Section 4.4.3, we give theoretical results for the successive local exploration method.

4.4.1 An Explicit Convex Proxy for the Feasible Set of GOPF

Let $(\hat{\mathbf{v}}, \hat{\mathbf{s}}^{Y,\Delta})$ be a known feasible point of GOPF and define

$$\epsilon^{\max}_{\hat{\mathbf{v}},\hat{\mathbf{s}}^{Y,\Delta}} = \left(\rho^{\ddagger}_{Y,\Delta}(\hat{\mathbf{v}}, \hat{\mathbf{s}}^{Y,\Delta})\right)^2, \tag{4.1}$$

$$\mathcal{B}^{\mathrm{aux}}(\hat{\mathbf{s}}^{Y,\Delta}, \epsilon) = \left\{\mathbf{s}^{Y,\Delta} \in \mathcal{S}^{Y,\Delta} : \xi^{Y,\Delta}\left(\mathbf{s}^{Y,\Delta} - \hat{\mathbf{s}}^{Y,\Delta}\right) < \epsilon\right\}, \tag{4.2}$$

where $\rho^{\ddagger}_{Y,\Delta}$, $\xi^{Y,\Delta}$ are given in Table 2.3 of Chapter 2.

By Theorem 2.2 and Proposition 2.2,

- If $(\hat{\mathbf{v}}, \hat{\mathbf{s}}^{Y,\Delta})$ satisfies $\rho^{\ddagger}_{Y,\Delta}(\hat{\mathbf{v}}, \hat{\mathbf{s}}^{Y,\Delta}) > 0$, then for any $\mathbf{s}^{Y,\Delta} \in \mathcal{B}^{\mathrm{aux}}(\hat{\mathbf{s}}^{Y,\Delta}, \epsilon^{\max}_{\hat{\mathbf{v}},\hat{\mathbf{s}}^{Y,\Delta}})$, there is a unique power-flow solution $\mathbf{v} \in \mathcal{D}_\rho(\hat{\mathbf{v}})$ with $\rho = \rho^{\ddagger}_{Y,\Delta}(\hat{\mathbf{v}}, \hat{\mathbf{s}}^{Y,\Delta})$ (see (2.21) for the definition of $\mathcal{D}_\rho$).
- Moreover,
  - $|\mathbf{v} - \hat{\mathbf{v}}|$ is controlled by $\xi^{Y,\Delta}\left(\mathbf{s}^{Y,\Delta} - \hat{\mathbf{s}}^{Y,\Delta}\right)$, which implies that $|\mathbf{i}_{\mathcal{E}}(\mathbf{v}) - \mathbf{i}_{\mathcal{E}}(\hat{\mathbf{v}})|$ is also controlled by $\xi^{Y,\Delta}\left(\mathbf{s}^{Y,\Delta} - \hat{\mathbf{s}}^{Y,\Delta}\right)$.
  - $\rho^{\ddagger}_{Y,\Delta}(\mathbf{v}, \mathbf{s}^{Y,\Delta}) > 0$ and the power-flow Jacobian $\mathbf{J}_{\mathbf{F}^{Y,\Delta}}\left(\mathbf{v}, \mathrm{diag}\left(\mathbf{H}\overline{\mathbf{v}}\right)^{-1}\overline{\mathbf{s}^{\Delta}}\right)$ is non-singular.

Based on these results, we give the following lemma and prove it in Appendix 4.A.

Lemma 4.1

Given a feasible point $(\hat{\mathbf{v}}, \hat{\mathbf{s}}^{Y,\Delta})$ of GOPF that satisfies

(a1) $\mathbf{v}^{\min} < |\hat{\mathbf{v}}| < \mathbf{v}^{\max}$,

(a2) $|\mathbf{i}_{\mathcal{E}}(\hat{\mathbf{v}})| < \mathbf{i}^{\max}$,

(a3) $\rho^{\ddagger}_{Y,\Delta}(\hat{\mathbf{v}}, \hat{\mathbf{s}}^{Y,\Delta}) > 0$.

For any $\mathbf{s}^{Y,\Delta} \in \mathcal{B}^{\mathrm{aux}}(\hat{\mathbf{s}}^{Y,\Delta}, \epsilon^{\max}_{\hat{\mathbf{v}},\hat{\mathbf{s}}^{Y,\Delta}})$, let $\mathbf{v}$ be the unique power-flow solution in $\mathcal{D}_\rho(\hat{\mathbf{v}})$, $\rho = \rho^{\ddagger}_{Y,\Delta}(\hat{\mathbf{v}}, \hat{\mathbf{s}}^{Y,\Delta})$ that is guaranteed by Theorem 2.2.

We have that there exists $\epsilon_0(\hat{\mathbf{v}}, \hat{\mathbf{s}}^{Y,\Delta}) \in (0, \epsilon^{\max}_{\hat{\mathbf{v}},\hat{\mathbf{s}}^{Y,\Delta}})$ such that for any $\mathbf{s}^{Y,\Delta} \in \mathrm{cl}\left(\mathcal{B}^{\mathrm{aux}}\left(\hat{\mathbf{s}}^{Y,\Delta}, \epsilon_0(\hat{\mathbf{v}}, \hat{\mathbf{s}}^{Y,\Delta})\right)\right)$, $(\mathbf{v}, \mathbf{s}^{Y,\Delta})$ is a feasible point of GOPF and satisfies (a1)–(a3).

By Lemma 4.1, if $(\hat{\mathbf{v}}, \hat{\mathbf{s}}^{Y,\Delta})$ satisfies (a1)–(a3) and $\epsilon \in (0, \epsilon^{\max}_{\hat{\mathbf{v}},\hat{\mathbf{s}}^{Y,\Delta}})$ is appropriately controlled, then for any $\mathbf{s}^{Y,\Delta} \in \mathrm{cl}\Big(\mathcal{B}^{\mathrm{aux}}(\hat{\mathbf{s}}^{Y,\Delta}, \epsilon)\Big)$, there exists a $\mathbf{v}$ such that $(\mathbf{v}, \mathbf{s}^{Y,\Delta})$ is a feasible point of GOPF (see Figure 4.2 for an illustration). This means that $\mathrm{cl}\Big(\mathcal{B}^{\mathrm{aux}}(\hat{\mathbf{s}}^{Y,\Delta}, \epsilon)\Big)$ is an explicit convex proxy for the feasible set of GOPF . Namely, knowing that $\mathbf{s}^{Y,\Delta} \in \mathrm{cl}\Big(\mathcal{B}^{\mathrm{aux}}(\hat{\mathbf{s}}^{Y,\Delta}, \epsilon)\Big)$ permits us to "forget" the constraints on $\mathbf{v}$.

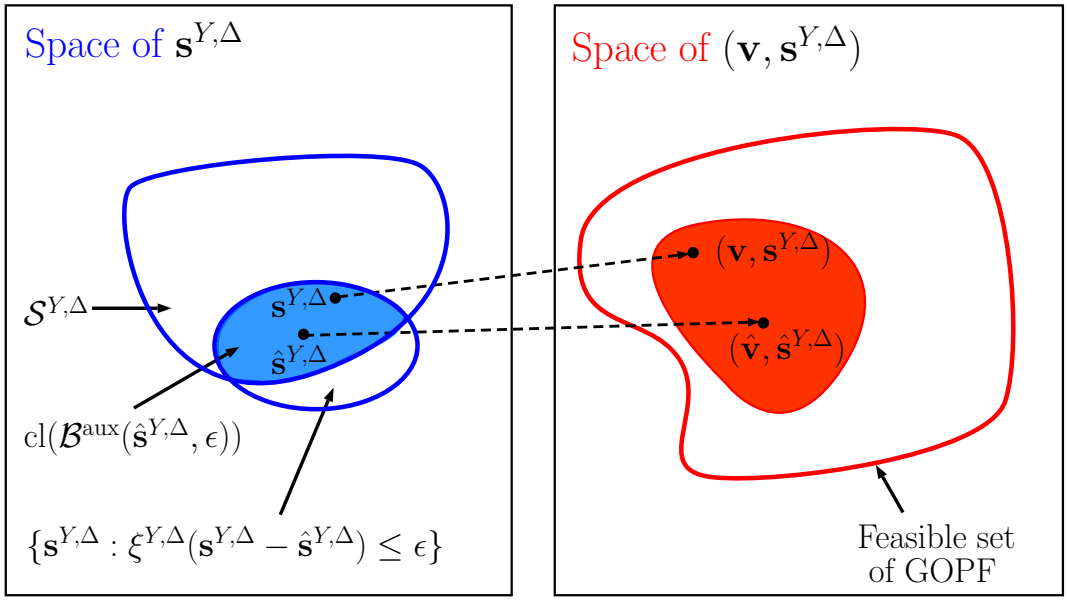

Figure 4.2 – If $(\hat{\mathbf{v}}, \hat{\mathbf{s}}^{Y,\Delta})$ satisfies (a1)–(a3) and $\epsilon \in (0, \epsilon^{\max}_{\hat{\mathbf{v}},\hat{\mathbf{s}}^{Y,\Delta}})$ is appropriately controlled, then for any $\mathbf{s}^{Y,\Delta} \in \mathrm{cl}\Big(\mathcal{B}^{\mathrm{aux}}(\hat{\mathbf{s}}^{Y,\Delta}, \epsilon)\Big)$, there exists a $\mathbf{v}$ such that $(\mathbf{v}, \mathbf{s}^{Y,\Delta})$ is a feasible point of GOPF .

4.4.2 The Successive Local Exploration Method

In Section 4.4.1, we have shown that: if $(\hat{\mathbf{v}}, \hat{\mathbf{s}}^{Y,\Delta})$ satisfies (a1)–(a3) in Lemma 4.1 and ϵ is appropriately controlled, then $\mathrm{cl}\Big(\mathcal{B}^{\mathrm{aux}}(\hat{\mathbf{s}}^{Y,\Delta}, \epsilon)\Big)$ is an explicit convex proxy for the feasible set of GOPF . In what follows, we use this result to develop a successive local exploration method for solving GOPF .

To begin with, let us introduce a linear approximation of $\mathbf{v}$ as follows:

$$\mathbf{v}^{\mathrm{approx}}_{\hat{\mathbf{v}}}(\mathbf{s}^{Y,\Delta}) = \mathbf{w} + \mathbf{Y}^{-1}_{LL}\left(\mathrm{diag}\left(\overline{\hat{\mathbf{v}}}\right)^{-1}\overline{\mathbf{s}^{Y}} + \mathbf{H}^{T}\mathrm{diag}\left(\mathbf{H}\overline{\hat{\mathbf{v}}}\right)^{-1}\overline{\mathbf{s}^{\Delta}}\right). \tag{4.3}$$

This linear approximation is the first step of the iterative power-flow method in (2.46). It generalizes the single-phase linear approximation in [30]. Compared to the common

first-order Taylor approximation, it has a much lower computational complexity.

With the linear approximation (4.3), we introduce the following optimization problem

$$[\mathbf{LOPF}(\hat{\mathbf{v}}, \hat{\mathbf{s}}^{Y,\Delta}, \epsilon)] \qquad \begin{aligned} &\min f\Big(\mathbf{v}_{\hat{\mathbf{v}}}^{\text{approx}}(\mathbf{s}^{Y,\Delta}), \mathbf{s}^{Y,\Delta}\Big) \\ &\text{s.t. } : \mathbf{s}^{Y,\Delta} \in \text{cl}\Big(\mathcal{B}^{\text{aux}}(\hat{\mathbf{s}}^{Y,\Delta}, \epsilon)\Big), \end{aligned}$$

which is a convex approximation of GOPF . Using $[\mathbf{LOPF}(\hat{\mathbf{v}}, \hat{\mathbf{s}}^{Y,\Delta}, \epsilon)]$, we develop the successive local exploration method as follows:

- In the initialization, we assume that there is a known feasible point $\Big(\mathbf{v}^{(0)}, (\mathbf{s}^{Y,\Delta})^{(0)}\Big)$ of GOPF that satisfies (a1)–(a3) in Lemma 4.1. Additionally, we specify some parameters $\zeta \in (0,1)$, $\epsilon^{\text{bound}} > 0$, and $\text{ErrBound} \geq 0$.
- Then, in each iteration $k \geq 0$, we find a feasible point $\Big(\mathbf{v}^{(k+1)}, (\mathbf{s}^{Y,\Delta})^{(k+1)}\Big)$ of GOPF such that
  - $f\Big(\mathbf{v}^{(k+1)}, (\mathbf{s}^{Y,\Delta})^{(k+1)}\Big) \leq f\Big(\mathbf{v}^{(k)}, (\mathbf{s}^{Y,\Delta})^{(k)}\Big)$,
  - $\Big(\mathbf{v}^{(k+1)}, (\mathbf{s}^{Y,\Delta})^{(k+1)}\Big)$ satisfies (a1)–(a3) in Lemma 4.1.

  To do so, we initialize $n = 0$ and take the following explorational steps:

  (S1) We solve the optimization problem $\text{LOPF}\Big(\mathbf{v}^{(k)}, (\mathbf{s}^{Y,\Delta})^{(k)}, \zeta^{n+1}\epsilon^{\max}_{\mathbf{v}^{(k)}, (\mathbf{s}^{Y,\Delta})^{(k)}}\Big)$ and obtain a minimizer $\tilde{\mathbf{s}}^{Y,\Delta}$.

  (S2) For $\tilde{\mathbf{s}}^{Y,\Delta}$, we compute the corresponding power-flow solution $\tilde{\mathbf{v}}$ that is guaranteed by Theorem 2.2.

  (S3) With the obtained $(\tilde{\mathbf{v}}, \tilde{\mathbf{s}}^{Y,\Delta})$, we consider the following cases:
    - In the case where $\mathbf{v}^{\min} < |\tilde{\mathbf{v}}| < \mathbf{v}^{\max}$, $|\mathbf{i}_{\mathcal{E}}(\tilde{\mathbf{v}})| < \mathbf{i}^{\max}$ and $f(\tilde{\mathbf{v}}, \tilde{\mathbf{s}}^{Y,\Delta}) \leq f\Big(\mathbf{v}^{(k)}, (\mathbf{s}^{Y,\Delta})^{(k)}\Big)$, we let $\Big(\mathbf{v}^{(k+1)}, (\mathbf{s}^{Y,\Delta})^{(k+1)}\Big)$ be $(\tilde{\mathbf{v}}, \tilde{\mathbf{s}}^{Y,\Delta})$.
    - In the case where $\mathbf{v}^{\min} < |\tilde{\mathbf{v}}| < \mathbf{v}^{\max}$, $|\mathbf{i}_{\mathcal{E}}(\tilde{\mathbf{v}})| < \mathbf{i}^{\max}$ and $f(\tilde{\mathbf{v}}, \tilde{\mathbf{s}}^{Y,\Delta}) > f\Big(\mathbf{v}^{(k)}, (\mathbf{s}^{Y,\Delta})^{(k)}\Big)$, we proceed according to the value of $\zeta^{n+1}\epsilon^{\max}_{\mathbf{v}^{(k)}, (\mathbf{s}^{Y,\Delta})^{(k)}}$. If $\zeta^{n+1}\epsilon^{\max}_{\mathbf{v}^{(k)}, (\mathbf{s}^{Y,\Delta})^{(k)}} \leq \epsilon^{\text{bound}}$, then we have already done enough explorations and should stop by letting $\Big(\mathbf{v}^{(k+1)}, (\mathbf{s}^{Y,\Delta})^{(k+1)}\Big)$ be $\Big(\mathbf{v}^{(k)}, (\mathbf{s}^{Y,\Delta})^{(k)}\Big)$.
    - In all the other cases, we have not yet done enough explorations. Consequently, we should increase n by 1 and repeat the explorational steps (S1)-(S3).
- When $\Big|f\Big(\mathbf{v}^{(k+1)}, (\mathbf{s}^{Y,\Delta})^{(k+1)}\Big) - f\Big(\mathbf{v}^{(k)}, (\mathbf{s}^{Y,\Delta})^{(k)}\Big)\Big| < \text{ErrBound}$, we terminate the method.

In the following, we give the pseudo code of the method and illustrate it in Figure 4.3.

Successive Local Exploration Method

Input: 1. Feasible point $\left(\mathbf{v}^{(0)}, (\mathbf{s}^{Y,\Delta})^{(0)}\right)$ of GOPF that satisfies (a1)–(a3) in Lemma 4.1.
2. Parameter $\zeta \in (0,1)$.
3. Parameter $\epsilon^{\text{bound}} > 0$.
4. Parameter $\text{ErrBound} \geq 0$.

Output: $\left\{\mathbf{v}^{(k)}, (\mathbf{s}^{Y,\Delta})^{(k)}, (\epsilon^{\text{seq}})^{(k)}\right\}$

$k \leftarrow 0$, flagA$\leftarrow 1$
while flagA **do**
  $n \leftarrow 0$, flagB$\leftarrow 1$
  while flagB **do**
    $\epsilon^{(n)} \leftarrow \zeta^{n+1}\epsilon^{\max}_{\mathbf{v}^{(k)},(\mathbf{s}^{Y,\Delta})^{(k)}}$
    Solve LOPF$\left(\mathbf{v}^{(k)}, (\mathbf{s}^{Y,\Delta})^{(k)}, \epsilon^{(n)}\right)$ and obtain a minimizer $\tilde{\mathbf{s}}^{Y,\Delta}$
    For $\tilde{\mathbf{s}}^{Y,\Delta}$, compute the corresponding $\tilde{\mathbf{v}}$ that is guaranteed by Theorem 2.2
    if $\mathbf{v}^{\min} < |\tilde{\mathbf{v}}| < \mathbf{v}^{\max}$ and $|\mathbf{i}_{\mathcal{E}}(\tilde{\mathbf{v}})| < \mathbf{i}^{\max}$ **then**
      if $f(\tilde{\mathbf{v}}, \tilde{\mathbf{s}}^{Y,\Delta}) \leq f\left(\mathbf{v}^{(k)}, (\mathbf{s}^{Y,\Delta})^{(k)}\right)$ **then**
        $\mathbf{v}^{(k+1)} \leftarrow \tilde{\mathbf{v}}$, $(\mathbf{s}^{Y,\Delta})^{(k+1)} \leftarrow \tilde{\mathbf{s}}^{Y,\Delta}$, $(\epsilon^{\text{seq}})^{(k)} \leftarrow \epsilon^{(n)}$, flagB$\leftarrow 0$
      else if $\epsilon^{(n)} \leq \epsilon^{\text{bound}}$ **then**
        $\mathbf{v}^{(k+1)} \leftarrow \mathbf{v}^{(k)}$, $(\mathbf{s}^{Y,\Delta})^{(k+1)} \leftarrow (\mathbf{s}^{Y,\Delta})^{(k)}$, $(\epsilon^{\text{seq}})^{(k)} \leftarrow \epsilon^{(n)}$, flagB$\leftarrow 0$
      else
        $n \leftarrow n+1$
      end if
    else
      $n \leftarrow n+1$
    end if
  end while
  if $\left|f\left(\mathbf{v}^{(k+1)}, (\mathbf{s}^{Y,\Delta})^{(k+1)}\right) - f\left(\mathbf{v}^{(k)}, (\mathbf{s}^{Y,\Delta})^{(k)}\right)\right| < \text{ErrBound}$ **then**
    flagA$\leftarrow 0$
  end if
  $k \leftarrow k+1$
end while
return $\left\{\mathbf{v}^{(k)}, (\mathbf{s}^{Y,\Delta})^{(k)}, (\epsilon^{\text{seq}})^{(k)}\right\}$

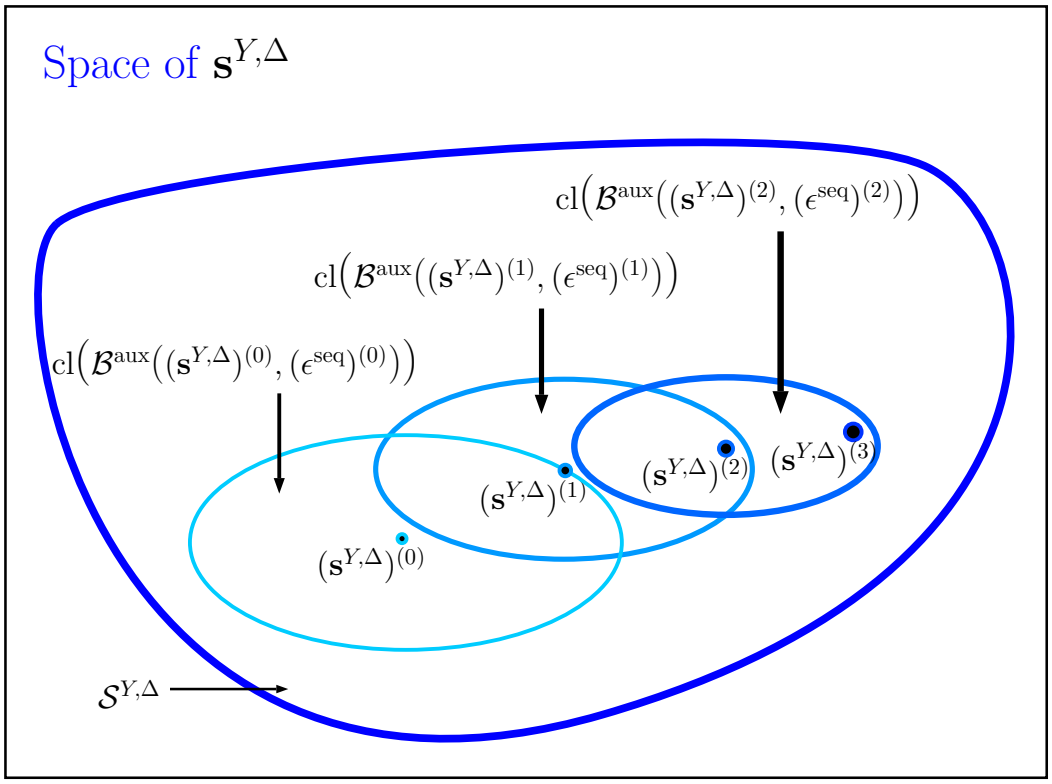

Figure 4.3 – Illustration of the successive local exploration method.

Remark 4.1 (*Comments on the Successive Local Exploration Method*)

For the successive local exploration method, we have the following comments:

- *In the initialization, we can either obtain* $\left(\mathbf{v}^{(0)}, (\mathbf{s}^{Y,\Delta})^{(0)}\right)$ *by state estimation processes or simply set it to* $(\mathbf{w}, \mathbf{0})$.
- *For* $(\tilde{\mathbf{v}}, \tilde{\mathbf{s}}^{Y,\Delta})$, *we do not need to verify* $\rho^{\ddagger}_{Y,\Delta}(\tilde{\mathbf{v}}, \tilde{\mathbf{s}}^{Y,\Delta}) > 0$, *as it is guaranteed by Proposition 2.2.*
- *If the objective function does not explicitly contain* $\mathbf{v}$, *then the condition in pseudo-code line 9 is always satisfied. Consequently, pseudo-code lines 11–14 do not come into effect.*

4.4.3 Theoretical Results for the Successive Local Exploration Method

We give the following theoretical results for the successive local exploration method. The proof is included in Appendix 4.B.

Theorem 4.1

For the successive local exploration method:

1. *In each iteration that is indexed by k, the inner loop (i.e., pseudo-code lines 5-18) terminates with a finite value of n.*
2. *When $\mathrm{ErrBound} = 0$, we get an infinite sequence $\left\{\mathbf{v}^{(k)}, (\mathbf{s}^{Y,\Delta})^{(k)}, (\epsilon^{\mathrm{seq}})^{(k)}\right\}$.*
   (a) *$\left\{f\left(\mathbf{v}^{(k)}, (\mathbf{s}^{Y,\Delta})^{(k)}\right)\right\}$ converges to a finite limit.*
   (b) *For each $k \geq 1$, if $(\mathbf{s}^{Y,\Delta})^{(k)} \in \mathcal{B}^{\mathrm{aux}}\left((\mathbf{s}^{Y,\Delta})^{(k-1)}, (\epsilon^{\mathrm{seq}})^{(k-1)}\right)$ and the objective function does not explicitly contain $\mathbf{v}$, then $\left(\mathbf{v}^{(k)}, (\mathbf{s}^{Y,\Delta})^{(k)}\right)$ is a locally optimal solution to GOPF .*
   (c) *Assume that*

$$\epsilon^{\min} = \liminf_{k\to\infty} (\epsilon^{\mathrm{seq}})^{(k)} > 0\,. \tag{4.4}$$

   Then for any limit point $\left(\mathbf{v}^*, (\mathbf{s}^{Y,\Delta})^*\right)$ of $\left\{\mathbf{v}^{(k)}, (\mathbf{s}^{Y,\Delta})^{(k)}\right\}$, we have
   (i) *$\mathbf{J}_{\mathbf{F}^{Y,\Delta}}\left(\mathbf{v}^*, \mathrm{diag}\left(\mathbf{H}\overline{\mathbf{v}^*}\right)^{-1}\overline{(\mathbf{s}^{\Delta})^*}\right)$ is non-singular,*
   (ii) *$\left(\mathbf{v}^*, (\mathbf{s}^{Y,\Delta})^*\right)$ is a locally optimal solution to GOPF if the objective function does not explicitly contain $\mathbf{v}$.*
   (d) *Assume that*

$$\epsilon^{\max} = \limsup_{k\to\infty} (\epsilon^{\mathrm{seq}})^{(k)} > 0\,. \tag{4.5}$$

   Then there exists a limit point $\left(\mathbf{v}^*, (\mathbf{s}^{Y,\Delta})^*\right)$ of $\left\{\mathbf{v}^{(k)}, (\mathbf{s}^{Y,\Delta})^{(k)}\right\}$ such that 2(c)(i)–2(c)(ii) hold.
3. *When $\mathrm{ErrBound} > 0$, the method terminates after solving a finite number of LOPF problems.*

Remark 4.2 (*On the Optimal Power Flow Solutions*)

In general, it is technically challenging to find an optimal solution to GOPF , because GOPF is a non-convex and NP-hard problem. According to the discussion in Section 4.3, GOPF might not have an optimal solution, due to the non-singularity constraint. For such a problem, our successive local exploration method at least finds sub-optimal solutions.

Moreover, in the case where the objective function does not explicitly contain $\mathbf{v}$*, we give a-posteriori conditions on the optimality:*

- *For each obtained* $\left(\mathbf{v}^{(k)}, (\mathbf{s}^{Y,\Delta})^{(k)}\right)$*, if* $(\mathbf{s}^{Y,\Delta})^{(k)} \in \mathcal{B}^{\mathrm{aux}}\left((\mathbf{s}^{Y,\Delta})^{(k-1)}, (\epsilon^{\mathrm{seq}})^{(k-1)}\right)$*, then* $\left(\mathbf{v}^{(k)}, (\mathbf{s}^{Y,\Delta})^{(k)}\right)$ *is a locally optimal solution to GOPF .*
- *If condition* (4.4) *holds, then any limit point* $\left(\mathbf{v}^{*}, (\mathbf{s}^{Y,\Delta})^{*}\right)$ *of* $\left\{\mathbf{v}^{(k)}, (\mathbf{s}^{Y,\Delta})^{(k)}\right\}$ *is a locally optimal solution to GOPF . Further, if a milder condition* (4.5) *holds, then there exists such a limit point. Note that if* (4.5) *does not hold, then we have that a limit point of* $\left\{\mathbf{v}^{(k)}, (\mathbf{s}^{Y,\Delta})^{(k)}\right\}$ *is an approximation of a locally optimal solution.*

4.5 Numerical Examples

In the following, we give the illustration and performance evaluation for the successive local exploration method. We assume that (i) the slack-bus voltage is nominal, (ii) the security bounds on the nodal-voltage magnitudes are 0.9 p.u. and 1.1 p.u., (iii) the security bounds on the branch-current magnitudes are 0.5 p.u., (iv) $\epsilon^{\mathrm{bound}} = 0.01$, (v) $\mathrm{ErrBound} = 0.0001$.

Illustration

Let us consider a single-phase two-bus network, where

- The PQ bus is directly linked to the slack bus via a transmission line.
- The transmission-line impedance is $0.3 + \jmath 0.7$ p.u.
- At the PQ bus, the power injection belongs to the triangular region in Figure 4.4, which specifies $\mathcal{S}^{Y,\Delta}$.
- f is quadratic and does not explicitly contain $\mathbf{v}$:

$$f(\mathbf{s}^{Y,\Delta}) = \left\| \begin{bmatrix} \Re(\mathbf{s}^{Y,\Delta}) \\ \Im(\mathbf{s}^{Y,\Delta}) \end{bmatrix} - \begin{bmatrix} 3 \\ 0 \end{bmatrix} \right\|_2^2. \tag{4.6}$$

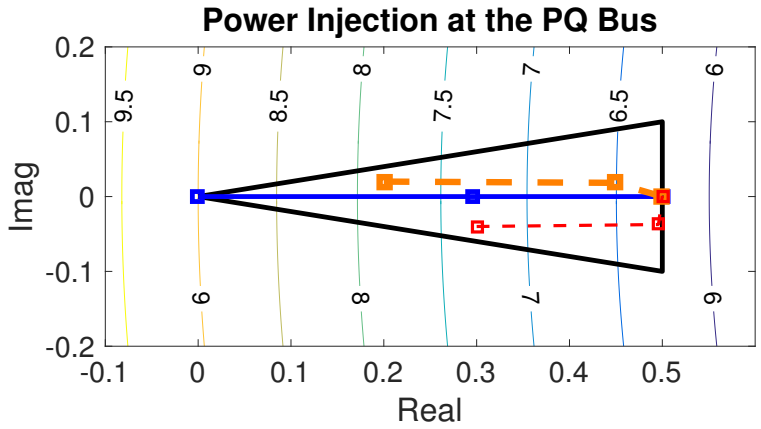

Figure 4.4 – The power injection at the PQ bus belongs to the triangular region. For each path of $\mathbf{s}^{Y,\Delta}$, the leftmost point represents $(\mathbf{s}^{Y,\Delta})^{(0)}$. (The thin colorful curves express the contour levels of the objective-function value.)

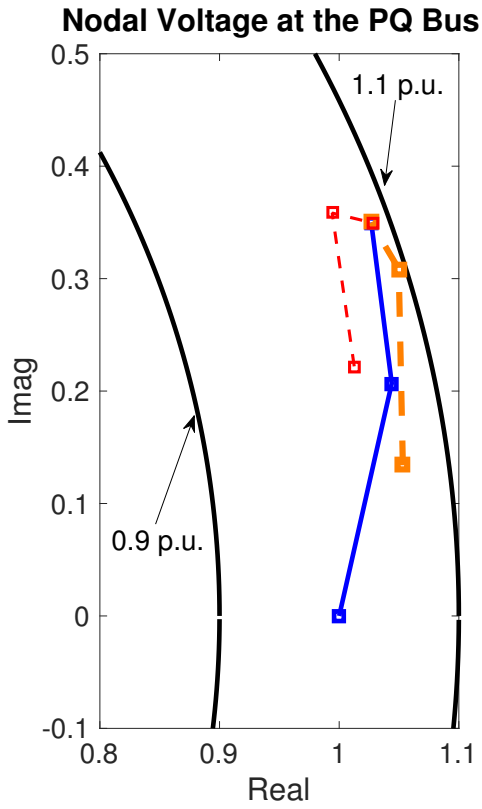

Figure 4.5 – The paths of $\mathbf{v}$ that correspond to those in Figure 4.4. For each path, the lowest point represents $\mathbf{v}^{(0)}$.

In this network, if $\left(\mathbf{v}^{(0)}, (\mathbf{s}^{Y,\Delta})^{(0)}\right) = (\mathbf{w}, \mathbf{0})$ and $\zeta = 0.9$, then the method terminates after solving 3 instances of LOPF problems. We plot the path of $(\mathbf{s}^{Y,\Delta})^{(k)}$ in Figure 4.4 and the corresponding path of $\mathbf{v}^{(k)}$ in Figure 4.5 via thick solid lines. As can be seen, $(\mathbf{s}^{Y,\Delta})^{(k)}$ converges to 0.5, which means that we reach the unique minimum value of f in $\mathcal{S}^{Y,\Delta}$. Similarly, we pick some other values for $\left(\mathbf{v}^{(0)}, (\mathbf{s}^{Y,\Delta})^{(0)}\right)$ and plot the obtained paths in Figures 4.4, 4.5 via dashed lines of different thickness. As can be seen, for every path, we have that $(\mathbf{s}^{Y,\Delta})^{(k)}$ converges to 0.5 .

In addition to the above results, we verify that the power-flow Jacobian is non-singular for all obtained paths. Moreover, if $\mathrm{ErrBound}$ is set to 0, we note that

$$\liminf_{k\to\infty}(\epsilon^{\mathrm{seq}})^{(k)} = \limsup_{k\to\infty}(\epsilon^{\mathrm{seq}})^{(k)} = 0.1211\ ,$$

which means that (4.4) and (4.5) hold.

Performance Evaluation

We evaluate the performance of the successive local exploration method on the IEEE 123-Bus Test Feeder [55, 56]. To create combined wye/delta connections, we add an additional delta-connected power injection $(-0.03-\jmath 0.01, -0.03-\jmath 0.01, -0.03-\jmath 0.01)^T$ p.u. to bus 1. Let us denote the modified benchmark system power injection by $(\mathbf{s}^{Y,\Delta})^{\mathrm{bench}}$ and take

$$\begin{aligned}\mathcal{S}^{Y,\Delta} = \Bigg\{\mathbf{s}^{Y,\Delta} : \kappa\Re\Big(\Big((\mathbf{s}^{Y,\Delta})^{\mathrm{bench}}\Big)_j\Big) \le \Re\Big((\mathbf{s}^{Y,\Delta})_j\Big) \le 0\ ,\\ \kappa\Im\Big(\Big((\mathbf{s}^{Y,\Delta})^{\mathrm{bench}}\Big)_j\Big) \le \Im\Big((\mathbf{s}^{Y,\Delta})_j\Big) \le 0\ ,\ \forall j\Bigg\}\ ,\end{aligned} \tag{4.7}$$

where $\kappa > 0$.

Our goal is to analyze how the number of LOPF problems depends on κ and ζ. More precisely,

- For a given ζ, we want to see whether the number of LOPF problems changes rapidly along with κ.
- For a given large κ, we want to find the best choice of ζ.

For this purpose, we initialize with $\left(\mathbf{v}^{(0)}, (\mathbf{s}^{Y,\Delta})^{(0)}\right) = (\mathbf{w}, \mathbf{0})$ and take the objective function as follows

$$f(\mathbf{v}, \mathbf{s}^{Y,\Delta}) = \left\|\mathrm{diag}(\mathbf{v}_0)\left(\overline{\mathbf{Y}_{00}}\,\overline{\mathbf{v}_0} + \overline{\mathbf{Y}_{0L}}\,\overline{\mathbf{v}}\right)\right\|_2^2 + 10\|\mathbf{s}^{Y,\Delta} - \mathbf{c}\|_2^2\ . \tag{4.8}$$

In this objective function,

- $\mathrm{diag}(\mathbf{v}_0)\Big(\overline{\mathbf{Y}_{00}}\overline{\mathbf{v}_0} + \overline{\mathbf{Y}_{0L}}\overline{\mathbf{v}}\Big)$ is the slack-bus power (see (2.10a) in Chapter 2),
- The entries of $\mathbf{c}$ are independent and randomly generated by uniform distribution over the square box $[-0.1, 0.1] \times [-0.1, 0.1]$.

With the above $\Big(\mathbf{v}^{(0)}, (\mathbf{s}^{Y,\Delta})^{(0)}\Big)$ and $f(\mathbf{v}, \mathbf{s}^{Y,\Delta})$, we fix $\zeta = 0.6$ and increase κ from 1 to 6. Using randomly generated objective functions, we obtain that

- For $\kappa = 1$, the method terminates after solving 2–3 instances of LOPF problems.
- For $\kappa = 6$, the method terminates after solving 9–15 instances of LOPF problems.

Thus, the number of LOPF problems is not very sensitive to κ.

Then, we fix $\kappa = 6$ and take ζ from $\{0.2, 0.4, 0.6, 0.8\}$. For each randomly generated objective function, we obtain that

- The number of iterations (indexed by k) in the successive local exploration method decreases as ζ increases.
- The average number of LOPF problems in the inner loop of each iteration increases as ζ increases.

From the numerical experiments, the best choice of ζ lies between 0.4 and 0.6.

4.6 Comparison with [83]

In this section, we compare with our work in [83]:

- In both this chapter and [83], we consider the multi-phase optimal power flow problem. Moreover, we make the same assumptions on the network topologies, transmission devices, and load/source connections.
- In [83], we formulate the problem as follows

$$\begin{aligned} &\min f(\mathbf{s}^{Y,\Delta}) \\ &\text{s.t. } : \mathbf{s}^{Y,\Delta} \in \mathcal{S}^{Y,\Delta}\,, \\ &\qquad \mathbf{v} = \mathbf{G}_{\mathbf{s}^{Y,\Delta}}(\mathbf{v})\,, \\ &\qquad \mathbf{v}^{\min} \le |\mathbf{v}| \le \mathbf{v}^{\max}\,. \end{aligned}$$

As can be seen,

- The objective function does not contain $\mathbf{v}$ hence cannot handle the slack-bus power.
- The branch-current constraints and the non-singularity constraint are not included.

- To solve this problem, we develop a successive linear approximation method in [83]. This method is very similar to the successive local exploration method. The major difference is that it successively solves the following local problem instead of LOPF, where $\widehat{|\mathbf{v}|}_{\mathbf{v}^{(k)},(\mathbf{s}^{Y,\Delta})^{(k)}}(\mathbf{s}^{Y,\Delta})$ is a linear approximation of $|\mathbf{v}|$.

$$\begin{aligned} &\min\ f(\mathbf{s}^{Y,\Delta}) \\ &\text{s.t.}\ : \mathbf{s}^{Y,\Delta} \in \mathcal{S}^{Y,\Delta}\ , \\ &\qquad \mathbf{v}^{\min} \leq \widehat{|\mathbf{v}|}_{\mathbf{v}^{(k)},(\mathbf{s}^{Y,\Delta})^{(k)}}(\mathbf{s}^{Y,\Delta}) \leq \mathbf{v}^{\max}\ , \\ &\qquad \xi^{Y,\Delta}\Big(\mathbf{s}^{Y,\Delta} - (\mathbf{s}^{Y,\Delta})^{(k)}\Big) \leq \epsilon^{(n)}\ . \end{aligned}$$

By inspection, the constraint $\mathbf{v}^{\min} \leq \widehat{|\mathbf{v}|}_{\mathbf{v}^{(k)},(\mathbf{s}^{Y,\Delta})^{(k)}}(\mathbf{s}^{Y,\Delta}) \leq \mathbf{v}^{\max}$ introduces more computational complexity and unnecessarily shrinks the feasible set of the local problem. As a result, the solution obtained in this local problem cannot be better than the one obtained in LOPF.

4.7 Conclusions

We have studied a multi-phase optimal power flow problem. In this problem, we have made generic assumptions on the network topologies and transmission devices, and we have considered various load/source connections. Moreover, we have incorporated the non-singularity constraint. In order to solve this problem, we have first shown that, by properly restricting the system power injection to some local domains, we can obtain an explicit convex proxy for its feasible set. Based on this, we have developed a successive local exploration method. In each iteration of the method, we obtain a feasible point of the problem, by exploring around the feasible point obtained in the previous iteration. We ensure that the objective-function values at the obtained feasible points are monotonically non-increasing. We have guaranteed that they converge to a finite limit. If the objective function does not explicitly contain $\mathbf{v}$, then we have given a-posteriori conditions to determine whether the obtained feasible points and their limit points are locally optimal solutions. We have numerically evaluated the successive local exploration method and have compared it with the successive linear approximation method in our work [83].

Appendix

4.A Proof of Lemma 4.1

By Proposition 2.2, for any $\mathbf{s}^{Y,\Delta} \in \mathcal{B}^{\text{aux}}(\hat{\mathbf{s}}^{Y,\Delta}, \epsilon^{\max}_{\hat{\mathbf{v}},\hat{\mathbf{s}}^{Y,\Delta}})$, we have that $\rho^{\dagger}_{Y,\Delta}(\mathbf{v}, \mathbf{s}^{Y,\Delta}) > 0$ and the power-flow Jacobian $\mathbf{J}_{\mathbf{F}^{Y,\Delta}}\left(\mathbf{v}, \text{diag}\left(\mathbf{H}\overline{\mathbf{v}}\right)^{-1}\overline{\mathbf{s}^{\Delta}}\right)$ is non-singular. Therefore, we only need to show that there exists $\epsilon_0(\hat{\mathbf{v}}, \hat{\mathbf{s}}^{Y,\Delta}) \in (0, \epsilon^{\max}_{\hat{\mathbf{v}},\hat{\mathbf{s}}^{Y,\Delta}})$ such that

$$\begin{aligned} & \xi^{Y,\Delta}(\mathbf{s}^{Y,\Delta} - \hat{\mathbf{s}}^{Y,\Delta}) \leq \epsilon_0(\hat{\mathbf{v}}, \hat{\mathbf{s}}^{Y,\Delta}) \\ \Rightarrow \quad & \mathbf{v}^{\min} < |\mathbf{v}| < \mathbf{v}^{\max}, \\ & |\mathbf{i}_{\mathcal{E}}(\mathbf{v})| < \mathbf{i}^{\max}. \end{aligned} \tag{4.9}$$

By Theorem 2.2, $\mathbf{v}$ is located in $\mathcal{D}_{\rho}(\hat{\mathbf{v}})$ with $\rho = \rho^{\dagger}_{Y,\Delta}(\hat{\mathbf{v}}, \hat{\mathbf{s}}^{Y,\Delta}, \mathbf{s}^{Y,\Delta})$. Since

- $\mathbf{v}^{\min} < |\hat{\mathbf{v}}| < \mathbf{v}^{\max}$,
- $|\mathbf{i}_{\mathcal{E}}(\hat{\mathbf{v}})| < \mathbf{i}^{\max}$,
- $\rho^{\dagger}_{Y,\Delta}(\hat{\mathbf{v}}, \hat{\mathbf{s}}^{Y,\Delta}, \hat{\mathbf{s}}^{Y,\Delta}) = 0$,
- $\rho^{\dagger}_{Y,\Delta}(\hat{\mathbf{v}}, \hat{\mathbf{s}}^{Y,\Delta}, \mathbf{s}^{Y,\Delta})$ is continuous in $\mathbf{s}^{Y,\Delta}$,

we have that there exists $\epsilon_0(\hat{\mathbf{v}}, \hat{\mathbf{s}}^{Y,\Delta}) \in (0, \epsilon^{\max}_{\hat{\mathbf{v}},\hat{\mathbf{s}}^{Y,\Delta}})$ such that

$$\begin{aligned} & \xi^{Y,\Delta}(\mathbf{s}^{Y,\Delta} - \hat{\mathbf{s}}^{Y,\Delta}) \leq \epsilon_0(\hat{\mathbf{v}}, \hat{\mathbf{s}}^{Y,\Delta}) \\ \Rightarrow \quad & \mathbf{v}^{\min} < \frac{1}{2}(\mathbf{v}^{\min} + |\hat{\mathbf{v}}|) \leq |\mathbf{v}| \leq \frac{1}{2}(|\hat{\mathbf{v}}| + \mathbf{v}^{\max}) < \mathbf{v}^{\max}, \\ & |\mathbf{i}_{\mathcal{E}}(\mathbf{v})| \leq \frac{1}{2}(|\mathbf{i}_{\mathcal{E}}(\hat{\mathbf{v}})| + \mathbf{i}^{\max}) < \mathbf{i}^{\max}, \end{aligned} \tag{4.10}$$

which completes the proof.

■

4.B Proof of Theorem 4.1

For Item 1

According to Lemma 4.1, there exists $\epsilon_0\left(\mathbf{v}^{(k)}, (\mathbf{s}^{Y,\Delta})^{(k)}\right) \in \left(0, \epsilon^{\max}_{\mathbf{v}^{(k)},(\mathbf{s}^{Y,\Delta})^{(k)}}\right)$ such that for $\epsilon^{(n)} \in \left(0, \min\left\{\epsilon_0\left(\mathbf{v}^{(k)}, (\mathbf{s}^{Y,\Delta})^{(k)}\right), \epsilon^{\text{bound}}\right\}\right]$ and $\tilde{\mathbf{s}}^{Y,\Delta} \in \text{cl}\left(\mathcal{B}^{\text{aux}}\left((\mathbf{s}^{Y,\Delta})^{(k)}, \epsilon^{(n)}\right)\right)$, the corresponding $\tilde{\mathbf{v}}$ computed in pseudo-code line 7 satisfies the conditions in

pseudo-code lines 8 and 11, hence triggers the termination of the inner loop. As $\epsilon^{(n)} = \zeta^{n+1}\epsilon^{\max}_{\mathbf{v}^{(k)},(\mathbf{s}^{Y,\Delta})^{(k)}}$ and $\zeta \in (0,1)$, we know that there exists a finite integer $\tilde{n} \geq 0$ such that $\epsilon^{(\tilde{n})} \in \left(0, \min\left\{\epsilon_0\left(\mathbf{v}^{(k)}, (\mathbf{s}^{Y,\Delta})^{(k)}\right), \epsilon^{\text{bound}}\right\}\right]$, which completes the proof.

For Item 2(a)

Consider that

- f is continuous,
- $\left(\mathbf{v}^{(k)}, (\mathbf{s}^{Y,\Delta})^{(k)}\right)$ belongs to a compact set,
- $f\left(\mathbf{v}^{(k+1)}, (\mathbf{s}^{Y,\Delta})^{(k+1)}\right) \leq f\left(\mathbf{v}^{(k)}, (\mathbf{s}^{Y,\Delta})^{(k)}\right)$.

We have that the sequence $\left\{f\left(\mathbf{v}^{(k)}, \mathbf{s}^{Y,\Delta})^{(k)}\right)\right\}$ is monotonically non-increasing and bounded below. By the monotone convergence theorem [96], $\left\{f\left(\mathbf{v}^{(k)}, (\mathbf{s}^{Y,\Delta})^{(k)}\right)\right\}$ converges to a finite limit.

For Item 2(b)

In this case, the objective function becomes $f(\mathbf{s}^{Y,\Delta})$. Accordingly, LOPF can be written as LOPF$\left((\mathbf{s}^{Y,\Delta})^{(k-1)}, (\epsilon^{\text{seq}})^{(k-1)}\right)$.

Let us define the following set

$$\mathcal{B} = \mathcal{B}^{\text{aux}}\left((\mathbf{s}^{Y,\Delta})^{(k-1)}, (\epsilon^{\text{seq}})^{(k-1)}\right) \bigcap \mathcal{B}^{\text{aux}}\left((\mathbf{s}^{Y,\Delta})^{(k)}, \epsilon_0\left(\mathbf{v}^{(k)}, (\mathbf{s}^{Y,\Delta})^{(k)}\right)\right), \tag{4.11}$$

where ϵ_0 is described in Lemma 4.1.

As $(\mathbf{s}^{Y,\Delta})^{(k)}$ minimizes LOPF$\left((\mathbf{s}^{Y,\Delta})^{(k-1)}, (\epsilon^{\text{seq}})^{(k-1)}\right)$, we have that $f\left((\mathbf{s}^{Y,\Delta})^{(k)}\right) \leq f(\mathbf{s}^{Y,\Delta})$, $\forall \mathbf{s}^{Y,\Delta} \in \mathcal{B}$. Therefore, $\left(\mathbf{v}^{(k)}, (\mathbf{s}^{Y,\Delta})^{(k)}\right)$ is a locally optimal solution to GOPF .

For Item 2(c)(i)

Consider that

- $\rho^{\ddagger}_{Y,\Delta}$ is continuous,

- $\rho^{\ddagger}_{Y,\Delta}\left(\mathbf{v}^{(k)}, (\mathbf{s}^{Y,\Delta})^{(k)}\right) > 0$,
- $\epsilon^{\max}_{\mathbf{v}^{(k)},(\mathbf{s}^{Y,\Delta})^{(k)}} = \left(\rho^{\ddagger}_{Y,\Delta}\left(\mathbf{v}^{(k)}, (\mathbf{s}^{Y,\Delta})^{(k)}\right)\right)^2 > (\epsilon^{\text{seq}})^{(k)}$,
- $\epsilon^{\min} = \liminf_{k\to\infty}(\epsilon^{\text{seq}})^{(k)} > 0$.

We have that $\rho^{\ddagger}_{Y,\Delta}\left(\mathbf{v}^*, (\mathbf{s}^{Y,\Delta})^*\right) > 0$. Then, by Proposition 2.2, we have that the power-flow Jacobian $\mathbf{J}_{\mathbf{F}^{Y,\Delta}}\left(\mathbf{v}^*, \text{diag}\left(\mathbf{H}\overline{\mathbf{v}^*}\right)^{-1}\overline{(\mathbf{s}^{\Delta})^*}\right)$ is non-singular.

For Item 2(c)(ii)

In this case, the objective function becomes $f(\mathbf{s}^{Y,\Delta})$.

Let $\{\sigma(k)\}$ denote the indexes of a convergent sub-sequence that corresponds to $\left(\mathbf{v}^*, (\mathbf{s}^{Y,\Delta})^*\right)$.

We proceed by creating a contradiction. Suppose that $\left(\mathbf{v}^*, (\mathbf{s}^{Y,\Delta})^*\right)$ is not a locally optimal solution to GOPF . Then, given any $\epsilon > 0$, $(\mathbf{s}^{Y,\Delta})^*$ is not a minimizer of LOPF$\left((\mathbf{s}^{Y,\Delta})^*, \epsilon\right)$. In particular, there exists $\tilde{\mathbf{s}}^{Y,\Delta} \in \mathcal{S}^{Y,\Delta}$ such that

$$\xi^{Y,\Delta}\left(\tilde{\mathbf{s}}^{Y,\Delta} - (\mathbf{s}^{Y,\Delta})^*\right) < \epsilon^{\min}, \tag{4.12}$$

$$f\left(\tilde{\mathbf{s}}^{Y,\Delta}\right) < f\left((\mathbf{s}^{Y,\Delta})^*\right). \tag{4.13}$$

As

- $(\mathbf{s}^{Y,\Delta})^{\sigma(k)} \to (\mathbf{s}^{Y,\Delta})^*$,
- $\xi^{Y,\Delta}$ is continuous,

there exists k' such that $\xi^{Y,\Delta}\left(\tilde{\mathbf{s}}^{Y,\Delta} - (\mathbf{s}^{Y,\Delta})^{\sigma(k')}\right) \leq \epsilon^{\min} \leq (\epsilon^{\text{seq}})^{\sigma(k')}$. Consequently, we obtain that $\tilde{\mathbf{s}}^{Y,\Delta} \in \text{cl}\left(\mathcal{B}^{\text{aux}}\left((\mathbf{s}^{Y,\Delta})^{\sigma(k')}, (\epsilon^{\text{seq}})^{\sigma(k')}\right)\right)$.

Since $(\mathbf{s}^{Y,\Delta})^{\sigma(k')+1}$ is a minimizer in $\text{cl}\left(\mathcal{B}^{\text{aux}}\left((\mathbf{s}^{Y,\Delta})^{\sigma(k')}, (\epsilon^{\text{seq}})^{\sigma(k')}\right)\right)$, it follows that

$$f\left(\tilde{\mathbf{s}}^{Y,\Delta}\right) \geq f\left((\mathbf{s}^{Y,\Delta})^{\sigma(k')+1}\right). \tag{4.14}$$

In addition, due to the fact that $\left\{ f\left((\mathbf{s}^{Y,\Delta})^{(k)} \right) \right\}$ is a monotonically non-increasing sequence, we have

$$f\left((\mathbf{s}^{Y,\Delta})^{\sigma(k')+1} \right) \geq f\left((\mathbf{s}^{Y,\Delta})^{*} \right) . \tag{4.15}$$

By combination of (4.14) and (4.15), we have

$$f\left(\tilde{\mathbf{s}}^{Y,\Delta} \right) \geq f\left((\mathbf{s}^{Y,\Delta})^{*} \right) , \tag{4.16}$$

which contradicts (4.13) and completes the proof.

For Item 2(d)

By definition of $\limsup$, we know that

- There exists a sequence $\{\varsigma(k)\}$ such that $(\epsilon^{\text{seq}})^{\varsigma(k)} \to \epsilon^{\max}$ as $k \to \infty$.
- For any $(\epsilon^{\min})' \in (0, \epsilon^{\max})$, there exists K_1 such that for all $k \geq K_1$, we have that $(\epsilon^{\text{seq}})^{\varsigma(k)} > (\epsilon^{\min})'$.

Let $\{\sigma'(k)\}$ be a sub-sequence of $\{\varsigma(k)\}$ such that $\left(\mathbf{v}^{\sigma'(k)}, (\mathbf{s}^{Y,\Delta})^{\sigma'(k)} \right) \to \left(\mathbf{v}^{*}, (\mathbf{s}^{Y,\Delta})^{*} \right)$ for some $\left(\mathbf{v}^{*}, (\mathbf{s}^{Y,\Delta})^{*} \right)$. Then, by replacing

- $\epsilon^{\min}$ with $(\epsilon^{\min})'$,
- $\{\sigma(k)\}$ with $\{\sigma'(k)\}$

in the proof for item 2(c), we complete the proof for item 2(d).

For Item 3

By item 2(a), the sequence $\left\{ f\left(\mathbf{v}^{(k)}, (\mathbf{s}^{Y,\Delta})^{(k)} \right) \right\}$ converges. Therefore, given any $\text{ErrBound} > 0$, there exists K_2 such that

$$\left| f\left(\mathbf{v}^{(k+1)}, (\mathbf{s}^{Y,\Delta})^{(k+1)} \right) - f\left(\mathbf{v}^{(k)}, (\mathbf{s}^{Y,\Delta})^{(k)} \right) \right| < \text{ErrBound} \ , \ \forall k \geq K_2 \ .$$

This means that the method terminates within a finite number of iterations that are indexed by k. Moreover, by item 1, we know that for each iteration k, there is a finite number of LOPF problems to solve. In this way, we complete the proof.

■

5 Conclusions

> In the morning, I gathered the angelica on the mountains.
> In the evening, I plucked the sedges of the islets.
> The days and months hurried on, never delaying.
> Springs and autumns sped by, in endless alternation.
>
> *Chu Ci*
> QU YUAN

In this thesis, we have addressed two inverse problems and one optimal power flow problem for ADNs.

In the first inverse problem (Chapter 2), we have focused on the solvability of the non-linear multi-dimensional power-flow equation in multi-phase ADNs. With respect to the model of ADNs, we have assumed that the network topologies are generic and the transmission devices can be either π-modelled transmission lines or complex-ratio transformers. Due to the non-linearity of the power-flow equation, the existence and uniqueness of the power-flow solution are not guaranteed in general. This creates an issue for network security. More precisely, when we have a target system power injection to implement, it is unknown whether this system power injection has a power-flow solution. Even if there is a power-flow solution, it might not satisfy the security constraints. To address the issue, we have first shown that the power-flow equation can be written in a fixed-point form, which leads to the implicit Z-bus formulation of the power-flow problem. Then, by applying the Banach fixed-point theorem to the implicit Z-bus formulation, we have established explicit sufficient conditions on the existence and uniqueness of the power-flow solution, which outperform the state of the art. When the conditions are satisfied, we guarantee the existence of a power-flow solution and analytically specify a domain in which this solution is unique. We have proved that this solution satisfies the non-singularity of the power-flow Jacobian hence fulfills the static voltage stability. To numerically compute this guaranteed solution, we have

developed an iterative method. Notably, the per-iteration complexity of this method is much lower than that of the widely deployed Newton-Raphson method, which is of significance for the real-time operation of ADNs. In addition to the above, we have further taken into account the specific load/source connections and have correspondingly extended all the established results. The considered load/source connections include not only grounded wye and ungrounded delta, but also a combination of them.

In the second inverse problem (Chapter 3), we have considered that the actual system power injection in ADNs might be uncertain and different from the target one. Consequently, the actual system electrical state cannot be exactly predicted, which makes it difficult to ensure the satisfaction of the security constraints. This issue motivates the definition of admissibility. More precisely, given an initial system electrical state $\mathbf{v}^{\text{initial}}$ that fulfills the security constraints and an uncertainty set $\mathcal{S}^{\text{uncertain}}$ that constrains the actual system power injection, we say that $\mathcal{S}^{\text{uncertain}}$ is admissible for $\mathbf{v}^{\text{initial}}$ if any continuous path of the system electrical state that starts at $\mathbf{v}^{\text{initial}}$ must satisfy the security constraints. To determine the admissibility, we have introduced the auxiliary concept of $\mathcal{V}$-control. Specifically, given a set $\mathcal{S}$ of system power injections and a set $\mathcal{V}$ of system electrical states, we say that $\mathcal{S}$ is a domain of $\mathcal{V}$-control if: any continuous path of the system electrical state that starts in $\mathcal{V}$ must stay in $\mathcal{V}$, as long as the corresponding path of the system power injection resides in $\mathcal{S}$. With the concept of $\mathcal{V}$-control, $\mathcal{S}^{\text{uncertain}}$ is admissible for $\mathbf{v}^{\text{initial}}$ if there exists a set $\mathcal{V}$ such that (i) every system electrical state in $\mathcal{V}$ fulfills the security constraints, (ii) $\mathbf{v}^{\text{initial}} \in \mathcal{V}$, and (iii) $\mathcal{S}^{\text{uncertain}}$ is a domain of $\mathcal{V}$-control. Through examples, we have shown that the "existence of a unique power-flow solution $\mathbf{v} \in \mathcal{V}$ for every $\mathbf{s} \in \mathcal{S}$" alone is neither sufficient nor necessary to ensure that $\mathcal{S}$ is a domain of $\mathcal{V}$-control. For $\mathcal{S}$ to be a domain of $\mathcal{V}$-control, we have given additional conditions that complement the existence and uniqueness of the power-flow solution. Moreover, we have proposed theorems to ensure that there exists a unique power-flow solution $\mathbf{v} \in \mathcal{V}$ for every $\mathbf{s} \in \mathcal{S}$. Due to the real-quadratic nature of the multi-dimensional power-flow equation, we have incidentally discovered that local uniqueness implies non-singularity, which is the converse of the inverse function theorem. Using the established theoretical results, we have developed two concrete methods for solving the admissibility problem. The first method is tight in the sense that it almost finds the largest $\mathcal{S}^{\text{uncertain}}$ that is admissible for some given $\mathbf{v}^{\text{initial}}$. However, due to relatively high complexity in both time and space, this method is not suitable for real-time deployment in large ADNs. Differently from the first method, the second method is less tight. But, through numerical evaluations, we see that it is suitable for real-time applications in large ADNs.

In the optimal power flow problem (Chapter 4), we have studied how to determine the optimal system power injection in generically modelled multi-phase ADNs. In particular, we have considered wye/delta load/source connections and have incorporated the non-singularity constraint. This problem cannot be solved by existent methods and might not have an optimal solution. To solve this problem, we have

exploited the results in Chapter 2 and have shown that, by properly restricting the system power injection to some local domains, we can obtain an explicit convex proxy for the feasible set of this problem. Based on this finding, we have developed a successive local exploration method. In each iteration of the method, we obtain a feasible point of this problem, by exploring around the feasible point obtained in the previous iteration. We ensure that the objective-function values at the obtained feasible points are monotonically non-increasing. We have guaranteed that they converge to a finite limit. If the objective function does not explicitly contain $\mathbf{v}$, then we have given a-posteriori conditions to determine whether the obtained feasible points and their limit points are locally optimal solutions. We have numerically evaluated the successive local exploration method and have compared it with the successive linear approximation method in our work [83].

Based on the work done in this thesis, the following topics are suggested for further studies:

- Improving the conditions on the existence and uniqueness of the power-flow solutions.
- Enhancing the time and space efficiency for the first solution method to the admissibility problem.
- Developing a-priori conditions to guarantee the optimality of the optimal power flow solutions.
- Extending the results to the networks with PV buses.

Bibliography

[1] J. D. Glover, M. S. Sarma, and T. Overbye, *Power system analysis and design (fifth edition)*. Cengage Learning, 2011.

[2] A. von Meier, *Electric power systems: a conceptual introduction*. John Wiley & Sons, 2006.

[3] M. Delfanti, M. Merlo, G. Monfredini, V. Olivieri, M. Pozzi, and A. Silvestri, "Hosting dispersed generation on italian mv networks: Towards smart grids," in *14th International Conference on Harmonics and Quality of Power (ICHQP)*, Sept. 2010, pp. 1–6.

[4] R. Verzijlbergh, L. De Vries, G. Dijkema, and P. Herder, "Institutional challenges caused by the integration of renewable energy sources in the European electricity sector," *Renewable and Sustainable Energy Reviews*, vol. 75, pp. 660–667, Aug. 2017.

[5] S. Alyami, Y. Wang, and C. Wang, "Overvoltage risk analysis in distribution networks with high penetration of pvs," in *2016 International Conference on Probabilistic Methods Applied to Power Systems (PMAPS)*, Oct. 2016, pp. 1–6.

[6] S. Adhikari, F. Li, and H. Li, "P-Q and P-V control of photovoltaic generators in distribution systems," *IEEE Transactions on Smart Grid*, vol. 6, no. 6, pp. 2929–2941, Nov. 2015.

[7] S.-H. Ko, S. R. Lee, H. Dehbonei, and C. V. Nayar, "Application of voltage- and current-controlled voltage source inverters for distributed generation systems," *IEEE Transactions on Energy Conversion*, vol. 21, no. 3, pp. 782–792, Sep. 2006.

[8] R. Majumder, A. Ghosh, G. Ledwich, and F. Zare, "Power management and power flow control with back-to-back converters in a utility connected microgrid," *IEEE Transactions on Power Systems*, vol. 25, no. 2, pp. 821–834, May 2010.

[9] L. M. Fernandez, C. A. Garcia, and F. Jurado, "Operating capability as a PQ/PV node of a direct-drive wind turbine based on a permanent magnet synchronous generator," *Journal of Renewable Energy*, vol. 35, pp. 1308–1318, 2010.

[10] S. Grillo, S. Massucco, A. Morini, A. Pitto, and F. Silvestro, "Microturbine control modeling to investigate the effects of distributed generation in electric energy networks," *IEEE Systems Journal*, vol. 4, no. 3, pp. 303–312, Sep. 2010.

[11] Q.-C. Zhong and G. Weiss, "Synchronverters: Inverters that mimic synchronous generators," *IEEE Transactions on Industrial Electronics*, vol. 58, no. 4, pp. 1259–1267, Apr. 2011.

[12] M. Torres and L. A. Lopes, "Virtual synchronous senerator: A control strategy to improve dynamic frequency control in autonomous power systems," *Energy and Power Engineering*, vol. 5, pp. 32–38, 2013.

[13] P. M. S. Carvalho, P. F. Correia, and L. A. F. M. Ferreira, "Distributed reactive power generation control for voltage rise mitigation in distribution networks," *IEEE Transactions on Power Systems*, vol. 23, no. 2, pp. 766–772, May 2008.

[14] R. Majumder, G. Ledwich, A. Ghosh, S. Chakrabarti, and F. Zare, "Droop control of converter-interfaced microsources in rural distributed generation," *IEEE Transactions on Power Delivery*, vol. 25, no. 4, pp. 2768–2778, Oct. 2010.

[15] J. M. Guerrero, J. C. Vasquez, J. Matas, L. G. de Vicuna, and M. Castilla, "Hierarchical control of droop-controlled AC and DC microgrids—a general approach toward standardization," *IEEE Transactions on Industrial Electronics*, vol. 58, no. 1, pp. 158–172, Jan. 2011.

[16] A. Bernstein, L. Reyes-Chamorro, J.-Y. Le Boudec, and M. Paolone, "A composable method for real-time control of active distribution networks with explicit power setpoints. Part I: framework," *Electric Power Systems Research*, vol. 125, pp. 254–264, Aug. 2015.

[17] L. Reyes-Chamorro, A. Bernstein, J.-Y. Le Boudec, and M. Paolone, "A composable method for real-time control of active distribution networks with explicit power setpoints. Part II: implementation and validation," *Electric Power Systems Research*, vol. 125, pp. 265–280, Aug. 2015.

[18] H. D. Nguyen and K. S. Turitsyn, "Appearance of multiple stable load flow solutions under power flow reversal conditions," in *2014 IEEE PES General Meeting | Conference Exposition*, July 2014, pp. 1–5.

[19] A. J. Korsak, "On the question of uniqueness of stable load-flow solutions," *IEEE Transactions on Power Apparatus and Systems*, vol. PAS-91, pp. 1093–1100, May 1972.

[20] B. K. Johnson, "Extraneous and false load flow solutions," *IEEE Transactions on Power Apparatus and Systems*, vol. PAS-96, no. 2, pp. 524–534, Mar. 1977.

[21] Y. Wang and W. Xu, "The existence of multiple power flow solutions in unbalanced three-phase circuits," *IEEE Transactions on Power Systems*, vol. 18, no. 2, pp. 605–610, May 2003.

[22] T.-H. Chen, M.-S. Chen, K.-J. Hwang, P. Kotas, and E. A. Chebli, "Distribution system power flow analysis - a rigid approach," *IEEE Transactions on Power Delivery*, vol. 6, no. 3, pp. 1146–1152, Jul. 1991.

[23] A. Quarteroni, R. Sacco, and F. Saleri, *Numerical mathematics*, 2nd ed., ser. 37. Springer, 2007.

[24] D. K. Molzahn, D. Mehta, and M. Niemerg, "Toward topologically based upper bounds on the number of power flow solutions," in *2016 American Control Conference (ACC)*, July 2016, pp. 1–6.

[25] B. Lesieutre and D. Wu, "An efficient method to locate all the load flow solutions - revisited," in *2015 53rd Annual Allerton Conference on Communication, Control, and Computing (Allerton)*, September 2015, pp. 1–8.

[26] J. Thorp, D. Schulz, and M. Ilic-Spong, "Reactive power-voltage problem: Conditions for the existence of solution and localized disturbance propagation," *International Journal of Electrical Power & Energy Systems*, vol. 8, pp. 66–76, Apr. 1986.

[27] M. Ilic, "Network theoretic conditions for existence and uniqueness of steady state solutions to electric power circuits," in *ICSAS*, San Diego, CA, 1992, pp. 2821–2828.

[28] H.-D. Chiang and M. E. Baran, "On the existence and uniqueness of load flow solution for radial distribution power networks," *IEEE Transactions on Circuits and Systems*, vol. 37, no. 3, pp. 410–416, Mar. 1990.

[29] K. N. Miu and H.-D. Chiang, "Existence, uniqueness, and monotonic properties of the feasible power flow solution for radial three-phase distribution networks," *IEEE Transactions on Circuits and Systems*, vol. 47, no. 10, pp. 1502–1514, Oct. 2000.

[30] S. Bolognani and S. Zampieri, "On the existence and linear approximation of the power flow solution in power distribution networks," *IEEE Transactions on Power Systems*, vol. 31, no. 1, pp. 163–172, Jan. 2016.

[31] S. Yu, H. D. Nguyen, and K. S. Turitsyn, "Simple certificate of solvability of power flow equations for distribution systems," in *2015 IEEE Power & Energy Society General Meeting*, 2015.

[32] J. W. Simpson-Porco, "A theory of solvability for lossless power flow equations – Part I: fixed-point power flow," *IEEE Transactions on Control of Network Systems*, vol. 5, no. 3, pp. 1361–1372, Sep. 2018.

[33] K. Dvijotham, H. Nguyen, and K. Turitsyn, "Solvability regions of affinely parameterized quadratic equations," *IEEE Control Systems Letters*, vol. 2, no. 1, pp. 25–30, Jan. 2018.

[34] K. Dvijotham, E. Mallada, and J. W. Simpson-Porco, "High-voltage solution in radial power networks: Existence, properties, and equivalent algorithms," *IEEE Control Systems Letters*, vol. 1, no. 2, pp. 322–327, Oct. 2017.

[35] M. Bazrafshan and N. Gatsis, "Convergence of the Z-bus method for three-phase distribution load-flow with ZIP loads," *IEEE Transactions on Power Systems*, vol. 33, no. 1, pp. 153–165, Jan. 2018.

[36] M. S. Chen and W. E. Dillon, "Power system modeling," *Proceedings of the IEEE*, vol. 62, no. 7, pp. 901–915, Jul. 1974.

[37] J. Arrillaga, D. Bradley, and P. Bodger, *Power system harmonics*. Chicester, U.K.: John Wiley & Sons, 1985.

[38] C. Wang, A. Bernstein, J.-Y. Le Boudec, and M. Paolone, "Explicit conditions on existence and uniqueness of load-flow solutions in distribution networks," *IEEE Transactions on Smart Grid*, vol. 9, no. 2, pp. 953–962, Mar. 2018.

[39] ——, "Existence and uniqueness of load-flow solutions in three-phase distribution networks," *IEEE Transactions on Power Systems*, vol. 32, no. 4, pp. 3319–3320, Jul. 2017.

[40] A. M. Kettner and M. Paolone, "On the properties of the power systems nodal admittance matrix," *IEEE Transactions on Power Systems*, vol. 33, no. 1, pp. 1130–1131, Jan. 2018.

[41] M. Bazrafshan and N. Gatsis, "Comprehensive modeling of three-phase distribution systems via the bus admittance matrix," *IEEE Transactions on Power Systems*, vol. 33, no. 2, pp. 2015–2029, Mar. 2018.

[42] S. Sarri, M. Paolone, R. Cherkaoui, A. Borghetti, F. Napolitano, and C. Nucci, "State estimation of active distribution networks: Comparison between WLS and iterated kalman-filter algorithm integrating PMUs," in *3rd IEEE PES Innovative Smart Grid Technologies Europe (ISGT Europe)*, 2012.

[43] J. Liu, J. Tang, F. Ponci, A. Monti, C. Muscas, and P. A. Pegoraro, "Trade-offs in PMU deployment for state estimation in active distribution grids," *IEEE Transactions on Smart Grid*, vol. 3, no. 2, pp. 915–924, Jun. 2012.

[44] M. Pau, P. A. Pegoraro, and S. Sulis, "Efficient branch-current-based distribution system state estimation including synchronized measurements," *IEEE Transactions on Instrumentation and Measurement*, vol. 62, no. 9, pp. 2419–2429, Sep. 2013.

[45] A. Primadianto and C.-N. Lu, "A review on distribution system state estimation," *IEEE Transactions on Power Systems*, vol. 32, no. 5, pp. 3875–3883, Sep. 2017.

[46] M. Pignati, L. Zanni, P. Romano, R. Cherkaoui, and M. Paolone, "Fault detection and faulted line identification in active distribution networks using synchrophasors-based real-time state estimation," *IEEE Transactions on Power Delivery*, vol. 32, no. 1, pp. 381–392, Feb. 2017.

[47] W. F. Tinney and J. W. Walker, "Direct solutions of sparse network equations by optimally ordered triangular factorization," *Proceedings of the IEEE*, vol. 55, no. 11, pp. 1801–1809, Nov. 1967.

[48] F. L. Alvarado, W. F. Tinney, and M. K. Enns, "Sparsity in large-scale network computation," *Advances in Electric Power and Energy Conversion System Dynamics and Control*, vol. 41, pp. 207–272, 1991.

[49] H. M. Markowitz, "The elimination form of the inverse and its application to linear programming," *Management Sci.*, vol. 3, no. 3, pp. 255–269, Apr. 1957.

[50] V. Ajjarapu and C. Christy, "The continuation power flow: A tool for steady state voltage stability analysis," *Transactions on Power Systems*, vol. 7, no. 1, pp. 416–423, Feb. 1992.

[51] P. W. Sauer and M. A. Pai, "Power system steady-state stability and the load-flow jacobian," *IEEE Transactions on Power Systems*, vol. 5, no. 4, pp. 1374–1381, Nov. 1990.

[52] G. Y. Cao and D. J. Hill, "Power system voltage small-disturbance stability studies based on the power flow equation," *IET Generation, Transmission and Distribution*, vol. 4, no. 7, pp. 873–882, Jul. 2010.

[53] W. H. Kersting, *Distribution system modeling and analysis (second edition)*. CRC Press, 2007.

[54] W. Rudin, *Principles of mathematical analysis (third edition)*. McGraw-Hill, 1976.

[55] W. H. Kersting, "Radial distribution test feeders," in *IEEE PES Winter Meeting*, vol. 2, Jan. 2001, pp. 908–912.

[56] ——, "Radial distribution test feeders," *IEEE Transactions on Power Systems*, vol. 6, no. 3, pp. 975–985, Aug. 1991.

[57] F. Milano, *Power system modelling and scripting*. Springer, 2010.

[58] R. C. Dugan and T. E. McDermott, "An open source platform for collaborating on smart grid research," in *2011 IEEE Power and Energy Society General Meeting*, July 2011, pp. 1–7.

[59] J. B. Lasserre, "Global optimization with polynomials and the problem of moments," *SIAM Journal on Optimization*, vol. 11, no. 3, pp. 796–817, 2001.

[60] H. Waki, S. Kim, M. Kojima, and M. Muramatsu, "Sums of squares and semidefinite program relaxations for polynomial optimization problems with structured sparsity," *SIAM Journal on Optimization*, vol. 17, no. 1, pp. 218–242, 2006.

[61] J. B. Lasserre, "Convergent SDP-relaxations in polynomial optimzation with sparsity," *SIAM Journal on Optimization*, vol. 17, no. 3, pp. 822–843, 2006.

[62] D. K. Molzahn and L. A. Roald, "Grid-aware versus grid-agnostic distribution system control: A method for certifying engineering constraint satisfaction," in *Proceedings of the 52nd Hawaii International Conference on System Sciences*, 2019, pp. 3445–3454.

[63] ——, "Towards an AC optimal power flow algorithm with robust feasibility guarantees," in *2018 Power Systems Computation Conference (PSCC)*, Aug. 2018, pp. 1–7.

[64] R. Louca and E. Bitar, "Robust AC optimal power flow," *IEEE Transactions on Power Systems*, vol. 34, no. 3, pp. 1669–1681, May 2019.

[65] K. Dvijotham and K. Turitsyn, "Construction of power flow feasibility sets," *arXiv*, 2015, 1506.07191v3.

[66] C. Josz, J. Maeght, P. Panciatici, and J. C. Gilbert, "Application of the moment-SOS approach to global optimization of the OPF problem," *IEEE Transactions on Power Systems*, vol. 30, no. 1, pp. 463–470, Jan. 2015.

[67] B. Ghaddar, J. Marecek, and M. Mevissen, "Optimal power flow as a polynomial optimization problem," *IEEE Transactions on Power Systems*, vol. 31, no. 1, pp. 539–546, Jan. 2016.

[68] D. K. Molzahn and I. A. Hiskens, "Sparsity-exploiting moment-based relaxations of the optimal power flow problem," *IEEE Transactions on Power Systems*, vol. 30, no. 6, pp. 3168–3180, Nov. 2015.

[69] Z. Wang, B. Cui, and J. Wang, "A necessary condition for power flow insolvability in power distribution systems with distributed generators," *IEEE Trans. on Power Systems*, vol. 32, no. 2, pp. 1440–1450, Mar. 2017.

[70] C.-K. Sim and G. Zhao, "A note on treating a second order cone program as a special case of a semidefinite program," *Mathematical Programming*, vol. 102, no. 3, pp. 609–613, Jan. 2005.

[71] L. Porkolab and L. Khachiyan, "On the complexity of semidefinite programs," *Journal of Global Optimization*, vol. 10, no. 4, pp. 351–365, Jun. 1997.

[72] M. V. Ramana, "An exact duality theory for semidefinite programming and its complexity implications," *Mathematical Programming*, vol. 77, no. 1, pp. 129–162, Apr. 1997.

[73] K. Strunz *et al.*, *Benchmark systems for network integration of renewable and distributed energy resources*. CIGRE Task Force C6.04.02, Apr. 2014.

[74] J. Lofberg, "YALMIP: a toolbox for modeling and optimization in MATLAB," in *IEEE International Symposium on Computer Aided Control Systems Design*, Sep. 2004, pp. 284–289.

[75] M. ApS, *The MOSEK optimization toolbox for MATLAB manual. Version 7.1 (Revision 28).*, 2015. [Online]. Available: http://docs.mosek.com/7.1/toolbox/index.html

[76] H. Waki, S. Kim, M. Kojima, M. Muramatsu, and H. Sugimoto, "SparsePOP: a sparse semidefinite programming relaxation of polynomial optimization problems," *ACM Transactions on Mathematical Software*, vol. 35, no. 2, Jul. 2008.

[77] J. O'Rourke, *Computational geometry in C (second edition)*. Cambridge University Press, 1998.

[78] Y. Makarov, D. Hill, and I. Hiskens, "Properties of quadratic equations and their application to power system analysis," *International Journal of Electrical Power and Energy Systems*, vol. 22, pp. 313–323, 2000.

[79] S. Kim and M. Kojima, "Exploiting sparsity in SDP relaxation of polynomial optimization problems," in *Handbook on Semidefinite, Conic and Polynomial Optimization,* M. F. Anjos and J. B. Lasserre, Eds. Published by Springer-Verlag, 2012.

[80] J. R. S. Blair and B. W. Peyton, "An introduction to chordal graphs and clique trees," in *Graph Theory and Sparse Matrix Computation,* A. George and J. R. Gilbert and J. W. H. Liu, Eds. New York, NY, USA: Springer-Verlag, 1993.

[81] R. Prada and L.J.Souza, "Voltage stability and thermal limit: Constraints on the maximum loading of electrical energy distribution feeders," *IEE Proceedings - Generation, Transmission and Distribution*, vol. 145, no. 5, pp. 573–577, 1998.

[82] K. Lehmann, A. Grastien, and P. V. Hentenryck, "AC-feasibility on tree networks is NP-hard," *IEEE Transactions on Power Systems*, vol. 31, no. 1, pp. 798–801, Jan. 2016.

[83] A. Bernstein, C. Wang, and J.-Y. Le Boudec, "Multiphase optimal and non-singular power flow by successive linear approximations," in *2018 IEEE Power Systems Computation Conf. (PSCC)*, Jun. 2018.

[84] P. Kessel and H. Glavitsch, "Estimating the voltage stability of a power system," *IEEE Transactions on Power Delivery*, vol. PWRD-1, no. 3, pp. 346–354, Jul. 1986.

[85] A. M. Kettner and M. Paolone, "A generalized index for static voltage stability of unbalanced polyphase power systems including Thévenin equivalents and polynomial models," *IEEE Transactions on Power Systems*, DOI 10.1109/TPWRS.2019.2922073.

[86] J. Nocedal and S. J. Wright, *Numerical optimization (2nd ed.)*. Springer-Verlag New York, 2006.

[87] S. Bruno, S. Lamonaca, G. Rotondo, U. Stecchi, and M. La Scala, "Unbalanced three-phase optimal power flow for smart grids," *IEEE Transactions on Industrial Electronics*, vol. 58, no. 10, pp. 4504–4513, Oct. 2011.

[88] S. Paudyal, C. A. Canizares, and K. Bhattacharya, "Optimal operation of distribution feeders in smart grids," *IEEE Transactions on Industrial Electronics*, vol. 58, no. 10, pp. 4495–4503, Oct. 2011.

[89] ——, "Three-phase distribution OPF in smart grids: Optimality versus computational burden," in *2011 2nd IEEE PES International Conference and Exhibition on Innovative Smart Grid Technologies*, Manchester, UK, Dec. 2011.

[90] L. R. Araujo, D. R. R. Penido, and F. A. Vieira, "A multiphase optimal power flow algorithm for unbalanced distribution systems," *International Journal of Electrical Power and Energy Systems*, vol. 53, pp. 632–642, 2013.

[91] E. Dall'Anese, H. Zhu, and G. B. Giannakis, "Distributed optimal power flow for smart microgrids," *IEEE Transactions on Smart Grid*, vol. 4, no. 3, pp. 1464–1475, Sep. 2013.

[92] S. Boyd, N. Parikh, E. Chu, B. Peleato, and J. Eckstein, "Distributed optimization and statistical learning via the alternating direction method of multipliers," *Foundations and Trends in Machine Learning*, vol. 3, no. 1, pp. 1–122, 2010.

[93] L. Gan and S. H. Low, "Convex relaxations and linear approximation for optimal power flow in multiphase radial networks," in *IEEE Proceedings of Power Systems Computation Conference*, 2014.

[94] A. S. Zamzam, N. D. Sidiropoulos, and E. Dall'Anese, "Beyond relaxation and Newton-Raphson: Solving AC OPF for multi-phase systems with renewables," *IEEE Transactions on Smart Grid*, vol. 9, no. 5, pp. 3966–3975, Sep. 2018.

[95] O. Mehanna, K. Huang, B. Gopalakrishnan, A. Konar, and N. D. Sidiropoulos, "Feasible point pursuit and successive approximation of non-convex QCQPs," *IEEE Signal Processing Letters*, vol. 22, no. 7, pp. 804–808, Jul. 2015.

[96] W. A. Sutherland, *Introduction to metric and topological spaces*. Oxford University Press, 1975.

List of Publications

Following is the list of all my publications written as a PhD student at EPFL.

- **Cong Wang**, Andrey Bernstein, Jean-Yves Le Boudec, Mario Paolone, "Explicit conditions on existence and uniqueness of load-flow solutions in distribution networks," *IEEE Transactions on Smart Grid*, vol. 9, no. 2, pp. 953–962, Mar. 2018
- **Cong Wang**, Andrey Bernstein, Jean-Yves Le Boudec, Mario Paolone, "Existence and uniqueness of load-flow solutions in three-phase distribution networks," *IEEE Transactions on Power Systems*, vol. 32, no. 4, pp. 3319–3320, Jul. 2017
- Andrey Bernstein, **Cong Wang**, Emiliano Dall'Anese, Jean-Yves Le Boudec, Changhong Zhao, "Load flow in multiphase distribution networks: Existence, uniqueness, non-singularity and linear models," *IEEE Transactions on Power Systems*, vol. 33, no. 6, pp. 5832–5843, Nov. 2018
- **Cong Wang**, Jean-Yves Le Boudec, Mario Paolone, "Controlling the electrical state via uncertain power injections in three-phase distribution networks," *IEEE Transactions on Smart Grid*, vol. 10, no. 2, pp. 1349–1362, Mar. 2019
- Andrey Bernstein, **Cong Wang**, Jean-Yves Le Boudec, "Multiphase optimal and non-singular power flow by successive linear approximations," *2018 Power Systems Computation Conference (PSCC)*, pp. 1–8, Jun. 2018
- **Cong Wang**, Eleni Stai, Jean-Yves Le Boudec, "A polynomial-time method for testing admissibility of uncertain power injections in microgrids," *arXiv:1810.06256 [math.OC]*, pp. 1–12, Oct. 2018
- Eleni Stai, **Cong Wang**, Jean-Yves Le Boudec, "Online battery storage management via Lyapunov optimization in active distribution grids," *IEEE Transactions on Control Systems Technology*, under review
- **Cong Wang**, Eleni Stai, Jean-Yves Le Boudec, "Admissibility of uncertain injections in quadratic algebraic systems," *IEEE Transactions on Control of Network Systems*, under review

- **Cong Wang**, Eleni Stai, Jean-Yves Le Boudec, "Scenario-based optimal power flow for three-phase radial distribution networks with energy storage," *IEEE Transactions on Control of Network Systems*, under review
- Roman Rudnik, **Cong Wang**, Lorenzo Reyes-Chamorro, Jagdish Achara, Jean-Yves Le Boudec, Mario Paolone, "Real-time control of an electric-vehicle charging station while tracking an aggregated power setpoint," *IEEE Transactions on Industry Applications*, under review

Cong WANG

Affiliation
School of Computer and Communication Sciences
École Polytechnique Fédérale de Lausanne (EPFL)
CH-1015, Lausanne, Switzerland

Contact Information
Phone: (+41) 021 693 12 63
Email: cong.wang@epfl.ch

EDUCATION

Ph.D., Computer and Communication Sciences — September 2014 - Present
École Polytechnique Fédérale de Lausanne (EPFL), Lausanne, Switzerland

B.Sc., Electronic Information Science and Technology — August 2009 - July 2013
Tsinghua University, Beijing, China

HONORS

Teaching Assistant Team Award 2015	École Polytechnique Fédérale de Lausanne (EPFL), 2015
IC Doctoral School Fellowship	École Polytechnique Fédérale de Lausanne (EPFL), 2014
Outstanding Graduate Award	Tsinghua University, 2013
ST Engineering China Scholarship	Singapore Technologies Engineering Ltd., 2013
Tsinghua Scholarship of Overall Excellence	Tsinghua University, 2012
ST Engineering China Scholarship	Singapore Technologies Engineering Ltd., 2012
Tsinghua Scholarship of Overall Excellence	Tsinghua University, 2011
ST Engineering China Scholarship	Singapore Technologies Engineering Ltd., 2011
First Prize in the National Competition of Physics	Beijing Physics Society, 2010
National Scholarship	Ministry of Education of the P. R. China, 2010
Freshman Academic Scholarship	Tsinghua University, 2009
Silver Medal in the National Final of Chinese Physics Olympiad	Chinese Society of Physics, 2008

PROFESSIONAL EXPERIENCE

TEACHING ASSISTANT

- Smart Grids Technologies (EE-472 EPFL) — Spring 2016/2017/2018
- TCP/IP Networking (COM-407 EPFL) — Autumn 2015/2016/2017/2018

RESEARCH INTERN

- National Laboratory for Information Science and Technology — October 2013 - April 2014
- Chinese Academy of Sciences — July 2012 - September 2012

MISCELLANEOUS

RESEARCH INTEREST

- Networked Systems, Control, Optimization, HPC, Signal Processing, Learning Methods

LANGUAGE SKILL

- Chinese, English, Japanese

**Ce document a été imprimé au Centre d'impression EPFL,
imprimerie climatiquement neutre, certifiée myClimate.**